



HAL
open science

Oligomerization and polymerization of ethylene by phenoxy-imine titanium catalysts

Astrid Cordier

► **To cite this version:**

Astrid Cordier. Oligomerization and polymerization of ethylene by phenoxy-imine titanium catalysts. Catalysis. Université de Lyon, 2019. English. NNT : 2019LYSE1229 . tel-03005971

HAL Id: tel-03005971

<https://theses.hal.science/tel-03005971v1>

Submitted on 15 Nov 2020

HAL is a multi-disciplinary open access archive for the deposit and dissemination of scientific research documents, whether they are published or not. The documents may come from teaching and research institutions in France or abroad, or from public or private research centers.

L'archive ouverte pluridisciplinaire **HAL**, est destinée au dépôt et à la diffusion de documents scientifiques de niveau recherche, publiés ou non, émanant des établissements d'enseignement et de recherche français ou étrangers, des laboratoires publics ou privés.



N°d'ordre NNT : 2019LYSE1229

THESE de DOCTORAT DE L'UNIVERSITE DE LYON

opérée au sein de
l'Université Claude Bernard Lyon 1

**Ecole Doctorale ED206
Chimie de Lyon**

Spécialité de doctorat : Chimie

soutenue publiquement le 15/11/2019, par :

Astrid CORDIER

Oligomerization and polymerization of ethylene by phenoxy-imine titanium catalysts

Devant le jury composé de :

Cipullo, Roberta Professeure, Université de Naples Federico II	Rapporteure
Sabo-Etienne, Sylviane Directrice de recherche, CNRS	Rapporteure
Amgoune, Abderrahmane Professeur, CNRS	Examineur
Michel, Typhène Ingénieure chercheuse, IFP Energies nouvelles	Examinatrice
Monteil, Vincent Directeur de recherche, CNRS	Directeur de thèse
Boisson, Christophe Directeur de recherche, CNRS	Co-directeur
Olivier-Bourbigou, Hélène Chef de projet, IFP Energies nouvelles	Invitée
Raynaud, Jean Chargé de recherche, CNRS	Invité

UNIVERSITE CLAUDE BERNARD - LYON 1

Président de l'Université

Président du Conseil Académique

Vice-président du Conseil d'Administration

Vice-président du Conseil Formation et Vie Universitaire

Vice-président de la Commission Recherche

Directeur Général des Services

M. le Professeur Frédéric FLEURY

M. le Professeur Hamda BEN HADID

M. le Professeur Didier REVEL

M. le Professeur Philippe CHEVALIER

M. Fabrice VALLÉE

M. Alain HELLEU

COMPOSANTES SANTE

Faculté de Médecine Lyon Est – Claude Bernard

Faculté de Médecine et de Maïeutique Lyon Sud – Charles Mérieux

Faculté d'Odontologie

Institut des Sciences Pharmaceutiques et Biologiques

Institut des Sciences et Techniques de la Réadaptation

Département de formation et Centre de Recherche en Biologie Humaine

Directeur : M. le Professeur J. ETIENNE

Directeur : Mme la Professeure C. BURILLON

Directeur : M. le Professeur D. BOURGEOIS

Directeur : Mme la Professeure C. VINCIGUERRA

Directeur : M. le Professeur Y. MATILLON

Directeur : Mme la Professeure A-M. SCHOTT

COMPOSANTES ET DEPARTEMENTS DE SCIENCES ET TECHNOLOGIE

Faculté des Sciences et Technologies

Département Biologie

Département Chimie Biochimie

Département GEP

Département Informatique

Département Mathématiques

Département Mécanique

Département Physique

UFR Sciences et Techniques des Activités Physiques et Sportives

Observatoire des Sciences de l'Univers de Lyon

Polytech Lyon

Ecole Supérieure de Chimie Physique Electronique

Institut Universitaire de Technologie de Lyon 1

Ecole Supérieure du Professorat et de l'Education

Institut de Science Financière et d'Assurances

Directeur : M. F. DE MARCHI

Directeur : M. le Professeur F. THEVENARD

Directeur : Mme C. FELIX

Directeur : M. Hassan HAMMOURI

Directeur : M. le Professeur S. AKKOUCHE

Directeur : M. le Professeur G. TOMANOV

Directeur : M. le Professeur H. BEN HADID

Directeur : M. le Professeur J-C PLENET

Directeur : M. Y. VANPOULLE

Directeur : M. B. GUIDERDONI

Directeur : M. le Professeur E. PERRIN

Directeur : M. G. PIGNAULT

Directeur : M. le Professeur C. VITON

Directeur : M. le Professeur A. MOUGNIOTTE

Directeur : M. N. LEBOISNE

Remerciements

Je voudrais en premier lieu remercier Timothy McKenna pour son accueil au laboratoire C2P2 et la région Auvergne Rhône-Alpes pour le financement de ce projet de thèse. Ce travail est le fruit d'une étroite collaboration entre l'IFP Energies nouvelles et le laboratoire C2P2.

Je souhaite remercier les membres du jury pour avoir évalué mon travail de thèse. Merci à Monsieur Amgoune pour avoir présidé le jury. Je tiens à exprimer ma gratitude à Madame Sabo-Etienne et Madame Cipullo pour avoir joué le rôle de rapporteur avec assiduité et bienveillance.

Je tiens à remercier l'IFPEN pour m'avoir fait profiter de ses diverses formations et événements scientifiques. Je remercie tous les thésards de l'IFPEN (Emile, Angélique, Alexis, Larissa, Audrey, Céline...) que j'avais plaisir à retrouver dès que l'occasion se présentait. Un grand merci à tous les membres de l'équipe Catalyse moléculaire avec qui j'ai eu plaisir à travailler lors de mon projet de fin d'étude. Parmi eux, je remercie chaleureusement Hélène Olivier-Bourbigou, Lionel Magna, Pierre-Alain Breuil et Typhène Michel pour m'avoir accompagnée ensuite pendant ces trois ans de thèse. J'ai beaucoup apprécié votre disponibilité et implication dans le projet malgré la distance. Travailler avec vous était un réel privilège, j'ai énormément appris de nos échanges lors de nos réunions. Je souhaite un bel avenir à toute l'équipe.

Ces trois années de thèse passées au laboratoire C2P2 ont été riches en rencontres professionnelles. Je remercie toute l'équipe de Chemspeed Technologies pour la plateforme de catalyse homogène, pour le chaleureux accueil en Suisse et pour votre accompagnement lors de la FAT, SAT et après. Merci tout particulièrement à Amira Abou-Hamdani, Jaroslav Padevet et Dominique Sauter pour leur disponibilité et leur aide. Merci à l'équipe d'Axel'One Campus pour leur disponibilité et leur assistance sans faille. L'installation de la plateforme n'a pas été simple mais le jeu en valait la chandelle !

Il est à présent temps de faire une standing ovation à tous les membres du laboratoire C2P2. Je veux remercier chaque permanent et étudiant que j'ai eu la chance de croiser pendant ces trois années. Au-delà d'un indéniable enrichissement scientifique, ces années ont été une expérience humaine inoubliable.

Je voudrais remercier toutes les personnes qui ont contribué de près ou de loin au bon déroulement de ces trois ans de thèse. Je remercie tous les collègues du C2P2 et particulièrement Kai Szeto, Nesrine Oueslati et Damien Montarnal. Un petit mot spécial à l'équipe d'analyse : désolée pour toutes ces fois où j'ai bouché la SEC avec mon PE... Merci à

Olivier pour ton aide et ton dévouement au labo comme en dehors. Merci à Franck Collas, l'expert de Mettler Toledo, pour ton investissement et ton partage de connaissance. Merci à Manel d'avoir été toujours disponible et prête à aider pour la SEC. Mention Spéciale pour Seb qui est toujours disponible pour épauler les étudiants avec bienveillance et toujours avec le sourire ! Merci de m'avoir aidée avec « la Ferrari » et bonne chance pour la suite. Je remercie également Pierre-Yves pour ta participation à chaque soirée (Vive la raclette !), Elodie pour nos échanges toujours intéressants aux pauses déjeuners. Merci à Franck et Muriel avec qui on a toujours l'occasion de bien rigoler. Je veux dire un grand merci à Nathalie sans qui le labo ne fonctionnerait pas aussi bien et l'ambiance ne serait pas la même (surtout à midi !). Merci pour toutes tes petites attentions et ton peps sur la piste de danse à la soirée de ma soutenance !

Je dois maintenant faire un big-up à tous les étudiants et post-docs avec qui j'ai pu travailler et échanger au laboratoire. Merci à mes co-labos pour la bonne ambiance et la bonne musique par 10 °C comme 40 °C : Islem, Benjamin, Wilfried et Nicolas. Merci aux co-bureaux du « bureau des intellos » pour l'ambiance studieuse mais surtout les fous-rires : Arne, Ali, Cédric, Matthieu, Priscilla (et Rémi l'incrust'). Merci aux autres étudiants pour la bonne atmosphère au labo et aux after-works : Amel, Douriya, Rita, James, Florian et tous les autres. J'en profite pour remercier ceux qui étaient des collègues et qui sont devenus des amis. Merci aux filles : Magali, Islem et Winnie + Anna, merci au maître du zouk, Wilfried et gracias Edgar pour ta générosité, droiture et gentillesse.

De ces années au laboratoire, je retiendrai les moments forts de partage qui vont me manquer : les crêpes, l'amigo secreto, le repas de Noël, le repas international, les restos, les bowlings, les pauses café et déjeuner, les after-works et les soirées (mais surtout celles dans un certain appart en presqu'île).

Ayant passé trois ans du « côté catalyse », j'adresse mes remerciements les plus sincères à mes encadrants de thèse. Lors de nos premiers échanges, j'ai pu mesurer la chance que j'avais de pouvoir travailler avec des experts en catalyse de polymérisation. Je vous remercie pour votre implication, votre partage de connaissance, votre aide et votre disponibilité alors que le sujet n'était pas entièrement de votre expertise à la base ! J'ai eu le privilège de travailler avec trois encadrants brillants scientifiquement et très riches humainement.

Jean, je salue ton enthousiasme et tes nombreux conseils qui m'ont permis d'avancer dans le projet. Christophe, j'ai beaucoup appris de ton expertise et de ta rigueur. Merci pour ton implication et pour nos partages de publis. Vincent, je n'aurais pas pu rêver meilleur directeur de thèse. Je te remercie sincèrement pour le dévouement sans limite que tu voues à tes étudiants pour la thèse et pas seulement. Mille mercis pour ton aide pour « l'après-thèse » et pour ces 1287 mails et 53 coups de téléphone passés à droite et à gauche qui ont permis le succès actuel de la plateforme Chemspeed.

Au cours de ces trois années de thèse, nous avons partagé de bons moments au laboratoire (réunions de plusieurs heures sans café, répétitions soporifiques de la soutenance...) et surtout en dehors : visite de Chemspeed, congrès à Geleen, Naples et Amsterdam (le plus visuellement et olfactivement mémorable). Je ressors grandie de ces trois ans de thèse grâce à vous, merci.

Une thèse c'est aussi une période pendant laquelle les amis s'éloignent (uniquement physiquement) ou se rapprochent.

Marie, Isa et Coline, on a pu finalement habiter toutes ensemble à Lyon. Vous êtes un pilier pour moi depuis la TS1. Chaque moment passés autour d'un verre, à un spectacle ou sur un canapé m'est précieux. 10 ans d'amitié obligent, la distance ne nous éloignera pas !

Je veux aussi remercier les copines de la prépa, la team Gossip : Chloé, Laurianne, Pénélope, Coralie, Blandine et Kath. Merci d'avoir fait partie de cette période de ma vie car sans vous, je ne serai jamais allée si loin ! A tous ces temps forts passés ensemble : des heures de pauses, aux soirées en passant par les visites en césure et maintenant les petits weekends escapade. Vous voir (quasi)toutes réunies pour ma soutenance m'a comblée de joie. Je vais faire en sorte que ces retrouvailles se perpétuent (#Tahiti2020).

I am also grateful to Becky who travelled from Belfast and contributed a lot to the success of my PhD defense. In 2014-2015, we spent one year together in the Netherlands. Since then, every time we meet is as if you were still living next-door. I would like to thank you from the bottom of my heart for your endless support.

J'ai eu aussi la chance de rencontrer sur ma route des personnes formidables : mes collègues stagiaires de l'IFPEN (Angélique, Jason & Alexis), (DJ) Jordan, (old) Martin, l'équipe d'UPBS (Caro, Mani, Gaëtan, Jenny, Marie-Mich, Audrey & Laura), Benji & Alex et mes colocs en or : Tatiana & Morgan. Je vous remercie pour tous les moments passés ensemble et j'espère vous recroiser à l'occasion.

Ces trois années de thèse ont été clairsemées de moments difficiles que je n'aurais pas pu surmonter sans l'aide inestimable de mes amis et mes proches. J'exprime toute ma gratitude à Marie, Isa, Yashmin, Audrey, Cédric, Benjamin et Becky pour avoir été là quand j'en avais besoin.

Pour finir, je tiens à remercier ma famille. Merci à Gérard & Sylviane, Eve, Rachelle, Robin & Arsène, pour être toujours là dans les moments difficiles mais surtout festifs. Je remercie mes parents pour avoir fait de moi qui je suis aujourd'hui et pour m'avoir donné les moyens d'arriver là où je voulais aller. Merci à mon frère Nico d'être toujours présent pour moi.

Pour clôturer mes remerciements, je me tourne vers les artistes qui m'inspirent (et qui m'ont indirectement aidé pendant la rédaction).

Will you lay yourself down and dig your grave or will you rail against your dying day.

The Lumineers

Cause you know, it's a dark, twisted road we are on. And we all have to walk it alone.

First Aid Kit

Y ahora puedo ver lo que a veces siempre se escondía. Las luces primeras

Les jours pétillent comme du soda, l'inconnu m'électrise. Brigitte

On réfléchit plus tard, maintenant, il faut rêver. Cœur de pirate

ABSTRACT

1-hexene is one of the most important olefin used as comonomer for the production of value-added polyethylenes (HDPE, LLDPE). In the field of selective ethylene trimerization employing titanium-based catalysts, specific single tridentate phenoxy-imine complexes (SFI) display the highest activity and 1-hexene selectivity upon activation with methylaluminoxane (MAO). However, ethylene polymerization is an unavoidable side reaction affecting both 1-hexene selectivity and process operations. Although being a major drawback, the causes of polymerization remain a grey area since few studies were dedicated to its deciphering. To tackle this challenge, an original “polymer-to-catalyst” strategy was implemented. An extensive temperature study (26-80°C) revealed that the highest 1-hexene activity is reached between 30 °C and 40 °C while polymer production is prominent above 50 °C. Polyethylenes obtained were analyzed by SEC, NMR DSC, and advanced techniques (CEF, SIST, rheology). Molar masses above 10^5 g mol⁻¹ were identified along with a 1-hexene content below 1 mol %. An increase of dispersity ($\bar{M}_w/\bar{M}_n > 2$) with at higher reaction temperature was ascribed to an evolution from single-site to multi-sites polymerization catalysis. Kinetic studies proved that polymer is continuously produced during the catalytic tests even at short reaction time, for any reaction temperature. Other parameters (addition of 1-hexene, hydrogen, use of trimethylaluminum) were found to impair the trimerization selectivity and/or activity of the system. Premix of the precursor with MAO can be beneficial for reducing the selectivity in polymer in some cases (depending on the composition of MAO). After analyzing the possible routes for the polymerization catalyst formation, the hypotheses of temperature- and MAO-induced complex alterations were considered. Regarding the latter, a molecular ligand-free Ziegler-Natta catalyst, modeled using TiCl₄/MAO. Formation of a polymerization species upon thermal alteration of the SFI complex was evidenced. This [O⁻,N,O⁻]-type species displays common features regarding catalytic response to 1-hexene compared to the polymerization catalyst in the SFI system although it could not reach the same catalytic performances. Investigations on the (FI)Ti^{III}Cl₂(THF) complex evidenced its disproportionation into a bis(phenoxy-imine) complex (FI)₂TiCl₂. Transformation of mono- to di-substituted complexes is a promising avenue worth exploring to rationalize the formation of secondary active species. Eventually, although the exact side polymerization active species has not yet been identified, this work enabled to guide the focus of further investigations on the activation process and potential complex rearrangements.

RESUME

L'hexène-1 est une des alpha-oléfinés linéaires les plus importantes puisqu'elle permet la fabrication de produits et de matériaux de la vie de tous les jours (détergents, lubrifiants, emballages...). Elle est notamment utilisée comme comonomère pour la production de polyéthylènes (HDPE, LLDPE) dont la demande explose à l'échelle mondiale (70 Mt/an en 2017). Un enjeu majeur pour les entreprises pétrochimiques est donc l'optimisation permanente des procédés de production de l'hexène-1, ce qui passe par la sélectivité de la réaction de trimérisation de l'éthylène.

De nos jours, cette trimérisation sélective est principalement réalisée par des catalyseurs au chrome. Néanmoins, des complexes de titane portant un ligand phenoxy-imine tridente (SFI ou (FI)TiCl₃) se sont aussi révélés être particulièrement efficaces pour la production d'hexène-1. La réaction associée implique une étape d'activation par l'oxyde de méthylaluminium (MAO) et l'éthylène conduisant à un complexe de titane (II) qui permet d'amorcer le mécanisme métallacycle (Schéma 1). Cependant, la polymérisation de l'éthylène est une réaction secondaire inhérente à ce système et dont l'origine reste indéterminée. La formation de ce polyéthylène impacte à la fois la sélectivité du système et le bon déroulement du procédé en phase liquide. S'il est primordial d'éviter cette réaction, peu d'études se sont focalisées sur sa rationalisation. En effet, plusieurs éléments limitent l'identification des espèces actives présentes dans le système : la structure mal définie du MAO et la présence de plusieurs espèces à différents degrés d'oxydation. Pour répondre à cette problématique, ce projet s'est appuyé sur une stratégie alternative et originale basée sur l'analyse du polymère pour récolter des informations sur le catalyseur. Le complexe étudié dans ce projet est celui présenté dans le Schéma 1.

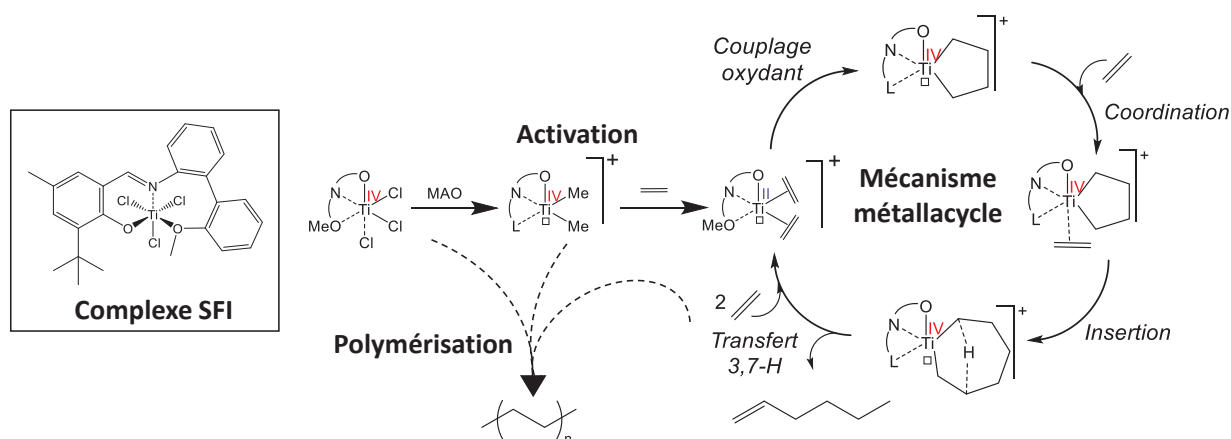


Schéma 1. Complexe phenoxy-imine pour la trimérisation sélective de l'éthylène et mécanisme métallacycle

Dans un premier temps, le comportement du système catalytique (activité, sélectivité) a été étudié sur une large gamme de températures (25-80 °C). Il a été montré que les meilleures activités et sélectivités en hexène-1 sont obtenues à basse température (30-40 °C). En revanche, la réactivité du système bascule vers la production modérée de polyéthylène à plus haute température ($T > 50$ °C) (Figure 1). En combinant des techniques d'analyses classiques (CES, RMN, DSC) et plus avancées (CEF, SIST, rhéologie), tous les polymères ont été identifiés comme ayant de hautes masses molaires ($> 10^5$ g mol⁻¹) et comportant un faible taux de ramifications (Figure 1). Ces éléments démontrent que l'espèce active en polymérisation incorpore peu d'hexène-1 et engendre peu de réactions de transfert. De plus, un élargissement des distributions de masses molaires à haute température ($\mathcal{D} > 2$) traduit l'évolution d'un système mono-site vers un système multi-sites.

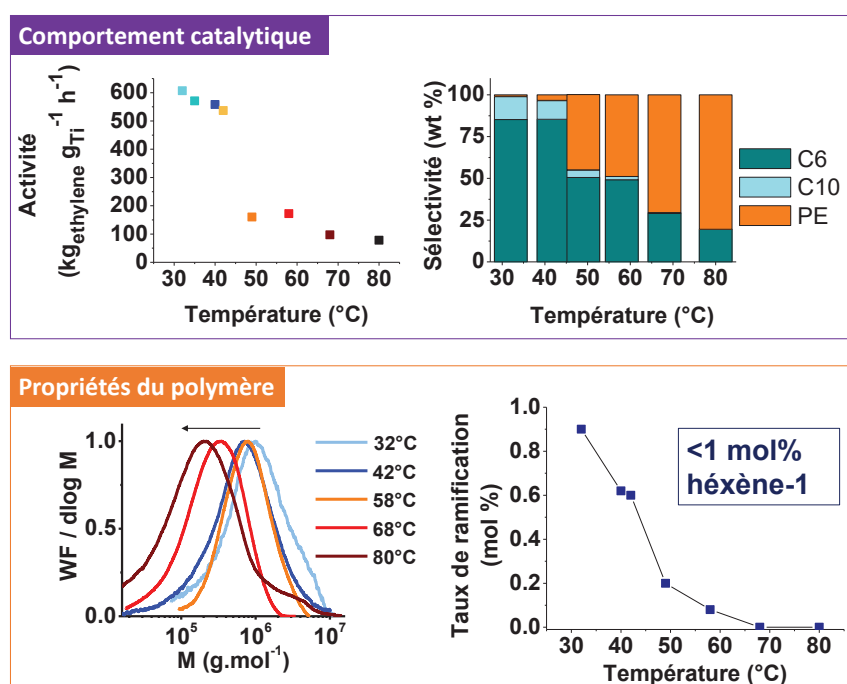


Figure 1. Effet de la température sur le système (Fi)TiCl₃/MAO en termes d'activité, sélectivité et propriétés des polymères

Des études cinétiques ont été menées sur une plateforme Chemspeed entièrement automatisée et sous atmosphère contrôlée (boîte à gants). Des tests réalisés à 40 °C et 80 °C à différents temps de réaction (5, 10, 20, 30 minutes) ont révélé une production continue de polymère. Il s'avère que cette dernière débute dès les premiers instants de la réaction, insinuant donc des déviations durant l'étape d'activation (Schéma 1). Pour étudier le comportement du système SFI, les conditions des tests catalytiques ont été modifiées (ajout d'hexène-1, d'hydrogène, un pré-mélange avec le MAO ou emploi du triméthylaluminium comme co-catalyseur). Dans tous les cas, l'activité et/ou la sélectivité en hexène-1 sont affectées.

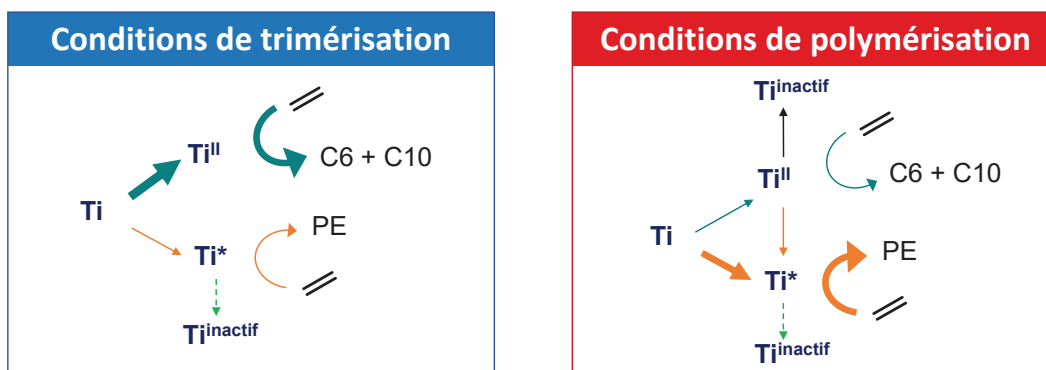


Schéma 2. Voies expliquant la formation des espèces actives d'après les études cinétiques

En étudiant finalement les voies potentielles menant à la formation d'espèces actives en polymérisation (Schéma 2), plusieurs hypothèses ont été considérées. Les causes possibles de formation d'une espèce active en polymérisation sont un changement du degré d'oxydation du titane, un échange de ligands ou encore une modification de la structure du ligand (Schéma 3). Les paramètres identifiés comme ayant un impact significatif sur ces réactions sont la température et le processus d'activation. Pour chaque système, les pré-catalyseurs ont été synthétisés, caractérisés et testés en polymérisation de l'éthylène. Une comparaison avec le système SFI en termes de performances catalytiques et de propriétés du polymère a été réalisée en fonction de la température de réaction et de la quantité d'hexène-1 présente dans le milieu réactionnel.

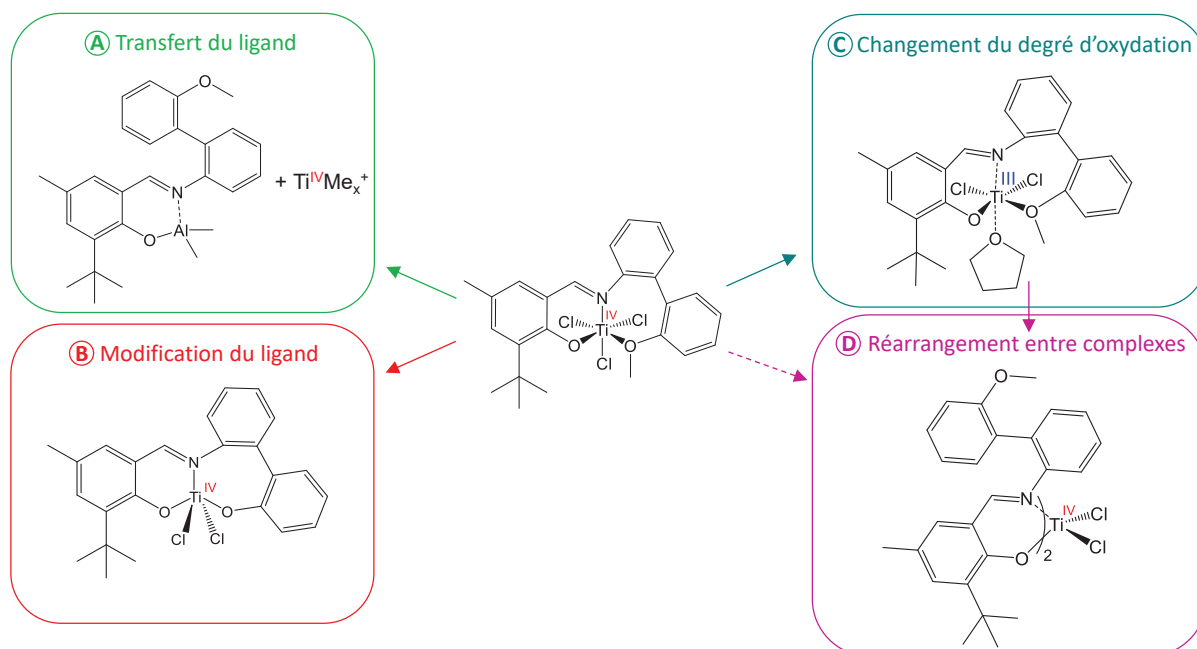


Schéma 3. Précurseurs de polymérisation dérivés du complexe SFI étudié

Concernant les réactions induites par le co-catalyseur, une espèce active « TiMe_x^+ » serait formée suite à l'abstraction du ligand par le triméthylaluminium contenu dans le MAO (Schéma 3, A). Ce transfert de ligand a été mis en évidence par l'analyse du mélange $(\text{FI})\text{TiCl}_3/\text{TMA}$ et la synthèse de $(\text{FI})\text{AlMe}_2$. Cette espèce dénuée de ligand a été modélisée par le système TiCl_4/MAO . Ce système devient inactif au cours des premières minutes de réaction, ce qui ne permet donc pas d'expliquer la production continue de polymère observée avec le système SFI.

La formation d'un précurseur de polymérisation par chauffage de $(\text{FI})\text{TiCl}_3$ a été mise en évidence. En étudiant la dégradation thermique du complexe par RMN en température, ATG et CG/MS, un complexe portant un ligand dianionique $[\text{O}^-, \text{N}, \text{O}^-]\text{-FI}$ a été identifié (Schéma 3, B). Le mécanisme de cette transformation reste indéterminé puisqu'une substitution intramoléculaire a été écartée par les calculs DFT. Après activation par le MAO, le catalyseur résultant possède des points communs avec le système SFI en termes de réponse à l'hexène-1. Cependant, sa faible activité même à haute température laisse penser qu'il ne s'agit pas de l'espèce de polymérisation principale du système $(\text{FI})\text{TiCl}_3/\text{MAO}$.

L'hypothèse d'une réduction partielle ou comproportionation menant à un composé de titane (III) a été vérifiée en testant le système $(\text{FI})\text{Ti}^{\text{III}}\text{Cl}_2(\text{THF})/\text{MAO}$ (Schéma 3, C). La formation d'un complexe de type bis(phenoxy-imine) $(\text{FI})_2\text{TiCl}_2$ par réarrangement (dismutation) du complexe $(\text{FI})\text{Ti}^{\text{III}}\text{Cl}_2(\text{THF})$ a été révélée (Schéma 3, D). Pour les hypothèses C et D, plusieurs espèces sont présentes en solution ce qui ne permet pas l'attribution de la formation de polymère à une espèce définie. Cependant, l'hypothèse de transfert de ligands est une piste sérieuse qui mérite d'être explorée d'avantage sachant que les complexes bis(phenoxy-imine) sont actifs en polymérisation de l'éthylène.

En conclusion, même si l'espèce active en polymérisation du système SFI n'a pas été formellement identifiée dans cette étude, ce projet a permis d'orienter de futures recherches en ciblant les paramètres clés influençant la formation d'espèces secondaires (étape d'activation et mobilité de ligands).

Table of content

Abbreviations	1
General introduction	3
Chapter 1. Literature review	7
<u>TABLE OF CONTENT</u>	8
<u>I. INTRODUCTION</u>	10
<u>II. FROM CONVENTIONAL TO POST-METALLOCENE GROUP 4-BASED ETHYLENE POLYMERIZATION CATALYSIS.....</u>	11
II.1. INTRODUCTION	11
II.2. POLYOLEFINS AND LINEAR ALPHA-OLEFINS	11
II.2.1. DEFINITION	11
II.2.2. APPLICATIONS AND MARKET.....	13
II.2.3. CATALYTIC POLYMERIZATION SYSTEMS	14
II.3. MULTI-SITE POLYMERIZATION CATALYSIS.....	14
II.3.1. POLYMERIZATION MECHANISM	14
II.3.2. DEVELOPMENT AND FEATURES OF ZIEGLER-NATTA CATALYSIS.....	17
II.4. SINGLE-SITE POLYMERIZATION CATALYSIS	19
II.4.1. METALLOCENES	19
II.4.2. POST-METALLOCENES	24
II.4.3. PHENOXY-IMINE (FI) CATALYST.....	25
<u>III. PROPERTIES OF POLYETHYLENES PRODUCED BY MULTI- AND SINGLE-SITE CATALYSIS</u>	35
III.1. INTRODUCTION	35
III.2. GENERAL ANALYSIS OF POLYETHYLENES	35
III.2.1. MULTI-SCALE ORGANIZATION OF POLYMER.....	35
III.2.2. CONVENTIONAL TECHNIQUES APPLIED TO POLYETHYLENE ANALYSES	36
III.2.3. ANALYTICAL FEATURES OF POLYETHYLENES MADE WITH SINGLE- AND MULTI-SITE CATALYSIS	37
III.3. ADVANCED CHEMICAL COMPOSITION ANALYSIS.....	38
III.3.1. CHEMICAL COMPOSITION DISTRIBUTION OF COPOLYMERS	38
III.3.2. BEYOND DSC: STEPWISE ISOTHERMAL SEGREGATION TECHNIQUE.....	39
III.3.3. BEYOND CHROMATOGRAPHY: CRYSTALLIZATION ELUTION FRACTIONATION	41
III.4. IN-DEPTH ANALYSIS OF HYDROCARBON MACROMOLECULE ORGANIZATION.....	44
III.4.1. ENTANGLEMENT IN THERMOPLASTICS	44
III.4.2. ENTANGLEMENT IN LINEAR POLYETHYLENE.....	46
III.4.3. ANNEALING APPLIED TO <i>DISUHMWPE</i>	51

IV. GROUP 4-BASED ETHYLENE OLIGOMERIZATION CATALYSIS	54
IV.1. INTRODUCTION	54
IV.2. EVOLUTION OF CATALYTIC SYSTEMS AND PROCESSES FOR ETHYLENE OLIGOMERIZATION	54
IV.2.1. LAOS PRODUCTION	54
IV.2.2. FROM FULL-RANGE TO ON-PURPOSE PROCESSES	55
IV.2.3. TITANIUM-BASED SELECTIVE OLIGOMERIZATION	58
IV.3. SINGLE FI CATALYST – A PROMISING TRIMERIZATION SPECIES	64
IV.3.1. STRUCTURE AND PRODUCTS	64
IV.3.2. UNDERSTANDING THE SFI SYSTEM	70
V. CONCLUSION AND SCOPE OF THE PHD PROJECT	77
V.1. MISSING ELEMENTS PREVENTING COMPREHENSION	77
V.2. MAIN HYPOTHESIS FOR POLYETHYLENE PRODUCTION	78
V.2.1. LIGAND ALTERATIONS	78
V.2.2. LIGAND TRANSFER	78
V.2.3. Ti ^{III} FORMATION	79
V.3. POLYMER-TO-CATALYST STRATEGY	79
VI. REFERENCES	81
 Chapter 2. Effect of temperature on (FI)TiCl ₃ /MAO system: reactivity and polymer features investigations	 87
TABLE OF CONTENT	88
I. INTRODUCTION	90
II. BEHAVIOR OF THE TRIMERIZATION SYSTEM WITH TEMPERATURE	91
II.1. REACTANTS AND PRODUCTS	91
II.1.1. CATALYTIC SYSTEM	91
II.1.2. PRODUCTS OF TRIMERIZATION AND POLYMERIZATION REACTIONS.....	93
II.1.3. CATALYTIC CONDITIONS OPTIMIZATION	94
II.2. TEMPERATURE EFFECT ON ACTIVITY AND SELECTIVITY.....	96
II.2.1. EVOLUTION OF THE ACTIVITY	96
II.2.2. EFFECT OF TEMPERATURE ON THE SELECTIVITY	98
II.2.3. DISCUSSION ON TEMPERATURE EFFECT ON POLYMERIZATION ACTIVE SPECIES FORMATION	101
III. IN-DEPTH POLYMER ANALYSIS	104
III.1. POLYMER FEATURES	104

III.1.1. MOLAR MASS DISTRIBUTION (MMD)	104
III.1.2. CHEMICAL COMPOSITION OF POLYMERS PE-SFS-26 TO PE-SFS-80	105
III.2. ADVANCES ANALYSIS OF PE-SFS-26 TO PE-SFS-80.....	112
III.2.1. CHEMICAL COMPOSITION DISTRIBUTION OF THE POLYMERS	112
III.2.2. POLYMER TOPOLOGY INVESTIGATION.....	119
<u>IV. CONCLUSIONS ON THE EFFECT OF TEMPERATURE AND POLYMER CHARACTERIZATION</u>	<u>124</u>
<u>V. EXPERIMENTAL SECTION.....</u>	<u>125</u>
V.1. GENERAL CONSIDERATIONS.....	125
V.2. ORGANIC AND COMPLEX SYNTHESIS	126
V.3. CATALYTIC TEST PROCEDURE	128
V.3.1. EQUIPMENT	128
V.3.2. PROCEDURE	128
V.4. PRODUCT ANALYSIS	129
V.4.1. OLIGOMER ANALYSES.....	129
V.4.2. POLYMER ANALYSES	130
<u>VI. REFERENCES</u>	<u>134</u>
Chapter 3. Kinetic studies and activation process investigations	135
<u>TABLE OF CONTENT</u>	<u>136</u>
<u>I. INTRODUCTION</u>	<u>138</u>
<u>II. KINETIC STUDIES.....</u>	<u>139</u>
II.1. KINETICS ACCORDING TO REACTION TEMPERATURE	139
II.1.1. KINETIC MODEL APPLIED TO THE SFI SYSTEM.....	139
II.1.2. REACTION RATE EVOLUTION FOR THE TEMPERATURE STUDY.....	142
II.1.3. EARLY STAGE REACTION	145
II.2. STUDY OF THE SFI SYSTEM AT SEVERAL REACTION TIMES	146
II.2.1. EQUIPMENT	146
II.2.2. KINETIC STUDIES AT 40, 60 AND 80 °C.....	147
II.3. DISCUSSION ON ACTIVE SPECIES FORMATIONS BASED ON KINETIC CONSIDERATIONS	158
<u>III. PARAMETERS INFLUENCING THE ACTIVATION PROCESS.....</u>	<u>160</u>
III.1. GOAL AND STRATEGY.....	160
III.2. INFLUENCE OF ADDITIONAL 1-HEXENE	161

III.2.1. ACTIVITY & SELECTIVITY.....	161
III.2.2. POLYMER PROPERTIES.....	164
III.3. INFLUENCE OF HYDROGEN.....	166
III.3.1. ACTIVITY & SELECTIVITY.....	166
III.3.2. PRODUCTS PROPERTIES.....	167
III.4. INFLUENCE OF TMA AND PREMIX.....	169
III.4.1. ACTIVITY & SELECTIVITY.....	169
III.4.2. INFLUENCE OF TMA AND MAO PREMIX ON POLYMER FEATURES.....	173
<u>IV. CONCLUSION.....</u>	<u>176</u>

V. EXPERIMENTAL SECTION.....178

V.1. GENERAL CONSIDERATION.....	178
V.2. CATALYTIC TESTS CONDITIONS FOR KINETICS STUDIES.....	178
V.2.1. STOPPED-FLOW REACTOR.....	178
V.2.2. SYNTHESIS AND CATALYTIC TEST ON CHEMSPEED UNIT.....	179
V.3. CATALYTIC TESTS WITH THE 1 LITER SFS REACTOR.....	180
V.3.1. INTRODUCTION OF 1-HEXENE.....	180
V.3.2. USE OF HYDROGEN.....	181
V.3.3. USE OF TMA AS CO-CATALYST.....	181
V.3.4. PREMIX COMPLEX I/MAO.....	181

VI. REFERENCES.....182

Chapter 4. Hypotheses of polymerization active species 183

TABLE OF CONTENT.....184

I. INTRODUCTION.....186

II. HYPOTHESIS OF LIGAND ABSTRACTION.....188

II.1. CHARACTERIZATION OF LIGAND TRANSFER TO TMA.....	188
II.1.1. REACTIVITY OF TMA TOWARD COMPLEX I.....	188
II.1.2. SYNTHESIS OF AND CHARACTERIZATION OF (FI)ALME ₂	190
II.2. TiCl₄/MAO AS MOLECULAR ZIEGLER-NATTA CATALYST.....	193
II.2.1. CATALYTIC PERFORMANCE OF TiCl ₄ /MAO IN ETHYLENE POLYMERIZATION AND COPOLYMERIZATION WITH 1-HEXENE.....	193
II.2.2. COMPARISON OF POLYMER FEATURES OBTAINED WITH COMPLEX I /MAO AND TiCl ₄ /MAO.....	195
II.3. DISCUSSION ON THE HYPOTHESIS OF LIGAND ABSTRACTION.....	198

III. HYPOTHESIS OF LIGAND ALTERATION.....	200
III.1. POSSIBLE MODIFICATIONS OF COMPLEX INDUCED BY A TEMPERATURE EFFECT	200
III.2. THERMAL MODIFICATION OF COMPLEX I	201
III.2.1. COMPLEX I DEGRADATION	201
III.2.2. SYNTHESIS OF COMPLEX III.....	205
III.3. CATALYTIC TEST WITH A MIXTURE OF COMPLEX I AND COMPLEX III.....	209
III.3.1. ACTIVITY AND SELECTIVITY WITH THE MIXTURE COMPLEX I + COMPLEX III	209
III.3.2. COMPARISON OF POLYMER PROPERTIES	210
III.4. TEST OF COMPLEX III/MAO TOWARD ETHYLENE POLYMERIZATION AND COPOLYMERIZATION WITH 1-HEXENE	212
III.4.1. INFLUENCE OF TEMPERATURE ON ACTIVITY OF COMPLEX III/MAO	212
III.4.2. POLYMERS PROPERTIES OBTAINED WITH COMPLEX III/MAO IN PRESENCE OF 1-HEXENE	214
III.5. RATIONALIZATION OF COMPLEX III FORMATION	215
III.5.1. PROPOSED MECHANISM	215
III.5.2. DFT CALCULATIONS.....	216
III.5.3. THERMAL ALTERATION DURING CATALYTIC TESTS	219
IV. HYPOTHESIS OF TI^{III} FORMATION.....	220
IV.1. HYPOTHESIS OF (FI)TI ^{III} Cl ₂ COMPLEX	220
IV.1.1. SYNTHESIS OF (FI)TI ^{III} Cl ₂ (THF)	220
IV.1.2. ACTIVITY, SELECTIVITY AND POLYMER PROPERTIES.....	223
IV.2. HYPOTHESIS OF A BIS(FI)TI ^{III} Cl ₂ SPECIES AS POLYMERIZATION ACTIVE SPECIES.....	225
IV.2.1. EVIDENCES OF THE FORMATION OF (FI) ₂ TiCl ₂	225
IV.2.2. ACTIVITY, SELECTIVITY AND POLYMER PROPERTIES.....	229
V. CONCLUSION.....	231
VI. EXPERIMENTAL SECTION.....	232
VI.1. DFT CALCULATION METHOD.....	232
VI.2. GENERAL CONSIDERATIONS.....	232
VI.3. COMPLEX SYNTHESIS AND CHARACTERIZATION.....	233
VI.4. HEATING AND DEGRADATION OF COMPLEX I.....	236
VI.5. CATALYTIC TESTS	237
VI.5.1. TESTS IN THE 1 LITER SFS REACTOR	237
VI.5.2. CATALYTIC TESTS WITH CHEMSPEED AUTOCLAVES.....	238
VII. REFERENCES	239
General conclusion	241

ABBREVIATIONS

\mathcal{D}	Dispersity
BHT	2,6-Di- <i>tert</i> -butyl-4-methylphenol
CCD	Chemical Composition Distribution
CEF	Crystallization Elution Fractionation
CGC	Constrained Geometry Catalyst
C_n	linear alpha-olefin with n carbons
Cp	cyclopentadienyl
Cp*	pentamethylcyclopentadienyl
CRYSTAF	Crystallization Analysis Fractionation
CGC	Constrained Geometry Catalyst
DFT	Density Functional Theory
DCB	<i>o</i> -dichlorobenzene
DSC	Differential Scanning Calorimetry
EPR	Electron Paramagnetic Resonance
FI	“Fenokishi-Imin”, japanese for Phenoxy-Imine (also stands for Fujita’s group Invention)
G', G''	Storage and loss modulus (MPa)
G_R	Strain hardening modulus (MPa)
G_N°	Normalized storage modulus on the rubbery plateau
GC(-MS)	Gas Chromatography (combined with Mass Spectrometry)
HDPE	High Density Polyethylene
HOMO	Highest Occupied Molecular Orbital
$k_{i, p, d}$	Rate constant of initiation/activation (s^{-1}), propagation ($mol^{-1} s^{-1}$), deactivation (s^{-1})
LCB	Long Chain Branching
LAO(s)	Linear Alpha-Olefin(s)
LLDPE	Linear Low Density Polyethylene
LUMO	Lowest Unoccupied Molecular Orbital
MAO	Methylaluminoxane
MMAO	Modified methylaluminoxane
MMD	Molar Mass Distribution
M_n	Number average molar mass ($g mol^{-1}$)
M_w	Weight average molar mass ($g mol^{-1}$)
M_e	Average molar mass between two entanglements
(HT-)NMR	(High Temperature) Nuclear Magnetic Resonance
PE	Polyethylene
PE-CR-T	Polyethylene produced in Chemspeed autoclave at temperature T
PE-SFS-T	Polyethylene produced in 1 liter SFS reactor at temperature T
PNP	Di(phosphino)amine
[O ⁻ ,N]-FI	Phenoxy-imine ligand
[O ⁻ ,N,O]-FI	Phenoxy-imine-ether ligand
[O ⁻ ,N,O ⁻]-FI	diphenoxy-imine ligand
R_p	Reaction rate ($mol s^{-1}$)
SCB	Short Chain Branching
SEC	Size Exclusion Chromatography
SFI	Single phenoxy-imine-ether
SHOP	Shell Higher Olefin Process
SIST	Stepwise Isothermal Segregation Technique

SNS	Bis(sulfanyl)amine
ssC	Single-site catalyst
$T_{c, m, g}$	Crystallization, melting and glass transition temperatures ($^{\circ}\text{C}$ or K)
TCB	1,2,4-trichlorobenzene
TEA	Triethylaluminum
THF	Tetrahydrofuran
TIBA	Triisobutylaluminum
TMA	Trimethylaluminum
TOF	Turn-Over Frequency (h^{-1})
TON	Turn-Over Number (unit specified in each case but most often $\text{mol}_{\text{reacted molecule}} \cdot \text{mol}_{\text{catalyst}}^{-1} \cdot \text{h}^{-1}$ or $\text{g}_{\text{reacted molecule}} \cdot \text{g}_{\text{catalyst}}^{-1} \cdot \text{h}^{-1}$)
TGIC	Temperature Gradient Interaction Chromatography
TREF	Temperature Rising Elution Fractionation
UHMwPE	Ultra High Molar mass Polyethylene
<i>dis</i> UHMwPE	disentangled Ultra High Molar mass Polyethylene
<i>un</i> UHMwPE	unentangled Ultra High Molar mass Polyethylene
ZN	Ziegler-Natta

General introduction

Linear alpha-olefins (LAOs) are major petrochemical derivatives employed in the production of a wide variety of chemicals from detergents, lubricants to special grades of polyethylenes (HDPE, LLDPE). Nowadays, meeting the increasing demand in LAOs is the main challenge faced by industrial companies. Economic and ecological requirements involve a continuous improvement of process efficiency. Since LAO production relies on catalytic oligomerization of ethylene, catalyst features are often leveraged to achieve higher activity and robustness. The first oligomerization processes, called “Full-range processes”, afforded a distribution of various sizes of LAOs. Over the past twenty years, significant efforts invested in the development of selective “On-purpose processes” gave rise to several systems able to produce 1-butene, 1-hexene or 1-hexene/1-octene mixture. Most of these processes employ chromium and titanium catalysts. These systems are still investigated to improve process performances.

In the case of selective trimerization reaction, several titanium catalysts proved their ability for selective 1-hexene production. However, they exhibit a lower activity and selectivity compared to chromium species. Generally speaking, all titanium-based systems that selectively trimerize ethylene are actually derived from polymerization metallocene and post-metallocenes catalysts. The first trimerization system reported in 2001 by Hessen *et al.* relies on hemi-metallocenes and affords up to 86 wt % of 1-hexene (Figure 1). As a matter of fact, the production of polyethylene is a side reaction that is inherent not only to Hessen’s system but also to all other titanium-based derivatives. A decade ago, Fujita and coworkers discovered a trimerization system with outstanding activity and 1-hexene selectivity reported so far for titanium catalysts. This system is based on a titanium complex bearing a single tridentate phenoxy-imine-ether (SFI) ligand and activated with a large excess of methylaluminoxane (MAO). Despite its promising performances, this system also undergoes ethylene polymerization as a minor side reaction. Even though the selectivity in polymer is very low (< 1 wt %), the accumulation of this solid product in a homogeneous and continuous process can lead to reactor fouling and pipe clogging. Therefore, improvement of the selectivity in 1-hexene is crucial for efficient process operating.

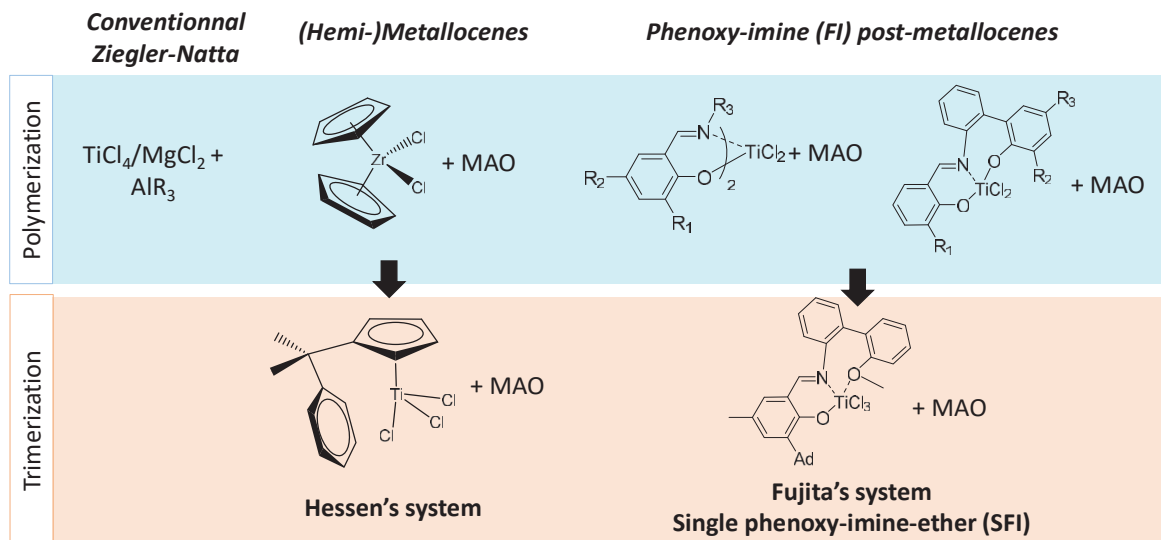


Figure 1. Example of Group 4-based systems for oligomerization and polymerization of ethylene

In this context, the C2P2 laboratory and IFP Energies nouvelles have combined their expertise in ethylene polymerization and oligomerization through this PhD project to further investigate the SFI system. Hence, the goal of this PhD is to identify the polymerization active species, understand the causes for their formation and eventually act on key parameters to prevent this side reaction. This project is focused on trimerization catalysts with a special attention paid to the polymerization active species. Therefore, polymer properties and catalytic behavior in oligo/polymerization are at the center of the strategy developed in this work and reported in this thesis.

This manuscript is divided into 4 chapters. Each chapter comprises its own experimental and bibliographic section.

Chapter 1. Literature review related to catalytic poly/oligomerization of ethylene

The first chapter aims at reviewing the main polymerization and oligomerization systems based on group 4 metals. This bibliographic section is dedicated to polymerization systems that are relevant as potential side active species. Given that a significant part of this project is focused on polymer analyses, a special section focuses on the polyethylene features and analytical techniques. The main studies reported for the trimerization SFI system are detailed and constitute the starting point of the works undertaken in this project.

Chapter 2. Effect of temperature on the SFI system: reactivity and polymer features investigations

This chapter relates the first systematic exploration on the influence of temperature on the activity and especially the selectivity of the SFI system. An extensive polymer investigation combining several conventional and advanced characterization techniques is presented. Following this temperature study, several hypotheses on the type of polymerization active species and the routes leading to their formation are discussed.

Chapter 3. Kinetics studies and activation process investigation

This chapter deals with the investigation on the stage of polymerization species production during the catalytic process. Studies are mainly focused on kinetics and the activation process. First, the evolution of product formation over time is investigated. Then, the influence of several parameters (introduction of 1-hexene, hydrogen and the impact of type and contact with activators) is reported. Combining both studies enables to exclude paths for active species formation and to hypothesize its origin.

Chapter 4. Side polymerization active species: hypotheses and investigations

The final part of the project consisted in studying the most plausible polymerization active species based on conclusions drawn in previous studies and assumptions made in the literature. The synthesis of the suspected catalytic systems and their assessment in terms of catalytic performance and polymer properties are presented. A discussion on the plausibility of each hypothesis is also proposed.

Chapter 1.

Literature review

TABLE OF CONTENT_Toc20673254

I. INTRODUCTION	10
II. FROM CONVENTIONAL TO POST-METALLOCENE GROUP 4-BASED ETHYLENE POLYMERIZATION CATALYSIS.....	11
II.1. INTRODUCTION	11
II.2. POLYOLEFINS AND LINEAR ALPHA-OLEFINS	11
II.2.1. DEFINITION	11
II.2.2. APPLICATIONS AND MARKET	13
II.2.3. CATALYTIC POLYMERIZATION SYSTEMS	14
II.3. MULTI-SITE POLYMERIZATION CATALYSIS	14
II.3.1. POLYMERIZATION MECHANISM	14
II.3.1.1. Phillips catalysis	14
II.3.1.2. Ziegler-Natta catalysis	15
II.3.2. DEVELOPMENT AND FEATURES OF ZIEGLER-NATTA CATALYSIS	17
II.3.2.1. Ziegler-Natta generations.....	17
II.3.2.2. Reactivity with LAOs and hydrogen.....	18
II.4. SINGLE-SITE POLYMERIZATION CATALYSIS	19
II.4.1. METALLOCENES	19
II.4.1.1. Precursors and activators	19
II.4.1.2. Mechanism and kinetics	21
II.4.1.3. Reactivity with LAOs and hydrogen.....	22
II.4.2. POST-METALLOCENES	24
II.4.2.1. Constrained Geometry Catalyst	24
II.4.2.2. Aryl-based systems.....	24
II.4.3. PHENOXY-IMINE (FI) CATALYST.....	25
II.4.3.1. Bis(phenoxy-imine) complexes.....	25
II.4.3.2. Mono(phenoxy-imine) complexes.....	29
II.4.3.2.1. Tridentate L ₂ X FI catalysts	29
II.4.3.2.2. Tridentate LX ₂ FI complexes	31
III. PROPERTIES OF POLYETHYLENES PRODUCED BY MULTI- AND SINGLE-SITE CATALYSIS	35
III.1. INTRODUCTION	35
III.2. GENERAL ANALYSIS OF POLYETHYLENES	35
III.2.1. MULTI-SCALE ORGANIZATION OF POLYMER.....	35
III.2.2. CONVENTIONAL TECHNIQUES APPLIED TO POLYETHYLENE ANALYSES	36
III.2.3. ANALYTICAL FEATURES OF POLYETHYLENES MADE WITH SINGLE- AND MULTI-SITE CATALYSIS	37
III.3. ADVANCED CHEMICAL COMPOSITION ANALYSIS.....	38
III.3.1. CHEMICAL COMPOSITION DISTRIBUTION OF COPOLYMERS	38
III.3.2. BEYOND DSC: STEPWISE ISOTHERMAL SEGREGATION TECHNIQUE.....	39

III.3.3. BEYOND CHROMATOGRAPHY: CRYSTALLIZATION ELUTION FRACTIONATION	41
III.4. IN-DEPTH ANALYSIS OF HYDROCARBON MACROMOLECULE ORGANIZATION.....	44
III.4.1. ENTANGLEMENT IN THERMOPLASTICS	44
III.4.2. ENTANGLEMENT IN LINEAR POLYETHYLENE.....	46
III.4.3. ANNEALING APPLIED TO <i>DISUHMWPE</i>	51
<u>IV. GROUP 4-BASED ETHYLENE OLIGOMERIZATION CATALYSIS</u>	<u>54</u>
IV.1. INTRODUCTION	54
IV.2. EVOLUTION OF CATALYTIC SYSTEMS AND PROCESSES FOR ETHYLENE OLIGOMERIZATION	54
IV.2.1. LAOs PRODUCTION	54
IV.2.2. FROM FULL-RANGE TO ON-PURPOSE PROCESSES.....	55
IV.2.2.1. Full-range process	55
IV.2.2.2. On-purpose process	56
IV.2.3. TITANIUM-BASED SELECTIVE OLIGOMERIZATION	58
IV.2.3.1. Dimerization	58
IV.2.3.2. Trimerization	60
IV.3. SINGLE FI CATALYST – A PROMISING TRIMERIZATION SPECIES	64
IV.3.1. STRUCTURE AND PRODUCTS.....	64
IV.3.1.1. Structure alteration	66
IV.3.1.2. Supported catalysis	67
IV.3.1.3. Tandem catalysis	68
IV.3.2. UNDERSTANDING THE SFI SYSTEM	69
IV.3.2.1. Activation process	69
IV.3.2.2. Trimerization mechanism.....	73
<u>V. CONCLUSION AND SCOPE OF THE PHD PROJECT.....</u>	<u>77</u>
V.1. MISSING ELEMENTS PREVENTING COMPREHENSION	77
V.2. MAIN HYPOTHESIS FOR POLYETHYLENE PRODUCTION	78
V.2.1. LIGAND ALTERATIONS	78
V.2.2. LIGAND TRANSFER	78
V.2.3. Ti^{III} FORMATION.....	79
V.3. POLYMER-TO-CATALYST STRATEGY	79
<u>VI. REFERENCES.....</u>	<u>81</u>

I. INTRODUCTION

This PhD project is focused on improving the selectivity of a catalytic system at the molecular scale to ultimately improve process performance at the industrial scale. The reaction targeted is the selective trimerization of ethylene mediated by titanium-based tridentate phenoxy-imine (SFI) systems. In addition to 1-hexene and higher trimers, polymer is formed as a minor side product (1 wt % selectivity) in optimized process conditions, i.e. low temperature and high pressure.¹ In the purpose of achieving the highest activity and selectivity in 1-hexene, polymerization must be avoided.

One approach to improve the selectivity in 1-hexene consists in modifying the catalytic systems, especially the SFI complex. As a matter of fact, the development of new complexes was implemented in previous studies but led to the enhancement of polymerization instead of trimerization reaction.² Since the design of new systems intends to avoid and not harness polymerization, our strategy is deliberately focused on the side product to find the reasons for its formation. In this context, this project was articulated around an original approach called “polymer-to-catalyst” strategy. From the analyses of the polymer, it is possible to collect useful information on the polymerization active species. These species can then be categorized among several families of polymerization catalysts. This requires to have a clear view on polymerization catalytic systems and relationship between catalyst features and polymer properties. Moreover, given that the polymer is produced from an unknown active species, it is necessary to combine conventional and advanced techniques to have a full picture of the polyethylene structure and composition. Eventually, polymerization cannot be utterly rationalized without an analysis of the core of this issue. Therefore, it is also important to lay the foundations of ethylene trimerization with SFI system regarding mechanism, related active species and parameters influencing its catalytic behavior (activity and selectivity). Having this overview in mind, it is possible to highlight potential parameters causing this side reaction and to address the missing elements for its rationalization.

This bibliographic study is organized on the basis of this “polymer-to-catalyst” approach. First, an overview is provided on ethylene polymerization with group-4 metals and associated polyethylene features. The second section focuses on conventional and advanced techniques for the analysis of polyethylene. Afterwards, ethylene oligomerization processes and their catalytic system are presented. A special attention is drawn to the selective trimerization SFI system regarding its discovery, mechanistic investigations and developments. Eventually, the last section summarizes the main hurdles to the comprehension of the side polymerization in the SFI system. A list of the potential causes of polymerization is extracted from the literature study and the strategy developed from these assumptions is explained.

II. FROM CONVENTIONAL TO POST-METALLOCENE GROUP 4-BASED ETHYLENE POLYMERIZATION CATALYSIS

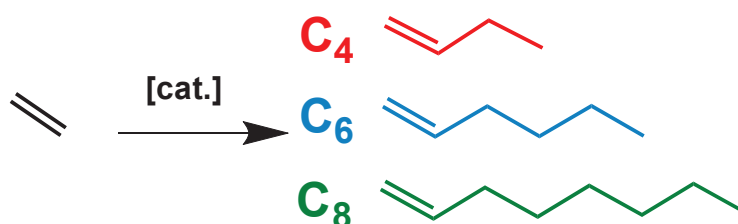
II.1. Introduction

In the case of the trimerization SFI system, the side reaction of polymerization has never been investigated from the perspective of the polymer. Yet, it is precisely by studying the polymer that one can have a glimpse into the type and number of polymerization active species. To apply the so-called polymer-to-catalyst strategy developed for this PhD project, it was necessary to set the bases of catalytic polymerization of ethylene with group 4 metals. Therefore, this section aims at providing a general overview catalytic systems for ethylene polymerization in terms mechanisms, active species and polymer features. Catalytic behavior and polymer properties are exemplified for relevant multi-site Ziegler-Natta catalysts as well as homogeneous single-site metallocenes and post-metallocenes. Eventually, this section focuses on phenoxy-imine derivatives displaying similarities with the trimerization SFI complexes employed for ethylene polymerization.

II.2. Polyolefins and Linear alpha-olefins

II.2.1. Definition

Ethylene is the smallest olefin used for the production of polyethylene (PE) and linear alpha-olefins (LAOs). Thus, these derivatives are simply made of a repetition of $-CH_2-$ groups. Chains of n carbons (C_n) are called oligomers when $2 < n < 100$ and polymers when n is above 100 carbons.³ Among oligomers, linear alpha-olefins with $n < 20$ are the most valuable ones. The LAO production relies on catalytic and anionic processes and is mainly oriented toward short 1-olefins, such as 1-butene, 1-hexene and 1-octene (Scheme 1).



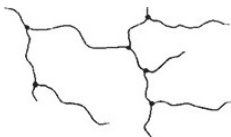


Scheme 1. Short linear alpha-olefin synthesis

Polyethylene is a polyolefin with a simple chemical structure but diverse features. Even though polyethylene is a mere sequence of $-CH_2-$ moieties, several polymer structures exist and display different physical properties (Table 1). In fact, the polymer chains can be linear or branched. Short chain branching (SCB), namely methyl to hexyl branching, is distinguished from long chain branching (LCB), since their impact on polymer properties is different. Long chain branching is defined as hydrocarbon side chain whose length is higher than the average critical entanglement distance of a linear polymer chain, often higher than 40 carbons.⁴

Regarding polymer properties, the higher the amount of branching in the hydrocarbon backbone, the lower the density and therefore the stiffness of the material.

Table 1. Main polyethylene structures and characteristics

PE molecular structure			
PE grade	HDPE	LLDPE	LDPE
Branching	quasi none	SCB	LCB and SCB
Melting temperature (°C)	135	125	105
Crystallinity (%)	70	50	40

Depending on the polymerization process, several grades of polyethylene can be produced. Free-radical polymerization under high temperature (above 100 °C) and high pressure (above 1 000 bar) affords low density polyethylene (LDPE) containing irregular long and short chain branchings. On the contrary, High Density Polyethylene (HDPE) and linear low density polyethylene (LLDPE) are linear polyethylenes that can only be obtained by means of a metal-based catalysis.⁵

These polymers contain SCB resulting from the copolymerization of ethylene with propylene, 1-butene, 1-hexene or 1-octene. It is noteworthy that some of these polymer grades comprise also LCB. The content of LAO in ethylene/LAO copolymers is referred as the chemical composition of the polymer. Generally speaking, the presence of branches in the linear chain affects the crystallinity of the polymer and decreases its melting temperature.⁶ While HDPE usually melts above 130 °C, the melting temperature of LLDPE varies from 120 °C to 135 °C when the 1-hexene or 1-octene molar content decreases from 2 mol % to 0 mol %.⁷

In addition to branching, the lengths of hydrocarbon chains and their homogeneity in size also play a crucial role on the toughness and processability of the resulting material. These parameters are defined as molar masses and their dispersity (Equation 1) and are extracted from the molar mass distribution of the polymer.⁸

$$M_n = \frac{\sum n_i M_i}{\sum n_i} \quad M_w = \frac{\sum n_i M_i^2}{\sum n_i M_i} \quad \mathcal{D} = \frac{M_w}{M_n}$$

Equation 1. Number-average molar mass (M_n), weight-average molar mass (M_w) and dispersity (\mathcal{D}) equations. n_i is the number of macromolecules of M_i molar mass.

From Equation 1, it is important to note that a polymer with a wide variety of hydrocarbon chain size will display a higher dispersity (\mathcal{D}) than a polymer with very homogeneous chain

length. In the case of linear hydrocarbon chains (produced by catalysis), polyethylenes can be classified from low molar mass ($< 10^4 \text{ g mol}^{-1}$) to high molar masses ($10^{4-5} \text{ g mol}^{-1}$) and ultra-high molar mass (UHMwPE, $> 10^6 \text{ g mol}^{-1}$). Chain length, distribution broadness and modality depend on the nature of the catalytic system employed as well as the polymerization conditions.⁹ It is important to stress that each catalyst is unique and leaves its fingerprint through the properties of the polymer it produces. A general view of the properties of polyethylenes afforded by two categories of catalyst (single-site and multi-site) will be detailed in the section “III. Properties of polyethylenes produced by multi- and single-site catalysis”.

II.2.2. Applications and market

Polyethylene is one of the most widely used polymer owing to its various structures providing versatile applications. The production of polyethylene increases each year from 68 Mt in 2006 to 86 Mt in 2015.¹⁰ The production in light linear alpha-olefins is mostly driven by the polyethylene demand since LLDPE contains 1-butene, 1-hexene or 1-octene.¹¹

Specific properties of HDPE, LLDPE and LDPE enable multi-disciplinary applications such as health and hygiene, electronic, construction and packaging.⁶ The assets of polyethylene are its strength, lightness, mechanical and chemical resistance. The range of products goes from flexible plastic bags and wrap films to rigid cables and pipes (Table 2).¹²

Table 2. Mechanical properties and applications of polyethylene grades

Polyethylene grade	Tensile strength (MPa)	Main applications
HDPE	20-32	pipes, cables, rigid packaging
LLDPE	10-22	Flexible tubing, bottles, plastic wrap
LDPE	8-12	grocery plastic bags

While polyolefins are being controverted, Mülhaupt *et al.* explained that these thermoplastics are decently included in a circular economy following the major principle of green chemistry and recycling materials.¹³ Moreover, polyolefins still bring innovation with the developments of new materials in the field of self-reinforced nanostructured all-hydrocarbon composites.¹⁴

II.2.3. Catalytic polymerization systems

Metal-based catalysis is the exclusive technique for linear polyethylene production. Owing to a low toxicity, group 4 metals are part of several polymerization processes that are either heterogeneous, i.e. supported catalyst, or homogeneous, i.e. molecular catalyst. Simple group 4 precatalysts are MX_4 species with X being a halide or alkoxide.^{15–18} They are distinguished from group-4 based complexes, which are precatalysts bearing permanent organic ligands from the simple cyclopentadienyl group (Cp) to sophisticated framework.^{19–21}

Concerning heterogeneous systems, precatalysts are supported on a carrier such as MgCl_2 and more rarely SiO_2 . This heterogeneity implies different environment around each active center and therefore inequivalent active sites. As a consequence, heterogeneous catalysis is synonym of multi-site catalysis. Conversely, single-site catalysis calls for molecular catalysts displaying the same structure. Organic complexes as well as homogeneous MX_4 species are considered as well-defined molecular precatalysts. Although precatalyst contains a transition metal (Ti, Cr, V...), cocatalysts are essential to activate this species toward ethylene.

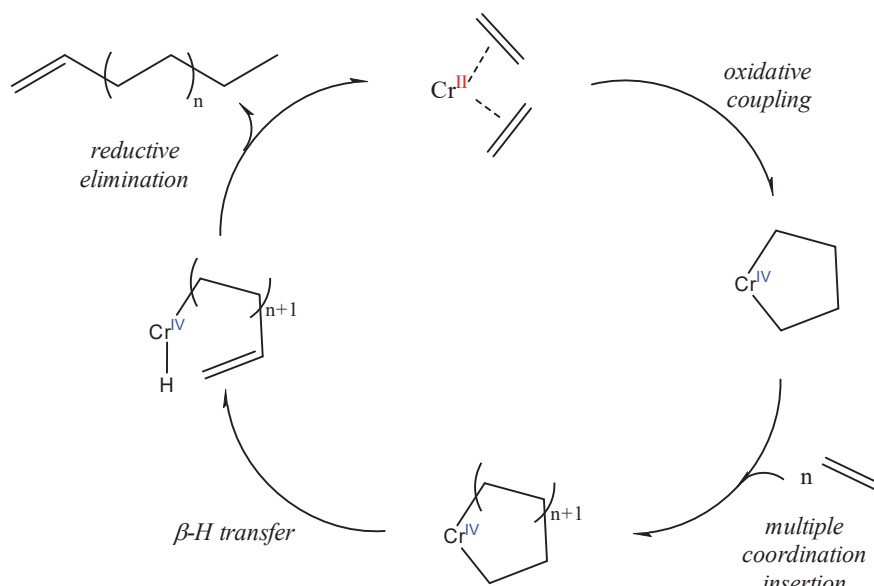
II.3. Multi-site polymerization catalysis

II.3.1. Polymerization mechanism

II.3.1.1. Phillips catalysis

Chromium-based Phillips catalysts were the first system to be industrialized 60 years ago for HDPE production.²² These catalysts are based on heterogeneous chromium oxide activated by a CO or C_2H_4 -assisted reduction from Cr^{VI} to Cr^{II} .²³ Investigation of the carrier (silica, alumina), cocatalyst (alkylaluminum) and promoters (titania, ammonium salts) led to activity enhancements and control of molar mass and its distribution.

Although 40-50 % of HDPE is produced by Phillips catalysis, the polymerization mechanism is still under debate and investigation. It has been proposed that ethylene polymerization occurs by an oxidative coupling followed by successive insertion of an ethylene unit in the loop before β -H transfer and reductive elimination (Scheme 2). Experimental and kinetics data are in favor of an expending metallacycle involving either $\text{Cr}^{\text{III}}/\text{Cr}^{\text{I}}$ or $\text{Cr}^{\text{IV}}/\text{Cr}^{\text{II}}$ but DFT calculations do not support this hypothesis.²⁴ Recent studies provide evidences for a Cr^{III} active species that polymerizes ethylene through a Cossee-Arlman mechanism detailed in the next section ("Ziegler-Natta catalysis", Scheme 3).²³ It was highlighted that the activation step corresponds to the heterolytic C-H bond cleavage of ethylene.²⁵ Details on Phillips catalysis will not be provided in this manuscripts but can be found in exhaustive reviews.^{26,27}



Scheme 2. "Growing loop" mechanism

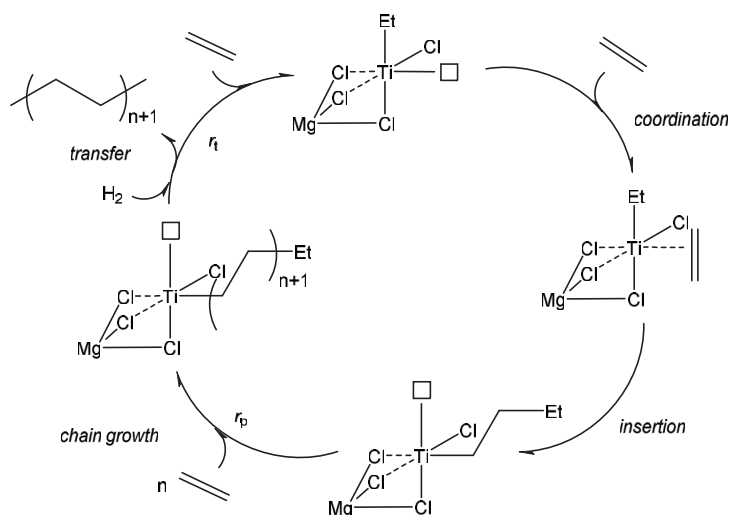
II.3.1.2. Ziegler-Natta catalysis

Heterogeneous Ziegler-Natta catalysis is based on a transition metal salt as precursor, namely TiCl_4 or VCl_4 supported on magnesium chloride or silica and combined with a cocatalyst. Among the common trialkylaluminums (AlR_3) used as co-catalysts, AlMe_3 (TMA), AlEt_3 (TEA), $\text{Al}(i\text{-Bu})_3$ (TIBA) are the most popular in this field although chlorinated species AlEt_2Cl is used to some extent. The activation process with AlR_3 involves several steps among which chlorine abstractions and metal alkylation but also reduction to Ti^{III} . Improvements of the activity and the control of molar masses distribution relied on implementation of the carrier and the use of Lewis base. The evolution of Ziegler-Natta systems will be explained in the next section Ziegler-Natta generations.

Catalytic polymerization relies on constructive interactions between orbitals of the metal center, the monomer and the growing chain. Indeed, favorable orbital interactions are crucial for the polymerization process. On the one hand, ethylene is a simple molecule made of two CH_2 moieties linked by one σ and one π bond.²⁸ On the other hand, titanium is a transition metal with vacant d-orbitals. The bonding process between the metal center and the monomer results from an electron-donation (and back-donation in the case of Ti^{III}). Ethylene donates π electrons from its HOMO to the LUMO of titanium. Simultaneously, the partially occupied d-orbital of Ti^{III} interacts with the vacant orbital of each carbon of the monomer. This interaction makes ethylene less stable and therefore, more active toward the carbon linked to the metal. Eventually, the ethylene molecule is inserted in the metal-carbon bond.

Ziegler-Natta catalytic polymerization follows a mechanism of successive coordination-insertions. One mechanism was described by Cossee and Arlman.²⁹ This process comprises several steps: initiation, propagation and transfer (Scheme 3). First, the alkylation of the

precatalyst by the alkylaluminum species affords a Ti-C bond. The resulting active species has an octahedral geometry with one vacant orbital, which is the right configuration to initiate the chain growth. After coordination of ethylene to the metal, a 4-center intermediate is formed between the Ti-C bond and the incoming ethylene. Ethylene is then inserted in the chain, which migrates to its previous position. The successive assembly of several ethylene molecules enables the growth of a hydrocarbon macromolecule. As soon as a transfer step occurs, a “dead chain” is obtained since it is no longer elongated. A transfer to the monomer, the alkylaluminum or hydrogen added in the reactor can occur depending on the type of catalyst and the polymerization conditions.

Scheme 3. Cossee-Arlman mechanism²⁹

Kinetics of multi-site Ziegler-Natta catalysis is important for the control of the molar masses distribution. Although miscellaneous polymerization species exist, each active site follows a simple kinetic scheme that can be divided into elementary steps (Scheme 4).³⁰ The length of a hydrocarbon chain is determined by the difference between the rate of the propagation (r_p) and transfer steps (r_t). When r_p is greater than r_t , long chains of polymer are afforded.³ However, the increase of the temperature induces higher transfer rate and therefore smaller polymer chains.

Activation	C	$\rightarrow C^*$	r_a, k_a
Initiation	$C^* + C_2H_4$	$\rightarrow C^*-P$	r_i, k_i
Propagation	$C^*-P_n + C_2H_4$	$\rightarrow C^*-P_{n+1}$	r_p, k_p
Transfer	C^*-P_x	$\rightarrow C^* + P_x$ or C^*-H	r_t, k_t
Deactivation	C^*-P_y	$\rightarrow C^\dagger + P_y$	r_d, k_d

Scheme 4. Kinetic steps for catalytic ethylene polymerization

C: Ti precursor, C^* : Ti- C_2H_4 or Ti-H (transfer to hydrogen),
P: hydrocarbon chain, C^\dagger : inactive species

II.3.2. Development and features of Ziegler-Natta catalysis

II.3.2.1. Ziegler-Natta generations

Ziegler-Natta catalysis is named after Karl Ziegler and Giulio Natta who dedicated their work to catalytic olefin polymerization systems. In 1949, Karl Ziegler was working on Aufbau ethylene oligomerization when he proved the ability of ethylene to be “inserted” in the Al-C bond of trialkylaluminum *via* an anionic process.³¹ Later on, he managed to produce linear polyethylene with the $\text{TiCl}_4/\text{AlR}_3$ homogeneous system under mild conditions. In 1954, Natta was the first to synthesize isotactic polypropylene by using $\text{TiCl}_3/\text{AlEt}_2\text{Cl}$.³² They were awarded the prestigious Nobel Prize in 1963 for their pioneer work on olefin polymerization.

Regarding polyethylene production, several generations of ZN catalysts were developed in order to reach better activity. Since the discovery of Ziegler in 1950s, Ziegler-Natta catalysis has greatly evolved.¹⁸ The first homogeneous systems had a rather low activity.³³ Consequently, the polymer needed to be purified from metallic residues, making the production process complex and expensive. In 1970s, scientists from Mitsui Chemical Inc. used MgCl_2 as a support for TiCl_4 . This heterogeneous system was a hundred times more active than the original homogeneous catalyst. Along with a high productivity, heterogeneous catalysis also enables a better control of the polymer morphology. New grades of polymer were developed such as HDPEs, LLDPEs and Ethylene Propylene Rubber.

Contrary to homogeneous system, active sites on a support are not equivalent. Multi-site catalysis involves several catalytic species affording various lengths of polymer chain.³⁴ The resulting broad molar mass distribution is an asset for the processing of the polymer. However, this multi-site nature of the active species makes ZN catalyst difficult to analyze and to understand. Nowadays, industrial production of polyolefin still largely relies on heterogeneous catalysts. Ziegler-Natta and chromium-based Phillips catalysis are the main systems used in the industry.

II.3.2.2. Reactivity with LAOs and hydrogen

Ziegler-Natta catalysts can react with LAOs higher than propylene. It was proven that the longer the alpha-olefin, the lower the reactivity of the catalyst. In fact, 1-hexene is fifty times less reactive than ethylene.³⁵ However, once used as comonomer with ethylene, the presence of LAO boosts the activity of the catalyst with an enhancement of the propagation rate r_p (Figure 1). This so-called “comonomer effect” decreases with the length of the olefin and its substitution. One explanation relies on transportation aspects. Since the monomers diffuse in the amorphous phase of the polymer, it would be easier for them to reach active sites in a LLDPE than HDPE.³⁰ However, depending on the type of alpha-olefin and its concentration, some heterogeneous ZN catalysts display a moderate to non-existing comonomer effect.³⁶ McDaniel and coworkers showed that it is not only a physical phenomenon but mainly a chemical effect that explains the improvement of activity upon addition of an alpha-olefin.³⁷ In fact, the coordination of a higher alpha-olefin electronically enriches the titanium center, thereby triggering the migratory insertion of ethylene in the Ti-alkyl bond.

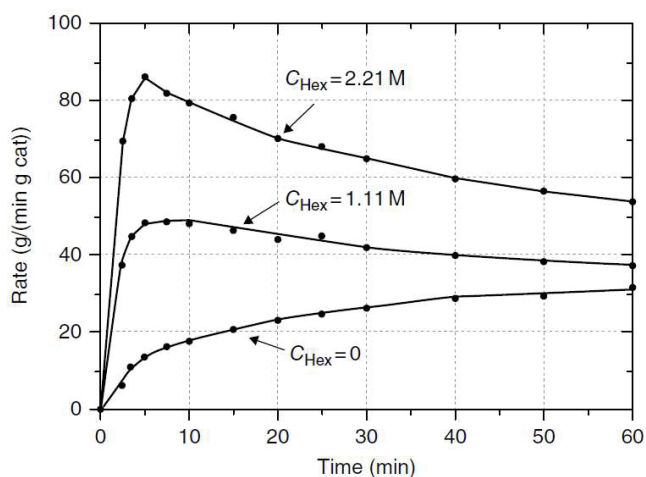


Figure 1. Positive “comonomer effect” of ethylene/1-hexene polymerization with a heterogeneous Ziegler-Natta catalyst Reprinted with permission from [35] Copyright (1999) Elsevier.

Hydrogen is widely used as transfer agent in ethylene and propylene polymerization. Therefore, the presence of hydrogen involves the reduction of polymer chain length, which features an alkylated chain end. For example, molar masses afforded by the heterogeneous system $TiCl_4/Mg(OEt)_2/SiO_2 + TEA$, decrease from 1.6×10^6 to 1.4×10^5 $g\ mol^{-1}$ when changing the gas feed from pure ethylene ($P_{C_2H_4} = 3.8$ bar) to a mixture of ethylene/hydrogen with $P_{C_2H_4} = 3.8$ bar and $P_{H_2} = 6.9$ bar.³⁵ Activity is also impaired by the presence of hydrogen for homo and copolymerization of ethylene with 1-hexene (Figure 2). In the first case, the presence of hydrogen decreases the activation rate by diminishing the number of active sites. For ethylene/1-hexene copolymerization, the only effect of hydrogen is the promotion of transfer reactions.

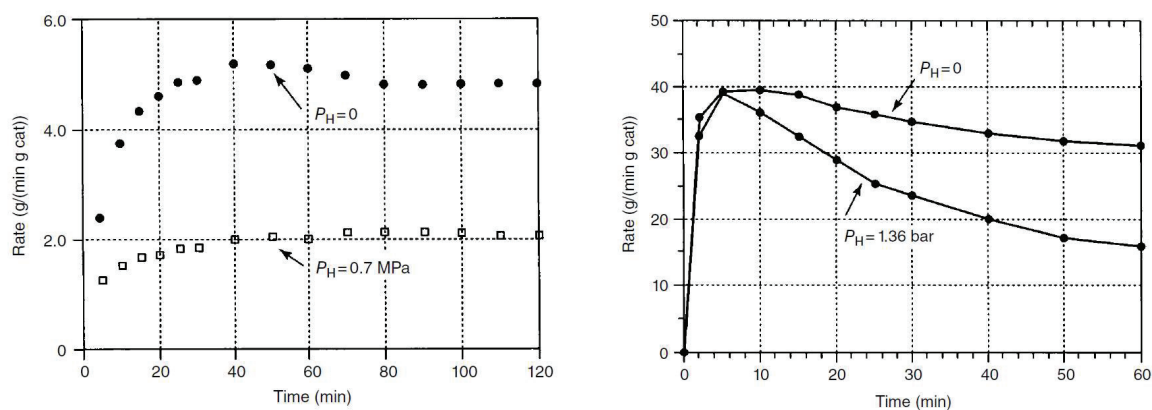


Figure 2. Impact of hydrogen on the activity of a heterogeneous Ziegler-Natta catalyst. The case of ethylene polymerization (left) and copolymerization with 1-hexene (right). Reprinted with permission from [35] Copyright (1999) Elsevier.

II.4. Single-site polymerization catalysis

II.4.1. Metallocenes

II.4.1.1. Precursors and activators

Single-site catalysis enabled significant breakthrough regarding polymerization mechanism and unprecedented polymer architecture. The first generation of single-site catalyst, for a precise control over polymerization of olefins, emerged with metallocenes. These complexes comprise two aromatic cycles, most often cyclopentadienyl ligands (Cp), bound to the metal center (Figure 3).

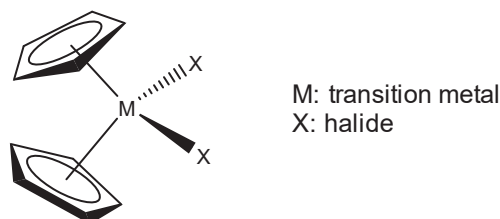


Figure 3. General structure of metallocenes

The first example of ethylene polymerization with a group 4 metallocene was reported by Natta in 1957.³³ Upon activation of Cp_2TiCl_2 with standard cocatalysts, Et_2AlCl or $AlEt_3$, the polymerization was very slow. In fact, such cocatalysts are not relevant for the activation of complexes bearing organic ligands. Consequently, further studies of metallocene systems were exclusively focused on mechanistic studies. Indeed, alkyl exchange and β -H transfer were studied with zirconocenes, being less prompt to be reduced than titanocenes. The discovery of the highly active Cp_2ZrCl_2/MAO system launched the diversification of metallocene precursors.³⁸

Discovered by chance in 1977, methylaluminoxane is a major activator for group 4 metallocene complexes. Indeed, Kaminsky and Sinn reported the polymerization of ethylene after that the system $\text{Cp}_2\text{TiMe}_2/\text{AlMe}_3$ was contaminated with water.^{38–40} A compound resulting from the hydrolysis of TMA with the general formula $(-\text{Al}(\text{Me})-\text{O}-)_n$ was identified as the most efficient cocatalyst for group 4 metal complexes in terms of catalytic activity.²⁰ Even though it is known that MAO is a mixture comprising MAO oligomers with free and MAO-bonded TMA, the precise structure of this cluster remains unclear.⁴¹ Assumptions of MAO structure evolved from a mixture of various oligomers to several structures depending on the ratio between MAO and bonded TMA (Figure 4).^{39,42–44} Addition of 2,2'-butylated hydroxytoluene (BHT) was efficient for trapping most of free-TMA. Recently, Zaccaria and coworkers determined the structure of BHT-modified MAO as a mixture of oligomers with the general formula $[\text{AlOMe}_{0.1}(\text{OAr})_{0.9}]_{62-96} + \text{AlMe}(\text{OAr})_2$.⁴⁵ Further developments of MAO derivatives gave rise to Modified MAO (MMAO). This compound results from the controlled hydrolysis of a mixture of TMA and TIBA enabling a better solubility in aliphatic solvents compared to MAO.⁴⁴

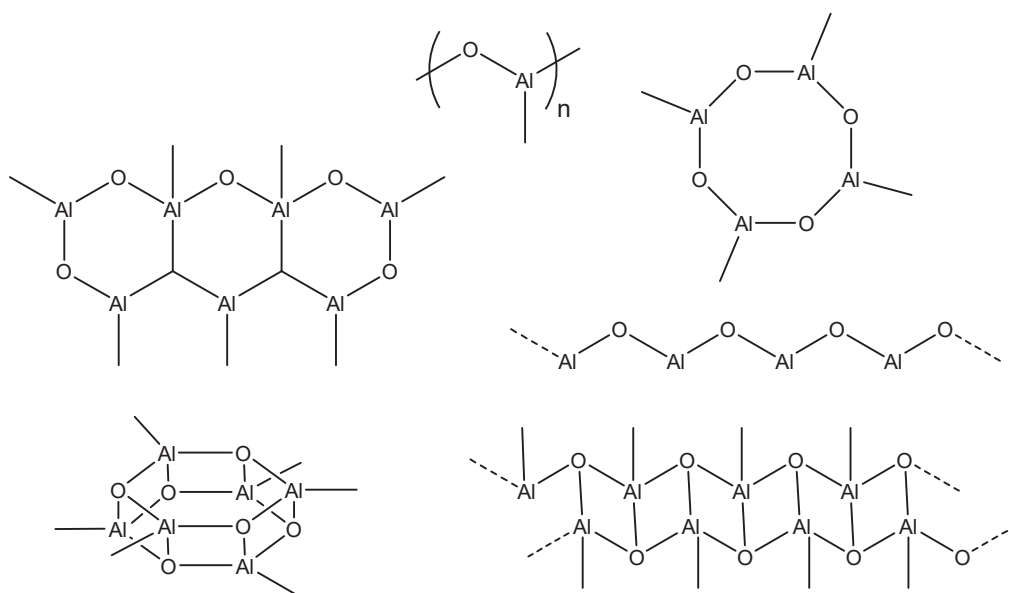
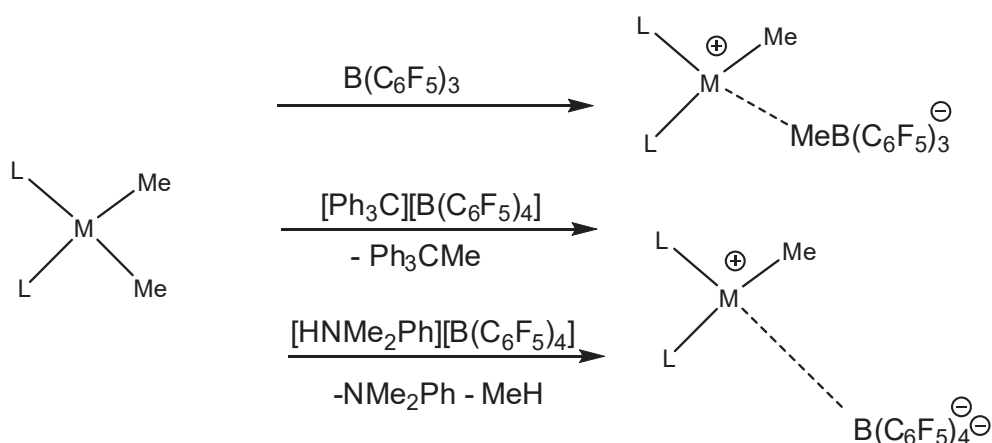


Figure 4. Examples of possible MAO structure

The exact role of MAO in the activation process of transition metal complexes is not fully understood. MAO being difficult to analyze, the characterization of the active species has not entirely succeeded yet. Besides, it is agreed that MAO achieves both metal methylation and cationization. For the latter, methyl/halide transmetallation and transfer of $[\text{AlMe}_2]^+$ from MAO to the precatalyst are proposed.^{44,46} For efficient ethylene transformation with MAO, the molar ratio Al/Zr usually amounts to one thousand. The requirement of a large excess of MAO has a direct financial impact for industrial companies. Consequently, research has been oriented toward stoichiometric activation.

In the range of equimolar and weakly coordinated cocatalysts, Lewis acid compounds are interesting alternatives. These cocatalyst systems involve an alkylaluminum compound and a bulk fluorinated Lewis acid or a frustrated Lewis acid compound combined with a non-coordinating anion for the complex alkylation and cationization of the precatalyst. Frustrated species are characterized by a large moiety on which the negative charge can be delocalized. Three cationizing agent families are mainly used for the formation of a frustrated ion pair with group 4 complexes (Scheme 5).⁴³ Tris(pentafluorophenyl)borane was the first to demonstrate its ability for group 4 complex activation.^{47,48} Later on, the increase of catalytic activity was observed with tetrakis pentafluorophenylborate salts, such as $[\text{Ph}_3\text{C}][\text{B}(\text{C}_6\text{F}_5)_4]$ and $[\text{HNMe}_2\text{Ph}][\text{B}(\text{C}_6\text{F}_5)_4]$.^{44,49,50}



Scheme 5. Main weakly coordinated Lewis agents for complex cationization

II.4.1.2. Mechanism and kinetics

Olefin polymerization mechanism with single site catalysts is similar to heterogeneous Ziegler-Natta (Scheme 3) at the expense of activation and transfer process.⁵¹ The activation process consists in subsequent alkylation and chlorine/alkyl abstraction to form a $\text{M}^{\text{IV}+}$ complex which has to be alkylated and cationic to be active towards LAOs. The propagation step, *i.e* chain growth on the metal center occurs *via* the Cossee Arlman mechanism (Scheme 3). Then, transfer reaction is commonly operated via β -H transfer in the case of single site catalysis. Therefore, all polymer chains display an unsaturated chain end and the resulting cationic $\text{M}^{\text{IV}+}$ -H complex can initiate a new chain growth. Similarly to heterogeneous ZN polymerization, co-catalyst and hydrogen can be involved in transfer reactions and the polymerization occurs until the deactivation of active species.

In the case of titanocenes, cationic Ti^{IV} species are commonly assumed as active species for ethylene polymerization. Nevertheless, ancient and recent works supported that Ti^{III} species are also prone to successively coordinates and insert linear alpha olefins. During the early-age of metallocenes, Natta reported that the $\text{Cp}_2\text{Ti}^{\text{III}}\text{Et}/\text{AlCl}_2\text{Et}$ was isolated when mixing Cp_2TiCl_2 and AlEt_3 , which produces polyethylene with a limited activity.³³ Based on EPR analysis, Maksimov ascribed a Ti^{III} as active species toward ethylene polymerization for the

heterogeneous system $\text{Ti}(\text{CH}_2\text{C}_6\text{H}_5)_4$ supported on silica.⁵² Very recently, Barr *et al.* exemplified this assumption with a phosphinimide post-metallocene $(\text{Ind})(t\text{Bu}_3\text{P}=\text{N})\text{TiCl}_2/\text{AlEt}_3$ involving a EPR-identified Ti^{III} species for ethylene polymerization.⁵³ Despite characterization limitations of paramagnetic Ti^{III} species, it is agreed that olefin polymerization is possible with these reduced titanium complexes.

Contrary to multi-site catalyst, single-site catalysis relies on a system based on well-defined active species that exhibit the same reactivity towards ethylene. Indeed, homogeneous metallocenes are considered as single sites since all active sites display the same structure and thus the same kinetic parameters. Consequently, polyethylene chains display the same length and their size is imposed by the ratio between transfer and propagation rate, which are unique for each active site. This homogeneity in macromolecule sizes explains the narrow molar mass distribution characterized by a dispersity of 2. This value arises from the Schulz-Flory statistics considering that all active sites follow fixed propagation and transfer rates.⁵⁴ Therefore single-site catalysis enables to tailor polyolefins by selecting the appropriate complex structure and process operations.⁵⁵

II.4.1.3. Reactivity with LAOs and hydrogen

Metallocene catalysis has been widely applied to polypropylene production given its ability to tailor the tacticity of PP by tuning the symmetry of the complex (Figure 5). C_n , C_2 and C_s symmetry of metallocene and ansa-metallocene gives access to atactic, isotactic and syndiotactic polypropylenes respectively (Figure 5).^{20,56} This catalyst/polymer relationship is an interesting illustration of the control of stereoselectivity through the choice of steric hindrance around the metal center.

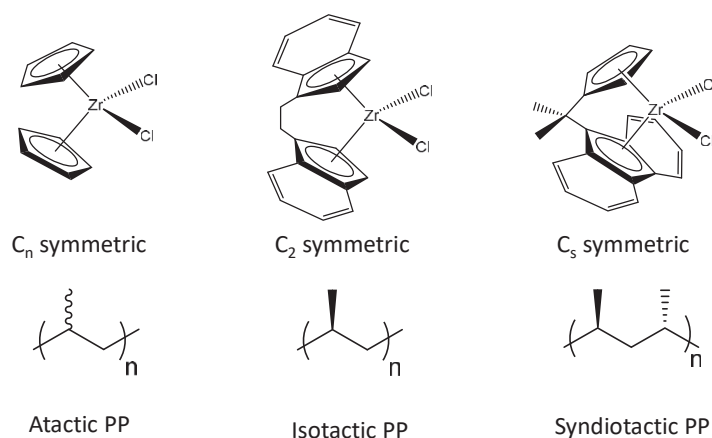


Figure 5. Metallocene geometries and resulting polypropylene tacticity

In the case of copolymerization of ethylene with LAOs, the comonomer effect depends on the type of metallocene and the operating conditions.⁵⁴ For instance, Et(Ind)₂ZrCl₂/MAO displays a higher activity with the increase of 1-hexene concentration in the reaction medium.⁵⁷ Conversely, 1-octene copolymerization with the same system leads to a lower activity than the corresponding ethylene homopolymerization.⁵⁸ Even though these experiments differ in terms of polymerization conditions, it is usually observed that the activity decreases as the comonomer concentration increases. In fact, the presence of comonomer affects the propagation rate but has no impact on the deactivation process. As a result, copolymers display a lower molar mass as their comonomer content increases. Noteworthy, as all active sites react in the same fashion towards ethylene and LAOs, they produce copolymers with the same comonomer composition. It is also possible to control the amount of comonomer content in the polymer with single site catalysis. Using Cp₂ZrCl₂/MAO, Saadat showed that the 1-hexene content in the polymer is proportional to the concentration in the reaction medium (Figure 6).⁵⁹ This relationship is generalized by the Mayo-Lewis equation that can be applied to all single site systems (Equation 2).⁶⁰

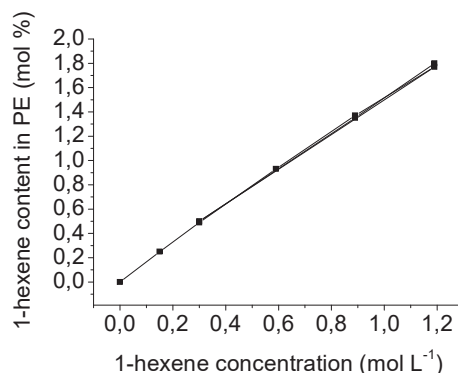


Figure 6. Linear relationship between 1-hexene concentration in the reaction medium and in the copolymer.

$$F_H = \frac{r_H f_H^2 + f_H(1-f_H)}{r_H f_H^2 + 2f_H(1-f_H) + r_E(1-f_H)^2}$$

F_H : molar fraction of 1-hexene in the polymer

f_H : molar fraction of 1-hexene in the reaction media

r_H and r_E : reactivity ratio of 1-hexene and ethylene respectively

Equation 2. Mayo-Lewis equation for copolymerization ethylene/1-hexene

As for heterogeneous Ziegler-Natta catalysis, hydrogen is a transfer agent that promotes dead chain formation. For Cp₂ZrCl₂/MAO, both ethylene propagation and deactivation rates are lowered at higher hydrogen concentration. A sharp decrease of molar masses from 168x10³ to 64x10³ g mol⁻¹ has been observed upon introduction of hydrogen with a concentration of 0.146 mmol L⁻¹.⁵⁹ Therefore, metallocenes are highly sensitive to the presence of hydrogen, which has a severe impact on the chain length of the polymer.

II.4.2. Post-metallocenes

II.4.2.1. Constrained Geometry Catalyst

The CGC catalyst developed by DOW and Exxon, is efficient to copolymerize ethylene and alpha-olefins.⁶¹ CGC catalysts are derivatives of silane-bridged *ansa*-monocyclopentadienyl-amido complexes (Figure 7). These half-sandwich complexes are less hindered than metallocenes owing to a small bite angle Cp-M-N of 107.6°.⁶² This open geometry promotes both the activity and the coordination of LAOs to the metal center. Therefore, CGC catalysts afford copolymers with a higher LAO content than most of metallocenes. R' and R groups (Figure 7) are crucial parameters to optimize the efficiency of LAO incorporation. As an example, activity and 1-octene incorporation are promoted in the case of titanium-based Cp* derivatives with R = *t*Bu (43 kg_{polymer} mmol_{Ti}⁻¹ h⁻¹, density_{P(E-co-O)} = 0.88) instead of Ph (7 kg_{polymer} mmol_{Ti}⁻¹ h⁻¹, density_{P(E-co-O)} = 0.93).⁶¹ Therefore, CGC catalysts are the first systems capable to produce copolymers with both high molar masses (> 2x10⁵ g mol⁻¹, Đ = 2.1) and high LAO content even at elevated temperature (160 °C).^{63,64} These appealing features were a driving force for their industrialization as first post-metallocene system producing high molar masses LLDPE.⁶⁵

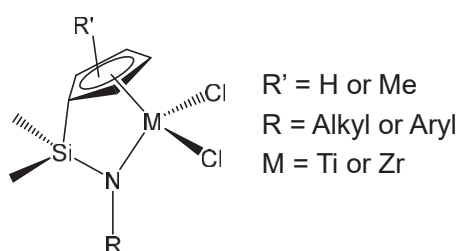


Figure 7. General structure of CGC catalysts

II.4.2.2. Aryl-based systems

Development of Aryl-based post-metallocenes has been stimulated by the endless possibilities of ligand design and thus polymer properties. For the sake of concision, this section will focus on selected examples of industrialized post-metallocenes for polyethylene and related copolymers with LAOs (Figure 8).⁶⁶ Numerous post-metallocenes are listed in dedicated reviews.^{21,67,68} Most post-metallocene systems are based on Hafnium and Zirconium for LAO homopolymerization and copolymerization with ethylene. It is the case of the imino-amido catalysts developed by Dow for the production of high molar masses poly(ethylene-co-1-octene) ($M_w = 10^6$ g mol⁻¹, Đ = 2.4).^{69,70} The same company utilizes a pyridyl-amido catalyst to produce Propylene-Ethylene Rubber in the VERSIFY process.⁷¹ This system can also afford versatile polymer grades from LLDPE to poly-1-octene.⁷² Univation commercializes the Unipol process PRODIGY that relies on a diamido complex associated with a metallocene for the production of bimodal HDPE.⁷³ Eventually, Fujita *et al.* investigated bis(phenoxy-imine) systems for olefin polymerization that were firstly patented by Mitsui Chemicals.⁷⁴ The potential of the bis(phenoxy-imine) systems was a milestone for the

development of new polyolefins grades. As far as we are concerned, such catalysts are not yet employed at the industrial scale besides several patent pending.⁷⁵ These systems being in the scope of this PhD project, they will be detailed in the next section.

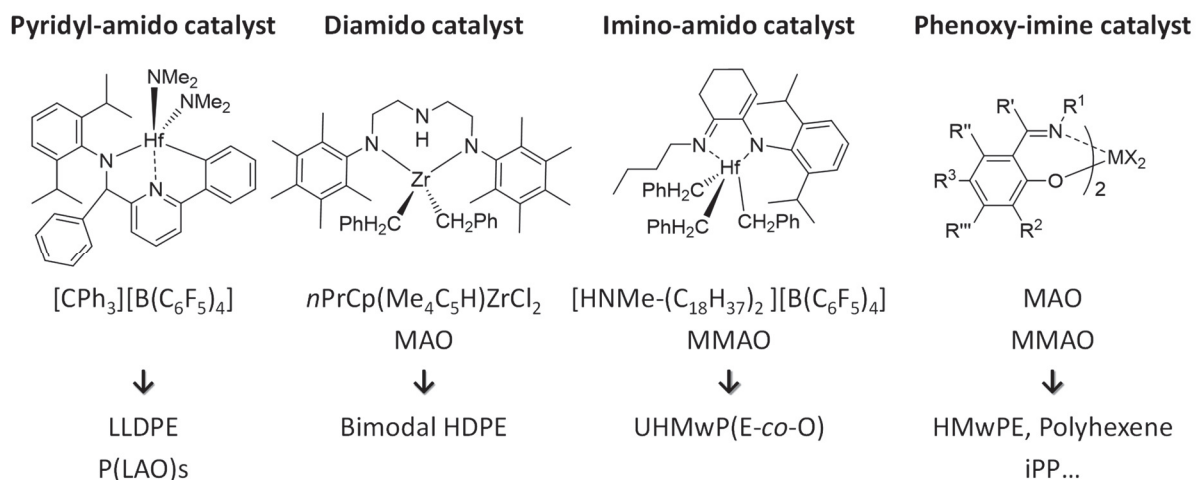


Figure 8. Industrialized post-metallocene catalysts and related polymer grades

II.4.3. Phenoxy-imine (FI) catalyst

II.4.3.1. Bis(phenoxy-imine) complexes

Phenoxy-imine (FI) catalysts belong to the family of post-metallocenes polymerization species. Scientists at Mitsui Chemicals Inc. have been studying these “phenoxy-imine” complexes since the 1990s.⁷⁶ The general formula of FI complexes is $(\text{FI})_2\text{MX}_2$ (Figure 9), where:

- FI is a non-symmetric, bidentate phenoxy-imine $[\text{O}^-, \text{N}]$ ligand;
- M is a group 4 transition metal, titanium or zirconium, with an octahedral geometry;
- X is an alkoxide, an amide, an alkyl or most often a halide (chloride or bromide).

Concerning the ligand, several criteria have been pointed out with respect to steric and electronic properties:

- a) Non-symmetrical ligand;
- b) Electronic flexibility with moderate electron-donating nature;
- c) Coordination in distorted octahedral fashion;
- d) Crucial position and nature of the ring substituents R^x .

Figure 9. General structure of Bis(FI) complexes

The geometry of the complex and its ligands provide peculiar hindered environment and electronic flexibility, which are essential for efficient olefin polymerization. It is noteworthy that most of FI precatalysts have a configuration such as that each oxygen atom is on the axial position while the two nitrogen atoms are *cis* in the equatorial plan (Figure 10). During the polymerization, the coordinated ethylene and the alkyl chain are located on the X positions. Consequently, R¹ and R² groups, being close to the metal center, have an impact on the polymerization process. It is often observed that a bulky R² substituent and a small R¹ group ensure high polymerization activity.⁷⁶⁻⁷⁸ In fact, the hindered R² limits the β -H transfer reaction and acts as a shield that protects the metal center from the counter-anion (Scheme 5).

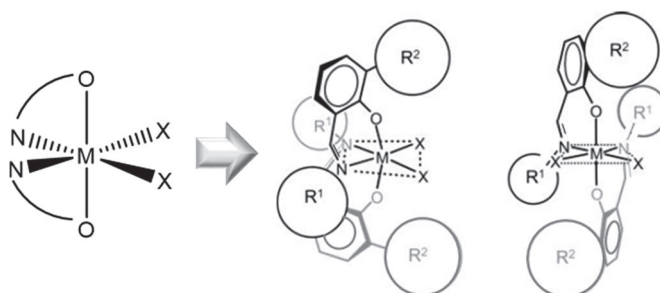


Figure 10. Usual configuration of Bis(FI) complexes

After the report of the first synthesis of bis(phenoxy-imine) complex in 1995 by Floriani *et al.*, the potential of these derivatives for olefin polymerization has been investigated by Fujita and coworkers.⁷⁹ In 1998, Mitsui Chemicals Inc. patented more than 300 bis(phenoxy-imine)-based complexes for olefin polymerization and copolymerization with LAOs and conjugated dienes in 1997.⁸⁰ Most of these bis(phenoxy-imine) ligands are associated with zirconium, hafnium and titanium. Similarly to metallocenes, zirconium is more active towards olefin than titanium owing to its larger ionic radius. This difference is emphasized in olefin polymerization with the bis(phenoxy-imine) complexes **1** and **2** (Figure 11). Zirconium complex **1** exhibits a high activity of 500-600 kg_{PE} mmol_{Zr}⁻¹ h⁻¹ between 25 °C and 40 °C but is highly deactivated at higher temperature with 100 kg_{PE} mmol_{Zr}⁻¹ h⁻¹ at 75 °C.^{81,82} In the same conditions, *viz.* 1.25 mmol of MAO with Al/Zr = 1 563-62 500 under 1 bar of ethylene for 5 min, a poor but temperature-stable activity of 4 kg_{PE} g_{Ti}⁻¹ h⁻¹ is observed for the titanium counterpart **2**. The deactivation of the Zr-based catalyst has been ascribed to complex degradation. The temperature robustness of zirconium complexes was achieved by the addition of a methoxy group on R³ position and cyclohexyl group in lieu of phenyl at R¹ position (Figure 9). The presence of this electron-donating group strikingly enhanced the activity from 63 to 1 374 kg_{PE} mmol_{Zr}⁻¹ h⁻¹ at 90 °C and under 9 bar of ethylene.⁷⁷ Therefore, temperature-sensitivity can be tuned by electronic effect of R³ group.

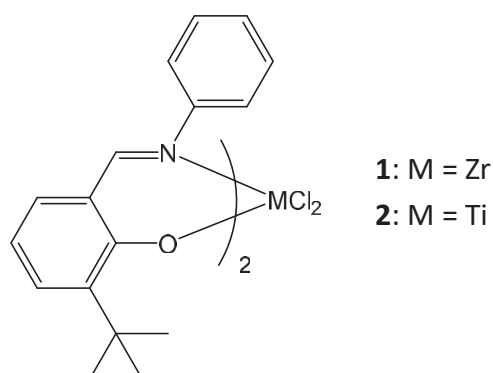


Figure 11. Bis(phenoxy-imine) complexes exhibiting temperature-dependence (complex **1**) and independence (complex **2**) of their activity

Alteration of the aforementioned titanium complex **2** also led to an outstanding change of its catalytic behavior. Fluorinated substituents on R^1 group (Figure 12) promotes a pseudo-living polymerization. Upon activation with 1 250 equivalents of MAO, the Bis[N-(3-*tert*-butylsalicylidene)pentafluoroanilinato] titanium dichloride (complex **3**) afforded a high molar mass polyethylene ($4.1 \times 10^5 \text{ g mol}^{-1}$) with an impressively narrow molar mass distribution ($\mathcal{D} = 1.13$).⁸¹ Such polymer was produced within 1 minute at 25 °C and 1 bar of ethylene with a tremendous activity of $34 \times 10^3 \text{ kg}_{\text{PE}} \text{ mmol}_{\text{Ti}}^{-1} \text{ h}^{-1}$. At 25 °C and 50 °C, M_n increases linearly overtime while a dispersity of 1.1 remains constant, which are indicators of ethylene polymerization in a living fashion. This exceptional behavior is most probably due to a β -H agostic interaction of the polymer chain with the *ortho*-fluorine instead of titanium, preventing the transfer reaction.⁸³

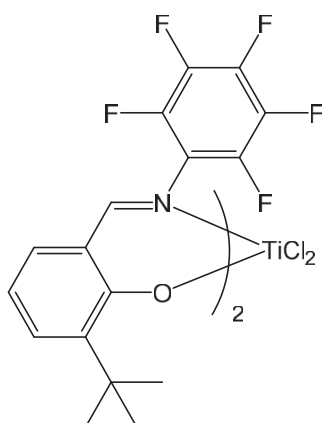


Figure 12. Bis(phenoxy-imine) complex (complex **3**) for pseudo-living polymerization

Bis(phenoxy-imine) complexes activated by MAO exhibit a limited reactivity towards LAOs as monomers and comonomer with ethylene. On the one hand, although the titanium complex **2** is very active towards ethylene, it exhibits limited activity for the homopolymerization of 1-hexene, 1-octene, 1-decene and 1-methyl-1-pentene.⁷⁷ However, switching the activator from MAO to *i*-Bu₃Al/Ph₃CB(C₆F₅)₄ induced the formation of high molar mass (10^5 g mol^{-1}) poly(LAOs) with ultra-random tacticity (more than 50 % atactic).⁸⁴ Surprisingly, the activity of the system increases with higher linear alpha olefins. On the other hand, the same complex activated by MAO afforded poly(ethylene-*co*-1-hexene) with a high molar mass but only

0.4 mol % of 1-hexene (Table 3, entry 2).⁸⁵ Contrary to the metallocene species, this post-metallocene complex copolymerized an insignificant amount of LAO (2 mg) compared to the quantity of 1-hexene introduced in the reaction media (6.73 g). However, in the case of the pseudo-living fluorinated complexes derived from **3**, a higher amount of 1-hexene incorporation is obtained at the expense of the activity.⁸⁶ For these systems, the steric hindrance at R² position is a key parameter for LAOs incorporation.⁸⁷ This is highlighted by the increase of 1-hexene content by a factor of 7 when the ligand bears no R² substituent (Table 3, entries 3 and 4). The same trend was observed in the case of 1-octene and 1-decene in addition to a decrease of incorporation ratio for longer LAOs. Thus, steric hindrance at R² position hampers the approach of LAO and its further incorporation in the polymer chain.

Table 3. Copolymerization ethylene/1-hexene with Bis(FI) complexes

Entry	Ti complex	Activity (kg _{P(E-co-H)} mol _{Ti} ⁻¹ h ⁻¹)	M _n (g mol ⁻¹)	Đ	1-hexene content (mol %)
1	Cp ₂ TiCl ₂	2 030	143 000	-	5.1
2	2	2 110	220 000	-	0.4
3	3^a	4 008	55 000	1.19	3.2
4	3^{a,b}	5 064	54 000	1.07	22.6

Conditions: 1 μmol complex, 1.25 mmol MAO, 250mL toluene, 25 °C, 1 bar ethylene, 10 mL 1-hexene, 5 min

^a 2.5 μmol complex, 1.25 mmol MAO, 200 mL toluene, 25 °C, 1 bar ethylene, 50 mL 1-hexene, 5 min

^b R² = H

Applying the so-called “ligand-oriented catalyst design” concept, Fujita and co-workers opened the access to a wide range of diverse new polymers (Figure 13). The most remarkable examples of these new polymers are vinyl-terminated low molar mass polyethylenes and polymerization of LAOs longer than 1-hexene.⁸⁸ Depending on the hindrance imparted by the R¹ group, zirconium complexes derivatives from **1** produce either UHMwPE or low molar masses polyethylenes.^{89,90} In the last case, polyethylene comprises short unsaturated chain-ends that can be further functionalized. High molar masses poly-1-hexene, poly-1-octene and poly-1-decene are used as performant lubricant base owing to the high viscosity of these amorphous polymers.⁸⁴ It was the first example of highly active catalyst for polymerization of LAOs higher than propylene since Ziegler-Natta or metallocene systems are poorly reactive toward such olefins. The versatility of the pseudo-living fluorinated catalysts allows the formation of very narrow distributions of high molar masses polyethylene as well as random and block copolymers of ethylene and linear alpha olefins.^{86,91}

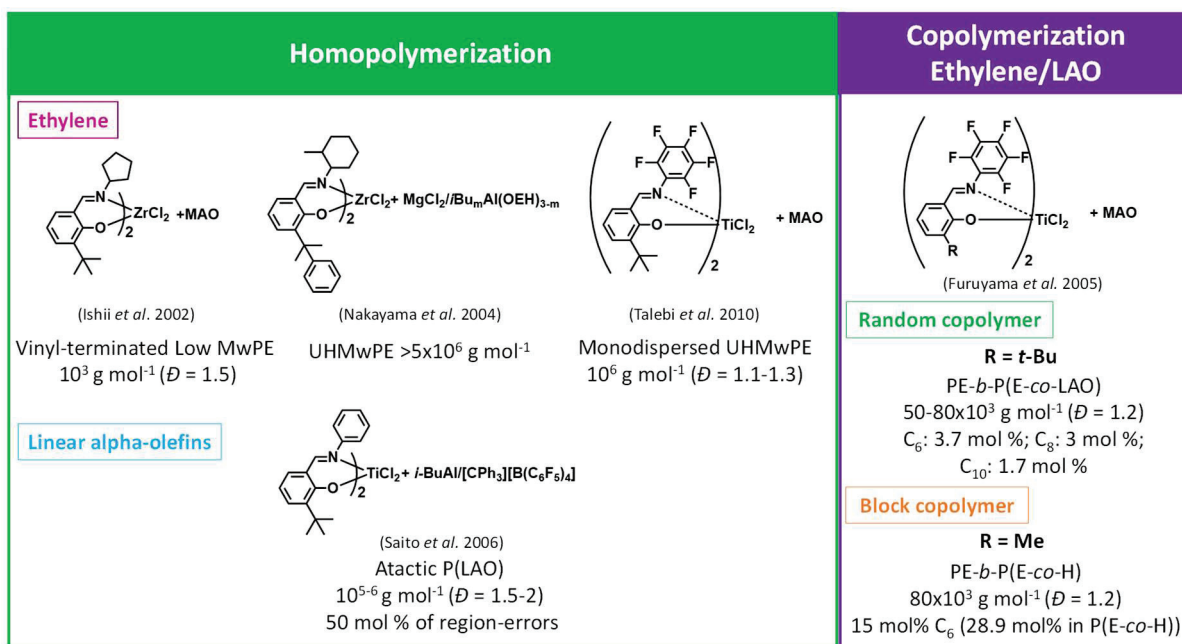


Figure 13. Examples of bis(phenoxy-imine) post-metallocenes and related polyolefin grades

II.4.3.2. Mono(phenoxy-imine) complexes

II.4.3.2.1. Tridentate L₂X FI catalysts

This section will mainly focus on single FI catalysts bearing a tridentate phenoxy-imine ligand of [O⁻,N,X]-type. In addition to the single phenoxy-imine-ether reported for ethylene trimerization (see section Single FI catalyst – a promising trimerization species), miscellaneous tridentate complexes for ethylene polymerization can be found in the review of Peng *et al.*⁹²

Among FI catalysts, single tridentate ([O⁻,N,O]-FI)TiCl₃ complexes polymerize ethylene and alpha-olefins. However, very few examples of such complexes were found in the literature. Tang *et al.* reported that complexes **4-7** (Figure 14) combined with MMAO polymerized ethylene with a moderate activity. A combination of steric hindrance and electronic effect explains the variations of activity, polyethylene molar mass and dispersity (Table 4, Figure 14).⁹³

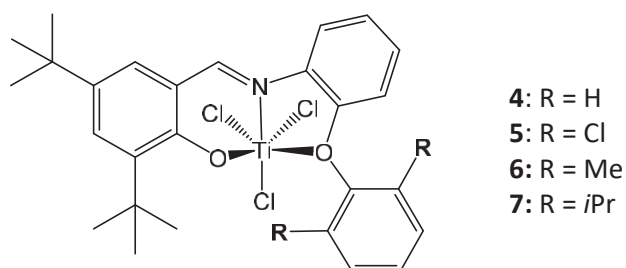
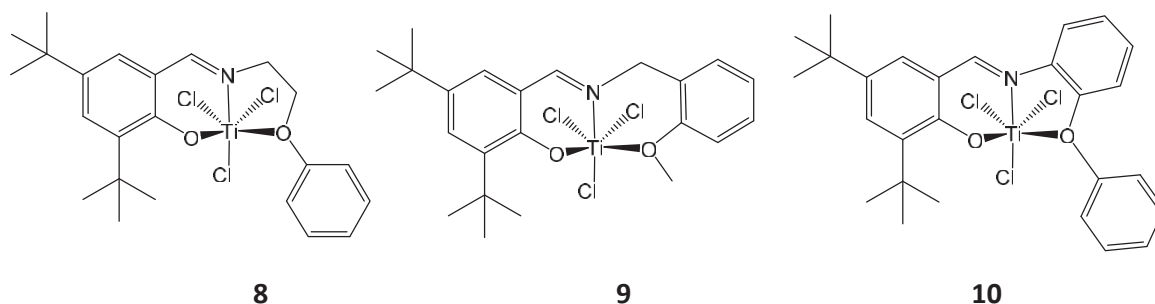
Figure 14. Structure of complexes **4-7**

Table 4. Catalytic performances and polymer properties of complexes **4-7** activated with MMAO

Complex	Activity (kgPE mol _{Ti} ⁻¹ h ⁻¹)	M _w (g mol ⁻¹)	Đ
4	20	25 000	4.07
5	23	39 600	3.84
6	2	48 900	3.31
7	3	115 000	14.9

Conditions: 3.5 μmol of complex, Al_{MMAO}/Ti = 500, 1 bar, 50 mL toluene, 50 °C, 15 min

Similar complex derivatives demonstrated their ability for the production of HDPE as well as poly(ethylene-co-1-hexene). Casagrande and co-workers designed complexes **8-10** bearing a phenoxy-imine ligand with pendant donor comprising a phenoxy group (Figure 15).⁹⁴ The peculiarity of these systems is the broad dispersity (24-40) of the HDPEs afforded, implying multi-site catalysis. Furthermore, high density poly(ethylene-co-1-hexene) was obtained with a rather low 1-hexene content (Table 5).

Figure 15. Structure of complexes **8-10**Table 5. Activity and polymer properties of the copolymerization ethylene/1-hexene with complex **8-10** activated with MAO

Complex	Activity (kgPE mol _{Ti} ⁻¹ h ⁻¹)	T _m (°C)	1-hexene incorporation (mol %)
8	220	127	1.0
9	160	126	1.3
10	500	124	1.4

Conditions: 10 μmol of complex, Al_{MAO}/Ti = 500, [1-hexene] = 0.4 mol L⁻¹, 5 bar, 120 mL toluene, 60 °C, 15 min

Most of the systems that are efficient for copolymerizing LAOs with ethylene are based on tridentate [O,N,P] phenoxy-imine complexes (Figure 16). Hu *et al.* described two main [O,N,P] derivatives exhibiting a high performance in ethylene polymerization even at a low MMAO/Ti ratio of 50. Complexes **11** and **12** are relevant for the copolymerization of ethylene with 1-hexene (Table 6) and norbornene.⁹⁵ It is worth noting that complex **13** was obtained

following the same procedure as complex **11** but using NaH instead of KH as deprotonating agent. The resulting bis-ligated ($[O^-,N,P]_2$ -FI) Ti complex was found to be inactive towards ethylene.

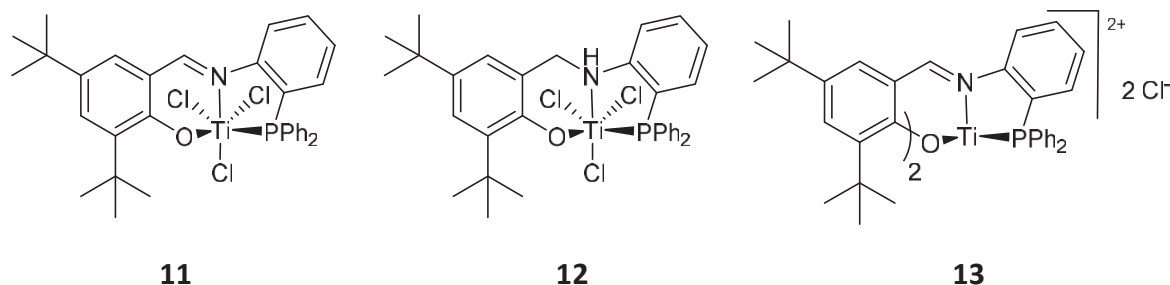


Figure 16. Example of tridentate $[O^-,N,P]$ -FI complexes

Table 6. Copolymerization ethylene/1-hexene with $[O^-,N,P]$ -FI complexes (Figure 16)

Complex	Activity ($\text{kg}_{\text{PE}} \text{ mol}_{\text{Ti}}^{-1} \text{ h}^{-1}$)	1-hexene incorporation (mol %) ^a	M_w (g mol^{-1}) ^b	\bar{D}
11	1 770	21	$4.8 \cdot 10^4$	1.26
12	580	15.8	$7 \cdot 10^4$	2.19

Conditions: 9.24 μmol of complex, $\text{Al}_{\text{MMAO-4}}/\text{Ti} = 250$, $[\text{1-hexene}] = 2.1 \text{ mol L}^{-1}$, 1 bar, 15 mL toluene, 50 °C, 15 min

^a determined by ^1H NMR

^b determined by GPC versus polystyrene standard

11.4.3.2.2. Tridentate LX_2 FI complexes

This section highlights the ability of tridentate $[(O^-,N,X^-)]\text{-FI}\text{TiCl}_2$ complexes for ethylene polymerization. A special attention is drawn on the few dianionic tridentate $[O^-,N,O^-]$ -FI complexes that resemble the trimerization SFI complex.

Owiny *et al.* synthesized both complex $(\text{FI})\text{TiCl}_2(\text{THF})$ (Figure 17) and the dimer $[(\text{FI})\text{TiCl}_2]_2$ without testing their reactivity toward ethylene.⁹⁶

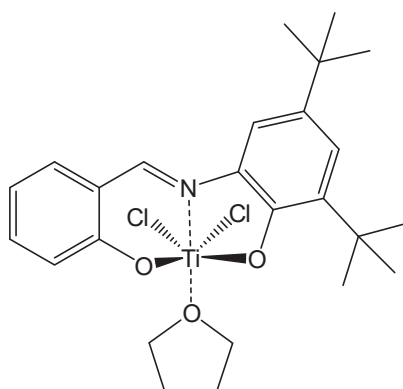
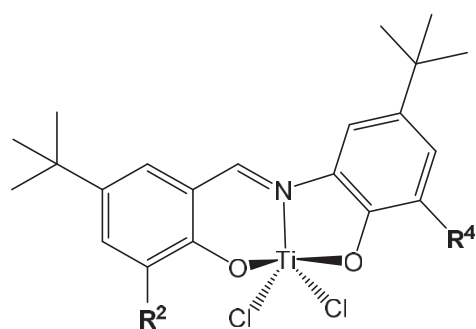


Figure 17. tridentate $[O^-,N,O^-]$ -FI complex **14**

Xu and coworkers synthesized a series of dianionic [O⁻,N,O⁻] complexes **15-19** on the basis of Owin's structure (Figure 18). Once activated with MAO, these complexes exhibit a moderate activity for 1-hexene and ethylene homopolymerization (Table 7).⁹⁷ Nevertheless, it was observed that complexes **18-20**, with bulky groups on ortho-position for both phenoxy rings exhibit an activity that is ten times higher than that of **15-17**. Consequently, steric hindrance close to phenoxy groups improves both catalytic activity and propagation reactions. Indeed, the hindered environment around the metal center protects the metal from the cocatalyst coordination and limits β -H transfer from the hydrocarbon chain to titanium.



15: R² = R⁴ = tBu

16: R² = Ad, R⁴ = tBu

17: R² = CMe₂Ph, R⁴ = tBu

18: R² = R⁴ = CMe₂Ph

19: R² = Si(Me₂)tBu R⁴ = CMe₂Ph

20: R² = Si(Me₂)tBu R⁴ = CMe₂Ph and THF coordinated to Ti

Figure 18. Dianionic [O⁻,N,O⁻]-FI complexes **15-20**

Table 7. Comparison of complexes **15-20** regarding catalytic performances for ethylene and 1-hexene homopolymerizations

Complex	Activity ^a (kg _{Polyethylene} mol _{Ti} ⁻¹ h ⁻¹)	M _n polyethylene (g mol ⁻¹) (dispersity)	Activity ^b (kg _{poly(1-hexene)} mol _{Ti} ⁻¹ h ⁻¹)	M _n poly(1-hexene) (g mol ⁻¹) (dispersity)
15	10	-	11.3	496 (1.16)
16	14	-	21.5	510 (1.18)
17	20	-	21.5	541 (1.17)
18	140	219 000 (2.0)	30.8	533 (1.21)
19	164	220 000 (1.8)	38.9	610 (1.15)
20	156	190 000 (2.1)	37.0	565 (1.22)

Conditions: 10 μ mol of complex, Al_{MAO}/Ti = 1 000, 20 °C

^a 5 bar ethylene, 100 mL toluene, 30 minutes

^b total volume 10 mL, toluene, 5 g (6 mmol) 1-hexene, 24 h

Other studies aimed at combining both Cp and tridentate FI ligands on the same metal center. Chen *et al.* managed to synthesize CpZr([O⁻,N,O⁻]-FI)Cl₂ (**21**) with a wide Cl-Zr-Cl angle of 151.71° (Figure 19).⁹⁸ Interestingly, after four hours reflux in THF, complex CpZr([O⁻,N,O⁻]-FI)Cl(THF) (**22**) was afforded. This observation was explained by a thermocyclization between Zr-Cl and O-Me bonds followed by elimination of chloromethane. Then activated with MAO, both complexes display a higher activity with the increase of

temperature, which has also been observed for some metallocene catalysts (Table 8).⁹⁹

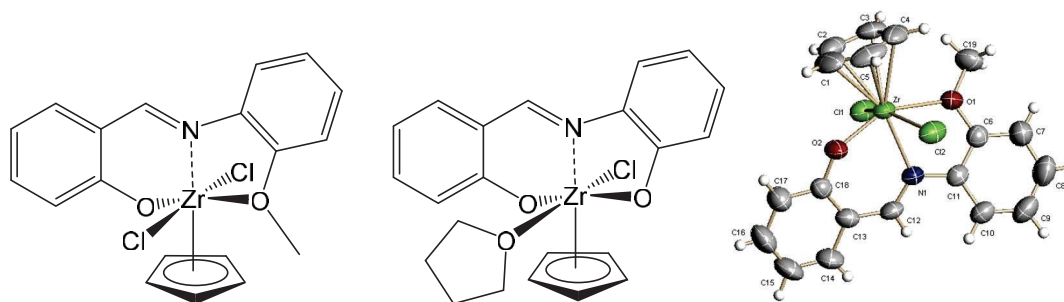


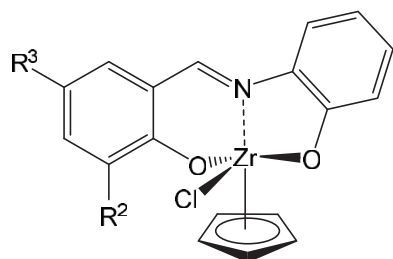
Figure 19. CpZr([O⁻,N,O⁻]-FI)Cl₂ (**21**) and CpZr([O⁻,N,O⁻]-FI)Cl(THF) (**22**) complexes and X-ray structure. Reprinted with permission from [99] Copyright 2005 Elsevier

Table 8. Thermal dependence of catalytic activity for Cp-(FI) complexes

Complex	Temperature (°C)	Activity (kg _{PE} mol _{Zr} ⁻¹ h ⁻¹)
21	30	59
21	50	231
21	80	769
22	30	10
22	50	35
22	80	221

Conditions: 5 μmol of complex, Al_{MAO}/Zr = 2 000, 1 bar, 50 mL toluene, 30 min

The development over these CpZr([O⁻,N,O⁻]-FI)Cl complexes was implemented by Zhang *et al.*¹⁰⁰ Among them, two half-metallocenes bearing a tridentate aryloxy-FI ligand were tested for ethylene polymerization (Figure 20). After 1 hour at 70 °C and under 1 bar of ethylene and with 1 500 equivalents of MAO, a higher activity was obtained with complex **23** (50 kg_{PE} mol_{Zr}⁻¹ h⁻¹) than complex **24**, which bears no substituent (32 kg_{PE} mol_{Zr}⁻¹ h⁻¹). This difference can be ascribed to the bulkiness of the *tert*-butyl group hampering the contact between the cocatalyst and the metal center.



23: R² = *t*Bu R³ = Me

24: R² = R³ = H

Figure 20. CpZr([O⁻,N,O⁻]-FI)Cl complex structures

Other complexes bearing a phenoxy-imine group bound to a phenyl-*ortho*-phenoxy group were described in a patent.¹⁰¹ Researchers at Mitsui Chemicals Inc. investigated the steric and electronic effect of R², R⁴ and R⁵ groups of twenty complexes (Figure 21). As already observed by Lu *et al.*, catalytic performances of complexes **25-28** with MAO are greatly improved by the bulkiness of the R^x groups (Table 9)⁹⁷ Moreover, catalytic tests with MAO showed that the increase of the temperature from 25 °C to 75 °C promoted the deactivation of the catalysts. Furthermore, activation with [CPh₃][B(C₆F₅)₄]/TIBA increased activities by a factor of ten compared to MAO activation, but these catalysts remained thermosensitive.

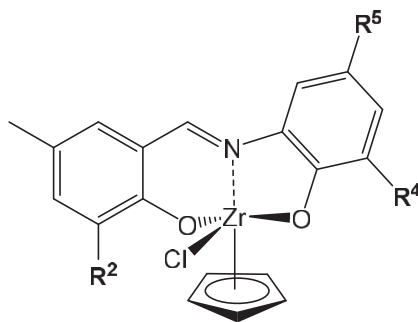


Figure 21. General structure of tridentate [O,N,O] FI complexes reported in the patent JP 2011016789 A

Table 9. Catalytic performances of tridentate FI complexes in Figure 21

Complex	R ²	R ⁴	R ⁵	Activity (kg _{PE} mol _{Ti} ⁻¹ h ⁻¹)
25	<i>t</i> Bu	<i>t</i> Bu	<i>t</i> Bu	140
26	Ph	<i>t</i> Bu	<i>t</i> Bu	130
27	CMe ₂ Ph	<i>t</i> Bu	<i>t</i> Bu	640
28	<i>t</i> Bu	CMe ₂ Ph	CMe ₂ Ph	280

Conditions: 5 μmol of complex, Al_{MMAO}/Ti = 250, 100 L h⁻¹ ethylene, 250 mL toluene, 50 °C, 10 min

After describing the miscellaneous catalytic systems for polyethylene production, the next section is dedicated to the techniques developed for the analysis of these polymers. A comparison between polymer produced by single-site and multi-site catalysis is also presented.

III. PROPERTIES OF POLYETHYLENES PRODUCED BY MULTI- AND SINGLE-SITE CATALYSIS

III.1. Introduction

To recall, the essence of this PhD project is the analysis of polymers to categorize polymerization active species among the families of catalysts described previously. Thus, the goal of this section is to describe the techniques and methods applied to the analysis of polyethylenes produced by single-site and multi-site catalysts. First, the conventional analytical techniques employed to determine the chemical composition and molar mass distribution of these PE are introduced. A comparison of polyethylene properties according to the nature of catalyst is proposed. Then, specific techniques for the analysis of chemical composition distribution (CCD) of polyolefins are detailed. Eventually, the concept of entanglement is defined and its impact on polyethylene topology and polymer analyses are discussed.

III.2. General analysis of polyethylenes

III.2.1. Multi-scale organization of polymer

Most polyethylene grades are semi-crystalline thermoplastics. These materials comprise an amorphous phase where chains are entangled, and a crystalline phase where macromolecules are well folded (Figure 22). The arrangements and entanglements of macromolecules is defined as the topology of the polymer.¹⁰² For semi-crystalline material, the crystallinity χ of a material depends on the composition of the polymer (comonomers, branching) and the conditions of its production (catalyst and process operation). Indeed, the presence of branching along the polymer chains hampers the alignment of macromolecules, lowering the crystallinity of the material. Polyethylene crystallites are assembled into lamellae. These ribbons share several polyethylene chains that act as connectors between crystallites. These lamellae organize radially to form spherulites. As its name implies, these structures result from the spherical assembly of lamellae after a nucleation step.

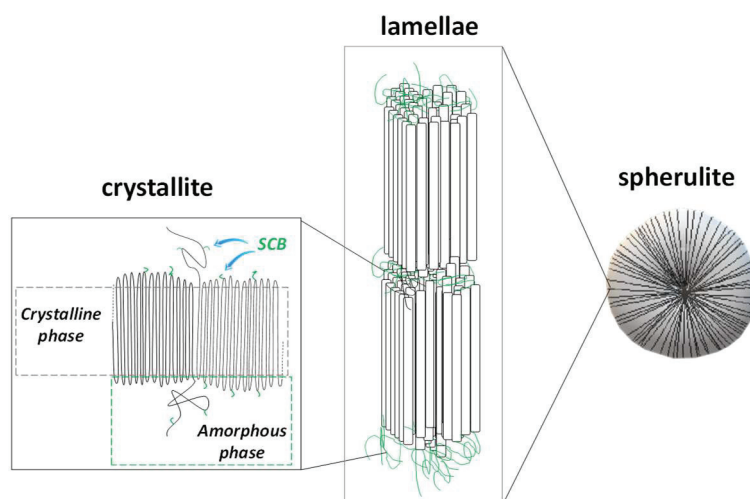


Figure 22. Simplified representation of polyethylene structures

Semi-crystalline materials can be found at the solid, rubbery or liquid state depending on its environment and especially the temperature. It is characterized by the glass transition temperature (T_g), crystallization (T_c) and melting (T_m) temperatures with $T_g < T_c < T_m$. A polymer is melted when local and global mobilities of the molecules are enhanced, i.e. $T > T_m$. At lower temperature, semi-crystalline material can adopt two main states:

- (i) the rubbery state, characterized by a limited mobility of chains at local scale. Above the crystallization temperature ($T_c < T < T_m$), macromolecules move along a virtual tube, which is also known as “reptation motion”. Below the crystallization temperature ($T_g < T < T_c$), the crystalline phase is formed.
- (ii) the solid state, where chains in amorphous and crystalline phase have a very limited mobility even at the local scale, typically below the glass transition temperature ($T < T_g$).

For linear polyethylene, typical glass transition temperature is between $-90\text{ }^\circ\text{C}$ and $-130\text{ }^\circ\text{C}$. T_c and T_m are both in the range of $110\text{ }^\circ\text{C}$ to $140\text{ }^\circ\text{C}$ depending on the chemical composition of the polymer. Therefore, HDPEs and LLDPEs are in the rubbery state at room temperature.

III.2.2. Conventional techniques applied to polyethylene analyses

Combining analytical techniques is essential to have a clear view of the unique feature of each polymer grade (Figure 23). Chemical composition of the polymer is determined through the thermal properties of the polymer. Indeed, the incorporation of comonomer such as LAO, creates side chains that hamper the folding of the polymer chains resulting in the formation of an amorphous area (Figure 22). As a consequence, branching can be assimilated to defects that limit the crystallization of the material. SCB has a direct impact on the crystallinity, temperature of crystallization and melting even with a few amount of comonomer. Therefore, these polymer properties are commonly assessed by thermal techniques such as Differential Scanning Calorimetry (DSC), which is based on the measurement of heat transfer upon heating of the material.

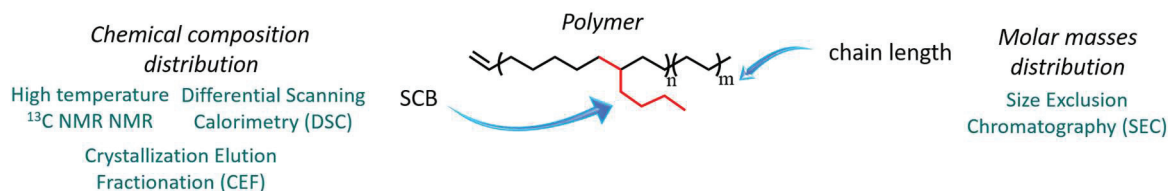


Figure 23. Poly(ethylene-co-1-hexene) structure and related analytical techniques.

Regarding the molar mass, chain length is evaluated by size exclusion chromatography (SEC) (Figure 23). This technique is based on the segregation of macromolecules according their hydrodynamic volume.¹⁰³ Alternative techniques based on rheological parameters have proven their efficiency for molar masses and molar mass distribution determination. Based on dynamic melt rheology, Rastogi and co-workers used the modulus model transposing

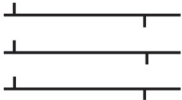
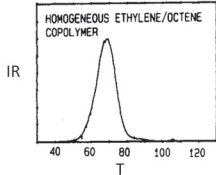
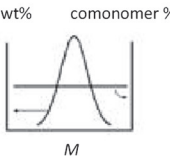

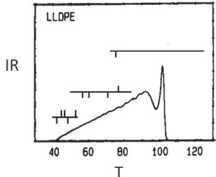
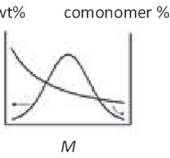
relaxation modulus data to molar mass distribution.⁹¹ This technique enables the analysis of molar masses up to 10^7 g mol⁻¹, which is not possible with standard SEC technique.

III.2.3. Analytical features of polyethylenes made with single- and multi-site catalysis

Differences between multi- and single-site catalysis are directly translated into a diversity of terms of polymer properties. Single-site catalysts are characterized by identical active species having the same behavior toward ethylene polymerization and copolymerization with LAO (Table 10).¹⁰⁴ As a result, similar polymer chain lengths are produced leading to a narrow molar mass distribution, i.e. dispersity is close to two. These well-defined catalysts offer the possibility to control the polymer molar masses along with comonomer content and distribution. Hence, single-site catalysts are often combined to facilitate the processing of these materials exhibiting specific mechanical properties.^{14,55,105} In 2009, 5 million tons of LLDPE were produced by single-site catalysis, representing 25 % of LLDPE production.¹⁰⁶

In contrast, multi-site catalysis can be seen as a mixture of different single-sites. Consequently, molar mass distributions are broader ($\mathcal{D} > 3$) and chemical composition distributions are often multimodal (Table 10).¹⁰⁷ In the case of heterogeneous Ziegler-Natta catalyst, the comonomer content varies with chain length. SCB is prevalent in short polymer chains but rare in long macromolecules. These peculiar properties of heterogeneous ZN-made polyethylenes were determined using advanced analyses of chemical composition distribution. The techniques and methods for HDPE and LLDPE fractionation are detailed in the next section.

Table 10. Properties of LLDPEs (same comonomer content) made by multi-site Ziegler-Natta and single-site catalysts adapted with permission from [107] Copyright 1997 John Wiley and Sons

Catalyst	Schematic view of hydrocarbon chains	Chemical composition distribution	Molar mass distribution
Single-site			
Ziegler-Natta Multi-site			

III.3. Advanced chemical composition analysis

III.3.1. Chemical composition distribution of copolymers

The chemical composition distribution of a copolymer is intrinsic to the active species producing it. Copolymers are defined by their CCD corresponding of the distribution of macromolecules in terms of comonomer content. In the case of copolymers of ethylene with linear alpha olefins, the CCD depends on the type and number of active species (Table 10). A single-site catalyst provides copolymers with the same specific comonomer content in each macromolecules. Thus, single-site catalysis is characterized by a narrow CCD. Moreover, the incorporation ability of a single-site is unique for each active species and it is governed by its structure.¹⁰⁸ In the case of heterogeneous Ziegler-Natta catalysts, the multiplicity of active sites cause the formation of macromolecules with various chemical composition. More precisely, short polymer chains exhibit higher LAO content than longer chains (Figure 24).¹⁰⁹

The analysis of olefin-based copolymers relies on the isolation of macromolecules according to their chemical composition. In fact, SCB highly affect the polymer properties, even at low comonomer content. Taking advantage of the relationship between SCB and characteristic temperatures of the copolymers (T_c and T_m), their segregation is usually performed by thermal fractionation of copolymers.¹¹⁰

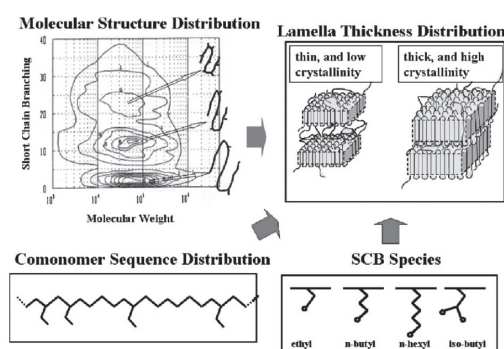


Figure 24. Chemical composition of P(E-co-4-methyl-1-pentene) produced by heterogeneous Ziegler-Natta catalysis¹⁰⁹

Reprinted with permission from [109] Copyright 2009 Elsevier.

III.3.2. Beyond DSC: Stepwise Isothermal Segregation Technique

Stepwise Isothermal Segregation Technique (SIST) enables the discrimination of copolymers according to their crystallization ability. Indeed, this thermal separation technique is based on the principle that the presence of SCB in the polymer induces smaller size of crystals and therefore lower crystallization temperature, according to the Gibbs-Thompson equation (Equation 3).

$$T_m = T_{m'} \cdot \left(1 - \frac{2\delta_e}{\Delta H \cdot l_c}\right)$$

Equation 3. Gibbs-Thompson equation

l_c : lamellae thickness (m); $T_{m'}$: melting temperature of 100 nm crystal (414.5 K); δ_e : surface energy of a PE crystal ($70 \times 10^{-3} \text{ J m}^{-2}$); ΔH : volumetric melting enthalpy of a PE crystal ($228 \times 10^6 \text{ J m}^3$) and T_m : measured melting temperature (K)

Thus, a mixture of copolymers with different comonomer content can be fractionated by forcing the crystallization of each population separately. More precisely, after erasing the thermal history of the material at 180 °C, a multiple-steps cooling forces the preferential crystallization of one copolymer with one specific comonomer content (Figure 25). For each plateau, the fraction of copolymer with $T_c \sim T_{\text{plateau}}$ crystallizes. Eventually, all fractions are isolated within the sample and melt separately during the final heating step. This way, a multimodal signal is obtained exhibiting as many peaks as the number of copolymers in the mixture.

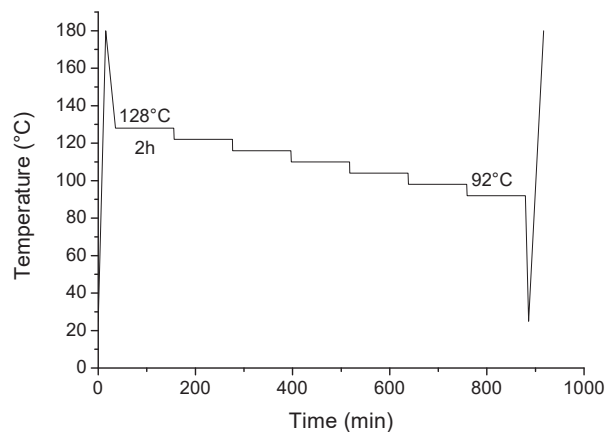


Figure 25. Example of SIST program for copolymer separation¹¹¹

Starck implemented the first SIST method (Figure 25) in view of isolating copolymers populations in a commercial poly(ethylene-co-1-butene) produced by heterogeneous Ziegler-Natta catalysis.¹¹¹ To achieve efficient copolymer segregation, the multiple crystallization steps need to be included in the range of temperature of the overall crystallization of the polymer, 92°C to 128°C in this case. Moreover, temperature is maintained during a long period

(2h) in order to allow the macromolecules to rearrange and form crystals. Eventually, this copolymer, with an overall comonomer content of 4.2 %, is composed of six fractions of copolymers revealed by the multimodal endothermal profile (Figure 26).

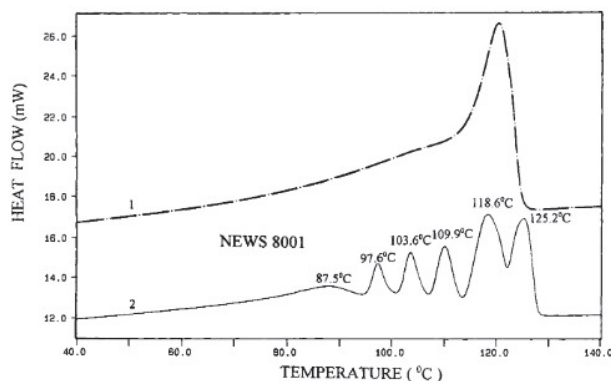


Figure 26. DSC melting profile of a poly(ethylene-*co*-1-butene) with standard DSC (dashed line) and SIST (solid line). Reprinted with permission from [111] Copyright 1999 Elsevier.

SIST experiments have been applied for the separation of poly(ethylene-*co*-1-hexene) produced by multi-site Ziegler-Natta and homogeneous metallocene catalysis. Lehmus *et al.* studied the composition of LLDPEs in term of chemical composition and molar mass at 3 stages of the polymerization.¹¹² These copolymers produced by an *ansa*-metallocene display a lower comonomer content, evolving from 15 to 9.5 mol %, as their molar mass increases from 40 000 to 62 000 g mol⁻¹ overtime. Performing successive isothermal steps each 9 °C from 125 °C to 80 °C, authors reported an evolution the endotherm profile (Figure 27). A significant portion of copolymer with a lower comonomer content is obtained after 30 minutes of reaction. It is noteworthy that signals corresponding to these HDPE fractions are overlapped, revealing a limited resolution of SIST technique. Such observation accounts for undesired chain-interactions between these long macromolecules expressed by the physical phenomenon of co-crystallization.

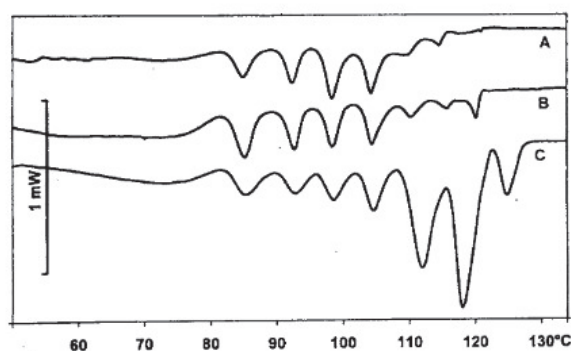


Figure 27. Endothermal signals for LLDPE (ethylene/1-hexene) obtained by an *ansa*-zirconocene. A: 6 min, 40 000 g mol⁻¹ (2.5) 15 mol % 1-hexene; B: 12 min, 49 000 g mol⁻¹ (2.5) 13 mol % 1-hexene; C: 30 min, 62 000 g mol⁻¹ (2.9) 9.5 mol % 1-hexene. Reprinted with permission from [112] Copyright 1997 Elsevier

In SIST experiments, the segregation occurs within the polymer melt, which most often leads to co-crystallizations. It was previously explained that the mobility of chains within the polymer melt is limited especially for high molar masses polymer. As a consequence, the chains that start crystallizing also initiate the crystallization of macromolecules proximately located. This co-crystallization effect affects the copolymers separation, which is translated by a limited resolution of the calorimetric profile. Therefore, SIST analyses are sensitive to intra and inter-macromolecular heterogeneity, restricting this technique to a qualitative fractionation of copolymer blends. This phenomenon of concomitant crystallization is inherent to the analysis of the polymer bulk but can be partially avoided in solution.

III.3.3. Beyond chromatography: Crystallization Elution Fractionation

Crystallization Elution Fractionation (CEF) is a brand-new technique specifically implemented for polyolefins with a low comonomer content. Similarly to SIST, the segregation is based on the difference of both crystallization and melting/solubilization temperatures of the copolymer. Indeed, unlike other chromatographic segregation techniques, CEF consists in two successive steps (Figure 28).¹¹³ First, a dynamic crystallization consists in a progressive cooling while the solution of copolymer in TCB flows in the column. This way, copolymer with low LAO content (high T_c and T_m) crystallizes prior to the one with a higher amount of SCB (low T_c and T_m). This separation is further improved during the temperature rising elution fractionation step as the last crystallized fraction is solubilized first (low T_c and low T_m) followed by the population with a low LAO content.

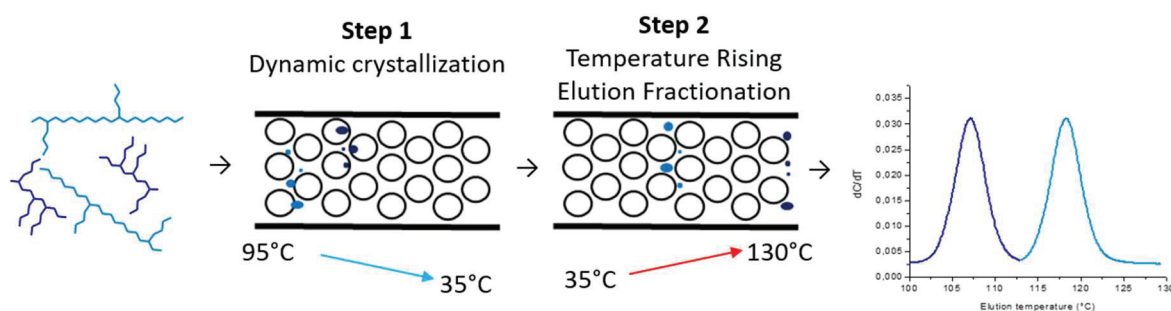


Figure 28. Principle of Crystallization Elution Fractionation

Among the chromatography techniques applied to copolymer segregation, CEF is the most appropriate with respect to linear polyethylene with low amount of SCB.¹¹³ Indeed, Temperature Rising Elution Fractionation (TREF) and Temperature Gradient Interaction Chromatography (TGIC) are based on the second step only, which does not afford a satisfactory resolution for mixture of copolymers with a close comonomer content.¹¹⁴ Likewise, Crystallization Analysis Fractionation (CRYSTAF) is based on a static crystallization of the polymer bulk. While temperature is decreasing, the fraction of polymer remaining in solution is analyzed. The superiority of CEF over former techniques lies in both its rapidity and

the limitation of the co-crystallization effect, enabled by the variation of temperature under dynamic flow. Monrabal *et al.* showed that a low cooling rate for step 1 is crucial to better isolate crystallites and ensure an efficient separation of signals.¹¹⁵ Thus, contrary to CRYSTAF and TREF, copolymer separation was successfully achieved since no broadening and merging of peaks is observed in CEF.

The few examples of polyolefin segregation, and especially poly(ethylene-co-1-olefin), have been mainly reported by the two research teams of Soares and Monrabal. As explained in section III.2. General analysis of polyethylenes, single-site catalysis affords very homogeneous polymers in terms of average molar mass and comonomer content. Thus, monomodal and narrow distributions are usual features for single-site LLDPEs. Soares *et al.* elected LLDPEs produced by metallocene catalysis to study the influence of their molar mass on the resulting CEF signal.¹¹⁶ For copolymer with similar comonomer content, it was shown that their elution temperature is concomitant whatever their average molar mass. Indeed, both LLDPEs m-1 and m-2 containing about 1.15 mol % of 1-octene have a common elution temperature although their molar masses are different (Figure 29).¹¹⁶ This observation implies that molar masses have no effect on CEF separation. Polymer segregation seems to be independent of the molar masses of the LLDPEs. It is important to note that such conclusion has been drawn for molar masses up to $50 \times 10^3 \text{ g mol}^{-1}$. Furthermore, signals exhibit a shoulder in the case of homopolyethylenes m-1 and m-2. However, no explanation is provided regarding this surprising pattern.

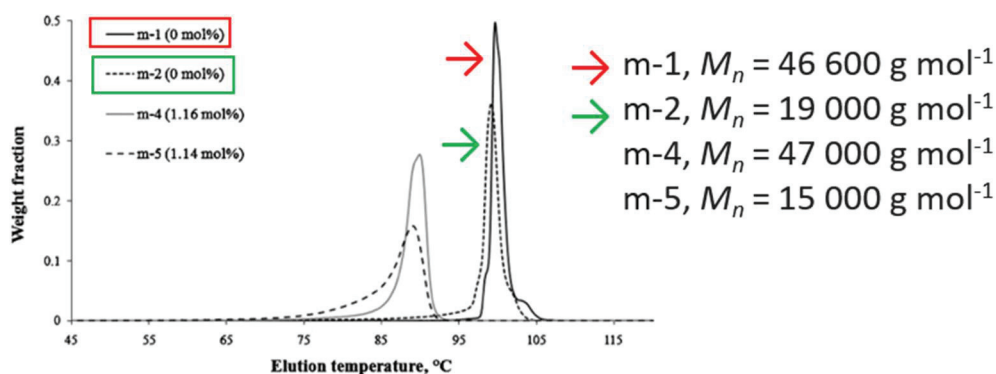


Figure 29. CEF profile of copolymer ethylene/1-octene made with a metallocene catalyst. Reprinted with permission from [116] Copyright 2012 Elsevier

Advanced segregation of ethylene/LAO copolymers were managed by combining thermal fractionation techniques. Ndiripo and coworkers isolated several fractions of a poly(ethylene-co-1-heptene) by preparative TREF and analyzed each population by DSC.¹¹⁷ The copolymer with a low comonomer content is composed of several fractions isolated by TREF at different temperature. Although the TREF profile displays a monomodal signal, DSC analysis of each fraction demonstrated that the bulk polymer is composed of several fractions of copolymers (Figure 30). Interestingly, crystallization profile for the 60 °C, 90 °C and 130 °C fractions are bimodal, which implies that these fractions are also composed of several sub-populations with different comonomer contents.

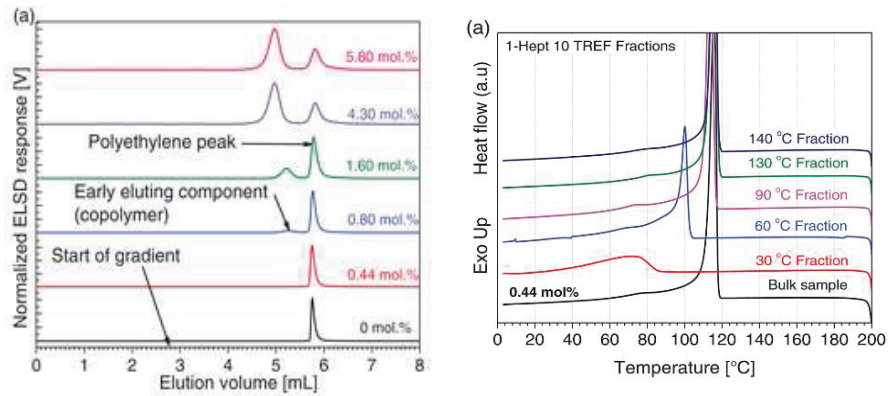


Figure 30. TREF profile (left) and DSC crystallization profiles (right) of a LLDPE with 0.44 mol% 1-heptene. Comparison between the bulk copolymer and TREF-isolated fractions. Reprinted with permission from [117] Copyright 2018 Elsevier

From these fractionation analyses overview, it was noted that high molar masses can have an impact on the separation. To rationalize such effects, the organization of the hydrocarbon chains at the macromolecular scale should be considered.

III.4. In-depth analysis of hydrocarbon macromolecule organization

III.4.1. Entanglement in thermoplastics

Entanglement is an inherent concept of macromolecules. Polymer chains overlap until the maximum entropy thermodynamic equilibrium state is reached (Figure 31). In polymer melt, entangled macromolecules move along a virtual tube in which they are confined.¹⁰² This phenomenon of reptation is a thermal motion, which only applies to linear polymers with high molar masses. In semi-crystalline polymers, macromolecules in the amorphous phase are interweaved, whereas chains constituting the crystalline phase are well-organized and folded. Each material is characterized by the density of entanglement, which corresponds to the molar mass between entanglements M_e . It is defined as the average chain fragment between two entanglement knots in the overall polymer. Consequently, low value of M_e means a high number of loops between the chains and therefore a high entanglement density. In the case of linear polyethylene, M_e is about $1\,200\text{ g mol}^{-1}$.¹¹⁸ As entanglement at macromolecular scale has ineluctable impacts at the material scale, M_e can be assessed by physical parameters.

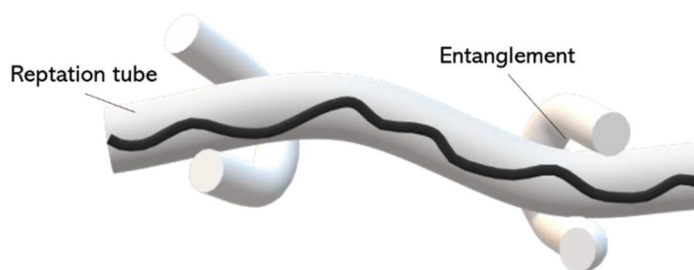


Figure 31. Representation of entanglement in polymer melt

The entanglement density is directly linked to the rheological and mechanical properties of the material.¹¹⁹ According to Ferry equation, M_e is inversely proportional to the rheological parameter G_N° (Equation 4.1).¹²⁰ This modulus is deduced from oscillatory shear experiments. In the theory of rubber elasticity, viscoelastic moduli evolve according to the shear frequency (Figure 32, a). From low to high frequencies, the state of material changes from melted to rubbery to glassy. In the rubbery domain, the storage modulus G' is constant whereas the loss modulus G'' varies with the angular speed. The modulus in the rubbery plateau region G_N° corresponds to the value of G' when G'' reaches its minimum value. The physical phenomenon behind the transition from the rubbery to liquid state is the disappearance of reptation in favor of a “free” chain motion. As macromolecules are diffusing outside their virtual tube, interactions of chains with their surrounding as well as entanglement density are altered. Therefore, reptation time τ_r is also linked to M_e (Equation 4.2).¹²¹ It is evaluated by the terminal relaxation time τ_d at which the relaxation modulus $G(t)$ falls off (Figure 32, b). Thus, higher entanglement density leads to longer terminal relaxation.

$$G^{\circ}_N = \frac{\rho RT}{M_e} \quad (1)$$

$$\tau_r = 3 \tau_e \left(\frac{M}{M_e}\right)^3 \quad (2)$$

Equation 4. Ferry equation (1) and reptation relaxation equation (2)

with ρ : density of polymer (g mol^{-1}); R : gas constant ($8.314 \text{ J mol}^{-1} \text{ K}^{-1}$); T : absolute temperature (K) and τ_e : Rouse time (s)

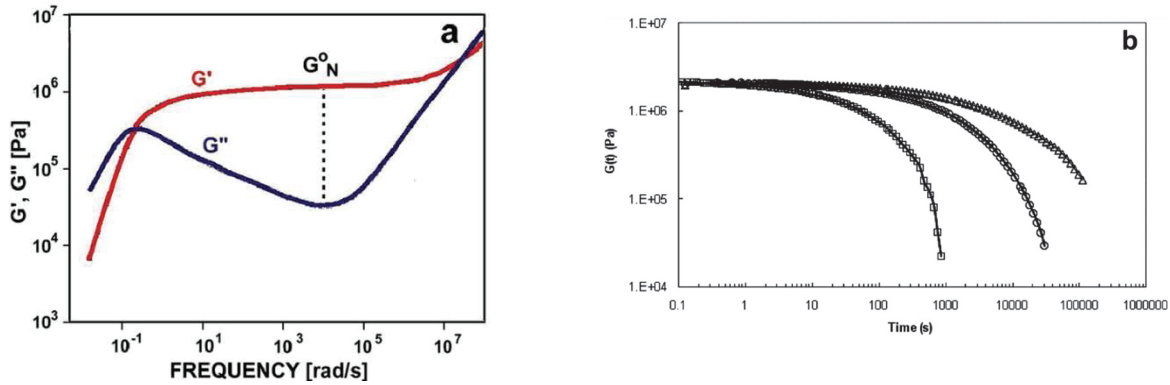


Figure 32. Viscoelastic response in oscillatory shear (a)¹²² and stress relaxation profile (b)⁹¹ of linear polyethylene. Reprinted with permission from [129] and [97]. Copyright 1996 AIP Publishing and Copyright 2010 American Chemical society

A high entanglement density provides interesting mechanical properties such as strength and stiffness. In stress-strain experiments, true stress σ gives access to the strain hardening modulus, G_R (Equation 5).¹²³ As long as the temperature is lower than T_m , applying a force on the material leads to a significant or moderate deformation. In the last case, this strain hardening phase is caused by the entanglements in the amorphous phase of the material. Consequently, low M_e , *i.e* high entanglement density, is characterized by high G_R value.

$$\sigma = Y + G_R \left(\lambda^2 - \frac{1}{\lambda} \right)$$

Equation 5. stress-strain equation¹²⁴

with G_R : strain hardening modulus; Y : yield stress; λ : extension ratio

Partial or complete reduction of the entanglement density can be achieved by appropriate polymer production or processing techniques. On the one hand, the dissolution of polymer in a solvent facilitates the separation of macromolecules leading to a reduced entanglement density. As a consequence, low concentration of polymer favors this disentanglement of macromolecules.¹²⁵ On the other hand, the direct production of non-entangled polyethylene was made possible thanks to the many possibilities offered by catalysts design. The production and properties of this unentangled polyethylene is discussed in the following section.

III.4.2. Entanglement in linear polyethylene

The diversity of polymerization catalysts enabled the study of various grades of linear polyethylenes. Rationalizing the relationship between unentangled/disentangled polymers and their physical properties lead to significant breakthrough and is still of interest nowadays.¹²² Several rheological and mechanical studies were applied to linear polyethylenes HDPE and LLDPE. For HDPE, higher molar masses lead to higher entanglement density. From $5.8 \times 10^4 \text{ g mol}^{-1}$ to $2 \times 10^6 \text{ g mol}^{-1}$, the molar mass of entangled fragments drops from 1 020 to 543 g mol^{-1} .^{126,127} Noteworthy, M_w and M_e are independent when the polymer is melted or dissolved. However, polyethylene with ultra-high molar mass has a different behavior in terms of mechanical and rheological properties. In the rest of this manuscript, a distinction is made between *unUHMwPE*, which is defined as a polyethylene that is synthesized without entanglement, and *disUHMwPE*, which was originally entangled and has been physically disentangled.

Unentangled ultra-high molar mass polyethylene (*unUHMwPE*) can be produced by supported Ziegler-Natta catalysts as well as homogeneous metallocenes and post-metallocenes. It is important to keep in mind that an unentangled polyethylene crystal is composed of a single folded polyethylene chain.¹²⁸ In the case of homogeneous catalysis, active sites are distant from one another, which prevent overlapping of PE chains. This condition limits the entanglement of the growing macromolecules. In heterogeneous systems, active sites are fixed on a support and surrounded by other active sites. This proximity of polymerization centers favors the contact between nascent polymer chains.¹²⁹ Moreover, polymerization rate is higher than crystallization rate in Ziegler-Natta catalysis but similar in homogeneous systems. Consequently, a higher density of entanglement is caused by this difference in kinetic parameters. More precisely, this phenomenon is related to a better control of temperature in a diluted reaction medium than in the confined environment of a support. As a result, entanglement is enhanced in the case of supported catalysts while a “single chain forming a single crystal” can be achieved by single-site catalysis (Figure 34).¹³⁰ For the records, an interesting combination of heterogeneous and homogeneous catalysis enabled to overcome the issues of reactor fouling and excess of cocatalyst in the production *unUHMwPE*.¹³¹

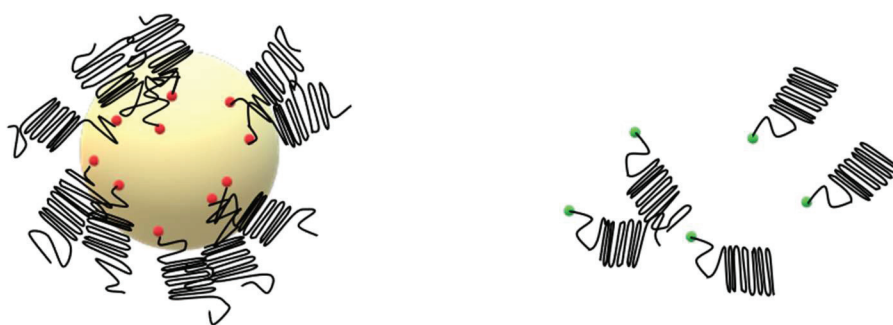


Figure 33. Schematic view of entanglement during PE production by a heterogeneous Ziegler-Natta (left) and a homogeneous metallocene or post-metallocene (right)

Chanzy and co-workers were the first to report a heterogeneous system for the production of unentangled polyethylene. Using VCl_3 supported on glass plate and activated by TIBA, low temperature polymerization ($-40\text{ }^\circ\text{C}$) were required for the synthesis of high melting temperature ($141\text{ }^\circ\text{C}$) and high molar masses polyethylene ($4 \times 10^6\text{ g mol}^{-1}$).¹³² These specific properties are linked to the microstructure of the polymer induced by polymerization temperature (Figure 34). These polymer features are explained by the unentanglement of chains as well as low transfer reactions. Both phenomena are governed by the very low polymerization temperature (T_{pol}) compared to the polymer dissolution temperature (T_{diss}). In fact, low temperature hampers macromolecules mobility and forces the crystallization of these linear chains. Consequently, polymerization temperature is essential for triggering the crystallization rate of macromolecules.

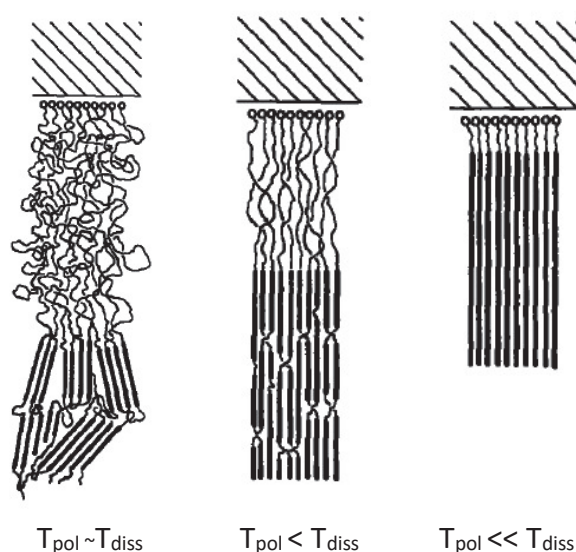


Figure 34. Entanglement effect with reaction temperature. Reprinted with permission from [132] Copyright 1987 Springer Nature

UHMwPE produced by heterogeneous Ziegler-Natta catalysis have specific rheological and mechanical properties. Rheology analysis of *un*UHMwPE is based on the principle that this material ineluctably entangles at high temperature to reach its equilibrium. Rheology is useful for the evaluation of the entanglement density as well as the molar masses distribution which cannot be easily measured by standard SEC technique. Stress relaxation of *un*UHMwPE is analyzed at low frequency, high temperature ($160\text{ }^\circ\text{C}$) and fixed strain. In the rubbery domain, G' is expected to be constant overtime. Besides, its increase until G'_N value is reached is observed instead. Based on Ferry equation (Equation 4), a lower G' is a sign of low entanglement density. As time passes by, molten polymer rearranges to reach its entanglement equilibrium, which explains the build-up of the storage modulus.⁹¹ Moreover, it has been also proven that the build-up time is proportional to $M^{2.6}$.¹²⁶ Indeed, a kinetic study reported by Pandey *et al.* showed that the entanglement density increases overtime as molar mass increases.¹³³ This evolution of molar masses was deduced from the longer time required for G' to reach the plateau value during the modulus build-up (Figure 35). Authors

explain that a long entanglement recovery is due to a limited reptation motion for the long and well-organized polyethylene macromolecules. Therefore, as long as the equilibrium is not reached, the entanglement density is not homogeneous within the molten polymer.

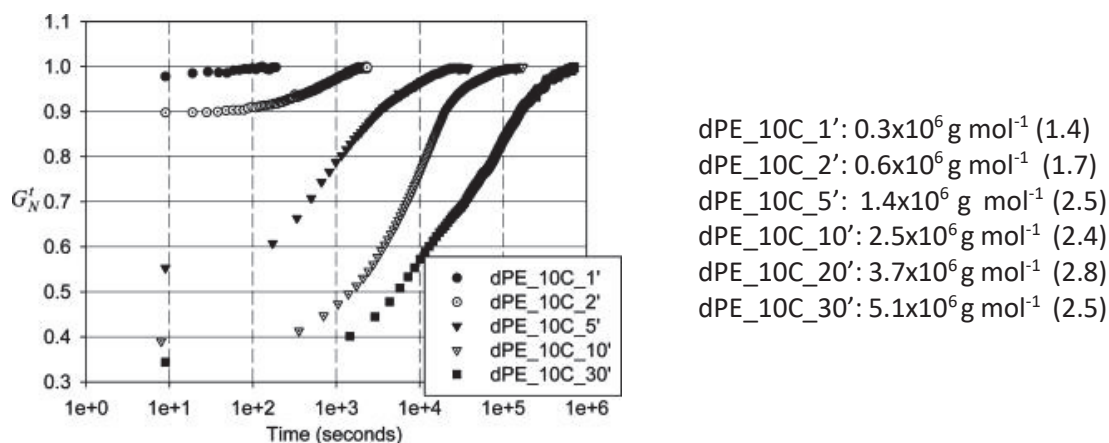


Figure 35. Build-up profile for *dis*UHMwPE dynamic time sweep experiment at 160 °C. Reprinted with permission from [133] Copyright 2011 American Chemical Society

Mechanical strain-stress experiments revealed a much pronounced strain hardening effect at higher molar mass (Figure 36).¹²⁷ This phenomenon is characterized by a higher force necessary to further deform the material. This increase of tensile module G_R results from the inhibition of macromolecules motion due to their progressive entanglement. It can be concluded that polyethylene with higher molar masses have a lower M_e value meaning a higher entanglement density. In other words, long macromolecules of UHMwPE have to entangle a numerous number of time before reaching the entanglement equilibrium.

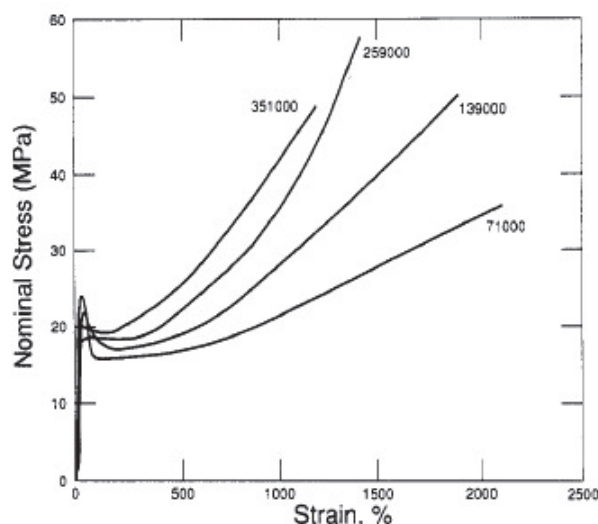


Figure 36. Strain-Stress of UHMwPE from 7×10^4 - $3 \times 10^5 \text{ g mol}^{-1}$. Reprinted with permission from [127] Copyright 1994 American Chemical Society

Interestingly, Gote *et al.* reported a Ti^{III} heterogeneous system able to produce *unUHMWPE* in a single-site manner.¹³⁴ Using $Ti(OEt)_4/MgCl_2$ activated with MMAO-12, a polyethylene of 10^7 g mol^{-1} displays the same rheological and mechanical properties as its homogeneous *unUHMwPE* counterpart.

Homogeneous production of *unUHMwPE* was reported with a pseudo-living bis(phenoxy-imine)-based catalyst (see II.4.3.1 Bis(phenoxy-imine) complexes, Figure 12). By using BHT to trap free TMA in MAO, Rastogi and coworkers aimed at enhancing the pseudo-living behavior of the catalyst in view of reducing the entanglement density in the polymer.¹²⁸ Therefore, all macromolecules display almost the same very high molar masses ($10^{6-7} \text{ g mol}^{-1}$). The *unUHMwPE* obtained by single-site catalysis has a different topology than the one afforded by heterogeneous Ziegler-Natta. In fact, it exhibits superior properties owing to its specific structure at the macromolecular scale.

As mentioned previously, unentanglement requires low temperature reaction to promote crystallization over polymerization rate. With the pseudo-living system, lower concentration of catalyst enables the formation of *unUHMwPE* even above $0 \text{ }^\circ\text{C}$ and 1 bar of ethylene.¹²⁸ This specific features combined with a low entanglement density explain the surprising pattern of stress-strain curves (Figure 37). The resulting *disUHMwPE* displays exceptional tensile modulus in solid-state (above 165 GPa) and tensile strength (above 4 GPa), which are correlated to a significant entanglement density. Indeed, drawing experiments revealed that the material can be elongated up to several times its initial length by applying a limited force. Most strikingly, this phenomenon is observed in the solid-state in a temperature range below but close to its melting temperature. Furthermore, crystallinity of drawn disentangled polyethylene increases as the material is elongated.¹³⁵ These properties make *disUHMwPE* an appealing material as for its ease of processability and the outstanding stiffness of the resulting films. This material has the unprecedented ability to be drawn in one or two directions in the large span of $125 \text{ }^\circ\text{C}$ - $145 \text{ }^\circ\text{C}$. Therefore, solvent-free *disUHMwPE* production was easily implemented by tuning the temperature of melting processing and injection molding steps.

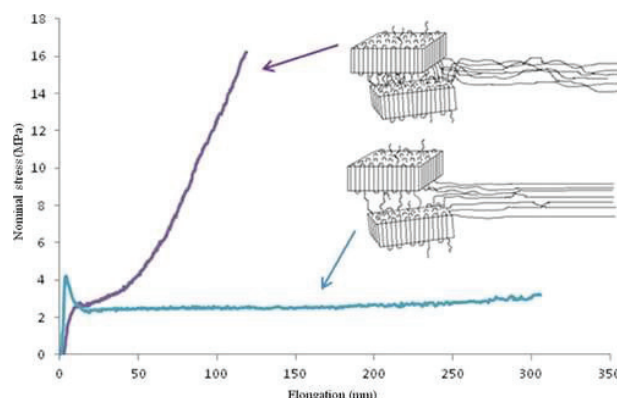


Figure 37. Stress-Strain curves at $125 \text{ }^\circ\text{C}$ of a commercial ZN UHMwPE (purple) and the homogeneous *unUHMwPE* (blue). Reprinted with permission from [128] Copyright 2012 John Wiley and Sons

Evolution of entanglement was studied according to reaction time and ethylene pressure through the stretching forces required for solid-state deformation.^{136,137} Higher ethylene concentration promotes entanglement density within the polymer. In fact, higher polymerization rate causes significant heat release, which favors the mobility and thus entanglement of the nascent polyethylene chains. Indeed, a difference of 0.2 MPa for G_N° is measured between polyethylenes of $11 \times 10^6 \text{ g mol}^{-1}$ (4.2) and $9 \times 10^6 \text{ g mol}^{-1}$ (3.4).

From an application point of view, the indisputable potential of homogeneous *dis*UHMwPE as tough and abrasion resistant material lies in the unprecedented topological structure of this material. *dis*UHMwPE processing requires ductility while the users of the final product demand stiffness. A compromise of these two conditions was found thanks to the special properties of the *dis*UHMwPE produced with the aforementioned homogeneous catalyst system. Thus, a process was developed for the production of shaped parts made of UHMwPE.¹³⁸ Catalytic conditions were optimized in terms of concentration and temperature to reach a very low entanglement density of the nascent polymer. Since stiffness of a material is provided by a high degree of entanglement, the processing issue relies on the control of the entanglement to manage the high melt viscosity of such high molar masses polymers. Thus, the idea is to tune the topology of the polymer by the means of temperature. First, a pre-heating of the polymer below its melting temperature initiates entanglements in the amorphous phase, while conserving low entanglement density in the disentangled domains.¹³⁸ Indeed, entanglement equilibrium takes longer to be reached in the disentangled region owing to a longer relaxation time. The resulting partially entangled melt is then shaped. Eventually, the material is heated above the melting temperature to promote entanglement of the disentangled region and therefore enhance the stiffness of the object. The first step of the process is known as “annealing” and is a useful technique to characterize the entanglement density from a disentangled material.

III.4.3. Annealing applied to *dis*UHMwPE

Annealing is a segregation technique based on the difference of polymer crystal size. In the case of *un*UHMwPE, the low entanglement density allow the macromolecules to properly organize and fold in a large monocystal. Conversely, a polymer with a similar molar mass but a lower M_e will only be able to generate more but smaller crystals. According to Gibbs-Thomson equation (Equation 3), the higher the crystal size, the higher the melting temperature. Therefore, DSC measurements can be quickly and easily implemented for distinguishing these two populations. This model defines an extended chain crystal with lamellae thickness above 100 nm that melts at 141.3 °C (T_m').

Practically, annealing consists in melting a polymer to modify its entanglement density. From a *un*UHMwPE or a *dis*UHMwPE it is possible to recover the equilibrium of entanglement in the melt state. At the macromolecular scale, creating entanglement highly impacts the ratio between crystalline and amorphous phase. Therefore, overall crystallinity is hampered as the molten polymer tends to reach its entanglement equilibrium. Moreover, imbrication of chains prevents their folding and therefore, the growth of large crystals. As a result, as long as the entanglement equilibrium is not reached in the polymer melt, the resulting polymer is composed of a partially entangled and a remaining disentangled area (Figure 38). It was previously stressed that dramatic changes at the molecular scale are visible through the physical properties of the material. Consequently, the alteration of thermal properties of a material can give insights in the reorganizations at the macromolecular scale. Bearing these phenomenon in mind, annealing techniques have been developed to better segregate the populations constituting the polymer.

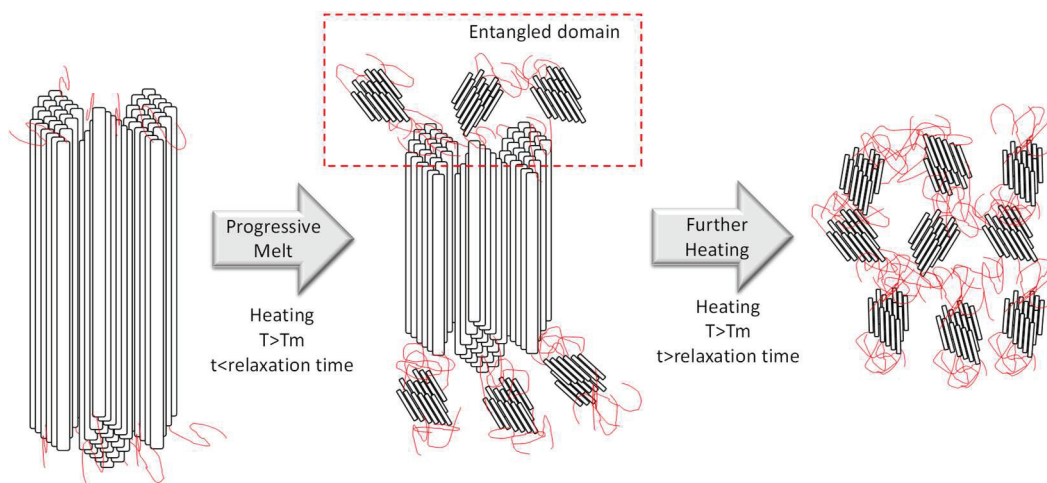
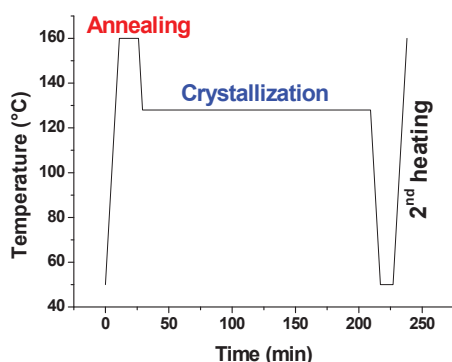


Figure 38. Schematic view of macromolecular structure of UHMwPE evolution with time in the molten polymer

Rastogi and coworkers shed light on the bipopulation in polymer melt in the case of *dis*UHMWPEs produced by both homogeneous and heterogeneous catalysis. They developed a DSC method for studying the impact of annealing on ultra-high density polyethylenes (Figure 39). It consists in annealing the polymer at 160 °C (above T_m) for a given time before a crystallization at 128 °C for 3 hours. For both polymers, the second endothermic profile are bimodal, revealing two populations of crystals of different lamellae size.¹³⁹ It is observed that homogeneous UHMwPE melts at 134.2 °C and 141.7 °C, while lower temperatures were observed in the case of the heterogeneous counterpart (131.2 °C and 135.4 °C). Authors explained this bimodality by a heterogeneity in the polymer melt. In fact, entanglement equilibrium is not fully achieved since annealing time is shorter than relaxation time. Indeed, kinetic of entanglement in the amorphous phase is lower than the melting of the crystalline phase. Hence, long and well organized chain of the crystalline phase melts but delays to entangle thus, it cannot reach its equilibrium in such conditions. As shown in Figure 35, a longer relaxation time is necessary for high molar mass macromolecules to reptate and reach the entanglement equilibrium. In fact, reptation time for UHMwPE usually exceeds 10^4 s while HDPE reaches its equilibrium within 10^3 s.¹⁴⁰ Thus, the bimodal DSC signal reveals the remaining disentangled domain in which crystals are larger than in the entangled domain after cooling. For the homogeneous system, a high degree of disentanglement and large crystal size remains after annealing ($T_m = 141.7$ °C). On contrary, macromolecules in the partially entangled domain will crystallize in smaller lamellae ($T_m = 134.2$ °C). As annealing time increases, macromolecules in the disentangled domains tend to entangle and form smaller crystals. Hence, population of crystals growing in the entangled domain increases at the expense of disentangled area. Entanglement equilibrium is a long process as it is reached by 90 % of the polymer within 10^5 minutes of annealing. In the case of heterogeneous catalysis, polymer chains grow proximately, and the resulting lamellae display several polymer chains. The mobility of chains with temperature is favored in this case, the entanglement equilibrium is easier to reach than in the case of homogeneous catalysis. As a consequence, heterogeneous UHMwPE displays lower melting temperature.



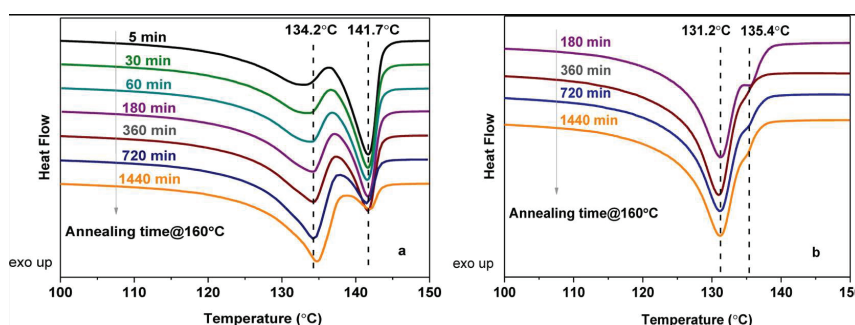


Figure 39. DSC annealing method (top) and resulting DSC profile of second heating for UHMWPE made with pseudo-living homogeneous system (left) and heterogeneous Ziegler-Natta (right). Reprinted with permission from [139] Copyright 2016 American Chemical Society

Differences in entanglement in the melt have an impact on the speed to reach the entanglement equilibrium.¹⁴¹ Yamazaki *et al.* proposed a relationship between entanglement density and annealing time in Equation 6.¹⁴² The exponential decay profile implies a fast re-entanglements followed and a slower process of more complex overlapping.

$$N \sim \ln[A \exp(\Delta t/\tau) + B]$$

Equation 6. Entanglement density according to annealing time with A and B: constant; Δt time of annealing in the melt (s); τ : melt relaxation time (s)

IV. GROUP 4-BASED ETHYLENE OLIGOMERIZATION CATALYSIS

IV.1. Introduction

This PhD is dedicated to the investigation of a titanium-based phenoxy-imine system that selectively trimerizes ethylene into 1-hexene. It is one example among other catalytic systems that produce LAOs by ethylene oligomerization. Therefore, this section provides an overview of these systems and especially those based on group 4-metals. First, the transition from non-selective to selective catalysts is presented with respect to oligomerization mechanisms and active species. Selective ethylene oligomerization assisted by titanium complexes is also reported with a special focus on the phenoxy-imine system studied in this project. For this peculiar SFI system, this section outlines the discovery, developments and mechanistic investigations reported in the literature.

IV.2. Evolution of catalytic systems and processes for ethylene oligomerization

IV.2.1. LAOs production

LAOs are valuable petrochemical intermediates composing a broad span of daily goods (Table 11). Their production amounted to 3.5 Mt in 2012 with a continuous increase to 4.3 Mt in 2016. Owing to the alpha chain end, these building blocks can be reacted with further chemicals, explaining their versatility of applications. Short LAOs namely 1-butene, 1-hexene and 1-octene represent more than 60 % of the overall LAO production given their use as comonomer for polyethylene grades.¹⁴³ In contrast, longer LAO are used for the synthesis of plasticizers, detergent and diesel fuel additives market.¹⁴⁴

Table 11. LAOs applications and global market

LAO range	Applications	Market share (%)
C ₄ -C ₈	comonomers for PE grades production	59
C ₆ -C ₁₀	plasticizers	16
C ₈ -C ₁₈	Lubricant and oil additives	12
C ₁₀ -C ₁₈	Intermediates for detergents	12
others	amines, mercaptans and other chemicals	13

IV.2.2. From Full-range to On-purpose processes

IV.2.2.1. Full-range process

Full-range processes are based on catalytic systems that afford a mixture of linear alpha-olefins. This non-selective oligomerization involves a Cossee-Arlman mechanism (Scheme 3) where transfer reactions are favored over propagation reaction. Indeed, β -H elimination is strongly promoted compared to coordination and insertion of ethylene. This specific kinetic features lead to the production of short hydrocarbon chains from C_4 to C_{30} .¹⁴⁴

Depending on the catalytic system, the chain-length distribution follows a Poisson or Schulz Flory trend (Figure 40).¹⁴⁵ On the one hand, Poisson distribution enables to target a specific range of LAOs. On the other hand, LAO size distribution based on Schulz Flory model displays an exponential decay function.

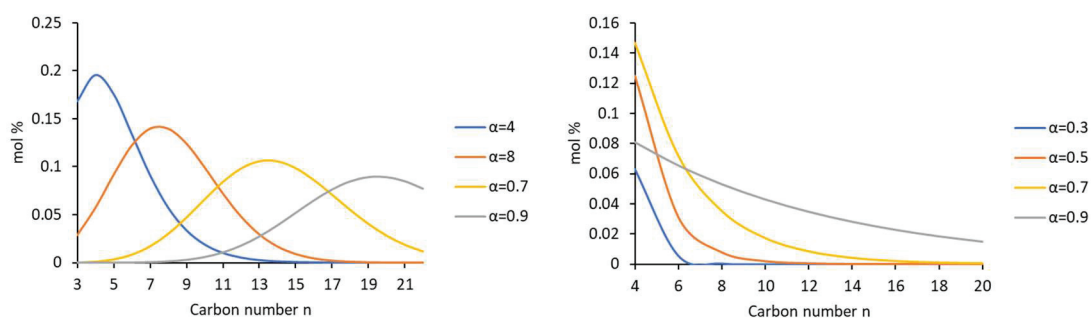


Figure 40. Comparison between Poisson (left) and Schulz Flory (right) LAO chain length distributions

The Schulz Flory equation translates the direct dependence of production between a olefin C_n production and the precedent shorter LAOs C_{n-2x} in the reaction media (Equation 7).¹⁴⁶

$$T_{n+2} = \alpha T_n$$

$$T_n/R = (1-\alpha)\alpha^{n-2}$$

T_n : molar amount of oligomer with n carbons

R : total moles of olefins produced in a given time.

α : probability of propagation

$(1-\alpha)$: probability of chain termination

Equation 7. Schulz Flory equation

The main full-range processes are based on aluminum or nickel species.¹⁴⁷ The Ethyl process of Ineos and the Gulftene process of Chevron-Phillips provide a mixture C_4 - C_{30} using alkylaluminum compounds. Shell Higher Olefin Process, known as SHOP, employs a nickel catalyst to oligomerize ethylene into C_4 to C_{40} products. In order to get a restricted range of linear alpha-olefin, an ingenious strategy was considered.¹⁴⁸ First, the $C_{>20}$ LAOs are isomerized by a Mo/Al_2O_3 catalyst to complete the migration of the double bond from a terminal to an

internal position. Afterwards, a $\text{Re}/\text{Al}_2\text{O}_3$ catalyst performs the metathesis between long internal olefin and C_4 to C_8 oligomers. Eventually, this clever combination of catalysts allows the production of the narrower range of C_{10} – C_{20} oligomers.

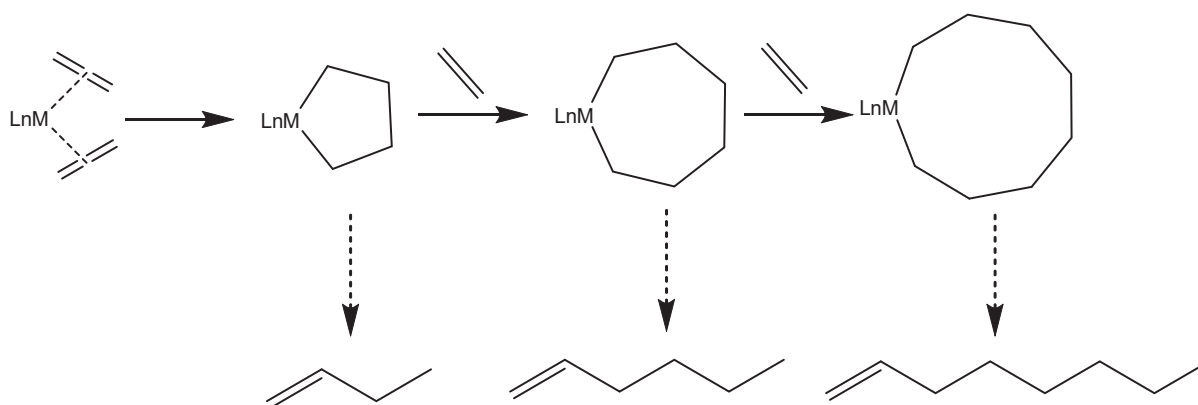
Group 4 metals are also implemented in several non-selective oligomerization processes (Table 12).¹⁴⁴ Although zirconium catalysts are well-known for their high efficiency in ethylene polymerization, specific species are able to oligomerize up to ten ethylene molecules. This ability is governed by the drastic limitation of chain growth. Both Alpha-Sablin and Idemitsu processes relies on zirconium complexes activated by trialkylaluminum or a mixture of chloroalkylaluminum with trialkylaluminum, respectively. Although the Alphaselect process gives access to a restricted range of short LAOs, it has not yet been commercialized.

Table 12. Full-range oligomerization processes based on group 4 metals

Process	Inventor	Distribution
Idemitsu ^{149,150}	Idemitsu	$\text{C}_4\text{-C}_{20}^+$
Alpha-Sablin ¹⁵¹	Sabir/Linde	$\text{C}_4\text{-C}_{18}$
Alphaselect®	IFPEN/Axens	$\text{C}_4\text{-C}_{10}$

IV.2.2.2. On-purpose process

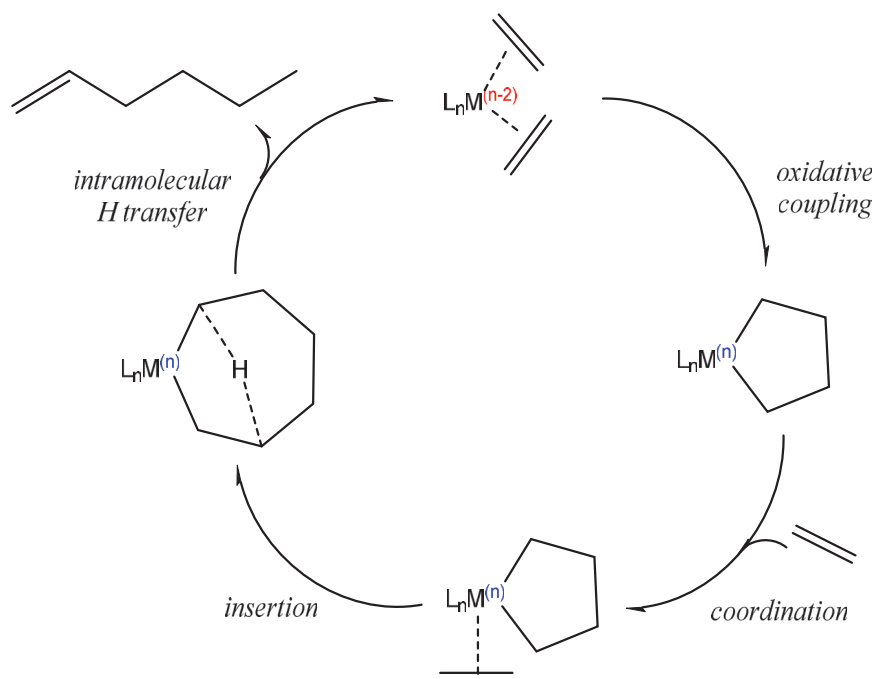
Contrary to Full-range processes, On-purpose processes employ a catalytic system that produces one specific 1-olefin. Among selective catalysts, Nickel-based species follow a coordination/insertion mechanism for the production of 1-butene while chromium and titanium-based metallacycle species are involved in the formation of 1-butene, 1-hexene and 1-octene.¹⁴⁷ The size of the resulting olefin depends on the stability of the cyclic intermediate (Scheme 6).



Scheme 6. Selective oligomerizations *via* metallacycle intermediate

The selectivity of oligomerization is governed by the ability of the catalyst to perform the metallacycle mechanism. Briggs *et al.* described this process as a growing ring around the metal center (Scheme 7).¹⁵² The activation of the precursor by the cocatalyst induces a reduced species with two available coordination sites. Once two ethylene molecules are

coordinated to the active center, an oxidative coupling generates a cyclic intermediate. As a result, the oxidation state of the metal switches from $(n-2)$ to (n) . In some cases, the metallacycle can further enlarge until the maximum ring strain is reached. Eventually, a β -H intramolecular transfer gives rise to a specific 1-olefin and the initial reduced active species $M^{(n-2)}$. The length of the LAO depends on the stability of the metallacycle intermediate. It can be modulated by tuning steric and electronic parameters that influence the metallacycle decomposition.



Scheme 7. Elementary steps of the metallacycle mechanism

For each linear alpha-olefin, several On-purpose processes were developed since the 1990's mainly driven by the increasing demand of LLDPE and HDPE (Table 13).¹⁴⁷ 1-butene production relies on titanium-based AlphaButol process whereas 1-hexene is mainly produced by chromium catalysts.

Table 13. On-purpose processes and their LAO production capacity

Cr-Process	Inventor	LAO	LAO capacity
AlphaHexol	Axens	1-hexene	50 kt/y
AlphaPlus	CPChem	1-hexene	397 kt/y
Mitsubishi	Mitsubishi	1-hexene	-
Sasol	Sasol	1-octene/1-hexene	100 kt/y
Ti-Process			
AlphaButol	Axens	1-butene	708 kt/y
MET	Mitsui	1-hexene	30 kt/y

Concerning chromium-based process, Phillips chromium trimerization catalyst is a “famous” system, which inspired the design of new ligands for selectivity adjustments (Figure 41). In contrast to Phillips polymerization system, a chromium precursor, often CrCl_3 species, is contacted with a N,S and/or P-based ligand as well as alkylaluminum derivatives to initiate the metallacycle mechanism. Despite extensive active species investigations, it is still unclear whether ethylene trimerization involves $\text{Cr}^{\text{III}}/\text{Cr}^{\text{I}}$ or $\text{Cr}^{\text{IV}}/\text{Cr}^{\text{II}}$ intermediates.^{153–155} Following the pyrrole ligand of the Phillips system, bidentates PN and SN derivatives were found to improve the activity with only 300 equivalents of MAO as activator.¹⁵⁶ Surprisingly, systems based on trifunctionalized PNP ligands yield a mixture of 1-hexene and 1-octene.¹⁵⁷ Selective chromium catalysis has been the subject of many studies related to performance improvements and intermediate identifications. Selective chromium catalysis will not be further detailed in this manuscript since the scope is restricted to group 4 catalysis. However, it is extensively discussed in abundant reviews and publications.^{144,158–160}

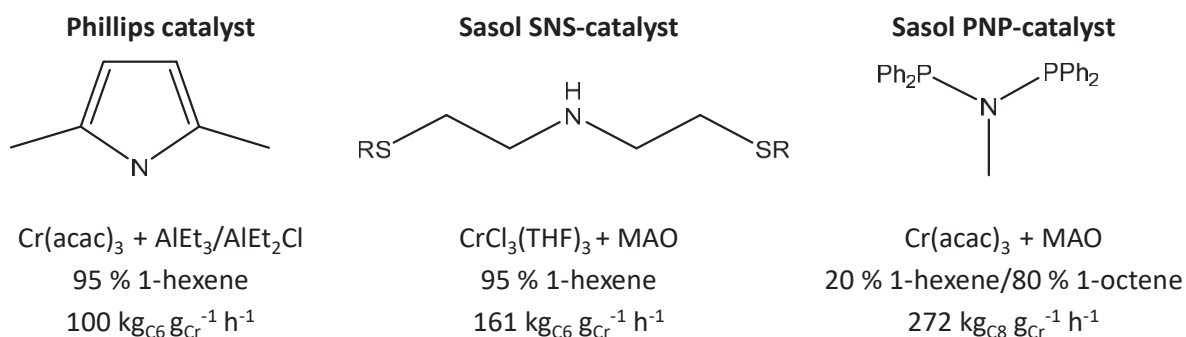


Figure 41. Examples of chromium-based systems for ethylene trimerization

IV.2.3. Titanium-based selective oligomerization

IV.2.3.1. Dimerization

Titanium is the prominent early transition metal for the oligomerization reactions especially for selective dimerization. Ziegler was first to discover the potential of titanium tetraalkoxide activated by TEA to produce 1-butene along with polymer.¹⁶¹ Investigations on the $\text{Ti}(\text{OR})_4$ system revealed the positive impact of additives, such as THF or PPh_3 , on the selectivity in 1-butene.¹⁶² Thus, AlphaButol catalytic system typically employs a titanium alkoxide and a trialkylaluminum species in the presence of specific additives. Since its first commercialization in the mid-1980s, its success was such that it became the largest dimerization process industrialized with 30 units worldwide and an annual production of 700 000 tons of 1-butene.¹⁶³ With an activity of $10 \text{ kg}_{\text{ethylene}} \text{ g}_{\text{Ti}}^{-1} \text{ h}^{-1}$ and a selectivity in 1-butene of 93 wt %, AlphaButol system exceeds all preceding dimerization processes.¹⁶⁴

The mechanism for selective dimerization is still under debate. A classic metallacycle mechanism was proposed by Chauvin *et al.*¹⁶⁵ However, recent mechanistic investigations contested this hypothesis. McGuinness *et al.* demonstrated that $\text{Ti}(\text{O}i\text{Bu})_4/\text{AlEt}_3$ does not dimerize ethylene in a metallacyclic fashion but rather through a Cossee-Arman process.¹⁶⁶ Indeed, using a mixture of C_2H_4 and C_2D_4 , a H/D scrambling of oligomers ($\text{C}_4\text{H}_{4-x}\text{D}_x$) was observed whereas a distribution of four isotopomers (C_4H_8 , C_4D_8 , $\text{C}_4\text{H}_2\text{D}_2$) is expected for metallacycle mechanism. Theoretical studies also support the Cossee-Arman mechanism for ethylene dimerization.¹⁶⁷

Contrary to McGuinness assumption of a coordination/insertion process, Girolami and coworkers demonstrated that ethylene insertion in Ti-H or Ti-Me bond does not occur when using the complexes shown in Figure 42.¹⁶⁸ Moreover, this observation explains why the metallacycle does not expand limiting the products to 1-butene. Until now, several antagonist results have been preventing the deciphering of the dimerization mechanism.

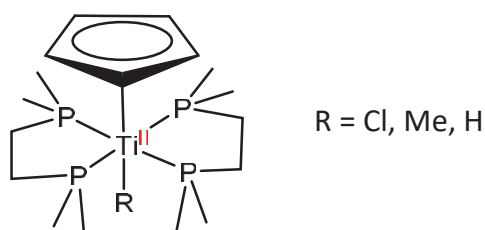


Figure 42. Titanium(II) complexes synthesized by Girolami and coworkers.

IV.2.3.2. Trimerization

The development of titanium-based trimerization system started in the 2000s with fruitful discoveries (Table 14). Throughout the years, investigations aimed at improving the selectivity of the systems by modulating the steric hindrance and electronic flexibility of titanium complexes.

Table 14. Historical background of the ethylene trimerization with titanium complexes

Year	Author	Discoveries and/or improvements
1999	Pellecchia ¹⁶⁹	Evidence of 1-hexene production and incorporation in PE chain with Cp*TiMe ₃ /B(C ₆ F ₅) ₃
2001	Hessen ¹⁷⁰	Development of hemi-labile ancillary ligands such as substituted-Cp types. Ph-CH ₂ -CpTiCl ₃ as first example of highly selective titanium-based catalyst
2002	Hessen ¹⁷¹	Diversification of ligand structures by combining electronic and steric properties
2003	Huang ¹⁷²	Hemi-labile cycle with heteroatom (sulphur) on the ligand
2004	Tobisch ¹⁷³	Proof of a metallacyclic mechanism supported by a theoretical study
2005	Biagini ¹⁷⁴	Selective trimerization by premixing CpTiCl ₃ /MAO prior to reaction with TMA and ethylene (patented procedure)
2010	Fujita ¹⁷⁵	Tridentate single phenoxy-imine catalyst with outstanding performances for selective ethylene trimerization

The first selective systems for ethylene trimerization rather than polymerization, are derivatives of monocyclopentadienyl complexes. After performing a standard catalytic test with ethylene and Cp*TiMe₃/B(C₆F₅)₃, Pellecchia and coworkers realized that the polymer comprised 5 % of butyl-branching. They logically deduced that 1-hexene was produced *in situ* and subsequently inserted in the polymer chains. Subsequently, Hessen and coworkers decided to deeply investigate Cp complexes in order to understand their reactivity and improve their selectivity. In 2001, they published the first example of metallocene complexes **29** able to produce 1-hexene after an activation with MAO (Figure 43).¹⁷⁰ This system has unprecedented high activity (TOF = 240 000 h⁻¹) and 1-hexene selectivity (86 wt %). Side products are mainly longer oligomers and polymer. On the one hand, C₁₀ oligomers results from the co-trimerization of 1-hexene with two ethylene. On the other hand, HDPE with a very low 1-hexene content was reported as solid side product.¹⁷⁶

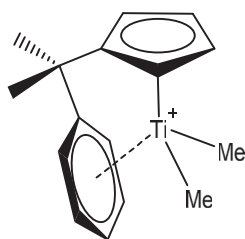


Figure 43. First titanium hemi-labile metallocene catalyst (**29**) selective for ethylene trimerization

Later on, miscellaneous derivatives of this complex were studied to target the parameters influencing the selectivity of these systems.^{170,172} It was concluded that the mobility of the pendant donor, its size and the presence of heteroatoms have a major impact on the reactivity of the active species (Figure 44). The electronic flexibility of the pendant hemi-labile group is key for the stabilization of the metal center whose oxidation state varies during the catalytic process. Efficient trimerization is achieved when the pendant group and the center remain proximate. Therefore, a quite rigid bridge is required for a moderate mobility of the pendant moiety. Table 14 gathers selected examples of hemi labile systems for the purpose of a relevant comparison of their performances. First, the bridging group should display a limited steric hindrance to allow the oxidative coupling. Indeed, complex **32**, with $C(Me)_2$ bridge, has a better activity and selectivity for trimerization than **30** and **31**, with a wider angle for Cp-bridge-Ph. Furthermore, the presence of a σ -donor heteroatom on the pendant group can also improve the trimerization selectivity but affects the activity. An illustrative example is complex **34** which is nearly two times less active than **33** owing to the sulfur coordination to titanium hampering the reactivity of the catalyst.

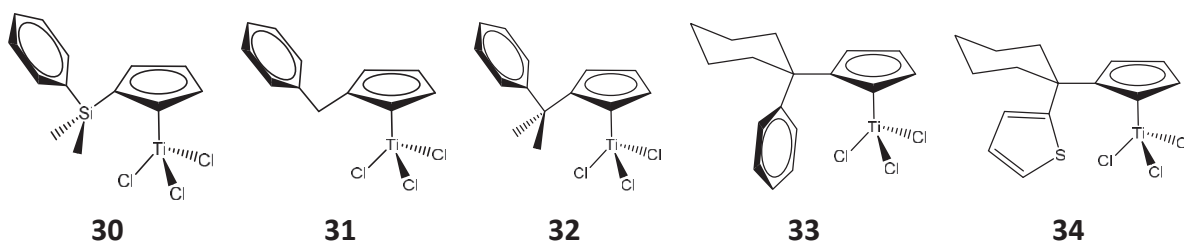


Figure 44. Selected examples of substituted-Cp derivatives

Table 14. Reactivity of hemi-labile metallocenes for selective ethylene trimerization

Complex	Activity (kg _{ethylene} g _{Ti} ⁻¹ h ⁻¹)	C ₆ (wt %)	C ₁₀ (wt %)	PE (wt %)
30	17	36	7	44
31	18	42	9	34
32	71	83	14	2
33	78	87	10	2
34 ^a	42	87	<i>nd</i>	13

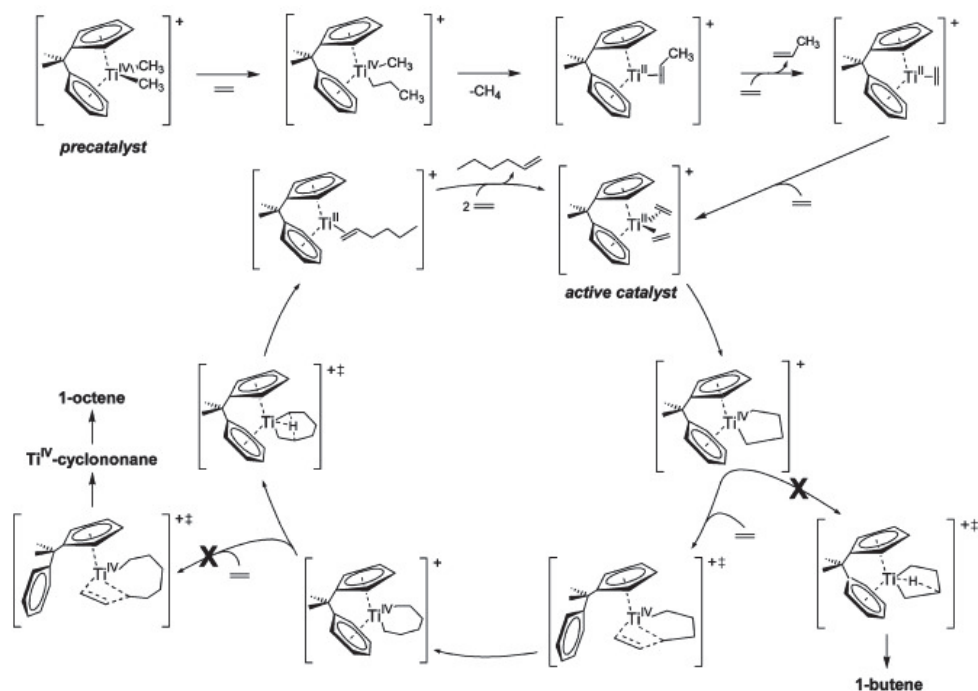
Conditions: 15 μmol Ti, Al_{MAO}/Ti = 1 000, 200 mL toluene, 30 °C, 5 bar, 30 min

^a 1.5 μmol Ti, Al_{MAO}/Ti = 1 000, 20 mL toluene, 30 °C, 5 bar, 30 min

Based on these diverse structure/reactivity relationships, mechanistic studies supported a reaction scheme that involves a metallacycle process (Scheme 8).¹⁷³ Hagen *et al.* conducted DFT calculations on the complex **32** (Figure 44) showing that:

- (i) the activation process relies on the insertion of ethylene in the Ti-Me bond followed by the β-H transfer and reductive elimination, affording methane, propylene and the Ti^{II} active species;
- (ii) the growth of the pentanacycle is favoured compared to its degradation, i.e 1-butene formation ($\Delta\Delta G^\ddagger = 25.5 \text{ kJ mol}^{-1}$). This step being first order regarding ethylene concentration, it is agreed to be the rate determining step;
- (iii) the elimination of 1-hexene is promoted compared to the further growth of the heptanacycle ($\Delta\Delta G^\ddagger = 36.8 \text{ kJ mol}^{-1}$). Indeed, both a high strain of the Ti-C₆H₁₂ intermediate and the fact that 9-members cycles are the least favoured rings explain this limitation.

Recently, Copéret *et al.* reported that polymerization and trimerization metallocene intermediates exhibit an alkylidenic character favoring further ethylene insertion in the Ti-C bond. Using solid state NMR and chemical shift tensor analysis, they showed that these species display two low lying frontier orbitals $\sigma(\text{Ti-C})$ and $\pi^*(\text{Ti-C})$.¹⁷⁷ They explain that the difference between polymerization and trimerization species emerges from the degree of π -bonding, in other words the alkylidenic character of the Ti-C bond. This study highlights that the selectivity of the catalyst depends on a subtle difference in terms of energy orbital. Thus, one can conceive that slight complex alteration can drastically orient the reactivity of these species toward polymerization or oligomerization.



Scheme 8. Metallacycle mechanism with hemi-labile metallocenes: process of activation and selective 1-hexene. Reprinted with permission from [173] Copyright 2004 American Chemical Society.

Among the few studies that considered the polymer production, Hagen *et al.* reported the continuous formation of polyethylene with the system **32**/MAO.¹⁷⁸ Their kinetic study revealed that polymer production is enhanced during the first ten minutes but also after 2h of reaction. At the early stage, it is suspected that the activation process is not completed and a CpTi^{IV}ClMe species undergoes ethylene polymerization. On the other hand, the progressive formation of a polymerization active species CpTi^{III}H resulting from the degradation of the trimerization system was hypothesized. Only three publications reported the analysis of polymer mentioning molar masses in the range of 10⁵-10⁶ g mol⁻¹.^{171,178,179} Nevertheless, neither active species and nor mechanism investigations have been undertaken concerning this side polymerization.

IV.3. Single FI catalyst – a promising trimerization species

IV.3.1. Structure and products

A decade after the unexpected discovery of Pellecchia, Fujita and co-workers reported outstanding phenoxy-imine catalysts with similar performances to Phillips chromium systems. These (FI)TiCl₃ complexes bearing a single tridentate phenoxy-imine ligand (Figure 45), named SFI complexes thereafter, belong to the restricted family of FI catalysts for ethylene trimerization.¹⁸⁰

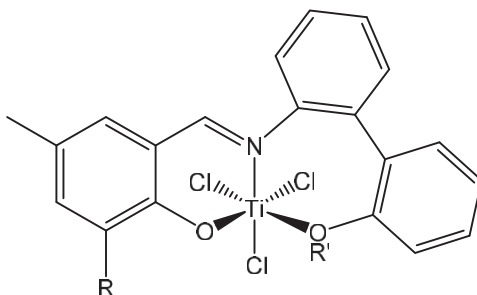


Figure 45. Single FI catalyst for the trimerization of ethylene

Trimerization SFI catalysts result from Fujita's "ligand-oriented catalyst design" strategy initiated in the 2000s and originally dedicated to polymerization species. It is important to recall that similar tridentate [O,N,O] and [O',N,O'] complexes were reported for ethylene polymerization (see Mono(phenoxy-imine) complexes). Investigations lead to a mono tridentate complex (FI)TiCl₃ (**35**) with a third donating heteroatom, which actually promotes ethylene trimerization rather than polymerization (Figure 46). This single phenoxy-imine-ether complex has a specific structure explaining its reactivity toward ethylene after activation with MAO.¹⁸⁰ Regarding the metal, titanium has the ability to undergo redox reactions especially by the Ti^{IV}/Ti^{II} couple which is suitable for the metallacycle mechanism. Additionally, the tridentate FI ligand is coordinated in such a fashion that the three chlorine atoms have a *fac* configuration. This specific geometry is essential for the oxidative coupling between two monomers and the metal center as well as for the metallacycle expansion. Furthermore, the criterion for a high activity relies on a constrained environment around the metal center, which is provided by the adamantyl group. The second requirement is a controlled electronic flexibility enabled by the ether function on the biphenyl group. Indeed, the moderate rotation of the anisole group stabilizes titanium when needed during the metallacycle mechanism.

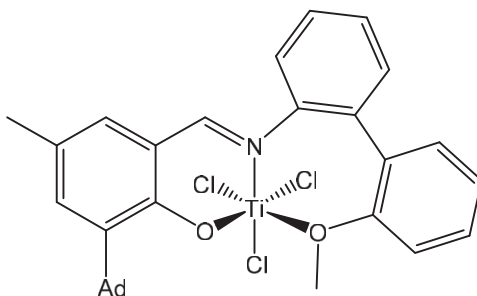
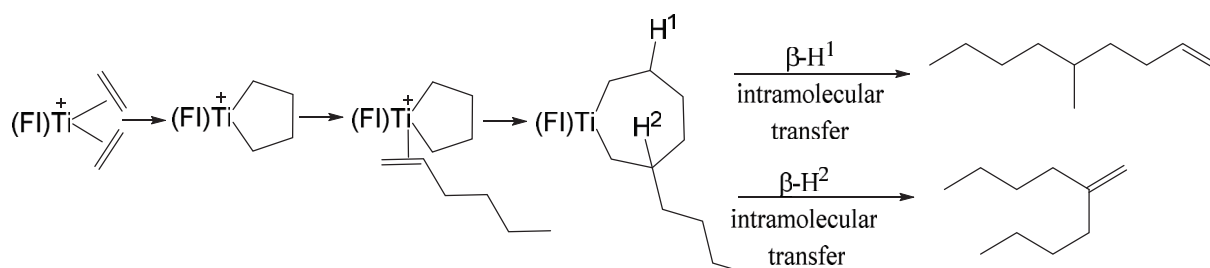


Figure 46. SFI complex (**35**) for ethylene trimerization

This trimerization SFI-system exhibits exceptional catalytic performances in terms of activity and 1-hexene selectivity compared to any preceding systems based on group 4 metals. Upon activation with 10 000 equivalents of MAO, complex **35** displays an impressive activity of $6.6 \text{ t}_{1\text{-hexene}} \text{ g}_{\text{Ti}}^{-1} \text{ h}^{-1}$ at $30 \text{ }^\circ\text{C}$ under 50 bar of ethylene.¹⁷⁵ Furthermore, a remarkable 1-hexene selectivity of 92.3 wt % exceeds all achievements of titanium-based trimerization catalysts. Owing to the high concentration of 1-hexene, co-trimerization of 1-hexene and two molecules of ethylene yields 7.3 wt % of C_{10} branched olefins as side products (Scheme 9). Three main C_{10} oligomers produced are a majority of 2-butyl-1-hexene then 3-propyl-1-heptene and 5-methyl-1-nonene. The other side reaction is the ethylene polymerization with 0.4 wt % of polyethylene produced. The cause of this polyethylene remains unknown and no publication dedicated to the investigation of its origin were found. In fact, the main interest being focused on oligomers, a limited literature relates the analysis of the polyethylene.



Scheme 9. Rationalization of main C_{10} oligomers production

The side reactions did not prevent Mitsui Chemical Inc. from developing the MET process with the SFI catalytic system (Figure 47).¹⁸¹ These undesired reactions impact the complexity and the cost of the process with additional separation and purification units. This continuous flow process requires several units for the polymer isolation given that the accumulation of this solid product could cause pipe clogging and reactor fouling. Thus, the inhibition of polymerization is the current challenge for the improvement of the efficiency of the process the enhancement of 1-hexene selectivity.

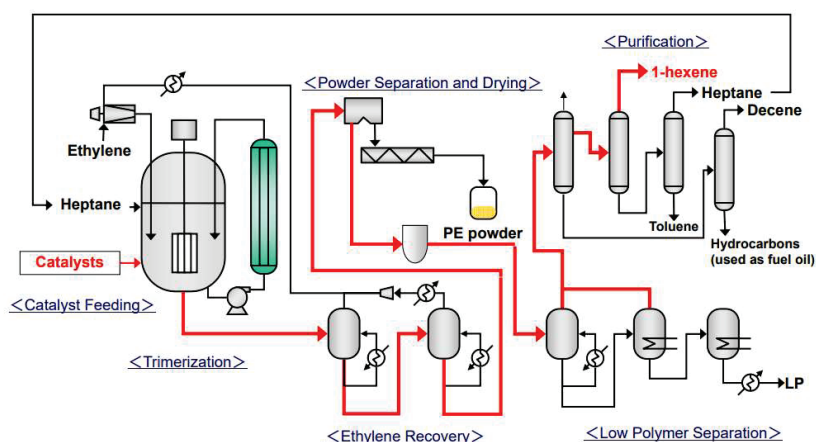


Figure 47. Mitsui Ethylene Trimerization (MET) Process¹⁸¹

IV.3.1.1. Structure alteration

The efficiency of the trimerization SFI catalyst shed light on the great potential of the development of this family of complexes. The first consideration was the understanding of their structure-reactivity relationship by altering the complex structure. Several studies revealed that most of ligand alterations shift the reactivity in favor of polymerization. Audouin *et al.* showed that one crucial parameter is the spacer between the nitrogen and the third neutral donor, which should be limited to the biphenyl group bearing the third heteroatom.^{2,182} In fact, this conjugated moiety generates more electronic flexibility than alkyl group.¹⁸³ Moreover, the third neutral donor group should be an aryl-based ether instead of amine or thioether, which are softer Lewis bases.¹⁸⁴ As a consequence, trimerization titanium-based complexes should bear a single tridentate ligand with the general framework presented in Figure 48.

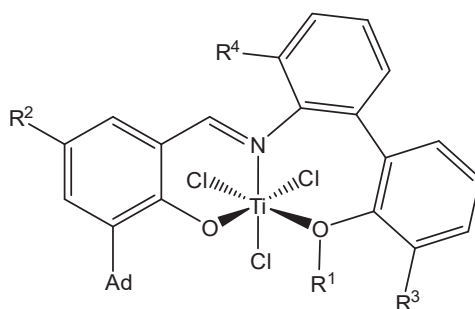


Figure 48. General structure of SFI complex

Subtle modifications of R^x substituents compared to the standard SFI complex (Figure 46) enable the tuning of the activity and 1-hexene selectivity.^{1,180,185} The adamantyl substituent is suitable for achieving a high activity but it can be replaced by another bulky group such as cumyl or *tert*-butyl without severe impact on catalytic performances. Regarding other substituents, the increase of steric hindrance of R^4 and electron-withdrawing property of R^2 can improve the activity and selectivity for trimers (Table 15). Among all SFI catalysts, the complex **38** with $R^2 = F$ (Figure 48) activated with MAO displays the highest activity and 1-hexene selectivity reported so far. Located on the para position relatively to the oxygen, this electron-withdrawing atom increases the electrophilicity of the metal center making the Ti-C bond more reactive. Regarding the bridging group bearing the ether, two trends are highlighted. First, steric hindrance close to the metal center, i.e. on R^1 and R^3 positions, affects the activity of the catalyst as revealed by both complex **37** and **39**. However, while **37**/MAO furnishes 1-hexene with a similar selectivity compared to its analogue **36**, the reactivity of **39**/MAO shifts in favor of C_{10} branched oligomers production. This second point is also observed when another alkyl group is added in the bridge between the imine and the ether on R^4 position. Substitutions of R^3 and R^4 are therefore strategic for blocking the 1-hexene in the coordination sphere before its reintroduction in trimerization reaction. It is noteworthy that, beyond its high activity, complex **40**/MAO displays a remarkable isoselectivity for

1-hexene and C₁₀ oligomers along with one of the lowest polyethylene selectivity found in the literature.

Table 15. Catalytic performances of selected altered SFI complex

Complex	R ¹	R ²	R ³	R ⁴	Activity (kg _{ethylene} g _{Ti} ⁻¹ h ⁻¹)	C ₆ (wt %)	C ₁₀ (wt %)	PE (wt %)
36	Me	Me	H	H	418.4	91.0	7.6	1.4
37	<i>i</i> -Bu	Me	H	H	92.1	93.6	2.5	3.9
38	Me	F	H	H	715.5	93.3	5.9	0.8
39	Me	Me	<i>i</i> -Pr	H	106.7	70.5	27.9	1.2
40	Me	Me	Me	Me	638.1	50.1	49.7	0.2

Conditions: 0.25 μmol Ti, 0.5 mmol MAO, 2 000 Al/Ti, 30 mL toluene, 25 °C, 8 bar, 1h

IV.3.1.2. Supported catalysis

To go further with catalyst alterations, a new strategy to improve catalytic performances of SFI catalyst is its immobilization on a support. Heterogeneous SFI systems were first developed by Duchateau and coworkers in 2015.¹⁸⁶ Their main purpose was to prevent reactor fouling by impregnating a solution of SFI precatalyst **35** on a MAO/SiO₂ support. This study revealed that the supported system is twenty times less active than the homogeneous species although selectivities are similar (Table 16). It is noteworthy that the difference of Al/Ti-ratio between heterogeneous and homogeneous systems is the main cause for the very low activity of the supported catalyst. Hence, once Al(*i*-Bu)₃/SiO₂ is introduced as scavenger, the activity increases by a factor of ten but remains lower than that of the homogenous counterpart.

Table 16. Comparison between homogeneous and MAO/SiO₂-supported SFI catalyst

Catalyst	Al _{MAO} /Ti	Activity (kg _{ethylene} g _{Ti} ⁻¹ h ⁻¹)	C ₆ (wt %)	C ₁₀ (wt %)	PE (wt %)
35 + MAO ^a	2 250	213.4	93.3	5.1	1.6
35/MAO/SiO ₂ ^b	121	10.5	89.6	8.3	2.1
35/MAO/SiO ₂ + Al(<i>i</i> -Bu) ₃ /SiO ₂ ^c	121	115.1	90.9	8	1.1

Conditions: 28 °C, 28 bar, 75 mL isopar, 1h

^a 1 μmol Ti

^b 100 mg of supported catalyst, 3.8 μmol Ti

^c same as *b* with 615 mg of supported triisobutylaluminum

Subsequently, Bercaw *et al.* claimed the synthesis of a SFI supported catalyst with a higher activity than the homogeneous system.¹⁸⁷ The supported catalyst was prepared with a similar method as described by Duchateau *et al.* except that 1.8 $\mu\text{mol Ti}/100 \text{ mg}$ of catalyst and a Al/Ti ratio of 300 were used. At 25 °C and under 1 bar of ethylene, the catalyst yields more than 95 % of trimers C₆, C₁₀ and C₁₄ and approximately 3 % of polyethylene in toluene after 24 hours. With a TON of $1.2 \times 10^5 \text{ mmol}_{\text{oligomerized ethylene}} \text{ mmol}_{\text{Ti}}^{-1} \text{ h}^{-1}$, this supported system exceeds the activity of its homogeneous analogous (TON = $9 \times 10^3 \text{ mmol}_{\text{oligomerized ethylene}} \text{ mmol}_{\text{Ti}}^{-1} \text{ h}^{-1}$). Immobilization of the catalyst limits the contact between metal centers and therefore avoid the deactivation of trimerization species. Indeed, isolating active species prevents the comproportionation of Ti^{IV} and Ti^{III} into a Ti^{III} decomposition product, which is assumed to be inactive.

IV.3.1.3. Tandem catalysis

Another field of application of SFI complexes is tandem reactions. Thanks to the combination of polymerization and trimerization systems, ethylene/1-hexene copolymers can be synthesized from a single ethylene feed.¹⁸⁸ The first tandem reaction, also known as dual functional catalysis, was reported by Kissin *et al.* in 1984.¹⁸⁹ The author showed that poly(ethylene-co-butene-1) could be produced from a single monomer feedstock by mixing an heterogeneous Ziegler-Natta catalyst TiCl₄/MgCl₂ with the dimerization complex Ti(Oi-Pr)₄ activated by TEA. The importance of chemical compatibility between the active centers as well as their process conditions were highlighted. Efficient comonomer production and copolymerization require that both catalysts operate within similar temperature, ethylene pressure and quantity of cocatalyst. Several other systems combine Ziegler-Natta or single-site catalysts with oligomerization catalysts that are usually based on chromium or nickel. However, they often afford a mixture of oligomers non-homogeneously incorporated in the polymer chains.^{188,190,191}

The *in-situ* production of poly(ethylene-co-1-hexene) targeting a majority of butyl-branching was achieved thanks to the development of single-site catalysts. In 2004, Ye and coworkers described the first homogeneous one-pot production of LLDPE using a trimerization group 4 complex and a single-site polymerization catalysts.¹⁷⁶ The tandem system comprises the CGC complex $[(\eta^5\text{-C}_5\text{Me}_4)\text{SiMe}_2(\text{tBuN})]\text{TiCl}_2$ (Figure 7) and Hessen's first trimerization metallocene $[(\eta^5\text{-C}_5\text{H}_4\text{CMe}_2\text{C}_6\text{H}_5)\text{TiCl}_3]$ (Figure 43) activated by MMAO. By varying the temperature and the pressure, several grades of LLDPE were obtained with more than 99 % of butyl branching. A decade later, the emergence of SFI catalyst as a tremendously active and 1-hexene selective species inspired Duchateau and Bercaw for ethylene trimerization and copolymerization. Given that the use of homogeneous single-site catalysts prevents the control over the morphology of the LLDPE produced, Duchateau and coworkers decided to immobilize both complexes on the same support or two distinctive carriers.¹⁹² The isolation of each precatalyst on its support $[(\text{FI})\text{TiCl}_3]$ **35**/MAO/SiO₂ + $(n\text{BuCp})_2\text{ZrCl}_2$ **41**/MAO/SiO₂ displayed better results

than cosupporting both precursors [(FI)TiCl₃]+(nBuCp)₂ZrCl₂/MAO/SiO₂ with respect to activity and 1-hexene incorporation in the polyethylene backbone (Table 17). This observation was soon confirmed by Bercaw *et al.* who combined the SFI and CGC complexes.¹⁹³ Experiments revealed the migration of 1-hexene out of the particles prior to its incorporation in the growing chain by the CGC catalyst.

Table 17. Comparison of catalytic performances and polymer properties with support-isolated and co-supported SFI complex (Ti) and (nBuCp)₂ZrCl₂ complex (Zr)

Tandem system	n _{Ti} (μmol)	Productivity (g _{PE} g _{Zr/SiO₂} ⁻¹)	Polymer melting temperature (°C)
35/MAO/SiO ₂ + 41/MAO/SiO ₂	0.5	252	123
35/MAO/SiO ₂ + 41/MAO/SiO ₂	1	336	118
35/MAO/SiO ₂ + 41/MAO/SiO ₂	1.5	341	115
35 + 41/MAO/SiO ₂	0.5	125	129
35 + 41/MAO/SiO ₂	1	142	128
35 + 41/MAO/SiO ₂	1.5	128	125

Conditions: 0.7 μmol Zr, 10.6 wt % MAO/SiO₂, 10 bar, 58 °C, 650 mg Al(*i*-Bu)₃/SiO₂, isopar, 1h

IV.3.2. Understanding the SFI system

IV.3.2.1. Activation process

Studies employing alkylaluminum compounds provide interesting insights of the potential species formed during the activation process. Investigations of Duchateau *et al.* demonstrated several effects of the use of trialkylaluminum in contact to MAO on the catalytic performances of the SFI catalyst (Table 18).¹⁸⁶ When mixing TMA with MAO, the activity is doubled and the 1-hexene selectivity is slightly improved. Similar activity and selectivity are obtained when premixing MAO with (FI)TiCl₃ and contacting with the same amount of TMA. Conversely, the premix with TMA instead of MAO provides a poorly active polymerization species. One hypothesis explaining these observations is the abstraction of the ligand from the titanium center by the trialkylaluminum. The resulting “TiR_x” species is assumed to behave as a homogeneous Ziegler-Natta polymerization catalyst.

Table 18. Influence of AlR₃ premix and mixture with MAO on SFI catalyst performances

Premix	Scavenger/ cocatalyst	Activity (kg _{ethylene} mmol _{Ti} ⁻¹ h ⁻¹)	C ₆ (wt %)	C ₁₀ (wt %)	PE (wt %)
-	MAO	10.2	93.3	5.1	1.6
-	MAO/TMA	23.4	95.4	3.9	0.7
MAO	TMA	19.9	95.1	3.9	1.0
TMA	MAO	2.6	13.6	0.7	85.7

Conditions: 1 μmol (FI)TiCl₃, Al_{MAO}/Ti = 2 250, TMA/Ti = 100, 28 °C, 28 bar, 75 mL isopar, 1h

To understand the reactivity of alkylaluminum compounds with the SFI system, characterizations of the generated species were attempted.¹⁹⁴ Upon contacting (FI)TiCl₃ precatalyst with ten equivalents of TMA, TEA or tBuBA, Redshaw *et al.* reported the formation of Ti^{III} complexes identified by EPR (Figure 49). Simultaneously, Bercaw *et al.* explained the formation of inactive Ti^{III} species by comproportionation of Ti^{IV} and Ti^{II} complexes throughout the activation and catalytic cycle.¹⁸⁷ This Ti^{III} production is concomitant with the deactivation of the catalytic system implying that Ti^{III} species are inactive decomposition products. Moreover, Audouin conducted EPR analysis on the mixture (FI)TiCl₃/MAO (500 equivalents) with a similar complex as the one shown in Figure 46 but with a *tert*-butyl group instead of an adamantyl substituent.² Two Ti^{III} species were identified, one appearing and one disappearing with time, which most probably correspond to (FI)TiMe₂ and (FI)TiClMe respectively.

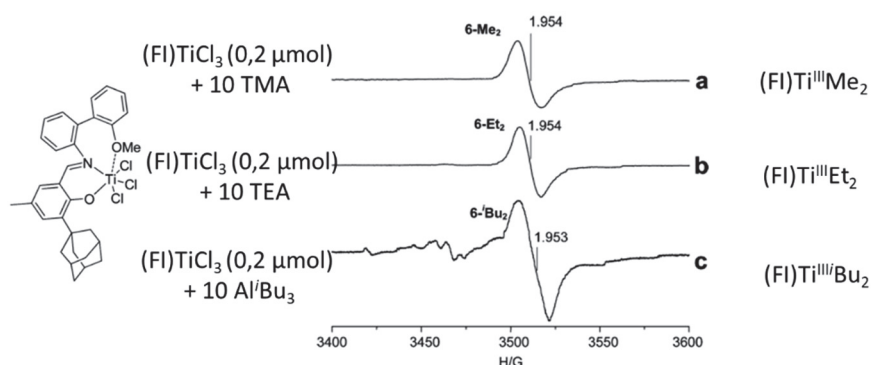
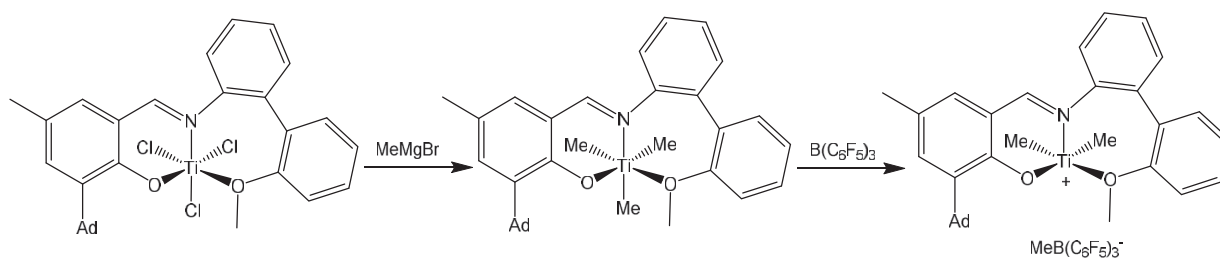


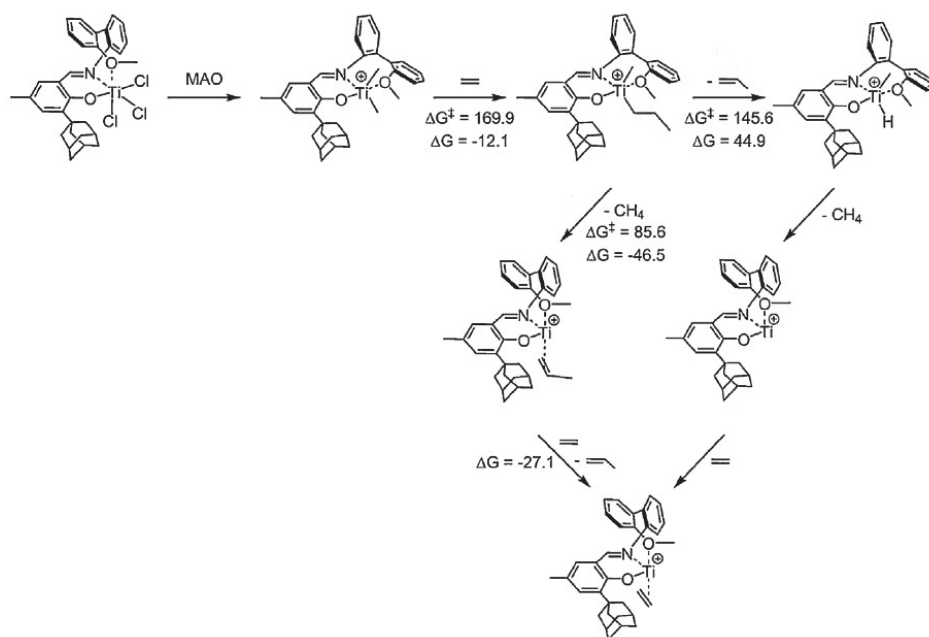
Figure 49. EPR spectra of [(FI)TiCl₃] **35** combined with AlR₃ in toluene at 25 °C. Reprinted from [187] with permission Copyright 2014 American Chemical Society

Even though the reduction mechanism has been partially elucidated, the main interrogations relative to the action of the MAO on the precatalyst remain unanswered. Deciphering the role of MAO in the activation process is essential to have a better understanding of single-site catalysis. Since MAO has a double function of alkylation and cationization, an alternative proposed by Bercaw *et al.* is to generate (FI)TiMe₂⁺ by the methylation of the precatalyst using MeMgBr before a methyl abstraction by the Lewis acid B(C₆F₅)₃ (Scheme 10).¹⁹⁵ This new stoichiometric system appears to mimic the MAO-based one. After data extrapolation of the (FI)TiCl₃/MAO system, it seems that both catalysts behave similarly with a TON of 4.5x10³ with MAO and 2.7x10³ mmol_{olefin oligomerized} mmol_{Ti}⁻¹ h⁻¹ with B(C₆F₅)₃. Although this well-defined system displays a higher trimers selectivity (> 99 wt %) than the MAO-activated one (< 97 wt %) at 1 bar, polymerization still occurs as a side reaction since less than 3 mg of polymer was produced. Consequently, polymerization active species seem to be generated either during the Ti^{IV} to Ti^{II} reduction or the metallacycle mechanism. However, MAO having a complex structure and composition, one could imagine many side reactions with the precatalyst such as partial methylation, reversed alkylation and cationization or even reactions with the ligand, all potentially promoting ethylene polymerization.

Scheme 10. [(FI)TiMe₂][MeB(C₆F₅)₃] trimerization system

Some deviations causing the unavoidable ethylene polymerization during trimerization process were identified in few studies. One of them is the structure modification of SFI complex during activation, which was highlighted by Bercaw *et al.* with the neosilylated and neopentylated precursors.¹⁹⁶ Once contacted with B(C₆F₅)₃ and ethylene, a transfer of the neosilyl group to the carbon of the imine results in the LX₂ complex (FI-CH₂-SiMe₃)Ti(CH₂-SiMe₃)⁺. Moreover, the alteration of the bis-neopentylated complex in the (FI)Ti(=CH-C(Me₃)⁺) and (MeOAr₂N=)Ti(OArHC=CHC(Me₃)⁺) species was observed. Even though these off-cycle species are inactive, their generation proves that B(C₆F₅)₃ is not innocent toward ligand modifications and so may be MAO.

Although few doubts remain about the 1-hexene production, the generation of the active species is still under discussion and investigation. In the publication reporting the first SFI catalyst for ethylene trimerization, Fujita proposed two possible paths for the formation of the active species that is the reduced Ti^{II} complex.¹ From the alkylated cationic complex (FI)Ti^{IV}Me₂, it was suspected that several ethylene molecules could be inserted in both Ti-C bonds. In one case, a β-H transfer to the metal and a reductive elimination afford the (FI)Ti^{II} species with two ethylene molecules coordinated to the metal center. The other expectation for the formation of this active species is a β-H transfer from one alkyl to another releasing an alkane and an olefin. A recent study of the same author supports the reduction of the cationic Ti^{IV} *via* a H-transfer route (Scheme 11).¹⁸⁰ Indeed, DFT calculations showed that the concerted mechanism, having an energy barrier of 85.6 kJ mol⁻¹, is more favorable than the β-H elimination, which activation energy reaches 145.6 kJ mol⁻¹. The concerted pathway was also preferred in the case of Hessen's catalyst **29** with a Gibbs energy barrier of 59.7 kJ mol⁻¹.¹⁹⁷ Furthermore, DFT considerations also indicate that the insertion of only one ethylene molecule is required before the β-H transfer from the resulting propyl to the methyl group providing the reduction of the metal.



Scheme 11. Routes for the formation of (FI)Ti^{II} active species and corresponding Gibbs free energies (ΔG , $\Delta^\ddagger G$ in $\text{kJ}\cdot\text{mol}^{-1}$)¹⁸⁰ Reprinted with permission from [180] Copyright 2017 Elsevier.

IV.3.2.2. Trimerization mechanism

SFI trimerization catalysts are agreed to occur through a metallacycle mechanism explaining the production of 1-hexene and trimers derivatives. In the first publication relating the SFI ability for ethylene trimerization, Fujita described the metallacycle mechanism as a “plausible” path for trimers formation.¹ Further studies employing deuterated ethylene supported this hypothesis. Sattler *et al.* reported no scrambling of olefins produced putting aside the Cossee-Arlman mechanism and reinforcing the hypothesis of a metallacycle.¹⁹⁵ Indeed, upon contacting $[(\text{Fl})\text{TiMe}_2][\text{MeB}(\text{C}_6\text{F}_5)_3]$ with a mixture $\text{C}_2\text{D}_4/\text{C}_2\text{H}_4$ (1/1), the resulting olefins do not display a random but even number of deuterium atoms: C_6H_{12} , $\text{C}_6\text{H}_8\text{D}_4$, $\text{C}_6\text{H}_6\text{D}_6$ and C_6D_{12} . By varying the monomer, this research team managed to reinforce the metallacycle hypothesis.¹⁹⁸ Longer alpha olefins, namely propylene, 1-butene, 1-hexene and 1-decene, are trimerized but also isomerized by the supported SFI catalyst described previously in section “Supported catalysis”. The major trimer product is 2,3,4-alkyl-1-hexene and is provided by (1,2) oxidative coupling of two LAOs with the titanium followed by (1,2) insertion of the third LAO in the titanacyclopentane. Internal alpha-olefins, branched alpha-olefins and non-conjugated diene were not transformed by this system except for butadiene which was polymerized.

Furthermore, parameters influencing the kinetics of reaction such as temperature, pressure and type of monomer, were studied to improve the understanding of catalytic process of the SFI system. Preliminary studies of the impact of ethylene pressure at 30 °C showed that, without significant change of selectivities, the 1-hexene productivity with the SFI catalyst is second order with respect to ethylene pressure (Figure 50).¹ This observation implies that the oxidative coupling of two ethylene molecules would be the rate-determining step of metallacycle mechanism. Therefore, under high pressure of ethylene, the SFI system supplies 1-hexene with high efficiency, bearing in mind that cotrimerizations are favored by the increase of 1-hexene concentration.

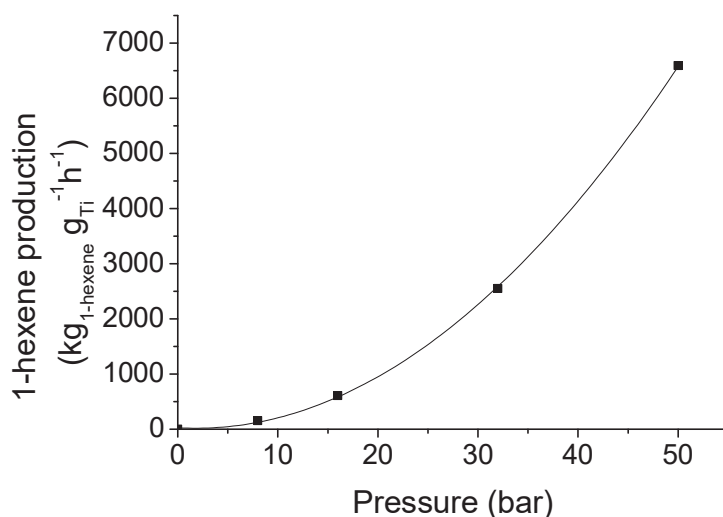


Figure 50. Second order dependence of 1-hexene formation activity with ethylene pressure

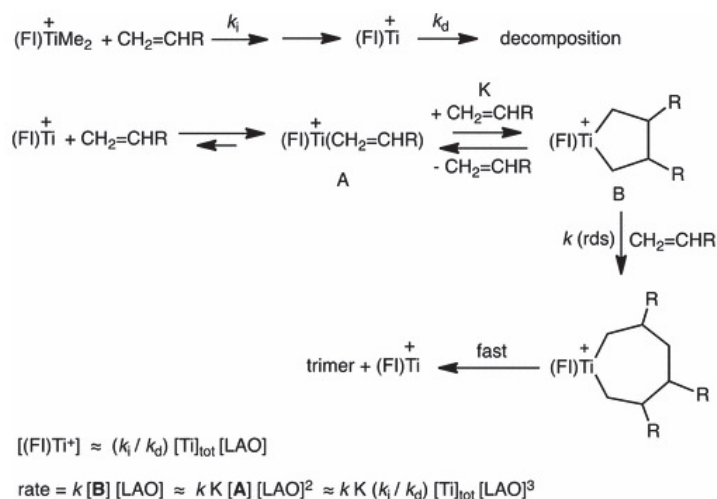
Few other studies relate the influence of temperature on the activity and selectivity of the SFI catalyst. While exploring the effect of supporting SFI catalyst on its performances, Duchateau *et al.* studied its behavior as homogeneous catalyst at 28 °C and 58 °C (Table 19). They clearly showed that the activity and trimers selectivity are affected by the temperature increase.¹⁸⁶ While the activity decreased from 213.4 to 169.5 kg_{ethylene} g_{Ti}⁻¹ h⁻¹, the 1-hexene selectivity dropped from 93.3 wt % to 79.8 wt %. This trend is typical from trimerization single-site systems since the same behavior regarding temperature and pressure was observed with hemi-metallocene such as $[(\eta^5\text{-C}_5\text{H}_4\text{CMe}_2\text{Ph})\text{TiCl}_3]$ (**32**).^{170,171} The reasons for this reactivity change with the increase of temperature has not yet been described in the literature.

Table 19. Catalytic performances of homogeneous SFI catalyst at two temperatures (28 and 58 °C) and pressures (10 and 28 bar)

n_{Ti} (μmol)	T (°C)	P (bar)	Activity (kg _{ethylene} g _{Ti} ⁻¹ h ⁻¹)	C ₆ (wt %)	C ₁₀ (wt %)	PE (wt %)
1	28	28	213.4	93.3	5.1	1.7
1	58	28	169.5	79.8	1.5	18.7
2	28	10	66.9	93.0	5.4	1.6
2	58	10	12.5	64.0	1.0	35.0

Conditions: MAO as cocatalyst, Al/Ti = 2 250, 75 mL isopar, 1h

Kinetic studies with alpha olefin higher than ethylene shed light on the catalytic behavior of SFI catalyst. In the study employing higher LAOs, Bercaw *et al.* described an initial rate of trimerizations with the supported SFI catalyst as a third order reaction toward LAOs concentration at both 0 °C and 25 °C.¹⁹⁸ Combining experimental results and proposed mechanism for ethylene trimerization, the author explained the third order kinetic considering a competition between catalytic initiation and decomposition as well as an equilibrium between alpha-olefins coordination and oxidative coupling (Scheme 12).



Scheme 12. Proposed mechanism and reaction rate equation for higher alpha-olefin trimerization with the supported SFI catalyst.

K: equilibrium constant k_i : initiation constant rate k_d : decomposition constant rate

Reprinted with permission [199] Copyright 2017 American Chemical Society.

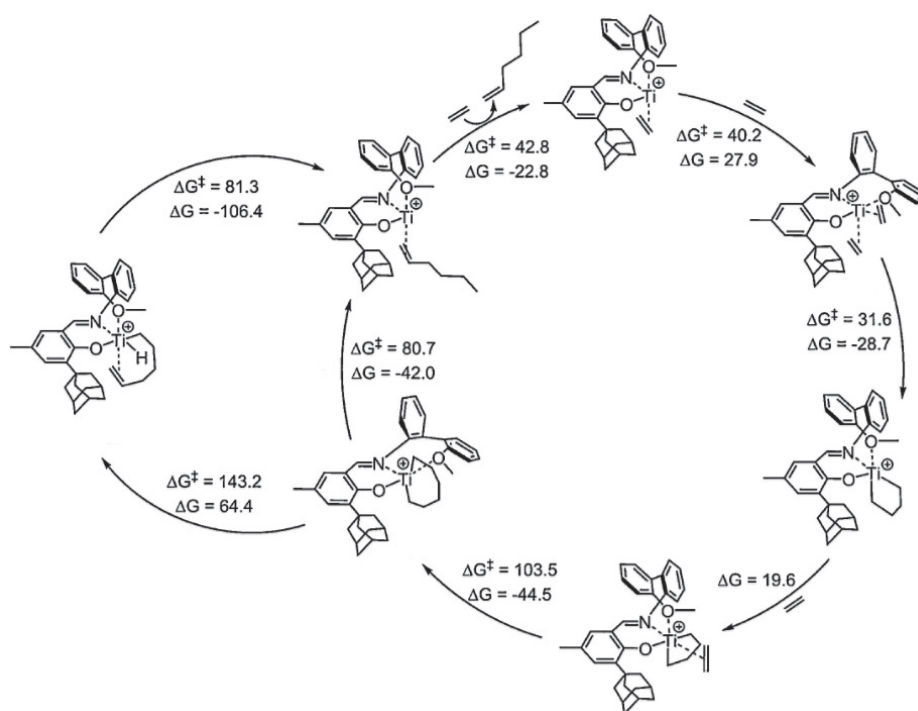
As mentioned previously, the formation of Ti^{III} species was linked to the deactivation of the system and demonstrated by kinetic considerations. In fact, the rate of deactivation of the homogeneous catalyst, more inclined to the comproportionation because not immobilized, is ten times higher than that of the supported system (Table 20). As a consequence, many parameters need to be taken into account or deeper investigated in order to explain the reactivity and activity of the SFI catalytic system.

Table 20. Kinetic parameters for homogeneous and supported SFI catalysts

Catalytic system	k_i (s^{-1})	k_t (s^{-1})	k_d (s^{-1})
(FI)TiMe ₃ /B(C ₆ F ₅) ₃	3.0×10^{-4}	6.2	2.4×10^{-3}
(FI)Ti(CH ₂ SiMe ₃)/B(C ₆ F ₅) ₃	3.0×10^{-3}	6.2	2.4×10^{-3}
(FI)TiCl ₃ /MAO/SiO ₂	5.8×10^{-5}	6.2	1.8×10^{-4}

DFT calculation is another powerful tool for deciphering favorable mechanistic routes of the SFI trimerization mechanism. In the latest publication of Fujita and coworkers, a DFT study enabled to solve uncertainty regarding key steps of the metallacycle mechanism (Scheme 13).¹⁸⁰ Although most of the elementary steps were elucidated, the final step affording the release of 1-hexene molecule was still unclear whether a concerted intramolecular 3,7-H transfer or standard β -H elimination followed by reductive elimination was preferential. Previous DFT studies relative to the titanacycloheptane hemi-metallocene (η^5 -C₅H₄(CH₂-Ph))Ti^{II}(CH₂)₆ suggest a one-step H-transfer with a Gibbs energy barrier between 42.6 and 81.5 kJ mol⁻¹.^{197,199} Recent Fujita's DFT calculations demonstrated that this concerted elementary step is more prone to occur. Indeed, its free energy barrier (80.7 kJ mol⁻¹) is almost the half of the corresponding β -H elimination (143.2 kJ mol⁻¹). Moreover, the rate determining step of the overall metallacycle process was demonstrated to be the ethylene insertion in

titanacyclopentane. Accordingly, this elementary step displays the highest free energy ($122.3 \text{ kJ mol}^{-1}$) contrary to previous beliefs ascribing the oxidative coupling as the rate determining step, but in line with a third order dependence on the trimerized linear α -olefin for the initial rate.¹⁹⁸ DFT calculations also gave new explanations on the selectivity of the system for trimerization instead of dimerization or tetramerization. First, this system does not produce 1-butene since the free energy barrier is higher for the pentanacycle degradation ($142.8 \text{ kJ mol}^{-1}$) than that of ethylene insertion ($123.1 \text{ kJ mol}^{-1}$). Moreover, the significant difference of energy barrier between the insertion of ethylene in the titanacycloheptane cycle ($\Delta\Delta G^\ddagger = 159.9 \text{ kJ mol}^{-1}$) and the 3,7-H transfer ($\Delta\Delta G^\ddagger = 80.7 \text{ kJ mol}^{-1}$) explains the preference for the latest elementary step. Besides, no DFT calculation regarding cotrimerizations or even polymerization was undertaken.



Scheme 13. Metallacycle mechanism elementary steps and comparison of concerted *versus* stepwise pathways for the titanacycle decomposition with corresponding Gibbs free energies (ΔG , $\Delta^\ddagger G$ in $\text{kJ}\cdot\text{mol}^{-1}$)¹⁸⁰ Reprinted with permission from [180] Copyright 2017 Elsevier.

V. CONCLUSION AND SCOPE OF THE PHD PROJECT

V.1. Missing elements preventing comprehension

The scope of the thesis is restricted to selective ethylene trimerization by means of a titanium-based phenoxy-imine-ether (SFI) catalyst (Figure 45). With a high activity at low temperature (30 °C) and unprecedented 1-hexene selectivity, these promising systems are worth being improved with respect to side reactions. Given that such SFI catalysts produce both trimers and polymer for unknown reasons, the literature review was purposely focused on ethylene polymerization and oligomerization based on group 4-metals catalysis. The bibliographic section outlines the endeavors invested by few research groups regarding trimerization mechanism and active species investigations. Even though it is currently agreed that a cationic Ti^{IV} complex trimerizes ethylene through a metallacycle process, there is no clear description of the activation process and related intermediates. More precisely, it has not yet been possible to understand the precise role of MAO on the precatalyst (FI)TiCl₃ for the formation of the active species [(FI)Ti^{IV}Me₂]⁺. Consequently, no reaction intermediates have been identified, which prevents a straightforward and detailed explanation of the activation steps. Additionally, this lack of information raises interrogations on the origin of side reactions. Indeed, ethylene polymerization remains unsuccessfully explained in the case of SFI and other titanium-based trimerization systems. Seldom studies shed light on two parameters influencing the selectivity of the system: the temperature and the type of cocatalyst.

Duchateau *et al.* initiated the study of the influence of temperature. They evidenced an alteration of reactivity at only two temperatures (28 °C and 58 °C). The temperature-promoted production of polyethylene raise several questions: Is the activity of polymerization species enhanced at higher temperature? Or are there other polymerization species formed? Or both? Is the transition from trimerization to polymerization catalysis thermally induced? What chemical transformation of the catalyst occurs in this case? A deeper investigation with respect to the temperature effect on this system would be beneficial to find part of the answers.

One can wonder whether polymerization species result from deviations during activation process and/or during the trimerization reaction. Regarding activation, doubts remain on the key steps for polymerization active species formation. Many reactions associated with MAO can be blamed such as partial precatalyst alkylations, ineffective cationization or even ligand alteration and/or abstraction caused by free TMA contained in the MAO. Duchateau *et al.* illustrated the complexity of activators effect when mixing cocatalyst and premixing pre- and co-catalysts.

Once in presence of ethylene, further active species transformations can be presumed. It is reasonable to consider an incomplete reduction to Ti^{II} leading to species that preferentially coordinate/insert olefins. Then, during the overall trimerization/polymerization process, alterations of the complex configuration or even the ligand structure can be caused by various factors: comproportionation, ligand transfer, structural changes etc. To clarify the overall scheme of active species formations, it would be worth studying the evolution of polymer, 1-hexene and $C_{>10}$ oligomers production throughout the catalytic process. Kinetic investigations would provide a potential correlation between polymerization and trimerization species. In this PhD project, the challenge lies in targeting and checking the most probable hypotheses for this side reaction of polymerization among multiple scenari.

V.2. Main hypothesis for polyethylene production

V.2.1. Ligand alterations

Literature investigation shed light on the sensitive structure/reactivity relationship of the system. To make matters even worse, phenoxy-imine complexes are subject to rearrangements: *fac/mer* configuration changes, ligand transfer or even chemical transformation often involving the imine group. For instance, the conversion of the imine into a secondary amine group induced by the cocatalyst was observed by Floriani *et al.*²⁰⁰ Moreover, this study shows that miscellaneous tridentate diphenoxy-imine complexes are known for ethylene polymerization. It has to be emphasized that some complexes and the trimerization SFI complex are very close in terms of ligand structure. In addition, the transformation of a dative to covalent bond related to the methoxy group was highlighted by Chen *et al.*⁹⁸ It turns out that such diphenoxy-imine complexes are moderately active as ethylene polymerization species.

V.2.2. Ligand transfer

The use of MAO as activator raises the concern on complex modifications by the action "free-TMA". Duchateau *et al.* ascribed polymerization to a " TiR_x^+ " species emerging from a ligand abstraction by TMA. Additionally, a ligand transfer to the aluminum affording a $(FI)AlMe_2$ species is found in the literature for $[C_6F_5N=CH(2-O-C_6H_3-3-tBu)]_2TiMe_2$ complex.²⁰¹ This phenomenon was revealed by the addition of TMA in the reaction media. The resulting "ligand-free" species would react similarly to the first homogeneous Ziegler-Natta catalysts reported by Natta.²⁰² Eventually, since original bis(phenoxy-imine) systems were developed for ethylene polymerization, it is not unreasonable to suppose the formation of such disubstituted complex by ligand transfer between two complexes or during the complex synthesis.

V.2.3. Ti^{III} formation

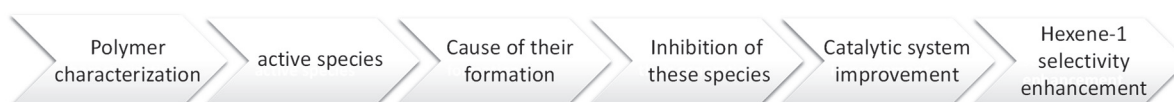
The progressive formation of a Ti^{III} species was observed by EPR analyses implemented by both Bercau and Talsi research teams.^{194,196} They advocate the comproportionation Ti^{II}/Ti^{IV} to explain the accumulation of this reduced species in the reaction media. Several examples of homogeneous Ti^{III} systems for ethylene polymerization exist, which supports the assumption of Ti^{III} as polymerization active species in the trimerization system (see II.4.1.2 Mechanism and kinetics).

Other hypotheses implicate radical process for the generation of Ti^{III}. One example of reduction of Ti^{IV} via homolytic cleavage and reversible transfer to toluene was given by Zaccaria *et al.*²⁰³ Besides, cationic Ti^{III} species is said to be inactive towards ethylene polymerization. In fact, the formation of a cationic Ti^{IV}-benzyl species, resulting from the combination with the benzyl radical, is the key step for further ethylene polymerization.

V.3. Polymer-to-catalyst strategy

In this work, an innovative strategy was implemented in order to get more insights into the SFI ethylene trimerization system. As mentioned previously, an unclear activation process limits the understanding of trimerization and polymerization process. The strategy adopted in this PhD project intend to focus on the cause of ethylene polymerization, which impairs the selectivity and process operation the most. This original approach corresponds to the so-called polymer-to-catalyst strategy. Although several publications are devoted to SFI trimerization systems, no polymerization rationalization has been reported so far.

In their respective field, researches on catalytic olefin oligomerization and polymerization only focused on the compound they target without paying attention to secondary products, purposely or not. In fact, Ye and coworkers are the only one who reported the analysis of the polyethylene in the case of ethylene trimerization with Hessen's hemi-metallocene.¹⁷⁶ Given that studies on the starting point of the process seem difficult, our strategy is oriented toward the end of chain products. In fact, collecting information about the polyethylene enables to identify the type of polymerization active species and to investigate further the reasons for their formation (Scheme 14).



Scheme 14. Innovative polymer-to-catalyst strategy focusing on polymer to improve 1-hexene selectivity

Based on this strategy, this PhD project was divided into three main axes of research.

The study of the effect of temperature on SFI system reactivity and resulting polymer is reported in chapter 2. Considering molar mass and chemical composition distributions of the polymers, conclusions on the nature of polymerization active species can be drawn.

To determine the relationship between trimerization and polymerization active species, the kinetic of product formation and polymer properties were concomitantly analyzed in chapter 3. It is also possible to play with the several parameters (premix, hydrogen, 1-hexene) to assess the reactivity of trimerization and polymerization active species. These studies provide further information regarding the behavior of active species. From the combination of the observed trends, some hypotheses can be put aside, which narrows down the scope of active species investigation.

Eventually, the second and third steps of Scheme 14 are part of the active species investigations based on hypotheses extracted from aforementioned studies. In chapter 4, it is not only question of testing the suspected species toward polymerization, but also finding explanation for their formation in the reaction medium. The main hypotheses include assumptions related to literature as well as behavioral study of the system according to the parameters considered (temperature, 1-hexene content in the liquid phase).

VI. REFERENCES

- 1 Y. Suzuki, S. Kinoshita, A. Shibahara, S. Ishii, K. Kawamura, Y. Inoue and T. Fujita, *Organometallics*, 2010, **29**, 2394–2396.
- 2 H. Audouin, phdthesis, Ecole normale supérieure de Lyon - ENS LYON, 2015.
- 3 Jadwiga. Skupinska, *Chem. Rev.*, 1991, **91**, 613–648.
- 4 A. Rudin, V. Grinshpun and K. F. O’driscoll, *J. Liq. Chromatogr.*, 1984, **7**, 1809–1821.
- 5 Y. Imanishi and N. Naga, *Prog. Polym. Sci.*, 2001, **26**, 1147–1198.
- 6 J. B. P. Soares and T. F. L. McKenna, *Polyolefin reaction and engineering*, Wiley-VCH, 2012.
- 7 E. Cossoul, L. Baverel, E. Martigny, T. Macko, C. Boisson and O. Boyron, *Macromol. Symp.*, 2013, **330**, 42–52.
- 8 A. Shrivastava, in *Introduction to Plastics Engineering*, ed. A. Shrivastava, William Andrew Publishing, 2018, pp. 17–48.
- 9 R. M. Patel, in *Multilayer Flexible Packaging (Second Edition)*, ed. J. R. Wagner, William Andrew Publishing, 2016, pp. 17–34.
- 10 PlasticsEurope, Berlin, 2016.
- 11 PlasticsEurope, *Plastics – the Facts 2017*, .
- 12 M. Demirors, in *100+ Years of Plastics. Leo Baekeland and Beyond*, American Chemical Society, 2011, vol. 1080, pp. 115–145.
- 13 R. Mülhaupt, *Macromol. Chem. Phys.*, 2013, **214**, 159–174.
- 14 T. Hees, F. Zhong, M. Stürzel and R. Mülhaupt, *Macromol. Rapid Commun.*, 2019, **40**, 1800608.
- 15 M. P. McDaniel, in *Handbook of Transition Metal Polymerization Catalysts*, John Wiley & Sons, Ltd, 2018, pp. 401–571.
- 16 Y. V. Kissin, T. E. Nowlin and R. I. Mink, in *Handbook of Transition Metal Polymerization Catalysts*, John Wiley & Sons, Ltd, 2018, pp. 189–227.
- 17 K. Nomura and X. Hou, in *Handbook of Transition Metal Polymerization Catalysts*, John Wiley & Sons, Ltd, 2018, pp. 313–337.
- 18 W. Kaminsky, Ed., *Polyolefins: 50 years after Ziegler and Natta I: Polyethylene and Polypropylene*, Springer-Verlag, Berlin Heidelberg, 2013.
- 19 R. A. Collins, A. F. Russell and P. Mountford, *Appl. Petrochem. Res.*, 2015, **5**, 153–171.
- 20 W. Kaminsky, *J. Polym. Sci. Part Polym. Chem.*, 2004, **42**, 3911–3921.
- 21 V. C. Gibson and S. K. Spitzmesser, *Chem. Rev.*, 2003, **103**, 283–316.
- 22 M. P. McDaniel, in *Handbook of Transition Metal Polymerization Catalysts*, John Wiley & Sons, Ltd, 2018, pp. 401–571.
- 23 C. Brown, A. Lita, Y. Tao, N. Peek, M. Crosswhite, M. Mileham, J. Krzystek, R. Achey, R. Fu, J. K. Bindra, M. Polinski, Y. Wang, L. J. van de Burgt, D. Jeffcoat, S. Profeta, A. E. Stiegman and S. L. Scott, *ACS Catal.*, 2017, **7**, 7442–7455.
- 24 E. Groppo, G. A. Martino, A. Piovano and C. Barzan, *ACS Catal.*, 2018, **8**, 10846–10863.
- 25 M. P. Conley, M. F. Delley, G. Siddiqi, G. Lapadula, S. Norsic, V. Monteil, O. V. Safonova and C. Copéret, *Angew. Chem. Int. Ed.*, 2014, **53**, 1872–1876.
- 26 M. P. McDaniel, in *Advances in Catalysis*, eds. D. D. Eley, H. Pines and P. B. Weisz, Academic Press, 1985, vol. 33, pp. 47–98.
- 27 M. P. McDaniel, in *Advances in Catalysis*, eds. B. C. Gates and H. Knözinger, Academic Press, 2010, vol. 53, pp. 123–606.
- 28 E. J. Baerends, D. E. Ellis and P. Ros, *Theor. Chim. Acta*, 1972, **27**, 339–354.
- 29 E. J. Arlman and P. Cossee, *J. Catal.*, 1964, **3**, 99–104.
- 30 Y. V. Kissin, R. I. Mink, T. E. Nowlin and A. J. Brandolini, *Top. Catal.*, 1999, **7**, 69–88.
- 31 K. Ziegler, *Angew. Chem.*, 1952, **64**, 323–329.

- 32 G. Natta and P. Corradini, *Il Nuovo Cimento 1955-1965*, 1960, **15**, 40–51.
- 33 G. Natta, P. Pino, G. Mazzanti and U. Giannini, *J. Am. Chem. Soc.*, 1957, **79**, 2975–2976.
- 34 N. Kashiwa, *J. Polym. Sci. Part Polym. Chem.*, 2004, **42**, 1–8.
- 35 Y. V. Kissin, R. I. Mink and T. E. Nowlin, *J. Polym. Sci. Part Polym. Chem.*, 1999, **37**, 4255–4272.
- 36 J. C. W. Chien and T. Nozaki, *J. Polym. Sci. Part Polym. Chem.*, 1993, **31**, 227–237.
- 37 M. P. McDaniel, E. D. Schwerdtfeger and M. D. Jensen, *J. Catal.*, 2014, **314**, 109–116.
- 38 H. Sinn, W. Kaminsky, H.-J. Vollmer and R. Woldt, *Angew. Chem. Int. Ed. Engl.*, 1980, **19**, 390–392.
- 39 W. Kaminsky, *Macromolecules*, 2012, **45**, 3289–3297.
- 40 W. Kaminsky, H.-J. Vollmer, E. Heins and H. Sinn, *Makromol. Chem.*, 1974, **175**, 443–456.
- 41 M. Linnolahti and S. Collins, *ChemPhysChem*, 2017, **18**, 3369–3374.
- 42 H. S. Zijlstra and S. Harder, *Eur. J. Inorg. Chem.*, 2015, **2015**, 19–43.
- 43 M. Bochmann, *Organometallics*, 2010, **29**, 4711–4740.
- 44 E. Y.-X. Chen and T. J. Marks, *Chem. Rev.*, 2000, **100**, 1391–1434.
- 45 F. Zaccaria, C. Zuccaccia, R. Cipullo, P. H. M. Budzelaar, A. Macchioni, V. Busico and C. Ehm, *ACS Catal.*, 2019, **9**, 2996–3010.
- 46 F. Ghiotto, C. Pateraki, J. R. Severn, N. Friederichs and M. Bochmann, *Dalton Trans.*, 2013, **42**, 9040–9048.
- 47 X. Yang, C. L. Stern and T. J. Marks, *J. Am. Chem. Soc.*, 1991, **113**, 3623–3625.
- 48 Fina Technologies, EP0427697, 1996.
- 49 Dow Chemicals, WO1999042467, 1999.
- 50 S. J. Lancaster, D. A. Walker, M. Thornton-Pett and M. Bochmann, *Chem. Commun.*, 1999, 1533–1534.
- 51 M. Bochmann, *J. Organomet. Chem.*, 2004, **689**, 3982–3998.
- 52 N. G. Maksimov, G. A. Nesterov, V. A. Zakharov, P. V. Stchastnev, V. F. Anufrienko and Yu. I. Yermakov, *J. Mol. Catal.*, 1978, **4**, 167–179.
- 53 J. L. Barr, A. Kumar, D. Lionetti, C. A. Cruz and J. D. Blakemore, *Organometallics*, 2019, **38**, 2150–2155.
- 54 H. H. Brintzinger, D. Fischer, R. Mülhaupt, B. Rieger and R. M. Waymouth, *Angew. Chem. Int. Ed. Engl.*, 1995, **34**, 1143–1170.
- 55 J. R. Severn and J. C. Chadwick, *Tailor-Made Polymers. Via immobilization of Alpha-Olefin polymerization Catalysis.*, Willey-VCH., 2008.
- 56 G. W. Coates, *Chem. Rev.*, 2000, **100**, 1223–1252.
- 57 R. Quijada, R. B. Scipioni, R. S. Mauler, G. B. Galland and M. S. L. Miranda, *Polym. Bull.*, 1995, **35**, 299–306.
- 58 S. Mehdiabadi and J. B. P. Soares, *Macromolecules*, 2016, **49**, 2448–2457.
- 59 S. Saadat, MSc, University of Alberta.
- 60 F. R. Mayo and F. M. Lewis, *J. Am. Chem. Soc.*, 1944, **66**, 1594–1601.
- 61 A. L. McKnight and R. M. Waymouth, *Chem. Rev.*, 1998, **98**, 2587–2598.
- 62 D. W. Carpenetti, L. Kloppenburg, J. T. Kupec and J. L. Petersen, *Organometallics*, 1996, **15**, 1572–1581.
- 63 J. C. Stevens, in *Studies in Surface Science and Catalysis*, eds. K. Soga and M. Terano, Elsevier, 1994, vol. 89, pp. 277–284.
- 64 J. Klosin, W. J. Kruper, P. N. Nickias, G. R. Roof, P. De Waele and K. A. Abboud, *Organometallics*, 2001, **20**, 2663–2665.
- 65 European Union, EP0416815A2, 1991.
- 66 M. C. Baier, M. A. Zuideveld and S. Mecking, *Angew. Chem. Int. Ed.*, 2014, **53**, 9722–9744.
- 67 G. J. P. Britovsek, V. C. Gibson and D. F. Wass, *Angew. Chem. Int. Ed.*, 1999, **38**, 428–447.

- 68 K. P. Bryliakov, *Russ. Chem. Rev.*, 2007, **76**, 253.
- 69 R. Figueroa, R. D. Froese, Y. He, J. Klosin, C. N. Theriault and K. A. Abboud, *Organometallics*, 2011, **30**, 1695–1709.
- 70 P. P. Fontaine, R. Figueroa, S. D. McCann, D. Mort and J. Klosin, *Organometallics*, 2013, **32**, 2963–2972.
- 71 P. S. Chum and K. W. Swogger, *Prog. Polym. Sci.*, 2008, **33**, 797–819.
- 72 R. D. J. Froese, P. D. Hustad, R. L. Kuhlman and T. T. Wenzel, *J. Am. Chem. Soc.*, 2007, **129**, 7831–7840.
- 73 Univation technologies, WO2010008964A1, 2010.
- 74 Mitsui Chemicals, US6309997B1, 2001.
- 75 Nova Chemicals, US20060122342A1, 2006.
- 76 H. Makio, H. Terao, A. Iwashita and T. Fujita, *Chem. Rev.*, 2011, **111**, 2363–2449.
- 77 H. Makio, N. Kashiwa and T. Fujita, *Adv. Synth. Catal.*, 2002, **344**, 477–493.
- 78 T. Matsugi and T. Fujita, *Chem. Soc. Rev.*, 2008, **37**, 1264–1277.
- 79 P. G. Cozzi, E. Gallo, C. Floriani, A. Chiesi-Villa and C. Rizzoli, *Organometallics*, 1995, **14**, 4994–4996.
- 80 Mitsui Chemicals, EP0874005B1, 2003.
- 81 J. Saito, M. Mitani, J. Mohri, Y. Yoshida, S. Matsui, S. Ishii, S. Kojoh, N. Kashiwa and T. Fujita, *Angew. Chem. Int. Ed.*, 2001, **40**, 2918–2920.
- 82 Y. Yoshida, S. Matsui, Y. Takagi, M. Mitani, M. Nitabaru, T. Nakano, H. Tanaka and T. Fujita, *Chem. Lett.*, 2005, **29**, 1270–1271.
- 83 G. Talarico and P. H. M. Budzelaar, *Organometallics*, 2016, **35**, 47–54.
- 84 J. Saito, Y. Suzuki, H. Makio, H. Tanaka, M. Onda and T. Fujita, *Macromolecules*, 2006, **39**, 4023–4031.
- 85 Y. Yoshida, T. Nakano, H. Tanaka and T. Fujita, *Isr. J. Chem.*, 2002, **42**, 353–359.
- 86 R. Furuyama, M. Mitani, J. Mohri, R. Mori, H. Tanaka and T. Fujita, *Macromolecules*, 2005, **38**, 1546–1552.
- 87 E. Yao, J. Wang, Z. Chen and Y. Ma, *Macromolecules*, 2014, **47**, 8164–8170.
- 88 M. Mitani, J. Saito, S. Ishii, Y. Nakayama, H. Makio, N. Matsukawa, S. Matsui, J. Mohri, R. Furuyama, H. Terao, H. Bando, H. Tanaka and T. Fujita, *Chem. Rec.*, 2004, **4**, 137–158.
- 89 Y. Nakayama, H. Bando, Y. Sonobe and T. Fujita, *J. Mol. Catal. Chem.*, 2004, **213**, 141–150.
- 90 S. Ishii, J. Saito, S. Matsuura, Y. Suzuki, R. Furuyama, M. Mitani, T. Nakano, N. Kashiwa and T. Fujita, *Macromol. Rapid Commun.*, 2002, **23**, 693–697.
- 91 S. Talebi, R. Duchateau, S. Rastogi, J. Kaschta, G. W. M. Peters and P. J. Lemstra, *Macromolecules*, 2010, **43**, 2780–2788.
- 92 D. Peng, X. Yan, C. Yu, S. Zhang and X. Li, *Polym. Chem.*, 2016, **7**, 2601–2634.
- 93 C. Wang, Z. Ma, X.-L. Sun, Y. Gao, Y.-H. Guo, Y. Tang and L.-P. Shi, *Organometallics*, 2006, **25**, 3259–3266.
- 94 F. da S. Gomes, A. L. Bergamo and O. de L. Casagrande, *Macromol. Chem. Phys.*, 2014, **215**, 1735–1743.
- 95 W.-Q. Hu, X.-L. Sun, C. Wang, Y. Gao, Y. Tang, L.-P. Shi, W. Xia, J. Sun, H.-L. Dai, X.-Q. Li, X.-L. Yao and X.-R. Wang, *Organometallics*, 2004, **23**, 1684–1688.
- 96 D. Owiny, S. Parkin and F. T. Ladipo, *J. Organomet. Chem.*, 2003, **678**, 134–141.
- 97 T. Xu, J. Liu, G.-P. Wu and X.-B. Lu, *Inorg. Chem.*, 2011, **50**, 10884–10892.
- 98 Q. Chen, J. Huang and J. Yu, *Inorg. Chem. Commun.*, 2005, **8**, 444–448.
- 99 P. A. do Couto Junior, M. Nele and F. M. B. Coutinho, *Eur. Polym. J.*, 2002, **38**, 1471–1476.
- 100 J. Zhang, Y.-J. Lin and G.-X. Jin, *Organometallics*, 2007, **26**, 4042–4047.
- 101 Mitsui Chemicals, JP2011016789, 2011.
- 102 P. G. de Gennes, *J. Chem. Phys.*, 1971, **55**, 572–579.

- 103 H. G. Barth, Christian. Jackson and B. E. Boyes, *Anal. Chem.*, 1994, **66**, 595–620.
- 104 W. Kaminsky and M. Fernandes, *Polyolefins J.*, 2015, **2**, 1–16.
- 105 J. R. Severn, in *Multimodal Polymers with Supported Catalysts: Design and Production*, eds. A. R. Albulnia, F. Prades and D. Jeremic, Springer International Publishing, Cham, 2019, pp. 1–53.
- 106 Metallocenes Rise Again | October 18, 2010 Issue - Vol. 88 Issue 42 | Chemical & Engineering News, <https://cen.acs.org/articles/88/i42/Metallocenes-Rise-Again.html>,
- 107 E. C. Kelusky, C. T. Elston and R. E. Murray, *Polym. Eng. Sci.*, 1987, **27**, 1562–1571.
- 108 W. Kaminsky, *Macromol. Chem. Phys.*, 1996, **197**, 3907–3945.
- 109 S. Hosoda, *Polym. J.*, 1988, **20**, 383–397.
- 110 A. J. Müller and M. L. Arnal, *Prog. Polym. Sci.*, 2005, **30**, 559–603.
- 111 P. Starck, *Polym. Int.*, 1996, **40**, 111–122.
- 112 P. Lehmus, O. Härkki, R. Leino, H. J. G. Luttikhedde, J. H. Näsman and J. V. Seppälä, *Macromol. Chem. Phys.*, 1998, **199**, 1965–1972.
- 113 B. Monrabal, N. Mayo, L. Romero and J. Sancho-Tello, Crystallization Elution Fractionation: A New Approach to measure the Chemical Composition Distribution in Polyolefins.
- 114 B. Monrabal, N. Mayo and R. Cong, *Macromol. Symp.*, 2012, **312**, 115–129.
- 115 B. Monrabal, J. Sancho-Tello, N. Mayo and L. Romero, *Macromol. Symp.*, 2007, **257**, 71–79.
- 116 A. A. Alghyamah and J. B. P. Soares, *Macromol. Symp.*, 2012, **312**, 43–50.
- 117 A. Ndiripo, P. S. E. Bungu and H. Pasch, *Polym. Int.*, 2019, **68**, 206–217.
- 118 J. F. Vega, S. Rastogi, G. W. M. Peters and H. E. H. Meijer, *J. Rheol.*, 2004, **48**, 663–678.
- 119 R. P. Wool, *Macromolecules*, 1993, **26**, 1564–1569.
- 120 J. D. Ferry, *Viscoelastic Properties of Polymers*, John Wiley & Sons, 1980.
- 121 S. T. Milner, *J. Rheol.*, 1996, **40**, 303–315.
- 122 A. Pawlak, *Macromol. Chem. Phys.*, 2019, **0**, 1900043.
- 123 R. N. Haward, *Macromolecules*, 1993, **26**, 5860–5869.
- 124 A. S. Argon, *J. Macromol. Sci. Part B Phys.*, 1973, **8**, 573–596.
- 125 P. Smith, P. J. Lemstra and H. C. Booij, *J. Polym. Sci. Polym. Phys. Ed.*, 1981, **19**, 877–888.
- 126 Z. Bartczak and M. Kozanecki, *Polymer*, 2005, **46**, 8210–8221.
- 127 M. A. Kennedy, A. J. Peacock and L. Mandelkern, *Macromolecules*, 1994, **27**, 5297–5310.
- 128 S. Rastogi, D. R. Lippits, G. W. M. Peters, R. Graf, Y. Yao and H. W. Spiess, *Nat. Mater.*, 2005, **4**, 635–641.
- 129 S. Rastogi, L. Kurelec, J. Cuijpers, D. Lippits, M. Wimmer and P. J. Lemstra, *Macromol. Mater. Eng.*, 2003, **288**, 964–970.
- 130 S. Ronca, D. Romano, G. Forte, E. Andablo-Reyes and S. Rastogi, *Adv. Polym. Technol.*, 2012, **31**, 193–204.
- 131 S. Ronca, G. Forte, H. Tjaden, Y. Yao and S. Rastogi, *Polymer*, 2012, **53**, 2897–2907.
- 132 P. Smith, H. D. Chanzy and B. P. Rotzinger, *J. Mater. Sci.*, 1987, **22**, 523–531.
- 133 A. Pandey, Y. Champouret and S. Rastogi, *Macromolecules*, 2011, **44**, 4952–4960.
- 134 R. P. Gote, D. Mandal, K. Patel, K. Chaudhuri, C. P. Vinod, A. K. Lele and S. H. Chikkali, *Macromolecules*, 2018, **51**, 4541–4552.
- 135 S. Rastogi, Y. Yao, S. Ronca, J. Bos and J. van der Eem, *Macromolecules*, 2011, **44**, 5558–5568.
- 136 D. Romano, N. Tops, E. Andablo-Reyes, S. Ronca and S. Rastogi, *Macromolecules*, 2014, **47**, 4750–4760.
- 137 B. P. Rotzinger, H. D. Chanzy and P. Smith, *Polymer*, 1989, **30**, 1814–1819.
- 138 Stichting Dutch Polymer Institute, US7671159B2, 2010.

- 139 K. Liu, E. L. de Boer, Y. Yao, D. Romano, S. Ronca and S. Rastogi, *Macromolecules*, 2016, **49**, 7497–7509.
- 140 D. R. Lippits, S. Rastogi and G. W. H. Höhne, *Phys. Rev. Lett.*, 2006, **96**, 218303.
- 141 Y. F. Yao, S. Rastogi, H. J. Xue, Q. Chen, R. Graf and R. Verhoef, *Polymer*, 2013, **54**, 411–422.
- 142 S. Yamazaki, M. Hikosaka, A. Toda, I. Wataoka and F. Gu, *Polymer*, 2002, **43**, 6585–6593.
- 143 C. P. Nicholas, *Appl. Catal. Gen.*, 2017, **543**, 82–97.
- 144 A. Forestière, H. Olivier-Bourbigou and L. Saussine, *Oil Gas Sci. Technol. - Rev. IFP*, 2009, **64**, 649–667.
- 145 G. R. Lappin and J. D. Sauer, *Routes to alpha-olefins. In alpha olefins application handbook*, 1992.
- 146 G. J. P. Britovsek, R. Malinowski, D. S. McGuinness, J. D. Nobbs, A. K. Tomov, A. W. Wadsley and C. T. Young, *ACS Catal.*, 2015, **5**, 6922–6925.
- 147 P.-A. Breuil, L. Magna and H. Olivier-Bourbigou, *Catal Lett*, 2014, **145**, 173–192.
- 148 W. Keim, *Chem. Ing. Tech.*, 1984, **56**, 850–853.
- 149 Idemitsu, US4814540 A, 1989.
- 150 Idemitsu, US6555633 B1, 2003.
- 151 Linde, DE 19812066 A1, 1998.
- 152 J. R. Briggs, *J. Chem. Soc. Chem. Commun.*, 1989, **0**, 674–675.
- 153 B. Venderbosch, J.-P. H. Oudsen, L. A. Wolzak, D. J. Martin, T. J. Korstanje and M. Tromp, *ACS Catal.*, 2019, **9**, 1197–1210.
- 154 I. Y. Skobelev, V. N. Panchenko, O. Y. Lyakin, K. P. Bryliakov, V. A. Zakharov and E. P. Talsi, *Organometallics*, 2010, **29**, 2943–2950.
- 155 D. S. McGuinness, D. B. Brown, R. P. Tooze, F. M. Hess, J. T. Dixon and A. M. Z. Slawin, *Organometallics*, 2006, **25**, 3605–3610.
- 156 D. H. Morgan, J. T. Dixon, M. J. Green and F. M. Hess, *J. Organomet. Chem.*, 2004, **689**, 3641–3668.
- 157 P. W. N. M. van Leeuwen, N. D. Clément and M. J.-L. Tschan, *Coord. Chem. Rev.*, 2011, **255**, 1499–1517.
- 158 J. T. Dixon, M. J. Green, F. M. Hess and D. H. Morgan, *J. Organomet. Chem.*, 2004, **689**, 3641–3668.
- 159 D. S. McGuinness, *Chem. Rev.*, 2011, **111**, 2321–2341.
- 160 T. Agapie, *Coord. Chem. Rev.*, 2011, **255**, 861–880.
- 161 K. Ziegler, M. Heinz, US2943125 A, 1960.
- 162 A. W. Al-Sa'doun, *Appl. Catal. Gen.*, 1993, **105**, 1–40.
- 163 A. Forestière, H. Olivier-Bourbigou and L. Saussine, *Oil Gas Sci. Technol. - Rev. IFP*, 2009, **64**, 649–667.
- 164 Institut Francais du Petrole, EP0135441 A1, 1985.
- 165 A. Bre and Y. Chauvin, *Nouv J Chim*, 1986, **10**, 535.
- 166 J. A. Suttill and D. S. McGuinness, *Organometallics*, 2012, **31**, 7004–7010.
- 167 R. Robinson, D. S. McGuinness and B. F. Yates, *ACS Catal.*, 2013, **3**, 3006–3015.
- 168 Y. You and G. S. Girolami, *Organometallics*, 2008, **27**, 3172–3180.
- 169 C. Pellecchia, D. Pappalardo and G.-J. Gruter, *Macromolecules*, 1999, **32**, 4491–4493.
- 170 B. Hessen, P. J. W. Deckers and J. H. Teuben, *Angew. Chem. Int. Ed.*, 2001, **40**, 2516–2519.
- 171 B. Hessen, P. J. W. Deckers and J. H. Teuben, *Organometallics*, 2002, **21**, 5122–5135.
- 172 J. Huang, T. Wu and Y. Qian, *Chem. Commun.*, 2003, 2816–2817.
- 173 S. Tobisch and T. Ziegler, *J. Am. Chem. Soc.*, 2004, **126**, 9059–9071.
- 174 Polimeri Europa, EP1514860A1, 2005.

- 175 Y. Suzuki, S. Kinoshita, A. Shibahara, S. Ishii, K. Kawamura, Y. Inoue and T. Fujita, *Organometallics*, 2010, **29**, 2394–2396.
- 176 Z. Ye, F. AlObaidi and S. Zhu, *Macromol. Rapid Commun.*, 2004, **25**, 647–652.
- 177 C. P. Gordon, S. Shirase, K. Yamamoto, R. A. Andersen, O. Eisenstein and C. Copéret, *Proc. Natl. Acad. Sci.*, 2018, **115**, E5867–E5876.
- 178 H. Hagen, W. P. Kretschmer, F. R. van Buren, B. Hessen and D. A. van Oeffelen, *J. Mol. Catal. Chem.*, 2006, **248**, 237–247.
- 179 Z. Ye, F. AlObaidi and S. Zhu, *Macromol. Rapid Commun.*, 2004, **25**, 647–652.
- 180 S. Ishii, T. Nakano, K. Kawamura, S. Kinoshita, S. Ichikawa and T. Fujita, *Catal. Today*, 2018, **303**, 263–270.
- 181 https://www.mitsuichem.com/en/techno/license/pdf/met_process.pdf
- 182 H. Audouin, R. Bellini, L. Magna, N. Mézailles and H. Olivier-Bourbigou, *Eur. J. Inorg. Chem.*, 2015, **2015**, 5272–5280.
- 183 J. A. Suttill, D. S. McGuinness, M. G. Gardiner and S. J. Evans, *Dalton Trans.*, 2013, **42**, 4185–4196.
- 184 J. A. Suttill, M. F. Shaw, D. S. McGuinness, M. G. Gardiner and S. J. Evans, *Dalton Trans.*, 2013, **42**, 9129–9138.
- 185 Mitsui Chemicals, WO2009005003 A1, 2009.
- 186 R. Duchateau, F. F. Karbach and J. R. Severn, *ACS Catal.*, 2015, **5**, 5068–5076.
- 187 J. E. Bercaw, A. Sattler, D. C. Aluthge, J. R. Winkler and J. A. Labinger, *ACS Catal.*, 2016, **6**, 19–22.
- 188 Z. J. A. Komon and G. C. Bazan, *Macromol. Rapid Commun.*, 2001, **22**, 467–478.
- 189 D. L. Beach and Y. V. Kissin, *J. Polym. Sci. Polym. Chem. Ed.*, 1984, **22**, 3027–3042.
- 190 S. Liu, A. Motta, M. Delferro and T. J. Marks, *J. Am. Chem. Soc.*, 2013, **135**, 8830–8833.
- 191 E. D. Schwerdtfeger, C. J. Price, J. Chai and S. A. Miller, *Macromolecules*, 2010, **43**, 4838–4842.
- 192 R. Duchateau, F. F. Karbach and T. Macko, *Macromolecules*, 2016, **49**, 1229–1241.
- 193 J. E. Bercaw, D. C. Aluthge, A. Sattler, M. A. Al-Harhi and J. A. Labinger, *ACS Catal.*, 2016, **6**, 6581–6584.
- 194 I. E. Soshnikov, N. V. Semikolenova, J. Ma, K.-Q. Zhao, V. A. Zakharov, K. P. Bryliakov, C. Redshaw and E. P. Talsi, *Organometallics*, 2014, **33**, 1431–1439.
- 195 A. Sattler, J. A. Labinger and J. E. Bercaw, *Organometallics*, 2013, **32**, 6899–6902.
- 196 A. Sattler, D. G. VanderVelde, J. A. Labinger and J. E. Bercaw, *J. Am. Chem. Soc.*, 2014, **136**, 10790–10800.
- 197 S. Tobisch and T. Ziegler, *Organometallics*, 2003, **22**, 5392–5405.
- 198 D. K. Steelman, D. C. Aluthge, M. C. Lehman, J. A. Labinger and J. E. Bercaw, *ACS Catal.*, 2017, 4922–4926.
- 199 A. N. J. Blok, P. H. M. Budzelaar and A. W. Gal, *Organometallics*, 2003, **22**, 2564–2570.
- 200 C. Floriani, E. Solari, F. Corazza, A. Chiesi-Villa and C. Guastini, *Angew. Chem. Int. Ed. Engl.*, 1989, **28**, 64–66.
- 201 H. Makio, T. Oshiki, K. Takai and T. Fujita, *Chem. Lett.*, 2005, **34**, 1382–1383.
- 202 G. Natta, P. Pino, G. Mazzanti, U. Giannini, E. Mantica and M. Peraldo, *J. Polym. Sci.*, 1957, **26**, 120–123.
- 203 F. Zaccaria, C. Ehm, P. H. M. Budzelaar, V. Busico and R. Cipullo, *Organometallics*, 2018, **37**, 2872–2879.

Chapter 2.
Effect of temperature
on (FI)TiCl₃/MAO
system: reactivity and
polymer features
investigation

TABLE OF CONTENT

I. INTRODUCTION	90
II. BEHAVIOR OF THE TRIMERIZATION SYSTEM WITH TEMPERATURE	91
II.1. REACTANTS AND PRODUCTS	91
II.1.1. CATALYTIC SYSTEM	91
II.1.1.1. Precatalyst	91
II.1.1.2. Co-catalyst	92
II.1.2. PRODUCTS OF TRIMERIZATION AND POLYMERIZATION REACTIONS.....	93
II.1.3. CATALYTIC CONDITIONS OPTIMIZATION	94
II.2. TEMPERATURE EFFECT ON ACTIVITY AND SELECTIVITY.....	96
II.2.1. EVOLUTION OF THE ACTIVITY	96
II.2.2. EFFECT OF TEMPERATURE ON THE SELECTIVITY	98
II.2.3. DISCUSSION ON TEMPERATURE EFFECT ON POLYMERIZATION ACTIVE SPECIES FORMATION	101
III. IN-DEPTH POLYMER ANALYSIS	104
III.1. POLYMER FEATURES	104
III.1.1. MOLAR MASS DISTRIBUTION (MMD)	104
III.1.2. CHEMICAL COMPOSITION OF POLYMERS PE-SFS-26 TO PE-SFS-80	105
III.1.2.1. Chain branching identification in polymers.....	105
III.1.2.2. 1-Hexene content in polymers PE-SFS-26 to PE-SFS-80	107
III.1.2.2.1. Evolution of 1-hexene content with reaction temperature	107
III.1.2.2.2. 1-hexene content in the polymer versus reaction medium.....	109
III.1.2.2.3. Link between melting temperature and 1-hexene content	110
III.2. ADVANCES ANALYSIS OF PE-SFS-26 TO PE-SFS-80.....	112
III.2.1. CHEMICAL COMPOSITION DISTRIBUTION OF THE POLYMERS	112
III.2.1.1. Stepwise Isothermal Segregation Technique (SIST)	112
III.2.1.2. Crystallization Elution Fractionation (CEF)	114
III.2.1.2.1. Observations and hypotheses	114
III.2.1.2.2. Investigation of the CEF technique.....	116
III.2.2. POLYMER TOPOLOGY INVESTIGATION.....	119
III.2.2.1. Entanglement in the polymers	119
III.2.2.1.1. Annealing.....	119
III.2.2.1.2. Rheology	121
III.2.2.2. Cocrystallization effect	122
IV. CONCLUSIONS ON THE EFFECT OF TEMPERATURE AND POLYMER CHARACTERIZATION	124

V. EXPERIMENTAL SECTION	125
V.1. GENERAL CONSIDERATIONS	125
V.2. ORGANIC AND COMPLEX SYNTHESSES	126
V.3. CATALYTIC TEST PROCEDURE	128
V.3.1. EQUIPMENT	128
V.3.2. PROCEDURE	128
V.4. PRODUCT ANALYSIS	129
V.4.1. OLIGOMER ANALYSES.....	129
V.4.2. POLYMER ANALYSES	130
V.4.2.1. High-Temperature Size Exclusion Chromatography (HT-SEC).....	130
V.4.2.2. High Temperature Nuclear Magnetic Resonance (HT-NMR)	130
V.4.2.3. Differential Scanning Calorimetry (DSC)	131
V.4.2.4. Crystallization Elusion Fractionation (CEF).....	132
V.4.2.5. Rheology.....	133
VI. REFERENCES	134

I. INTRODUCTION

The single phenoxy-imine-methoxy (SFI) catalytic systems display a dual reactivity toward ethylene. Based on literature data, polymerization reaction seems negligible at low temperature but becomes significant at higher temperature. For the records, experiments performed by Duchateau *et al.* at 28 °C and 58 °C highlighted a change of selectivity from 93 wt % to 64 wt % for 1-hexene and 1.6 to 35 wt % for polyethylene.¹ Therefore, detailed temperature studies are essential to get a better understanding of the catalytic behavior of the SFI trimerization systems and the side reaction of polymerization. Such study allows to identify the optimum conditions to reach the highest activity and selectivity in 1-hexene.

In this work, the aim is to determine the effect of temperature on the activity, product selectivities and the properties of the polymer generated by a selected SFI catalytic system under fixed conditions. This chapter reports the polymer-to-catalyst investigation illustrated in Figure 1, in two main sections. First, the influence of temperature on the activity and selectivity and related hypotheses regarding the route of polymerization catalyst formation are presented. Then, a focus on molar mass distribution and chemical composition distribution of polymer as well as advanced polymer analyses are detailed.

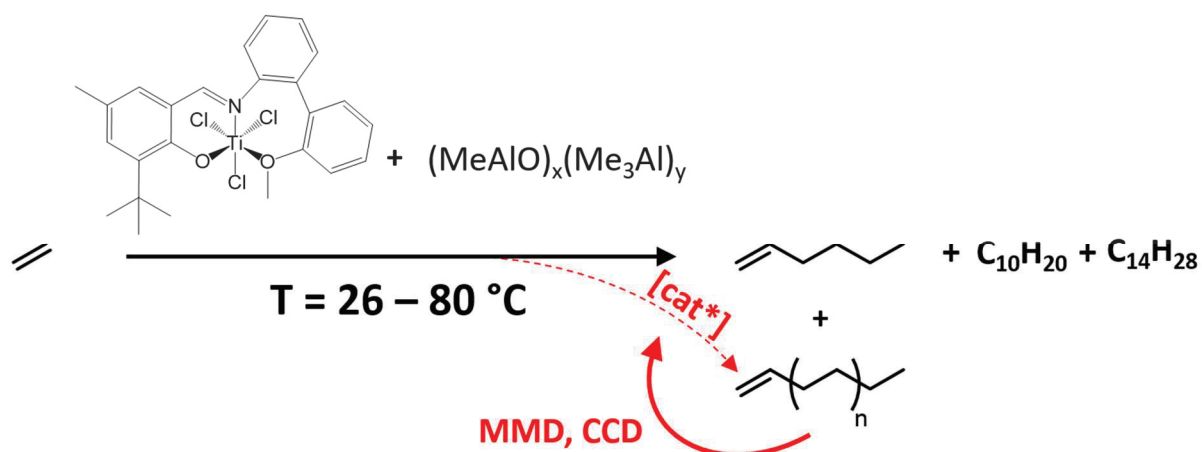


Figure 1. Schematic view of the polymer-to-catalyst strategy

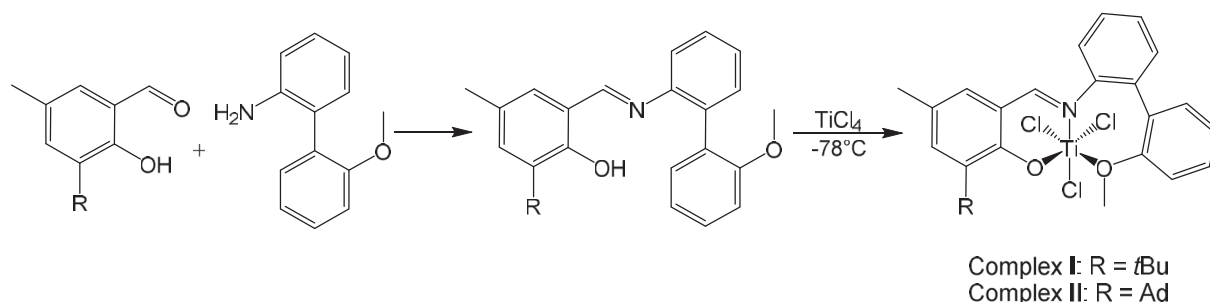
II. BEHAVIOR OF THE TRIMERIZATION SYSTEM WITH TEMPERATURE

II.1. Reactants and products

II.1.1. Catalytic system

II.1.1.1. Precatalyst

The choice of a titanium-based SFI complex was guided towards species displaying a high activity and 1-hexene selectivity upon MAO activation. As illustrated in the bibliographic section, minor structural modifications of the complex can cause the decline of 1-hexene selectivity. Thus, complex I presented in Scheme 1 was selected among the restricted number of phenoxy-imine complexes described by Fujita *et al.*² Studies carried out by Audouin showed that the adamantyl group of this SFI complex could be replaced by another bulky substituent without dramatic reactivity change.^{3,4} Complex I bearing a hindered *tert*-butyl group was synthesized according to a standard procedure (Scheme 1). Ligand moiety were obtained by orthoformylation of 2-*tert*-butyl-4-methyl-phenol and Suzuki coupling of 2-bromo-aniline and 2-methoxy-boronic acid. A simple acid-catalyzed Schiff base condensation afforded the ligand, which is further complexed to TiCl₄ at low temperature.



Scheme 1. Synthesis of SFI complex I and the original complex II described by Fujita *et al.*

Complex I was characterized by ¹H, ¹³C NMR and elemental analysis (see the experimental section). The titanium complex is obtained with a high yield of 79 %. Importantly, no side product was identified by ¹H NMR in toluene-*d*₈ (Figure 2). Characteristics chemical shifts of this complex are the *tert*-butyl and methyl groups (1.57 ppm and 1.94 ppm respectively), the methoxy group (4.07 ppm) and the imine proton (7.44 ppm). These signals were used as reference for further complex comparisons and alterations, detailed in Chapter 4.

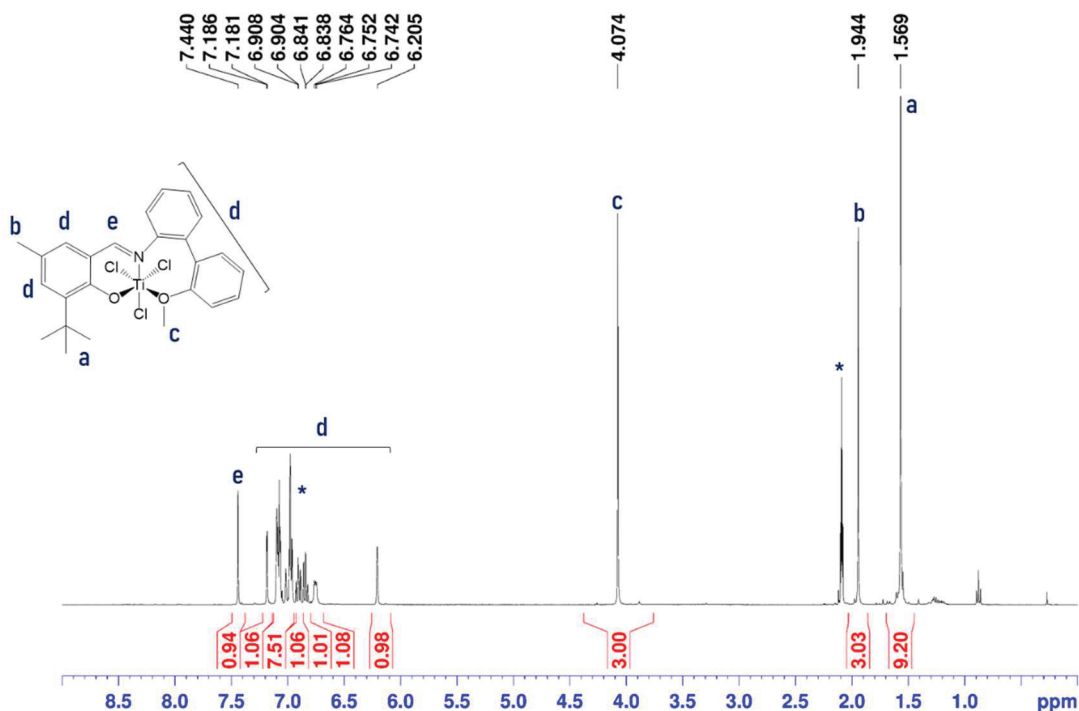


Figure 2. ¹H NMR of complex I in toluene-*d*₈ (*)

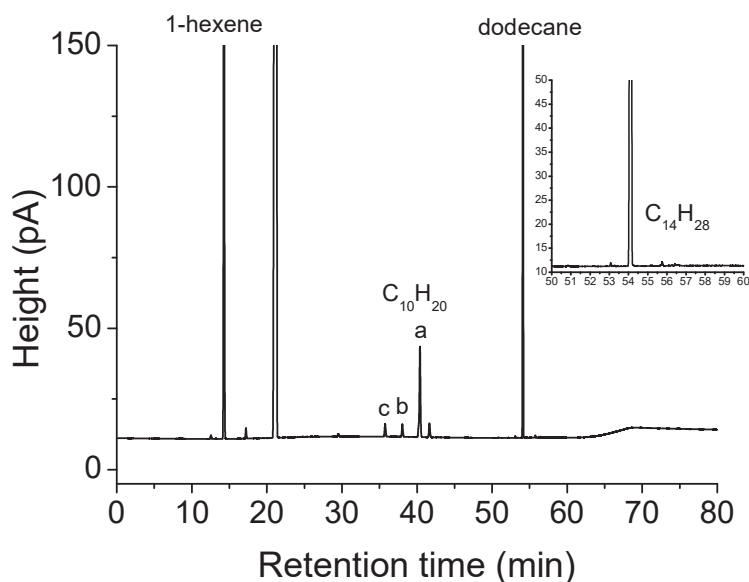
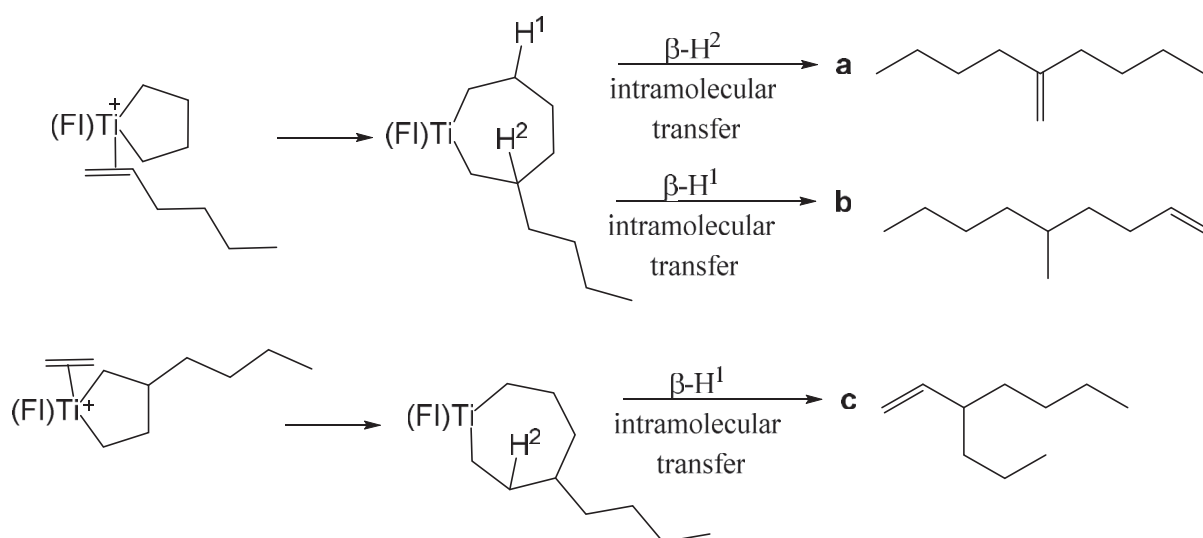
II.1.1.2. Co-catalyst

The trimerization system was studied according to the procedure developed by Fujita using complex II (Scheme 1) and methylaluminoxane as co-catalyst. They reported a large excess of 10 000 equivalents of activator to reach a high activity (6 600 kg_{1-hexene} g_{Ti}⁻¹ h⁻¹) and selectivity in 1-hexene (92.3 wt %) under 50 bar of ethylene. In this project, methylaluminoxane 30 wt % in toluene provided by Albermarle (now Grace) was employed as co-catalyst of complex I.

It has to be emphasized that the use of methylaluminoxane prevents direct characterization of active species. This limitation is intrinsically linked to the undefined structure of this ambiguous activator. Despite this hurdle, suppliers developed a ¹H NMR method to determine the general formula of the manufactured MAO.⁵ According to the specifications provided by Albermarle, the formula of MAO employed in this study is (Me_{1.44}AlO_{0.78})_{5.8}(AlMe₃). The amount of TMA was evaluated to 5.24 wt % (Al_{TMA} = 14.6 mol % of Al_{TMA+MAO}) by gas (methane) analysis. One should bear in mind that the TMA present within the MAO can possibly undergo side reactions with the SFI complex.

II.1.2. Products of trimerization and polymerization reactions

As explained in the previous chapter, the system affords C_{2+4x}H_{4+8x} (1 ≤ x ≤ 3) oligomers and polymer. Oligomers are liquid products that were analyzed by GC(-MS). The identification of C₁₀ and C₁₄ oligomers was reported by Sattler *et al.*⁶ Three C₁₀H₂₀ and several C₁₄H₂₈ oligomers are yielded as side trimerization reactions involving 2 ethylene molecules and 1-hexene or decenes (Scheme 2). Formation of decene (a) is predominant given the preferred 1,2-insertion of alpha-olefins into the Ti-C bond of the heptanacycle. Moreover, no isomerization occurs with titanium-based catalysts contrary to other oligomerization systems. Besides, no dimers were identified by GC.



Scheme 2. Formation of C_{2+4x}H_{4+8x} (1 ≤ x ≤ 3) oligomers and an example of GC chromatogram

Regarding the polymer, a jelly fish-like substance is collected as the solid is swollen by toluene (Figure 3). After treatment with acidic methanol, washing with methanol and drying under vacuum, polymer is purified from alumina and toluene residues. On average, the mass of swollen polymer is ten time higher than the dry solid. Despite a lack of reported PE analyses in literature, Audouin presumed a polyethylene of high to ultra-high molar masses because of a unsuccessful dissolution of the solid at high temperature (150 °C) in 1,2,4-trichlorobenzene.⁴

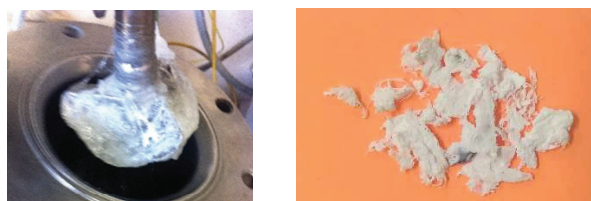


Figure 3. Polymer after reaction (left) and after drying (right)

II.1.3. Catalytic conditions optimization

The starting point of the temperature study was the optimization of catalytic conditions based on literature procedure (Table 1). From the conditions reported by Audouin (Table 1, entry 3), the quantity of pre-catalyst and co-catalyst were first set to 17.5 μmol and 420 equivalents.⁴ For studying the complex I/MAO system, it was decided that all reactions would be carried out for 30 minutes under 10 bar of ethylene in a 1-L semi-batch SFS reactor. The reactor is pressurized shortly after the successive introduction of MAO and precatalyst solution. The ethylene consumption is monitored from a 5-L ballast depressurization, while the pressure in the reactor is maintained constant during the catalytic test.

Table 1. Comparison of catalytic conditions and results with complex II (1,2) and complex I (3-5)

entry	Ref	T (°C)	P (bar)	t (min)	[Ti] ($\mu\text{mol L}^{-1}$)	Al/Ti	Solvent	Activity $\text{kg}_{\text{ethylene}} \text{g}_{\text{Ti}}^{-1} \text{h}^{-1}$	C ₆ ^c (wt %)	C ₁₀ ^c (wt %)	PE (wt %)
1	Fujita ⁷	30	8	60	16.7	10 000	30 mL Cyclohexane	169	91.4	6.4	2.1
2	Duchateau ¹	28	10	60	13.33	2 250	75 mL Isopar	67	93	5.4	1.6
3	Audouin ³	30	10	30	200	500	10 mL Toluene	294	86	12	2
4 ^a	SFS ^b	30	10	12	58.6	420	300 mL Toluene	147	71	12	17
5	SFS ^b	30	10	38	11.5	1 310	300mL Toluene	380	85	14	1

^a test time limited by ethylene feed capacities

^b 1 liter-reactor employed in this study

^cYield of oligomers quantified by GC analysis

Compared to literature procedures, a lower concentration of precatalyst was used to be able to manage temperature control. Higher titanium concentration often leads to a temperature overshoot. Indeed, ethylene trimerization and polymerization are known to be exothermic reactions.⁸ Hence a high catalyst concentration of 58.6 $\mu\text{mol L}^{-1}$ led to a violent temperature overshooting of $\Delta T = 10\text{ }^{\circ}\text{C}$ within 4 minutes (Figure 4). At low temperature, a fast ethylene uptake is observed and correlates with the fast increase of temperature. In fact, the combination of a high catalyst and ethylene concentration induces a higher reaction rate and heat released.⁹ As a result, the temperature control was achieved by decreasing the amount of precatalyst by a factor of 6 and subsequently lower the amount of MAO to 1 300 equivalents to ensure a high activity and still benefit from the reactor-scavenging role of the co-catalyst.

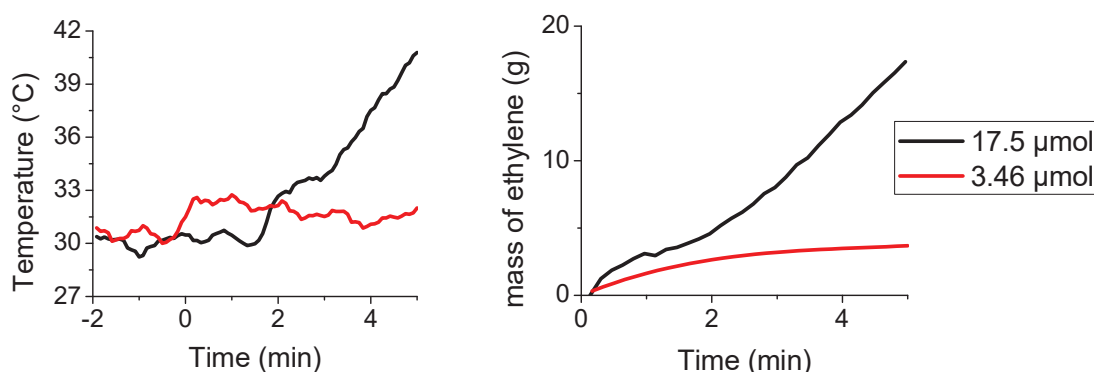


Figure 4. Evolution of the temperature (left) and ethylene consumption (right) at the early stage of the catalytic test for two precatalyst loadings (Table 1, entries 4 and 5)

Relating these exothermal effects to product selectivities, it can be observed that a decent 85 wt % selectivity was obtained when decreasing the precatalyst concentration (Table 1, entry 4 versus 5). This difference is ascribed to the uncontrolled temperature increase that surely promoted the formation of polymerization active species. This trend supports that the temperature is a crucial parameter for catalytic activity and selectivity. Indeed, from the temperature and consumption profiles, two conclusions are made:

- (i) The improvement of the activity and selectivity by the limited exothermal phenomenon enabled by diluted conditions;
- (ii) An induction period lasting 2 minutes after the pressurization to 10 bar

After optimization, it is noteworthy that activity and 1-hexene selectivity exceeded results reported by Audouin (Table 1, entry 3). Further studies will therefore be conducted under these conditions using 3 μmol of complex I ($[\text{Ti}] = 10\text{ } \mu\text{mol L}^{-1}$), MAO as cocatalyst with Al/Ti = 1 000-1 700, 300 mL of toluene, 10 bar of ethylene and 30 minutes of reaction. The impact of temperature on the reactivity of the system being scarcely assessed, a precise study of the behavior of the SFI system was carried out within a wide range of temperature.

II.2. Temperature effect on activity and selectivity

II.2.1. Evolution of the activity

To assess the impact of temperature on the activity of the SFI system, nine experiments were conducted at 10 bar of ethylene for 30 minutes from 26 °C to 80 °C. In this thesis, the activity is calculated assuming that all titanium centers introduced in the reaction media are active, which is conceivable given the homogeneous catalysis conditions. As it is not possible to discriminate trimerization and polymerization species, the activity represents the global activity for trimerization and polymerization reaction. The average activity values for each run are summarized in Table 2.

Table 2. Effect of temperature on SFI catalyst activity

Entry	n _{Ti} (μmol)	Al/Ti	T (°C)	t (min)	Activity (kg _{ethylene} g _{Ti} ⁻¹ h ⁻¹)
1	2.8	1 650	26	29	419
2	3.5	1 300	32	35	607
3 ^a	2.5	1 800	35	18	571
4	3.1	1 500	40	27	558
5	3.8	1 200	42	32	537
6	3.4	1 350	49	31	160
7	4.6	1 000	58	31	172
8	3.2	1 400	68	28	97
9	3.9	1 200	80	31	78

Conditions: complex I, 300 mL toluene, MAO 30 wt % in toluene, 10 bar of ethylene

^a test time limited by ethylene feed capacities

This study stresses that the activity of the SFI system highly depends on the temperature of reaction. After reaching its climax between 30 °C and 40 °C (Table 2, entries 2-5), the catalytic system is less active as the reaction temperature increases. In these conditions, 32 °C is the optimum temperature to reach the highest productivity. Above 42 °C, a decay is observed to the point where the activity at 80 °C is divided by almost tenfold compared to the maximum value (Table 2, entry 9 versus 2). To sum up, complex I/MAO is a highly active system between 26 and 42 °C but its activity decreases as the reaction temperature increases.

Such trend is in line with data reported in the literature for the original system complex II/MAO. Comparing these results with literature, the activity at 26 °C (entry 1) is similar to the 418 kg_{ethylene} g_{Ti}⁻¹ h⁻¹ reported with the adamantly-substituted complex in similar conditions (0.25 μmol of precatalyst in 30 mL of toluene, 2 000 equivalents of MAO, 8 bar of ethylene at 25 °C).² It is noteworthy that the bulkiness of the *tert*-butyl group has a similar impact as the adamantyl group on activity. Moreover, the overall trend of activity decay is also consistent with the activity decrease from 66.9 to 12.5 kg_{ethylene} g_{Ti}⁻¹ h⁻¹ between 28 °C and 58 °C reported by Duchateau *et al.*¹ Compared to these values, activities obtained in our study

are almost a tenfold higher, which is probably due to a lower concentration of precatalyst and a lower Al/Ti ratio. In fact, higher active species concentration promotes the exothermic phenomenon as well as the contact between active sites. For the records, comproportionation Ti^{II}/Ti^{IV} can lead to the deactivation of the system.⁶

This investigation is the first study that clearly quantifies the impact of temperature on the activity of the SFI trimerization systems. In fact, activity is paramount at low temperature (32 °C, entry 2) and within a narrow range of 10 °C. The deactivation at higher temperature is counter-intuitive as one would expect the activity to be enhanced. These results have to be combined with selectivities to distinguish the thermal influence on the behavior of trimerization and polymerization system separately.

II.2.2. Effect of temperature on the selectivity

The quantification of each product enables to extract the preferential path between oligomerization or polymerization. This way, the yield of each product and the corresponding selectivities are gathered in Table 3.

Table 3. Yields and selectivities according to the reaction temperature for the SFI system complex I/MAO

Entry	n _{Ti} (μmol)	T (°C)	t (min)	C ₆ (g) (wt %)	C ₁₀ (g) (wt %)	C ₁₄ (g) (wt %)	PE (g) (wt %)
1	2.8	26	29	22.20	4.49	0.03	0.08
				82.9%	16.7%	0.1%	0.3%
2	3.5	32	35	49.86	8.00	0.12	0.55
				85.37%	13.7%	0.2%	0.9%
3	2.5	35	18	17.98	2.57	0.00	0.15
				86.9%	12.4%	0.0%	0.7%
4	3.1	40	27	30.96	5.14	0.07	0.83
				83.7%	13.9%	0.2%	2.2%
5	3.8	42	32	44.21	5.75	0.10	1.69
				85.4%	11.1%	0.2%	3.3%
6	3.4	49	31	6.80	0.59	0.01	6.07
				50.4%	4.4%	0.1%	45.1%
7	4.6	58	31	9.61	0.38	0.00	9.55
				49.2%	1.9%	0.0%	48.9%
8	3.2	68	28	2.00	0.03	0.00	4.84
				29.1%	0.5%	0.0%	70.4%
9	3.9	80	31	1.44	0.00	0.00	5.93
				19.6%	0.0%	0.0%	80.4%

Conditions: complex I, 300 mL toluene, MAO 30 wt % in toluene, 10 bar

First, liquid phase analysis revealed that C₁₀H₂₀ and C₁₄H₂₈ branched alkenes are produced along with 1-hexene especially for reactions conducted below 49 °C (entries 1-6). Consequently, their production is directly linked to the production of 1-hexene. It is interesting to verify whether this side trimerization results from an effect of the 1-hexene concentration or 1-hexene remaining in the coordination sphere of the metal. The higher the 1-hexene concentration in the reaction media, the higher the amount of these branched oligomers (Figure 5). It is important to note that co-trimerization reactions decrease the 1-hexene selectivity, thereby should be taken into account for further industrial process developments.

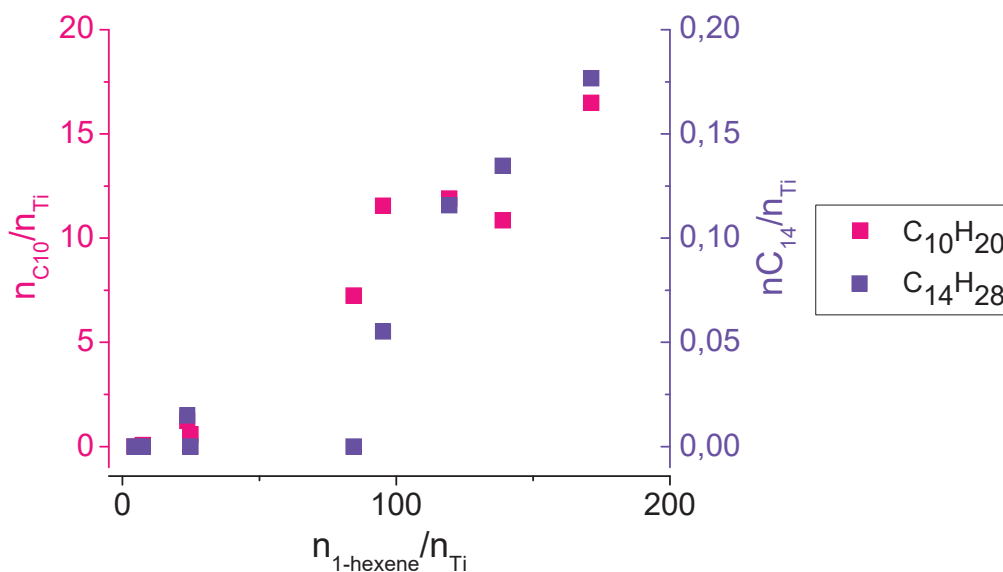


Figure 5. Evolution of C₁₀H₂₀ and C₁₄H₂₈ oligomers production according to 1-hexene concentration (Table 3)

Concerning the influence of the temperature on the selectivity of the SFI system, the highest 1-hexene selectivities are obtained for reactions performed below 42 °C (entries 1-5). In these cases, polyethylene production is limited and could even be considered as negligible below 35 °C (entries 1-3). These selectivities are slightly lower than that reported using complex II at low temperature (about 90 wt % at 30 °C).² This difference would be ascribed to a higher 1-hexene concentration compared to Duchateau's conditions (Table 1, entry 2). A substantial gap is observed between 42 °C and 49 °C (entries 5-6) as 1-hexene and polyethylene are almost isoselective with 50 wt % and 45.1 wt % respectively. Above 49 °C, the mass and selectivity of produced polymer increases to the detriment of 1-hexene. At 80 °C, the selectivity to polymer (entries 9, 80 wt %) is comparable to the selectivity to 1-hexene at low temperature (entries 1-5, around 85 wt %). This switch of selectivity has to be tempered as the activity decreases. Thus the yield of polyethylene at 80 °C is lower than that of 1-hexene at 32 °C (Table 3, entries 2 versus 9).

Having in mind the target of understanding polymer production, a focus on its production over temperature evolution gives information regarding the behavior of polymerization active species with temperature. Polymerization activity is calculated assuming that the amount of polymerization active species is constant whatever the temperature, by simply multiplying the activity by the selectivity. Figure 6 reveals the increase of polymerization activity with temperature, which is typical in catalytic ethylene polymerization. The production of polyethylene is rather constant below 42 °C and above 49 °C with a sudden increase in-between. Such evolution implies either an enhancement of activity of polymerization catalyst or the formation of more active species. In the first case, such increase may be due to an effect of temperature, which has an impact on the kinetics of polymerization species. The second assumption is supported by the deactivation of the trimerization system at higher

temperature. One could assume that temperature probably favors a partial transformation of trimerization species into polymerization catalysts.

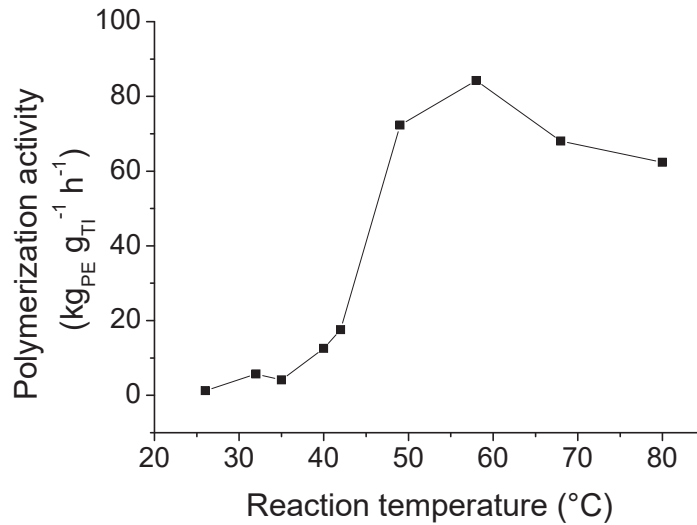


Figure 6. Polymer productivity according to reaction temperature

If one considers that 10 mol % of Ti species polymerizes ethylene at 80 °C for instance, the overall activity would be 600 kg_{polyethylene} g_{Ti}⁻¹ h⁻¹. This activity being utterly conceivable, this calculation proves that the polymer could be produced by a small portion of the overall titanium introduced in the reaction medium. Moreover, as the increase of polymer production is concomitant with the deactivation of the trimerization catalyst, one could hypothesize:

- (i) A transformation of trimerization to polymerization catalyst;
- (ii) The formation of another species inactive toward ethylene;
- (iii) The death of the catalyst trapped in the polymer.

II.2.3. Discussion on temperature effect on polymerization active species formation

Based on both activity and selectivity data, there are indisputable evidences of a thermal effect on the reactivity of the system. A clear trend was extracted:

- (i) the highest activity and 1-hexene selectivity are reached between 30 and 40 °C;
- (ii) the trimerization system rapidly deactivates above 50 °C and polymerization is predominant although moderate.

For the sake of clarity, each range of temperature are called “trimerization conditions” (i) and “polymerization conditions” (ii) thereafter.

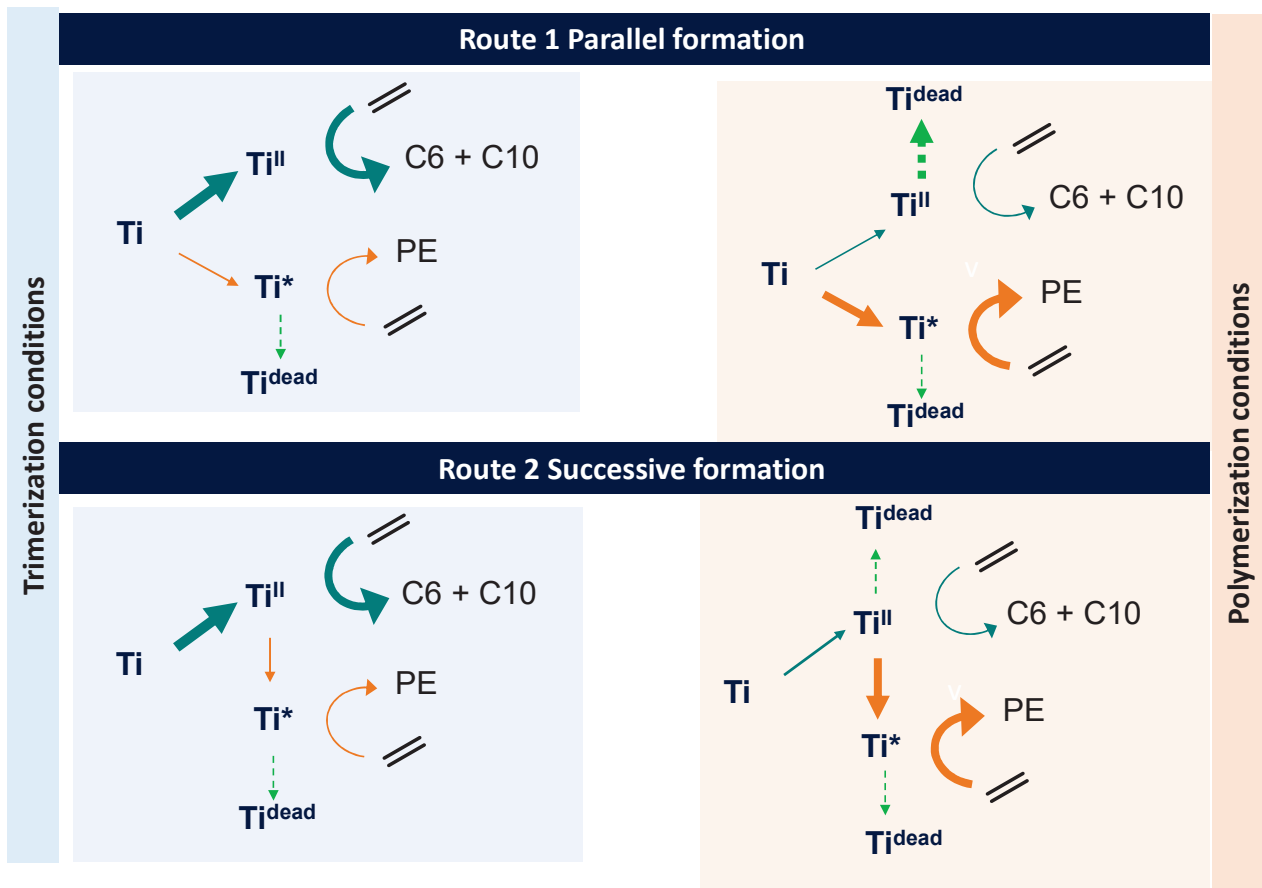
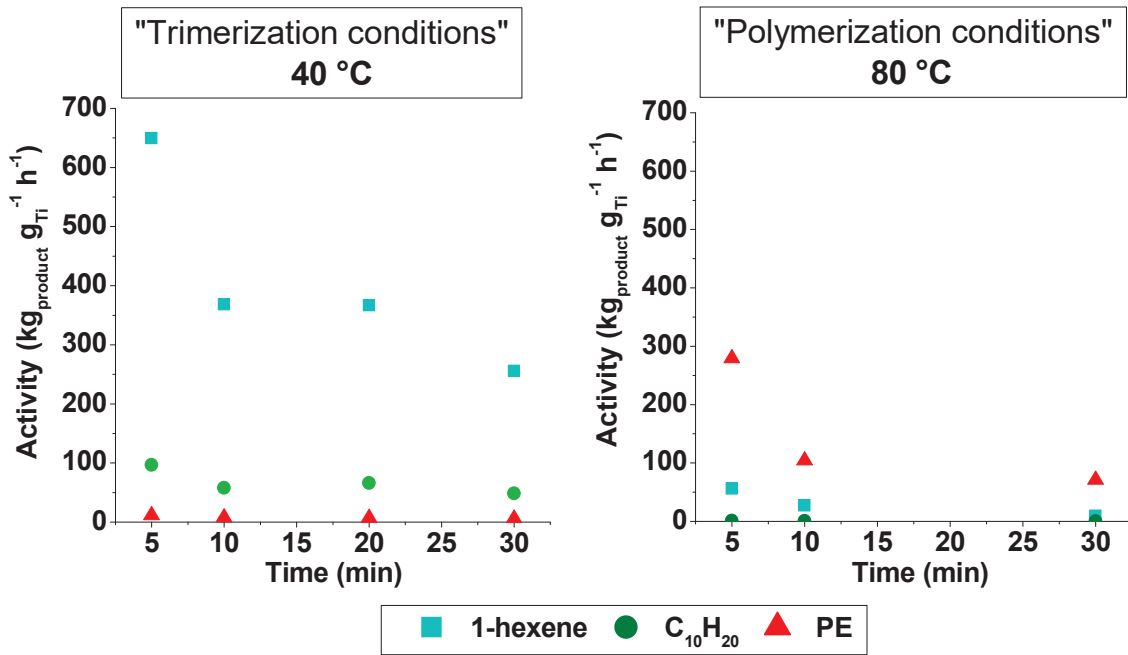
Temperature study is an important source of information regarding the formation of active species. From this evolution it is clear that the number of trimerization active species is decreased. From the kinetic point of view, this limitation of trimerization can be explained by two mechanisms (Scheme 3). One can consider either a lower activation rate compared to the parallel polymerization active species formation (*Route 1*) or a deactivation, *i.e* conversion of trimerization catalysts into dead species or polymerization species (*Route 2*).

The main hypothesis for *Route 1* is related to deviations in the activation process. Proposed side reactions are the incomplete activation leading to a Ti^{IV} or Ti^{III} polymerization catalyst or a ligand alteration or abstraction by TMA. Thus, a post-metallocene or a molecular Ziegler-Natta species (ligand-free) respectively are assumed. As these species behave differently towards ethylene and 1-hexene, the identification of the actual polymerization specie can be probed by the chemical and molar mass distribution of the polymer.

Regarding *Route 2*, a thermally-induced structure changes can cause the conversion from trimerization into polymerization species. In fact, this alteration could occur in the crucial temperature range of 40 and 50 °C, leading to a polymerization catalyst displaying a different activity. The polymer features (comonomer content and molar mass distribution) would also differ depending on the temperature.

It is noteworthy that for both *Route 1* and *Route 2*, the deactivation of trimerization species can occur by the death of active species. Apart from the formation of polymerization species, the generation of species being inactive toward catalytic transformation of olefins is plausible. Another possible reaction for *Route 2* is the comproportionation of Ti^{II} and Ti^{IV} species that would lead to the concomitant deactivation of trimerization and the formation of two Ti^{III} species. These reduced complexes can either polymerize ethylene (Ti*) or be catalytically inactive (Ti^{dead}). Kinetics and evolution of products over time are indispensable to discriminate *Route 1* from *Route 2* at higher reaction temperature. These investigations will be reported in the next chapter.

In conclusion, this study contributed to clarify the reactivity of the SFI catalytic system between 26 and 80 °C. By combining the evolution of activity and selectivity according to temperature, a switch of selectivity from trimerization to polymerization was identified around 50 °C. Keeping in mind that the focus of this project is the identification of polymerization active species, it is now interesting to implement the polymer-to-catalyst strategy based on this detailed investigation.



Scheme 3. Catalytic behavior of SFI trimerization system with temperature and possible routes for trimerization and polymerization activation/deactivation routes according to reaction temperature

III. IN-DEPTH POLYMER ANALYSIS

III.1. Polymer features

III.1.1. Molar mass distribution (MMD)

The assessment of molar mass distribution provides details on the frequency of transfer reactions. High steric hindrance of the ligand hampers transfer reactions especially β -H elimination, leading to long chain length and high molar masses. Based on the span of the distribution it can be concluded whether polymer chain length are homogeneous or rather dispersed. For a molecular catalyst, a narrow MMD is observed and the dispersity ($\mathcal{D} = \frac{M_w}{M_n}$) is close to 2 whatever the type and number of transfer reaction. Most often, a broad distribution witnesses the presence of several active species.

The molar mass distribution analysis informs on the average molar masses (M_n and M_w) and the homogeneity of chain size. To evaluate the length of macromolecules of the polymer produced, molar mass distributions were measured by high temperature size exclusion chromatography (HT-SEC). In the case of polyolefin, an elevated temperature (150 °C) is required for a proper polymer dissolution in a high boiling point-solvent such as 1,2,4-trichlorobenzene (TCB) in presence of 2,6-di(*tert*-butyl)-4-methylphenol (BHT) as anti-oxidizing agent. Although dissolution issues were often encountered, efforts in sample preparation were invested to analyze as many polymers as possible.

For the sake of clarify, polymers obtained in this study (Table 3) at the temperature T with the 1-liter SFS reactor are labeled PE-SFS-T. Note that a distinction is made between the 1 liter reactor and other reactors mentioned in the next chapters. Thus, the average molar masses of the polymer obtained from 26 to 80 °C, PE-SFS-26 to PE-SFS-80, are gathered in Figure 7.

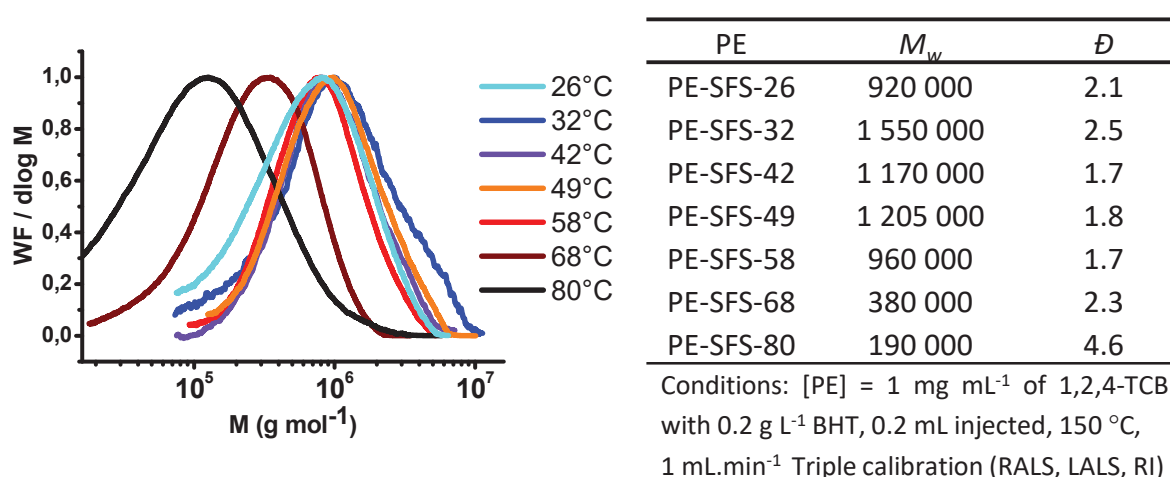


Figure 7. Molar mass distributions of PE-SFS-32 to PE-SFS-80 corresponding to polymers mentioned in Table 3

On the one hand, all polymers are high molar mass polyethylenes with M_w in the range 10^{5-6} g mol⁻¹. For reactions carried out below 58 °C, a remarkably high average molar mass of $1-1.5 \times 10^6$ g mol⁻¹ is observed (Table 3, entries 1-5). A brutal decrease of molar masses is observed when $T > 60$ °C since M_w is reduced by 3. This drastic reduction in chain size could be explained by kinetic effect where transfer reactions are favored compared to propagation reactions at higher temperature (Table 3, entries 6-7).

On the other hand, the broadness of distribution also evolves with the reaction temperature (Figure 7). When 30 °C $< T < 80$ °C (Table 3, entries 1-6), polymer dispersity is about 2. This low value is synonym of a homogeneity in size of the macromolecules. Such narrow distribution can only be obtained with a single-site catalyst. At 80 °C, a higher dispersity of 4.3 (Table 3, entry 7) reveals a wider range of macromolecules size between 10^4 and 10^6 g mol⁻¹. Consequently, a broad MMD could be linked to diverse active species, thus multi-site catalysis.

From this study, the evolution of the molar mass distributions of the polymer gives clues regarding the number and type of active species according to reaction temperature. Below 60 °C, polymers are composed of a mixture of very long hydrocarbon chains and display a narrow MMD. It is probably afforded by well-defined single-site catalysis, such as a post-metallocene. Indeed, the steric hindrance provided by the bulkiness of the ligands favors the polymer chain growth by hampering β -H elimination. Above 60 °C, lower molar masses and a higher dispersity presumes a heterogeneity in active sites. Thus, one could think of a mixture of single-site catalysts that polymerize ethylene at higher reaction temperature. Indeed, this assumption supports the thermal conversion from trimerization to polymerization hypothesized in Discussion on temperature effect on polymerization active species formation.

III.1.2. Chemical composition of polymers PE-SFS-26 to PE-SFS-80

III.1.2.1. Chain branching identification in polymers

The chemical composition is defined by the molar ratio between the amount of comonomer and the total amount of monomer and comonomers of a polymer. In this case, 1-hexene is mainly produced during the trimerization reaction and can potentially be incorporated in the hydrocarbon chains. Thus, analyzing the content of Short Chain Branching (SCB) in the polymer will give information about the ability of the polymerization catalyst to incorporate higher alpha-olefins. It will eventually be possible to conclude on the nature of this polymerization active species as explained in Chapter 1.

The branching identification and quantification in a polymer is possible using high temperature ¹³C NMR. This analysis is operated at 120 °C in *o*-DCB-*d*₄/*o*-DCB to ensure the dissolution and the homogeneity of the sample during the signal recording. As for SEC analysis, some polymers could not be analyzed for dissolution or quantity issues. An example of ¹³C NMR spectrum is presented in Figure 8. Branchings are identified using the notation from Galland *et al.*¹⁰

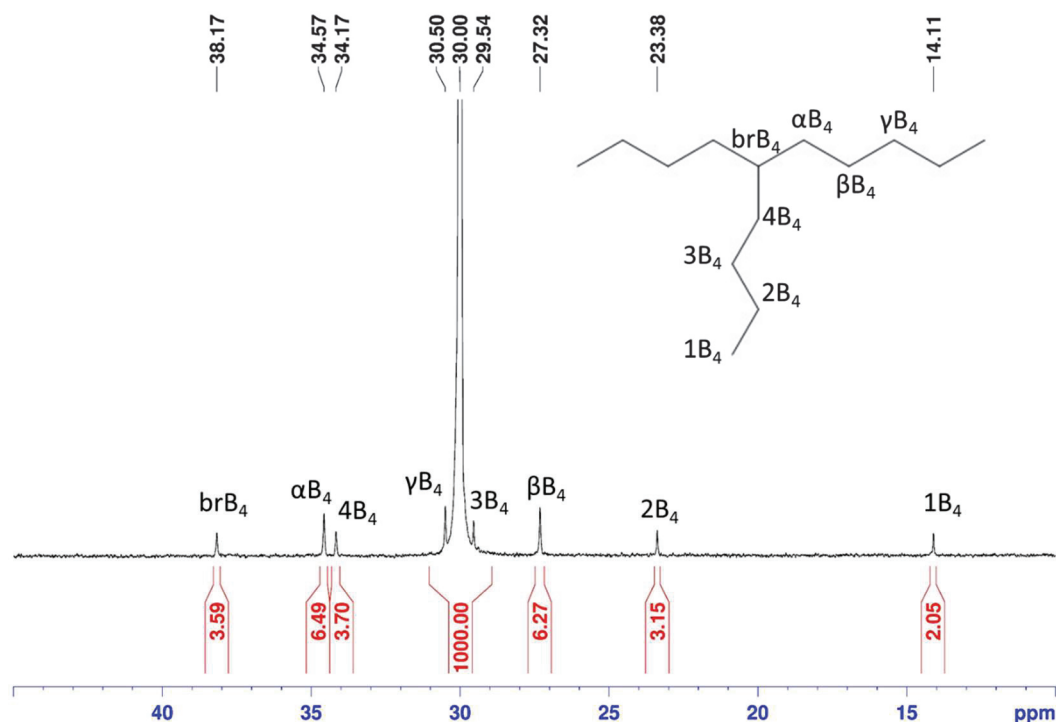


Figure 8. HT ¹³C NMR of PE-SFS-42 in *o*-DCB-*d*₄/*o*-DCB (1/9) at 120 °C

For the polymer produced at 42 °C (PE-SFS-42, Figure 7), only short chain branching of butyl groups were identified by high-temperature ¹³C-NMR. More precisely, the polymer obtained at this low temperature comprises about 3.4 SCB/1000C meaning 0.6 mol % of 1-hexene. Note that among all polymers analyzed, solely C₄ branching were identified. Branched oligomers (C₁₀H₂₀ and C₁₄H₂₈) were not incorporated in the polyethylene backbone for steric reasons.

Unfortunately, chain end groups could not be identified by HT-¹³C NMR owing to the high molar masses of polymers. It would have been very informative regarding transfer reactions and therefore the nature of polymerization active species. Indeed, post-metallocenes are inclined to perform β-H elimination resulting in an unsaturated vinyl chain end whereas homogeneous Ziegler-Natta species generate polymer chains after transfer to the co-catalyst leaving saturated alkyl-chain ends as fingerprints.

In summary, only C₄ branching is observed and the average 1-hexene content of the polymer could be determined by HT-¹³C NMR. 1-hexene content can also be assessed indirectly by DSC analysis combined with HT-¹³C NMR results (see next section). This thermal analysis is faster and sample preparation is easier compared to NMR spectroscopy. It also gives additional information regarding the crystallinity of the polymer.

III.1.2.2. 1-Hexene content in polymers PE-SFS-26 to PE-SFS-80

III.1.2.2.1. Evolution of 1-hexene content with reaction temperature

As illustrated in Chapter 1, Differential Scanning Calorimetry is a thermal technique that enables to assess the comonomer content by providing the melting (T_m) and crystallization (T_c) temperatures of the polymer. In fact, the amount of SCB in polyethylene has a pronounced impact on characteristic properties of the material. It is therefore possible to combine DSC and HT-¹³C NMR to express the comonomer content as a function of T_m and T_c . Then, it is possible to evaluate the comonomer content based on the DSC profile and without having to perform high temperature ¹³C NMR spectroscopy.

Thermal analysis of polyethylene comprises 3 main steps:

- The first heating step aims at erasing the “thermal past” of the material. A quick increase of temperature from 25 °C to 180 °C ($T \gg T_m$) at 20 °C min⁻¹ ensures the polymer to melt and form a homogeneous rubbery phase.

- The cooling step enables the crystallization of this homogeneous melt from 180 °C to 25 °C at 5 °C min⁻¹ and gives access to T_c .

- The last step consists in the melting of the newly formed crystallites from 25 °C to 180 °C with the same speed as the previous step. Therefore the exothermal profile provides the actual melting temperature (T_m) of the material.

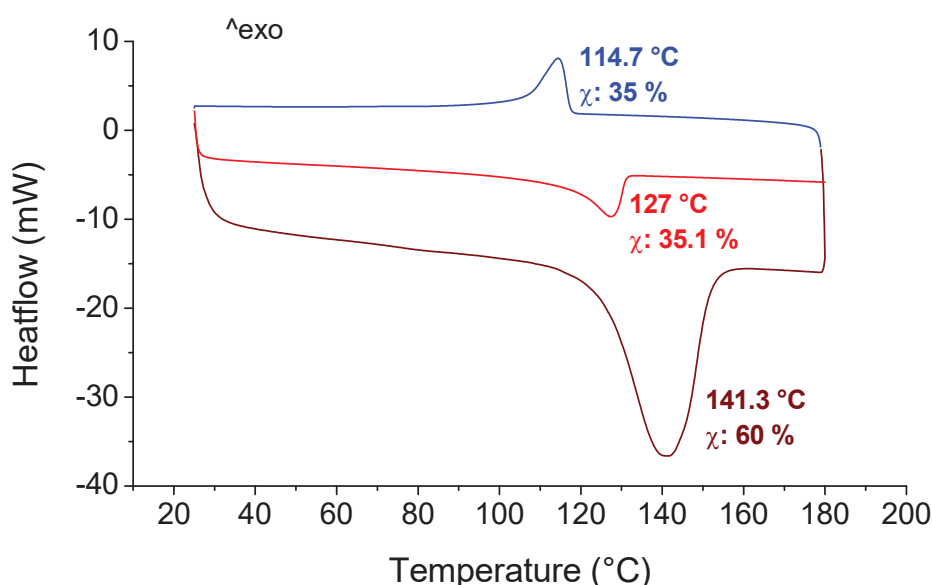


Figure 9. DSC profile of PE-SFS-42 containing 0.6 mol % of 1-hexene. First melting (brown), crystallization (blue) and second melting (red) curves.

DSC analysis of the sample PE-SFS-42 displays a crystallization temperature of 114.7 °C and a melting temperature of 127 °C with a specific heat of 109.8 J g⁻¹ amounting to 35 % crystallinity. The calculation of crystallinity is detailed in the experimental section. It is noteworthy that the first melting temperature is substantially higher than the actual melting

point. The same observation is made regarding the crystallinity with a decrease of more than 40 % between the first and second heating step. Such difference is ascribed to the rearrangement of the polymer chains during the first heating. Indeed, macromolecules are more mobile, they form smaller crystallites and thus have a lower melting temperature according to the Gibbs-Thomson relationship. Moreover, similar temperature and crystallinity values were reported in the case of UHMwPE.¹¹

DSC endothermal and exothermal profiles were recorded for each polymer made from 30 to 80 °C. The extracted melting point values are compared with the comonomer content calculated from high-temperature ¹³C NMR signals. Figure 10 displays the evolution of the polymer melting temperature and 1-hexene content according to the reaction temperature.

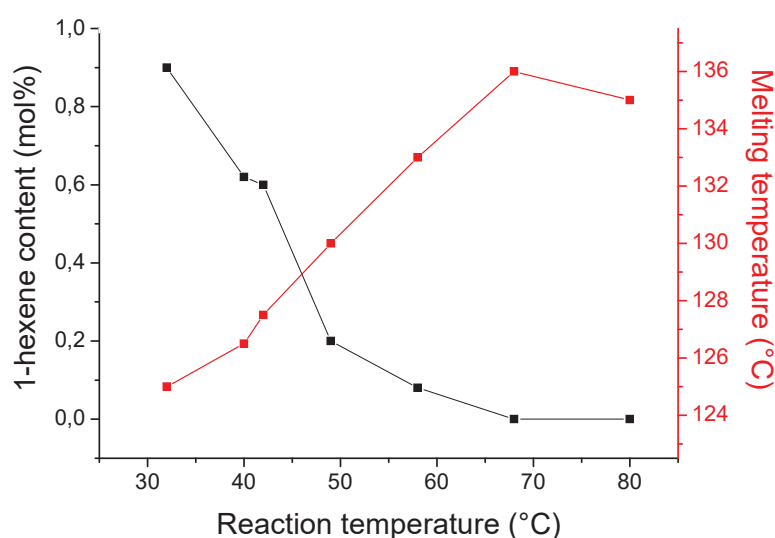


Figure 10. Variation of the chemical composition of polyethylenes according to reaction temperatures

From Figure 10, it is clear that all 1-hexene contents are lower than 1 mol %, which is considered as a limited incorporation rate. 1-hexene content decreases as reaction temperature increases, which is reflected by higher T_m . This evolution must be put in perspective with the 1-hexene content in the reaction medium to draw conclusion on the catalyst ability for 1-hexene incorporation in the polyethylene backbone.

Keeping in mind that the aim of this polymer-to-catalyst strategy is to identify the PE properties and compare them with other polymer systems, two relationships can help in this view:

- The link between the comonomer content in the polymer ($\%_{C_6 PE}$) according to the reaction medium ($\%_{C_6 RM}$);
- The evolution of the melting temperature (T_m) measured by DSC and comonomer content from high temperature ¹³C NMR analysis.

III.1.2.2.2. 1-hexene content in the polymer versus reaction medium

First, in order to have more information about the polymerization active species, it is important to determine its ability to incorporate 1-hexene according to the amount of comonomer available in the reaction medium. In the literature, it was demonstrated that, in the case of single-site catalysis, the amount of comonomer incorporated in the polymer chain is proportional to the concentration of olefin in the reaction medium.¹²

From Figure 10 it can be seen that polymer properties depend on the reaction temperature and therefore, the amount of 1-hexene produced during the reaction (Figure 11). At low temperature, the overall 1-hexene content does not exceed 1 mol %, which is a low value compared to the amount of 1-hexene available in the reaction media. At $T > 50\text{ }^{\circ}\text{C}$, a decrease of the comonomer content is directly correlated to the lower amount of 1-hexene produced by the trimerization system.

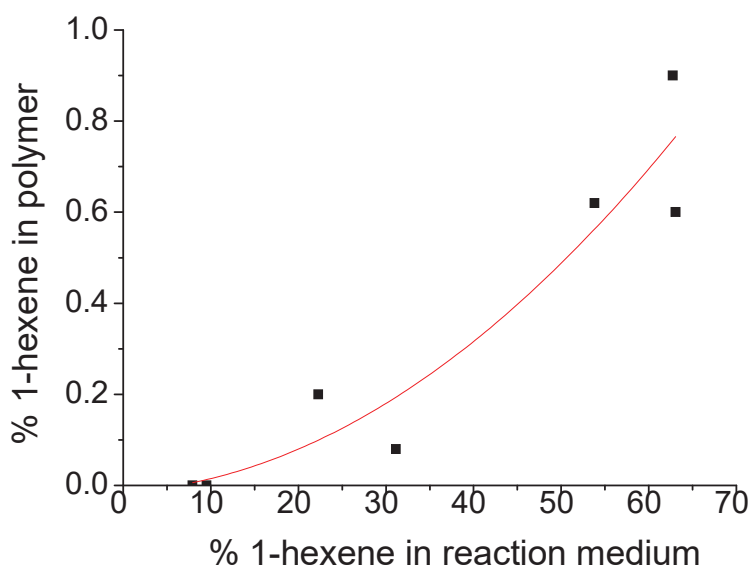


Figure 11. Relationship between 1-hexene content in the polymer and in the reaction media (at the end of reaction)

Consequently, the polymerization species very poorly incorporate higher alpha-olefins. This feature is often associated with Ziegler-Natta species. Metallocene and post-metallocene catalysts could also exhibit a limited copolymerization ability depending on the steric hindrance provided by the ligand.

In addition, this low comonomer content has to be pondered by the production of polymer over time. Kinetic parameters need to be taken into account to confirm the hypothesis of a poor copolymerization catalyst. Indeed, polymerization could occur during the early stage of the test, when the 1-hexene concentration is low. If the polymerization species deactivates rapidly, it is expected that the amount of 1-hexene content would be limited. This aspect will be further studied in Chapter 3.

III.1.2.2.3. Link between melting temperature and 1-hexene content

From Figure 10, it is observed that the melting temperature decreases as the 1-hexene content increases. This trend is in line with the classical behaviour reported in the literature. Moreover, the comonomer content decreases as the reaction temperature increases. A linear relationship is described with respect to SCB and melting temperature for ethylene/1-hexene copolymers produced by Ziegler-Natta catalysis (Equation 1.1).¹³ A study conducted at the C2P2 laboratory reports a different equation for LLDPEs produced by (*n*BuCp)₂ZrCl₂/MAO (Equation 1.2).¹⁴ Moreover, each trend is catalyst-dependant as highlighted in the case of other poly(ethylene-co-LAO).¹⁵

$$\%_{C6} = 15.3 - 0.11 T_m \quad (1)$$

$$\%_{C6} = 19 - 0.15 T_m \quad (2)$$

Equation 1. Relationships between melting temperature and 1-hexene content for HDPEs produced by a heterogeneous ZN (1) and a metallocene catalyst (2)

As the comonomer content is very low, a polynomial formula (Equation 2.1) is more representative of the results obtained experimentally in this study. Interestingly, such equation also accurately fits data obtained for (*n*BuCp)₂ZrCl₂/MAO-HDPEs in the restricted range of 0-1 mol % 1-hexene content (Figure 12, Equation 2.2).

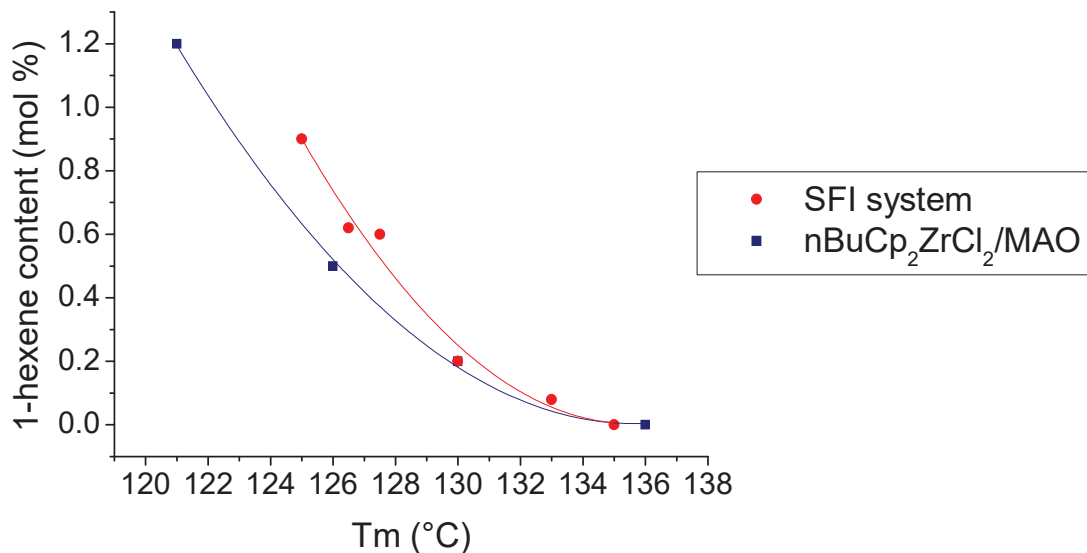


Figure 12. Evolution of 1-hexene content according to the melting point of HDPEs made by the SFI system (red) and (*n*BuCp)₂ZrCl₂/MAO (blue)

$$\%_{C6} = 147.01 - 2.168 T_m + 0.00799 T_m^2 \text{ with } R^2 = 0.97 \quad (1)$$

$$\%_{C6} = 101.97 - 1.50 T_m + 0.005 T_m^2 \text{ with } R^2 = 0.99 \quad (2)$$

Equation 2. Polynomial relationships between melting temperature and 1-hexene content for the HDPEs obtained with the SFI system (1) and (*n*BuCp)₂ZrCl₂/MAO (2)

The general trend regarding melting temperature and comonomer content for HDPE produced by the SFI system is non concomitant with the one for the polymer made with a heterogeneous catalyst. Interestingly, this trend is similar with a single-site catalyst. The evolution of %_{C6 PE} according to %_{C6 RM} will be used as a comparison tool when investigating PE obtained with potential active species investigated in Chapter 4.

After assessing the average composition of these poly(ethylene-co-1-hexene), chemical composition distribution will provide further information regarding the number of active species.

III.2. Advances analysis of PE-SFS-26 to PE-SFS-80

III.2.1. Chemical composition distribution of the polymers

III.2.1.1. Stepwise Isothermal Segregation Technique (SIST)

HDPEs obtained in this study contains a very limited amount of 1-hexene. The idea now is to verify whether 1-hexene is homogeneously or heterogeneously distributed among all polymer chains. The assessment of such chemical composition distribution is linked to the number of active species. In fact, multimodal signals imply several copolymers, which are associated with several active species in the reaction medium. A drift in 1-hexene production during the catalytic test would also impact the modality of the signal. A convenient method for obtaining a qualitative chemical composition distribution is the Stepwise Isothermal Segregation Technique (SIST) performed by DSC.

Knowing that crystal size depends on the comonomer content in the polymer, SIST analyses have been applied to segregate possible mixture of copolymers. Based on the literature, this method involves isothermal steps lasting 60 minutes every 10 °C from 130 °C to 50 °C (Figure 13).¹⁶

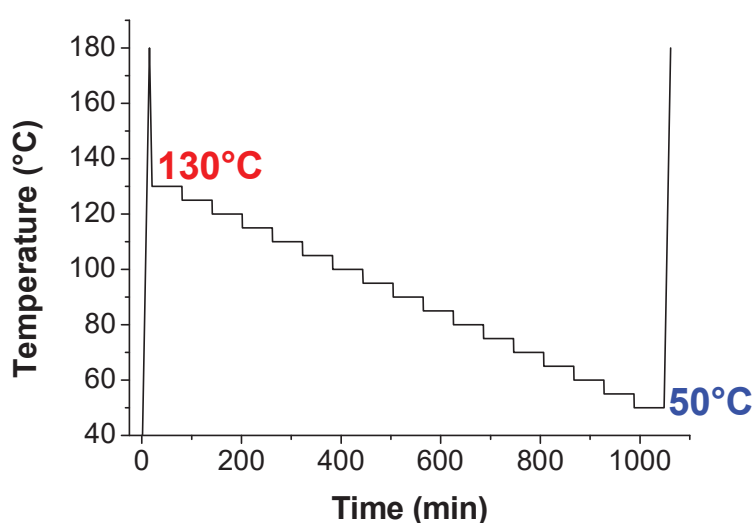


Figure 13. SIST method for HDPE segregation

The thermal profile of the last heating was analyzed for PE-SFS-42 (0.6 mol % 1-hexene) and PE-SFS-80 (0 mol % 1-hexene). For both endothermal profiles in Figure 14, a multi-modal signal reveals the presence of copolymers with a different comonomer content. After deconvolution, 5 populations of copolymers are identified for the PE made at 40 °C with melting temperatures between 108 °C and 131 °C. In contrast, the polymer made at 80 °C comprises solely two populations of copolymers with higher melting temperatures (131.3 °C and 135.7 °C). Thus, PE-SFS-42 made at low temperature is a mixture of several copolymers contrary to PE-SFS-80, which is composed of two populations. Such difference reveals that either the number of polymerization active species decreases at higher reaction temperature or several copolymers are produced over time as 1-hexene is produced in the reaction medium. The latter

assumption can be verified by analyzing the evolution of the polymer composition for different reaction time, which is detailed in Chapter 3. It is still interesting to analyze the distribution in terms of comonomer content for each fraction of the polymer.

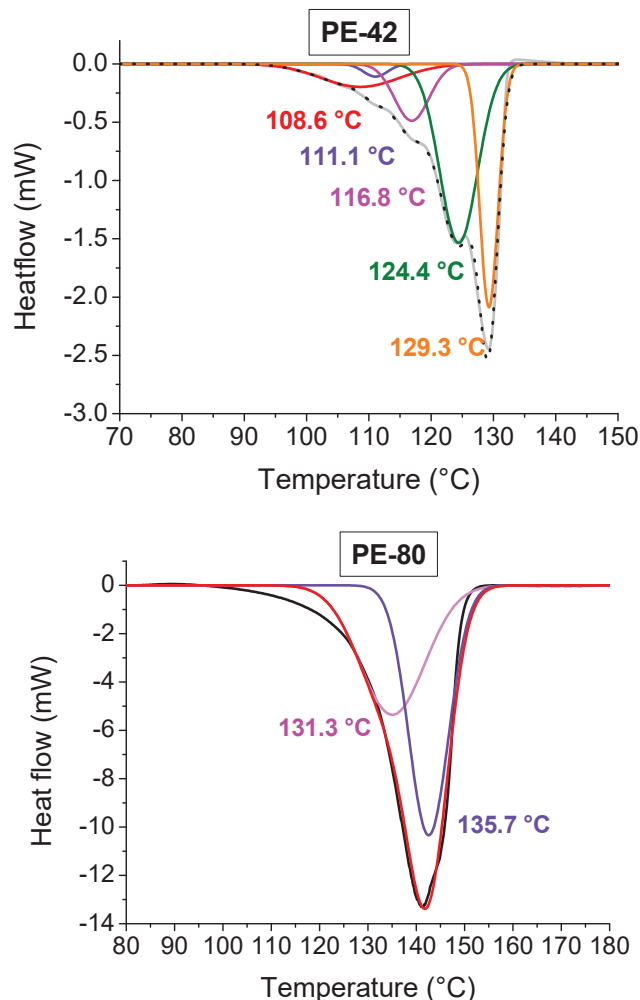


Figure 14. DSC-SIST heatflow deconvolution for PE-SFS-42 (top) and PE-SFS-80 (bottom)

From the melting temperature extracted after deconvolution, the resulting average lamellae thickness and comonomer content for each HDPE were calculated using Equation 2.2. and Gibbs-Thomson equation respectively. For both PEs, the proportion of each copolymer fraction according to their average lamellae thickness is represented in Figure 15. It is observed that PE-SFS-42 is composed of fractions with a higher 1-hexene content than that of PE-SFS-80, which is in agreement with the decrease in comonomer content observed at higher reaction temperature (Figure 10).

However, results obtained with SIST do not accurately represent the actual chemical composition of the polymers. Regarding PE-SFS-42, four fractions accounting for 71 % of the polymer, contain more than 1 mol % of 1-hexene whereas an average content of 0.9 mol % was calculated from ¹³C NMR (Figure 10). The same observation is less pronounced for PE-SFS-80 with 0.12 mol % instead of 0 mol % by ¹³C NMR.

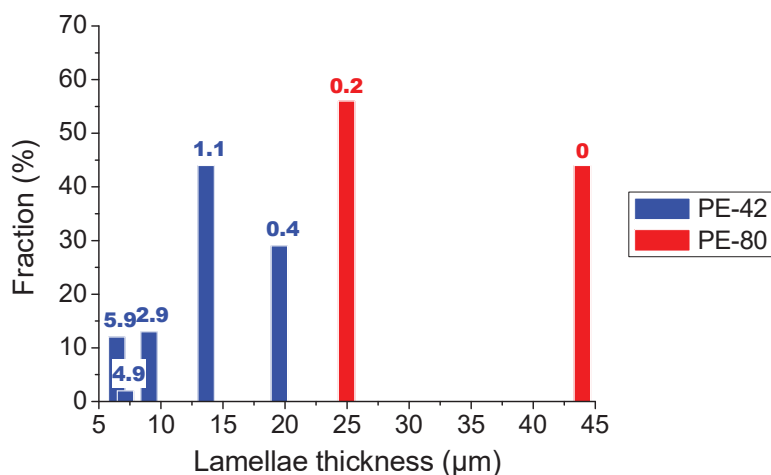


Figure 15. Polymer fractions distribution according to lamellae thickness and corresponding comonomer content (on top of bars) from SIST experiments for PE-SFS-42 (blue) and PE-SFS-80 (red)

At first glance, 5 and 2 polymerization active species would be identified at 42 °C and 80 °C respectively, based on the distributions obtained by SIST. However, the low dispersity in molar masses (Figure 7) for PE-SFS-42 stresses that the presence of more than two polymerization active species is not conceivable. One explanation for the presence of these multiple fractions is the drift of 1-hexene composition in the reaction medium over time. Indeed, the concentration in 1-hexene in the reactor at the end of reaction is significantly higher at 42 °C rather than at 80 °C. A more accurate alternative for the analysis of chemical composition distribution is a chromatography technique called Crystallization Elution Fractionation (CEF).

III.2.1.2. Crystallization Elution Fractionation (CEF)

III.2.1.2.1. Observations and hypotheses

CEF enables the separation of polymer according to the comonomer content regardless of the macromolecule chain size. The use of CEF in this study is relevant as all polymers studied feature a poor comonomer content below 1 mol % (Figure 10). Copolymer blends can be efficiently isolated resulting in a multi-modal CEF signal. Indeed, the segregation is monitored from a diluted polymer and under a continuous flow of solvent, making CEF separation superior to DSC segregation in terms of resolution. To recall, a multi-modal CEF signal implies multi-site catalysis whereas monomodal and narrow signal correlates to single-site catalysis.¹⁷

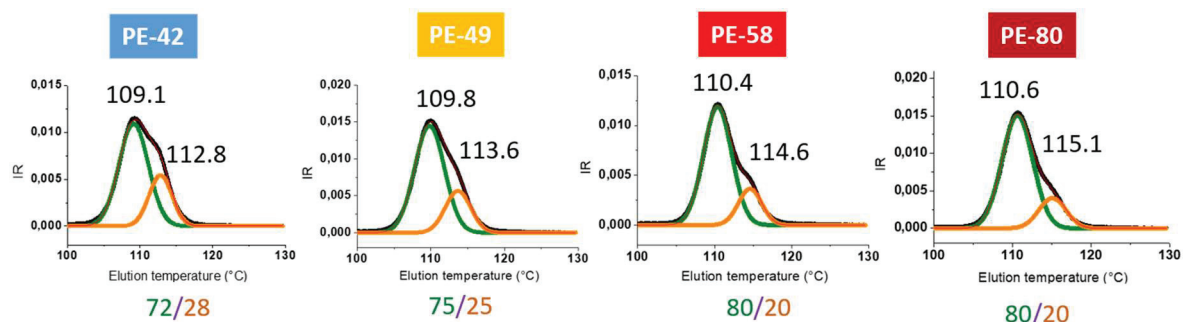
The principle of CEF is to isolate copolymers based on the difference in terms of crystallization and solubilization/elution temperature depending on the SCB content. The program for the dynamic crystallization and temperature rising elution fractionation is detailed in the experimental section. Regarding the assessment of comonomer content in the polymer, a polymer calibration is performed by correlating the elution temperature with the 1-hexene content in the polymer measured by high temperature ¹³C NMR. Several poly(ethylene-co-1-hexene)s used for CEF calibration were synthesized using (*n*BuCp)₂ZrCl₂ (1) and Et(Ind)₂ZrCl₂ (2) activated by MAO (Table 4). It is important to note that an elution temperature above 111.7 °C is expected for homopolyethylenes.

Table 4. Poly(ethylene-co-1-hexene)s features of selected polymers for CEF calibration

Catalyst	1-hexene content (mol %)	Elution temperature (°C)	M _w (g mol ⁻¹)	Dispersity
1	0	111.7	74 200	2.7
2	0.11	109	135 500	2.9
1	0.2	109.5	48 700	3.0
1	0.5	107.1	24 400	3.4
2	0.72	106.8	113 500	3.1
2	1	105.6	40 400	2.6
2	2	97.1	35 200	1.8

CEF was performed for each polymer made from 42 °C to 80 °C (Figure 16). First, CEF analysis revealed a bimodal chemical composition distribution for all polymers. After deconvolution, two populations are distinguished: one (fraction 1) displaying a lower elution temperature, thus a potentially higher 1-hexene content, than the other (fraction 2). Unlike SIST results (Figure 14), the two polymer fractions were identified for PE-SFS-42. Therefore, it seems that there is a couple of polymerization active sites in the SFI system between 40 and 80 °C. In addition, the 1-hexene content determined using the polymers calibration (Table 4) is 0.55 mol % for the polymer made at 42 °C and 0.6 mol % was calculated from ¹³C NMR spectrum (Figure 10).

When the reaction temperature is increased, the two populations evolve regarding their elution temperature and content in the polymer. On the one hand, elution temperatures of fraction 1 (T₁) and 2 (T₂) increase from 109.1 to 110.6 (fraction 1) and 112.8 to 115.1 °C (fraction 2) between 42 and 80 °C. Thus, fraction 1 and 2 are composed of a lower 1-hexene content as the reaction temperature increases. On the other hand, fraction 1, which exhibits a higher 1-hexene content than fraction 2, is more prominent for PE-SFS-80 than for PE-SFS-32 with 80 % and 72 % respectively.



1-hexene content (mol %) ^a	PE-SFS-42	PE-SFS-49	PE-SFS-58	PE-SFS-80
Fraction 1	0.30	0.19	0.11	0.08
Fraction 2	< 0	< 0	< 0	< 0

^acalculated from the calibration in Table 4

Figure 16. Chemical composition distribution and average 1-hexene content (mol %) of selected polyethylenes made from 42 to 80 °C

In view of these results, one could doubt regarding the inverted evolution compared to the trend observed in Figure 10, where 1-hexene content is reduced as the polymer is made at higher temperature. The key element to support this caution is the elution temperatures of fraction 2, which are out of calibration. Consequently, the bimodality would not witness a difference in chemical composition. Further investigations of this recent technique are required to clarify the phenomenon behind the presence of a shoulder at higher elution temperature.

III.2.1.2.2. Investigation of the CEF technique

The first idea is to focus on the method to identify parameters that could cause signals to be out of calibration. The classical method used by PolymerChar involves a starting temperature of the dynamic crystallization step at 95 °C. However, this temperature is far below the crystallization temperature of our copolymers. As a consequence, it could lead to a brutal crystallization affecting the efficiency of the separation, which is also known as cocrystallization effect. The idea was therefore to increase this temperature to perform a gradual crystallization from 160 °C to 35 °C followed by the second heating step (see the experimental section for more details).

Applying this modified method aims at checking the modality of the signal. One would expect that a more homogeneously dissolved polymer is injected in the column, and a monomodal signal would be observed. Nevertheless, as all polymers analyzed are high molar masses polyethylenes, these very long hydrocarbon chains could also cause physical phenomenon hampering the CEF separation. It is noteworthy that CEF analyses of polymers with such high molar masses have not been reported.

Applying CEF-160 method, the signal obtained for all polymers from 42 to 80 °C exhibit bimodal profiles that are similar to the signals obtained with the standard method. Moreover, the ratio and elution temperature are close for each polymer. For each population, T₁ and T₂ are slightly higher than the ones observed with the standard method. Although signals are similar, a better separation of the populations is observed when crystallization is initiated at 160 °C instead of 95 °C. Therefore, CEF-160 provides a better separation of the two populations but fraction 2 still exhibits an elution temperature out of the corresponding calibration. As a consequence, this change of method implies that the separation is affected by a parameter other than the SCB in the polymer.

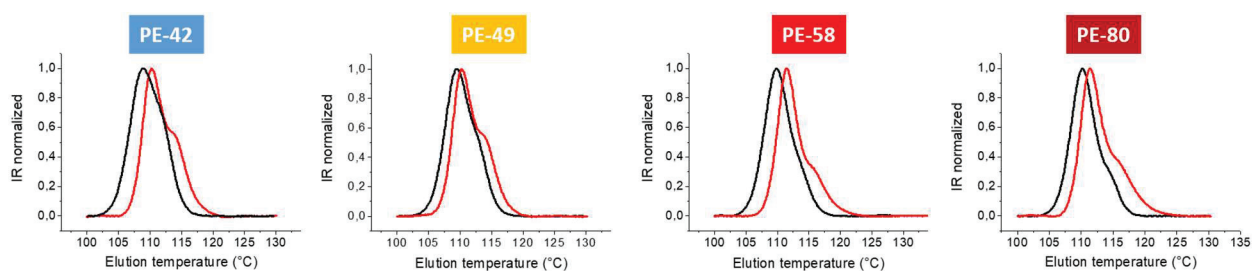


Figure 17. CEF profiles for polyethylenes produced between 42 and 80 °C with the standard method (black) and the CEF-160 method (red)

Bearing this in mind, the evolution of fraction 1 and 2 with reaction temperature observed by CEF is in line with the decreasing homogeneity in molar masses. In fact, polymer made at low temperature displays a narrow distribution of high molar masses. In this case, most of polymer chains are not fully entangled which is translated into a higher population of polymer that is eluted at T₂ compared to T₁. As the temperature increases, the molar mass distribution broadens and the ratio of entangled polymer increases. Thus, there is more polymer entangled that solubilizes at lower temperature leading to a predominant population at T₁.

An alternative to check the influence of molar masses on the CEF signal modality is the analysis of homopolyethylenes made by ZN and ssC. These polymers do not contain any SCB, thus their CEF distributions are expected to be monomodal and narrower for PE-ssC than PE-ZN. Two polymers with molar masses above 10⁵ g mol⁻¹ were selected and analyzed using the standard method (Figure 18). CEF analysis of these comonomer-free high molar mass polyethylenes will enable to conclude regarding a physical effect due to the hydrocarbon chain length.

For both PE-ZN and PE-ssC, a bimodal signal is observed whereas the polymers are pure polyethylenes. As a result, it is concluded that the bipopulation is not related to the comonomer content, in these cases. Moreover, elution temperatures T₁ and T₂ are consistent

with the ones obtained for the PE-SFS-80 (Figure 16). Therefore, all signals obtained at $T_{\text{elution}} > 109\text{ }^{\circ}\text{C}$ reveal most probably the absence of SCB in the polymer, in the case of high molar masses PE. Consequently, the bimodality of the CEF signal for elution temperature above $190\text{ }^{\circ}\text{C}$ is linked to an effect of the high molar masses.

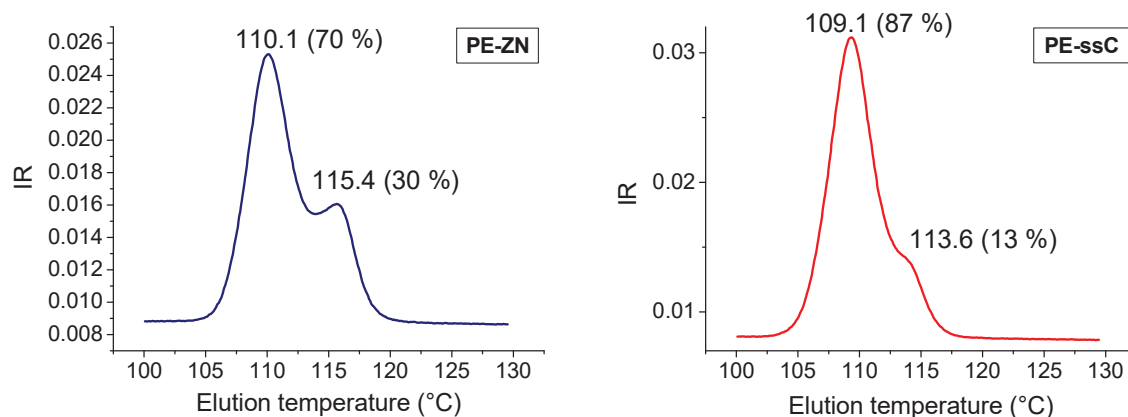


Figure 18. Comparison of CEF signal for homopolyethylenes made by a heterogeneous ZN ($2.7 \cdot 10^5\text{ g mol}^{-1}$, $\bar{D} = 2.6$, left) and homogeneous Et(Ind)₂ZrCl₂/MAO (10^5 g mol^{-1} , $\bar{D} = 2.3$, right)

Assuming that the CEF pattern is connected with an effect of the high molar masses, the question of the relative proportion between the two populations remains. In both PE-ZN and PE-ssC, the major population ($> 70\%$) has the lower elution temperature, which is also the case for the polymers obtained with the SFI system (Figure 16). In analogy with the Mark-Houwink relationship, a higher elution temperature would be correlated with a higher M_w . According to CEF results, PE-ZN and PE-ssC would display a bimodal or at least broad molar mass distribution. Nevertheless, such MMD profile was not observed except for PE-SFS-80 (Figure 7).

To sum up, the bipopulation at high elution temperature does not translate the presence of a mixture of copolymers but rather an effect caused by the high molar masses of polymers. In this particular case, the bimodality of the CEF signals cannot be explained by a bimodality in chemical composition distribution. Consequently, other physical effects have to be investigated. One can assume that cocrystallization occurs although the CEF technique is claimed to avoid such effect. This phenomenon is most probably linked to the topology of the polymer, which corresponds to the organization of macromolecules (interactions, arrangements and entanglements between hydrocarbon chains). The topology of polyethylenes PE-SFS can be assessed by several methods detailed hereafter.

III.2.2. Polymer topology investigation

III.2.2.1. Entanglement in the polymers

III.2.2.1.1. Annealing

To explain the distribution obtained by CEF, one should consider the specific topology of linear polyethylene with high molar masses. As highlighted in the bibliography study, this type of polyethylene has a high entanglement density. Fully entanglement is reached after the equilibrium time, which is proportional to molar mass cubed. In several cases, these high molar mass polyethylenes display two domains: one with entangled polymer chains and one with unentangled macromolecules. This dual composition could explain the bimodality of CEF signal.

Polymer annealing is an appropriate thermal method to highlight the heterogeneity in entanglement in the polymer. Performing annealing by DSC directly informs on the nature of the organization of the polyethylene chains. As explained in the bibliography study, the polymer is heated above its melting temperature (160 °C) for a certain time during which the amount of entanglement increases. Once the equilibrium is reached, no more evolution is observed. Thus, the idea is to verify the topology of the polymers PE-SFS-42 to PE-SFS-80 to identify whether entanglement density could impact the CEF technique results. The DSC method employed is the one applied by Rastogi *et al.* for the analysis of UHMwPE.¹⁸ More details on the method are provided in the experimental section.

The polymers made at 42, 58 and 80 °C were analyzed by DSC with this annealing method. After 5 minutes at 160 °C followed by a crystallization plateau at 136 °C, the second heating profile differs from one polymer to another (Figure 19). For both PE-SFS-42 and PE-SFS-58, a monomodal melting signal is obtained and is concomitant with the second heating of the standard DSC method (Figure 9). Only annealing profile after 5 minutes are presented as the duration of the annealing step has no effect on the endothermal signal. Melting curve for PE-SFS-80 exhibits a shoulder after 5 minutes of annealing. After deconvolution, the two populations have a melting temperature of 133.8 °C (67 %) and 141.5 °C (33 %) corresponding to the entangled and disentangled domains respectively. Increasing the annealing time to 15 minutes leads to a monomodal profile with the melting temperature of 136.5 °C. This evolution reveals a modification of the topology in the polymer as the annealing time increases. For PE-SFS-80, the entanglement equilibrium is reached between 5 and 15 minutes of annealing.

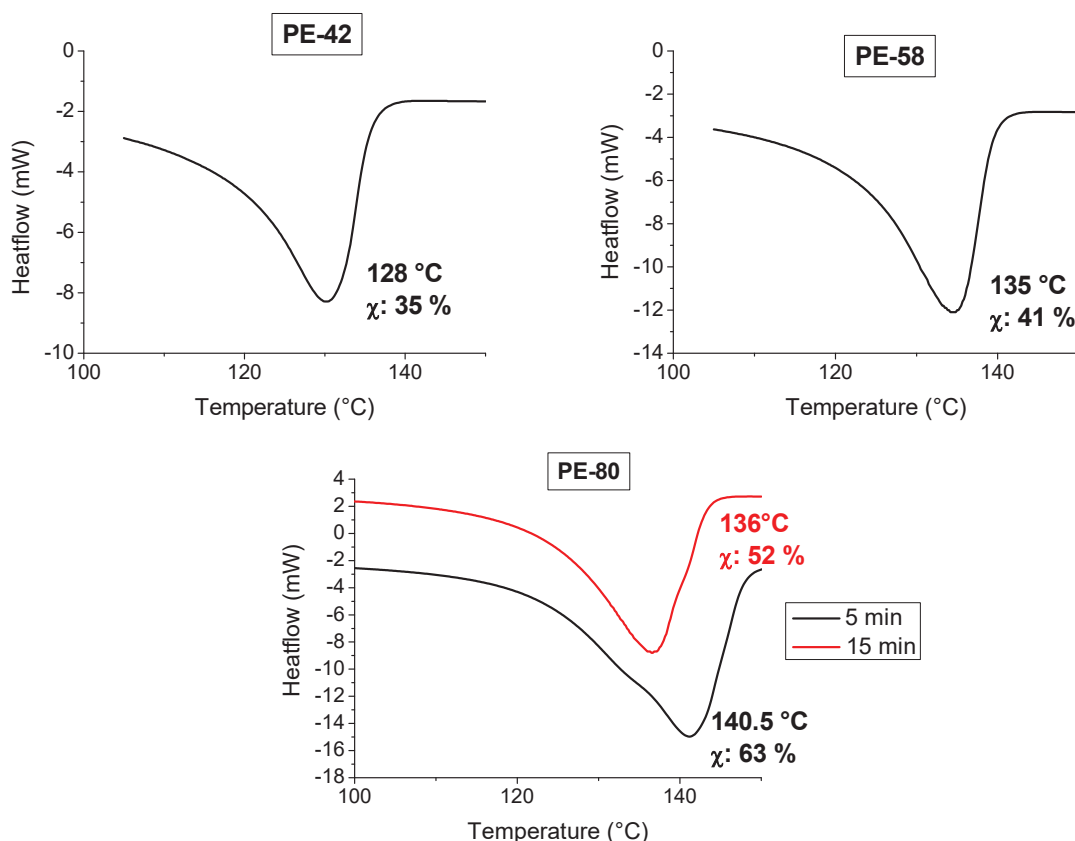


Figure 19. DSC profiles for PE-SFS-42, PE-SFS-58 and PE-SFS-80 after 5 minutes (black) and 15 minutes (red) of annealing at 160 °C

These annealing experiments reveal a difference of the polymer topology depending of the temperature of reaction. High molar mass HDPEs PE-SFS-42 and PE-SFS-58 seem to entangle during the 5 minutes of annealing. Even though this short time is surprising with respect to results from the literature, it is in line with the significant decrease of melting temperature observed in Figure 9. In spite of lower molar masses, molten PE-SFS-80 requires a longer time to reach the entanglement equilibrium. This dual topology would imply that part of macromolecules of higher molar mass (Figure 7) are very linear and non-entangled. One may also speculate that this fraction is generated by a polymerization active species that is not present at lower temperature. To go further, rheology characterization is a relevant technique to analyze the entanglement in PE-SFS-80.

III.2.2.1.2. Rheology

To determine the topology of the polymer, i.e its entanglement state, the evolution of the storage modulus G' of PE-SFS-80 was verified. In this purpose, time sweep experiment was conducted following the procedure described by Rastogi *et al.*¹⁸ Conditions were set at 160 °C under a 0.5 % strain and at 1 Hz. Such conditions are within the span of the rubbery plateau, which was checked beforehand.

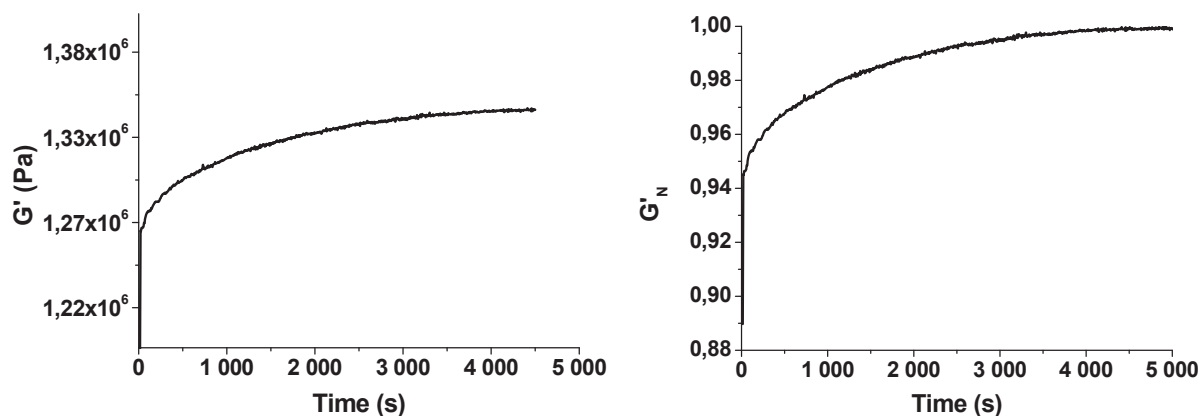


Figure 20. Time sweep experiment of PE-SFS-80 at 160 °C, 0.5 % strain, 1 Hz. Absolute (left) and relative (right) values of the storage modulus

From Figure 20, it is shown that G' value of PE-SFS-80 increases from 1.27 to 1.34 MPa over time. Indeed, the evolution of storage modulus is described as a fast increase of G' amounting from 89 to 95 % of its maximal value, while 90 minutes are necessary to reach the equilibrium. This modulus build-up reveals that PE-SFS-80 display not fully entangled macromolecules, as a progressive increase of entanglement density is observed. In the first stage, macromolecules with the lowest molar masses quickly reach their entanglement equilibrium. The remaining 5 % increase corresponds to cumbersome entanglement of the highest molar masses chains. As a result, the nonequilibrium polymer melt reflects an inhomogeneity of entanglement.

In comparison with polymers analyzed by Rastogi in the same conditions, PE-SFS-80 is closer to UHMwPE made by conventional Ziegler-Natta than by pseudo-living bis(phenoxy-imine) system. Thus, PE-SFS-80 would probably result from multi-site catalysis. Indeed, a similar G' span (1.4 MPa) and equilibration time (60-180 minutes) for PE of $4.5 \times 10^6 \text{ g mol}^{-1}$ implies that PE-SFS-80 contains high molar mass macromolecules with partial entanglement.¹⁸ Such high molar masses can also be responsible for CEF bimodal pattern, especially the population at high elution temperature (fraction 2). If time to reach entanglement equilibrium is long, so is the time for a complete dissolution of the polymer that allows a limited interaction in between macromolecules.

III.2.2.2. Cocrystallization effect

High molar masses most probably induce crystallization that would explain the bimodality in CEF experiment. It is relevant to check whether a cocrystallization effect is observed by DSC for the mixture of polymer in TCB. DSC temperature program is the same as CEF for the standard method but also includes a first heating step to mimic the dissolution step of CEF (Figure 21, top). The second endothermal profiles of PE-SFS-42, PE-SFS-58 and PE-SFS-80 were compared in Figure 21. Note that polymers are a thousand times more concentrated than in CEF experiments.

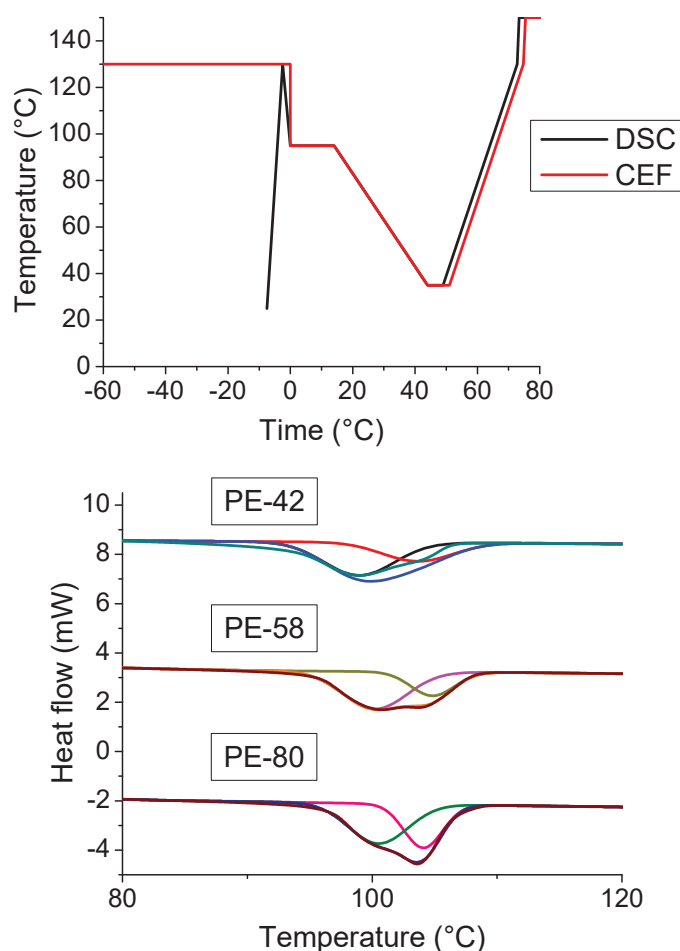


Figure 21. DSC program based on CEF method and last heating profile for PE-SFS-42 (1.17 g L⁻¹), PE-SFS-58 (1.2 g L⁻¹) and PE-SFS-80 (1.0 g L⁻¹) in 1,2,4-TCB

For the three polymers analyzed, a bimodal endothermal signal is obtained. Interestingly, characteristic temperatures (T_1' and T_2') are in a broader range for PE-SFS-42 (64 % at 99 °C; 36 % at 104.6 °C) and PE-SFS-58 (70 % at 100.2 °C; 30 % at 104.8 °C) than for PE-SFS-80 (58 % at 100.5 °C; 42 % at 104 °C). The increase of T_1' with the reaction temperature is consistent with the trends observed in CEF so far. Despite this similarity, T_2' of PE-SFS-80 is surprisingly lower than that of PE-SFS-42 and PE-SFS-58 whereas this HDPE fraction is prominent for PE-SFS-80 compared to other polymer in SIST analyses (Figure 17). Putting in perspective

higher T_2' and higher molar masses (Figure 7), one could assume that co-crystallization induced by longer macromolecules is responsible for the bimodal signal.

A higher entanglement density hampers the dissolution of longer polyethylene macromolecules in the last heating step. As a result, an inhomogeneous solution of polymer in the TCB is strongly suggested by the bimodality. Both entangled and unentangled domains constitute the polymer based on the storage modulus build-up for PE-SFS-80 (Figure 20). Therefore, dissolution of polymer would occur in the following order: lower molar masses, entangled and partially entangled high molar masses. Indeed, longer induction time is observed for initiating reptation of non-fully entangled polymer. Such effect could also occur in solution especially with the high concentration of polymer and the static mode of DSC measurement. In the case of less concentrated solution, this phenomenon is less pronounced since macromolecules are better isolated, resulting in a lower proportion of polymer eluted at higher temperature in CEF (Figure 17).

IV. CONCLUSIONS ON THE EFFECT OF TEMPERATURE AND POLYMER CHARACTERIZATION

In this chapter, the reactivity of a phenoxy-imine-ether system (FI)TiCl₃/MAO has been studied towards selective ethylene trimerization. This study combined to the original polymer-to-catalyst strategy provided information on the nature and number of polymerization active species.

A considerable insight has been gained with respect to the influence of temperature on the activity and the selectivity of the SFI system. This SFI system was shown to either trimerize or polymerize ethylene depending on the reaction temperature. Its selectivity switches from a significant production of the trimerization product, 1-hexene (85 wt %, from 520 to 450 kg_{1-hexene} g_{Ti}⁻¹ h⁻¹) between 32 and 42 °C, to a moderate polyethylene formation (70-80 wt %, 60-70 kg_{polyethylene} g_{Ti}⁻¹ h⁻¹) at higher reaction temperature (T > 60 °C). This binary behavior outlines the thermal deactivation of the trimerization catalyst and promotion of polymerization active species formation and/or enhancement of their activity.

The resulting polymers were analyzed combining miscellaneous characterization techniques and comparing them with single and multi-sites catalyst. Using DSC, SEC and high temperature ¹³C NMR analyses, polyethylenes were found to exhibit high molar masses (> 10⁵ g mol⁻¹) and a low 1-hexene content (< 1 mol %) at any temperature. Regarding chemical composition distribution, advanced segregation techniques (SIST, annealing, CEF) were found to be high molar mass-sensitive. Co-crystallization effects are strongly suggested by complementary rheological time sweep and PE/TCB DSC experiments. The increase of molar mass distribution dispersity at elevated temperature implies a change from single to multi-site catalysis. The poor comonomer incorporation ability of the active species echoes of a molecular Ziegler-Natta or a bulky post-metallocene catalyst. Eventually, this study narrowed the field of possibilities for polymerization active species to ligand-free "TiR_x" catalyst or post-metallocene Ti^{III} or Ti^{IV} derivatives.

To further clarify our understanding of the SFI system and the nature of the polymerization active species, the reactivity and polymer properties were studied over time and under altered conditions. Studies related to kinetics as well as the influence of selected parameters (1-hexene used as comonomer or monomer, introduction of hydrogen...) are presented in the following chapter.

V. EXPERIMENTAL SECTION

V.1. General considerations

All air and moisture sensitive reactions were carried out under argon atmosphere using Schlenk line, glovebox, Young NMR tube and vacuum techniques. Toluene, heptane and pentane were purchased from Biosolve and dried from a MBRAUN solvent purification system with activated alumina and copper catalyst columns. Dichloromethane was dried over CaH₂ and distilled before use. Deuterated solvents were stored under molecular sieves in the glovebox.

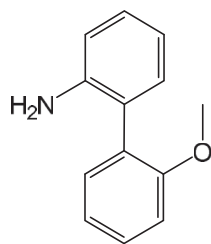
Chemicals and solvents used for the organic and complex synthesis are gathered in the following table:

Chemical	Supplier
2-bromoaniline, 98 %	Alfa Aesar
2-methoxybenzeneboronic acid, 95 %	TCI
2-tert-butyl-4-methylphenol, 99 %	Alfa Aesar
acetic acid, 99.5 %	Acros organics
magnesium chloride, ultra dry, 99.99 %	Alfa Aesar
magnesium sulfate, 99.9 9%	Sigma Aldrich
palladium dichloride, 99 %	Sigma Aldrich
paraformaldehyde 90 %	TCI
sodium carbonate	Sigma Aldrich
titanium tetrachloride, 1M in toluene	Acros organics
triphenylphosphine, 99 %	Sigma Aldrich
Solvent	Supplier
diethylether, anhydrous, > 99 %	Sigma Aldrich
dimethylformamide, anhydrous, 99.8 %	Sigma Aldrich
ethyl acetate, anhydrous, 99 %	Alfa Aesar
methanol, anhydrous 99.8 %	Sigma Aldrich

Methylaluminoxane 30 % in toluene (13.6 wt % of aluminum, 5.24 wt % TMA, 26.2 wt % MAO) was purchased from Albemarle. MAO was stored under inert atmosphere at -21 °C except when sampled at room temperature before catalytic tests. Ethylene (99.95 %) was purchased from Air liquid and was purified by passing through three columns containing activated molecular sieves, alumina and BASF cooper oxide catalyst.

V.2. Organic and complex syntheses

Synthesis of 2'-methoxy-[1,1'-biphenyl]-2-amine

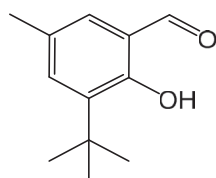


In a 15 mL Schlenk, PdCl₂ (0.50 g, 3.1 mmol) and P(Ph)₃ (1.57 g, 5.99 mmol) are mixed for 20 minutes in DMF (5 mL). In a 100 mL Schlenk, 2-bromoaniline (5.30 g, 31 mmol) in DMF (15 mL) is degassed for 15 minutes before the addition of 2-methoxyphenylboronic acid (4.72 g, 31 mmol). Then, a saturated solution of Na₂CO₃ (10 mL) is added before the addition of the solution containing the catalyst. The reaction mixture is stirred at 90 °C overnight for 16h. 20 mL of EtOAc + 20 mL of water are added at room temperature. The organic phase is extracted by 3x20 mL of EtOAc and 2x20 mL of water. The organic phase is dried over MgSO₄, filtered and concentrated. The crude product is purified by flash chromatography using silica gel and a mixture heptane/EtOAc (3/1). The product (R_f of 0.30) is a beige solid after drying under vacuum. Yield: 1.78 g, 8.9 mmol, 29 %.

¹H NMR (CD₂Cl₂, 300 MHz): δ (ppm) 7.45-7.40 (td, *J* = 2 Hz, *J* = 8 Hz, 1H, ArH), 7.30-7.06 (m, 5H, ArH), 6.87-6.77 (m, 2H, ArH), 3.85 (s, 3H, OCH₃), 3.73 (br, 2H, NH₂)

¹³C NMR (CD₂Cl₂, 75 MHz): δ (ppm) 157.05 (C), 145.14 (C), 132.01(CH), 131.40 (CH) 129.34 (CH), 128.73 (CH), 128.61 (C), 125.28 (C), 121.39 (CH), 118.14 (CH) 115.77 (CH), 111.49 (CH), 55.84 (CH₃)

Synthesis of the 3-tert-butyl-5-methylsalicylaldehyde

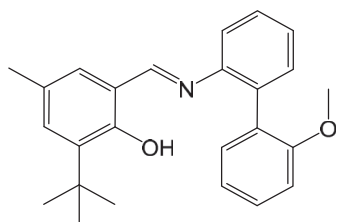


In a 100mL Schlenk, MgCl₂ (2.7 g, 28.1 mmol) and paraformaldehyde (6.9 g, 42.2 mmol) are mixed for 15 minutes in THF (15 mL). Triethylamine (2.8 g, 28.1 mmol) is then added to the solution. A solution of 3-(tert-butyl)-4-methylphenol (0.42 g, 14 mmol) in THF (50 mL) is added *via* cannula and the mixture is stirred at 75 °C overnight. After cooling, the yellow solution is diluted with diethylether (20 mL) and a solution of HCl 1N (15 mL). The organic phase is washed with 2x10 mL of HCl 1N and 2x10 mL of water. It is dried over MgSO₄, filtered and concentrated under vacuum. The residue is purified by recrystallization in pentane at -18 °C to afford yellow needles. Yield: 1.2 g, 6.2 mmol, 44 %.

¹H NMR (CD₂Cl₂, 300 MHz): δ (ppm) 11.65 (s, 1H, OH), 9.83 (s, 1H, O=CH), 7.37 (d, 1H, ArH), 7.21-7.20 (m, 1H, ArH), 2.33 (t, 3H, *J* = Hz, Ar-CH₃), 1.42 (s, 9H, ArC(CH₃)₃)

¹³C NMR (CD₂Cl₂, 75 MHz): δ (ppm) 197.73 (CH), 159.43 (C), 138.16 (C), 135.82 (CH), 131.88 (CH), 128.76 (C), 120.82 (C), 35.02 (C), 29.39 (3 CH₃), 20.66 (CH₃)

Synthesis of the phenoxy-imine-ether ligand (ligand 1)



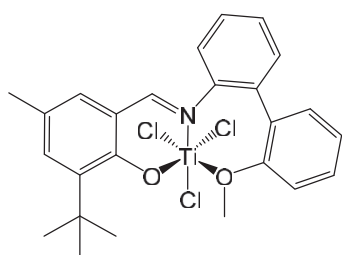
In a 100 mL Schlenk, 2'-methoxy-[1,1'-biphenyl]-2-amine (0.5 g, 2.51 mmol) and 3-*tert*-butyl-5-methylsalicylaldehyde (0.483 g, 2.51 mmol) are mixed in 20 mL of methanol before adding a drop of acetic acid. The reaction medium is stirred overnight at room temperature with molecular sieve. Some yellow solid precipitates while concentrating the reaction medium. Yield: 0.7 g, 1.88 mmol, 75 %.

¹H NMR (CD₂Cl₂, 300 MHz): δ (ppm) 13.31 (s, 1H, OH), 8.50 (s, 1H, N=CH), 7.45-7.32 (m, 4H, ArH), 7.24-7.20 (m, 2H, ArH), 7.14 (d, 1H, *J* = 2 Hz, ArH), 7.03-6.94 (m, 3H, ArH), 3.71 (s, 3H, O-CH₃), 2.27 (s, 3H, Ar-CH₃), 1.35 (s, 9H, Ar-C(CH₃)₃)

¹H NMR (toluene-*d*₈, 300 MHz): δ (ppm) 13.67 (s, 1H, OH), 8.10 (s, 1H, N=CH), 7.29-7.26 (m, 1H, ArH), 7.16-7.06 (m, 5H, ArH), 6.88-6.84 (m, 2H, ArH), 6.62-6.61 (m, 2H, ArH), 3.36 (s, 3H, O-CH₃), 2.14 (s, 3H, Ar-CH₃), 1.49 (s, 9H, Ar-C(CH₃)₃)

¹³C NMR (CD₂Cl₂, 75 MHz): δ (ppm) 163.50 (CH), 158.57 (C), 157.05 (C), 147.77 (C), 137.51 (C), 134.56 (C), 131.72 (CH), 131.66 (CH), 131.45 (CH), 130.56 (CH), 129.44 (CH), 128.97 (CH), 128.91 (C), 127.25 (C), 126.84 (CH), 120.73 (CH), 119.21 (C), 118.40 (C), 110.99 (CH), 55.54 (CH₃), 35.00 (C), 29.43 (3 CH₃), 20.72 (CH₃)

Synthesis of the phenoxy-imine-ether complex I



In a 100 mL Schlenk, a solution of titanium tetrachloride 1.0 N in toluene (1.1 mL, 1.1 mmol) is added to a solution of the phenoxy-imine-ether ligand (340.1 g, 0.91 mmol) in 10 mL of toluene at -78 °C. The solution is brought back to room temperature and stirred overnight. 50 mL of pentane is added to precipitate the catalyst. The brown-red particles are washed with 3x10 mL of pentane and dried under vacuum at 40 °C.

Yield: 0.38 g, 0.72 mmol, 79 %.

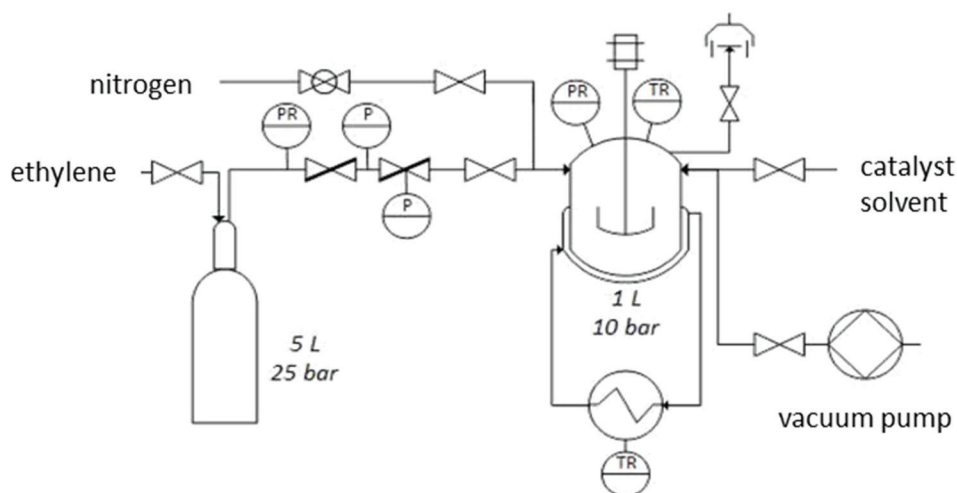
¹H NMR (CD₂Cl₂, 300 MHz): δ (ppm) 8.14 (s, 1H, N=CH), 7.53-7.47 (m, 3H, ArH), 7.41-7.30 (m, 5H, ArH), 7.16 (m, 2H, ArH), 4.34 (s, 3H, O-CH₃), 2.34 (s, 3H, Ar-CH₃), 1.50 (s, 9H, Ar-C(CH₃)₃)

¹³C NMR (CD₂Cl₂, 75 MHz): δ 169.23 (CH), 158.39 (C), 151.84 (C), 147.77 (C), 136.48 (C), 136.01 (CH), 134.61 (C), 133.09 (CH), 131.66 (CH), 131.58 (C), 131.02 (C), 130.51 (C), 130.13 (CH), 129.48 (CH), 128.79 (CH), 127.80 (C), 126.15 (C), 123.40 (CH), 72.53 (CH₃), 35.33 (C), 29.87 (3 CH₃), 21.02 (CH₃)

Elemental Analysis calculated (C₂₅H₂₆Cl₃NO₂Ti): C, 57.01; H, 4.98; N, 2.66 %. Found: C, 57.18; H, 5.01; N, 2.61 %.

V.3. Catalytic test procedure

V.3.1. Equipment



- 1L jacketed SFS reactor with gas inlet, liquid/vacuum inlet, injection chamber, a venting outlet, temperature and pressure sensor.
- 5L gas ballast with pressure sensor.
- Heating/cooling system (-60 to 80 °C)

V.3.2. Procedure

The reactor is heated at 80 °C under vacuum for 20 minutes. It is cleaned with 300 mL of a solution of TEA in heptane (15 mol L⁻¹). After 20 minutes, the solution is removed and the reactor is placed under vacuum for 10 minutes. The reactor is cooled down to the desired temperature and a commercial solution of MAO 30 wt % (1 mL, 1 200 eq) in 280 mL of toluene is injected. Once temperature is stable, the solution of complex (3 μmol) in 20 mL of toluene is introduced before feeding the reactor with purified ethylene. The catalytic test is carried out at 10 bar and the ethylene consumption is followed with the pressure drop of the ballast. After 30 minutes of reaction, the ethylene feed is stopped and 5 mL of methanol are introduced in the reactor *via* an injection sas. The reactor is cooled to 6 °C to condense the 1-hexene produced. The pressure is slowly released before opening the reactor. The liquid phase is treated with sulfuric acid and analyzed by GC with dodecane as internal standard. The solid is cleaned with acidified methanol then methanol and it is dried under vacuum at 90 °C for two hours.

V.4. Product analysis

V.4.1. Oligomer analyses

Gas Chromatography (GC)

Gas chromatography analyses were performed on a HP 6890 instrument using a HP5 column made of 5 % of diphenyl and 95 % dimethyl polysiloxane (32 m length, 0.32 mm diameter, 0.25 µm film) and a flame ionization detector. The injection volume is 1 µL and nitrogen is used as mobile phase with a flow of 1 mL min⁻¹. The temperature program is:

- 35 °C plateau for 10 min;
- heating to 76 °C at 0.6 °C min⁻¹;
- heating to 280 °C at 21 °C min⁻¹;
- 280 °C plateau for 20 min.

Dodecane was used as internal reference to determine the amount of oligomers produced after each catalytic test. After treating the liquid phase with an aqueous solution of H₂SO₄ and methanol, 0.5 mL of *n*-dodecane (anhydrous > 99 %, analytical grade) is introduced in the medium. 1 mL of the solution is analyzed without further dilution.

Gas Chromatography-Mass Spectrometry (GC-MS)

GC-MS analyses were performed on an Agilent 6850 instrument equipped with a HP5 column made of 5 % of diphenyl and 95 % dimethyl polysiloxane (32 m length, 0.32 mm diameter, 0.25 µm film) and an Agilent 5975C EI detector. The same temperature program as for GC analysis is used.

V.4.2. Polymer analyses

V.4.2.1. High-Temperature Size Exclusion Chromatography (HT-SEC)

HT-SEC analyses were performed using a Viscotek system (Malvern Instruments) equipped with three columns (PLgel Olexis 300 mm × 7 mm from Agilent Technologies). Samples volume of 200 μL and concentrations between 1-2 mg mL⁻¹ were eluted in 1,2,4-trichlorobenzene using a flow rate of 1 mL min⁻¹ at 150 °C. The mobile phase was stabilized with 2,6-di(*tert*-butyl)-4-methylphenol (200 mg L⁻¹). Online detection was performed with a differential refractive index detector, a dual light scattering detector (RALS LALS) and a viscometer detector for absolute molar mass measurement.

V.4.2.2. High Temperature Nuclear Magnetic Resonance (HT-NMR)

¹³C NMR analysis were performed with a Bruker Avance II 400 spectrometer operating at 100.6 MHz. In a 10 mm PA-SEX probe, about 100 mg of polymer are dissolved in 6 mL of solvent. A mixture of *o*-dichlorobenzene/*o*-dichlorobenzene-*d*₄ (9/1) was employed as solvent to record each spectrum at 120 °C.

The calculation of 1-hexene content in the polymer was made based on the method reported by Cossoul *et al.*¹⁴ They considered the integral of the polyethylene backbone I(CH₂) as well as αB₄ and βB₄, i.e Iα and Iβ respectively.

The region between 29 and 31 ppm is calibrated to 1 000 carbons. This range is composed of signals corresponding to CH₂ from the ethylene units (E) in the polyethylene backbone excluding 1-hexene moiety as well as CH₂ in 3B₄ position of 1-hexene (H) units. Therefore, its integral I(CH₂) is defined as:

$$I(\text{CH}_2) = 2(\text{E}-\text{H})$$

αB₄ and βB₄ counting for two 1-hexene molecules, their integrals (Iα at 34.5 ppm and Iβ at 27.3 ppm) were averaged to quantify the number of 1-hexene units:

$$H = (I\alpha + I\beta)/4$$

Consequently, the 1-hexene content was calculated as follow:

$$\text{mol \% 1-hexene} = H/(\text{E}+\text{H}) = (I\alpha + I\beta)/(2x(I(\text{CH}_2) + I\alpha + I\beta)$$

V.4.2.3. Differential Scanning Calorimetry (DSC)

Polyethylene melting temperature, crystallization temperature and crystallinity were determined using a Mettler Toledo DSC1.

Standard procedure

An average of 7 mg of PE was analyzed in 40 μ L aluminum crucible. After a first heating from 25 °C to 180 °C at 20 °C min⁻¹, the samples were cooled and heated within the same range of temperature at 5 °C min⁻¹. Only the second heat was considered. The measured specific enthalpy (Δh) and the enthalpy of fusion/crystallization of a 100 % crystalline PE ($\Delta h_c = 293 \text{ J g}^{-1}$) enabled the calculation of crystallinity:

$$\chi = 100 \times \frac{\Delta h}{\Delta h_c}$$

Stepwise Isothermal Segregation Technique

Sample preparation is identical to the standard procedure. Program temperature for SIST consists in the following steps:

- heating to 180 °C (20 °C min⁻¹);
- cooling to 130 °C (20 °C min⁻¹);
- successive plateaux lasting 60 minutes every 5 °C from 130 °C to 50 °C;
- heating to 180 °C (20 °C min⁻¹).

Annealing

Sample preparation is identical to the standard procedure. The temperature program used was based on the procedure described by Liu *et al.*¹⁸

- heating from 25 °C to 160 °C (25 °C min⁻¹);
- annealing plateau at 160 °C;
- cooling to 136 °C (-20 °C min⁻¹);
- crystallization plateau at 136 °C for 180 min;
- cooling to 25 °C (-20 °C min⁻¹);
- heating to 180 °C (20 °C min⁻¹).

Only the profile of the last heating is considered for deconvolution analysis.

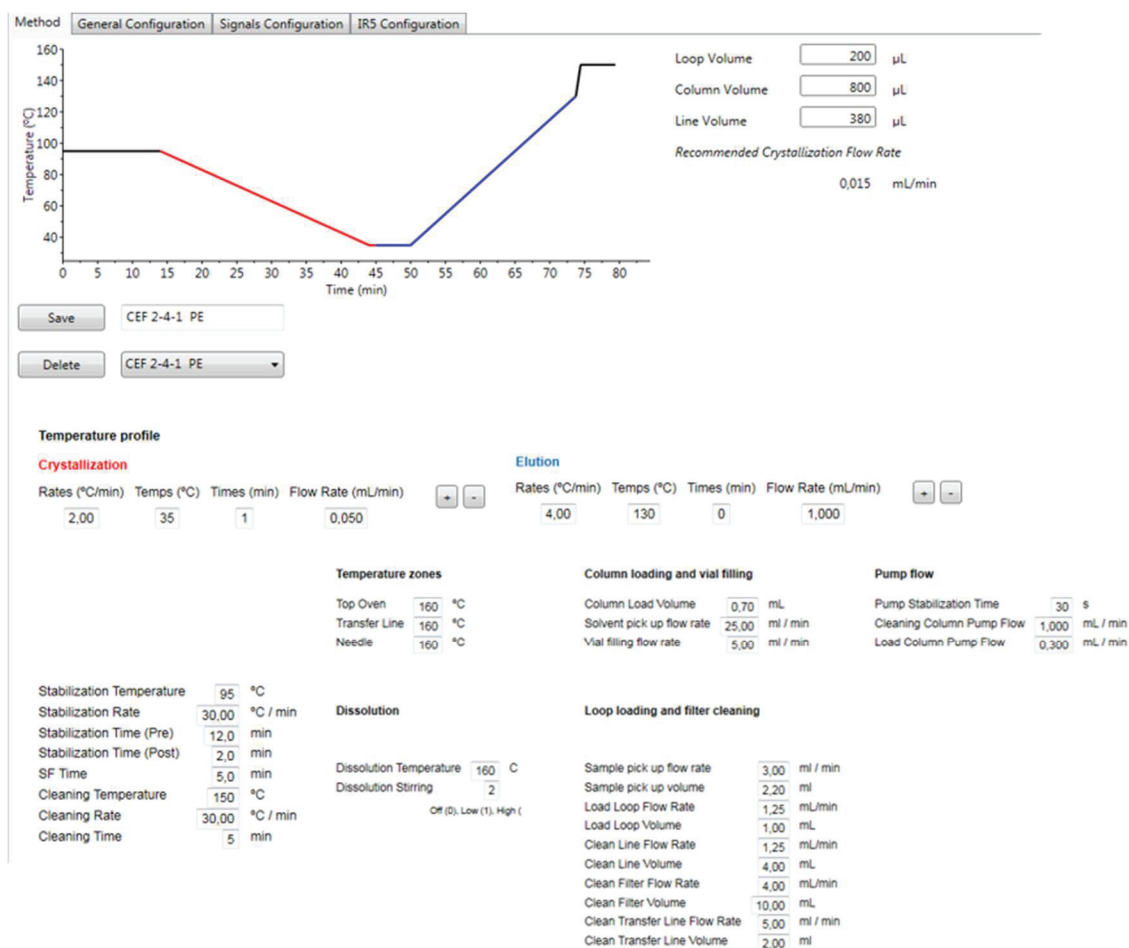
Procedure for PE/TCB analysis

An average of 1 mg of polyethylene is weighed in a medium-pressure 120 μ L-crucible. About 12 mg of TCB is added and the crucible is sealed with a Viton[®] O-ring. Temperature program is the same as for the standard CEF method detailed hereafter.

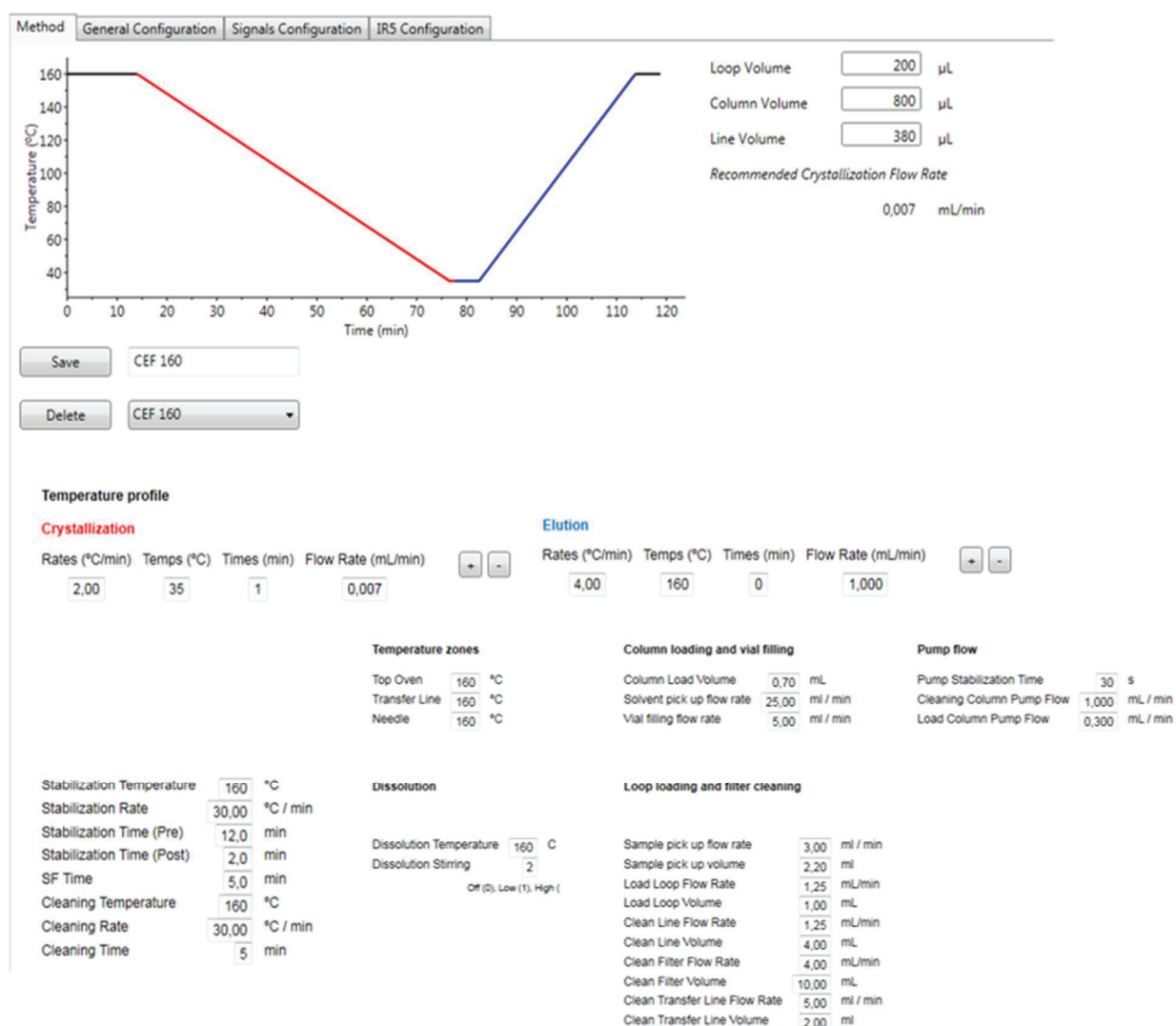
V.4.2.4. Crystallization Elution Fractionation (CEF)

Crystallization Elution Fractionation technique was carried out with an apparatus manufactured by Polymer Char S.A. The fractionation in CEF is based on dynamic crystallization of polymers on an inert support by temperature decrease within the CEF column. The polymer is thus segregated according to its chemical composition. Afterward, the fractions are further separated during a temperature rising elution cycle. Experimentally, about 3 mg of sample were dissolved at high temperature (135 °C) in 8 mL of 1,2,4-trichlorobenzene stabilized with 2,6-di(*tert*-butyl)-4-methylphenol. 0.5 ml of the sample solution is automatically loaded into the CEF column. The comonomer content for each fraction was determined by measuring CH₃ and CH₂ absorption using an IR detector. Calibration with poly(ethylene-*co*-1-hexene) containing a precise comonomer content enables to assess the molar percentage of 1-hexene in the polymer.

Standard procedure The temperature was slowly decreased to 35 °C at 2 °C min⁻¹ under a flow of 6.5 μL min⁻¹ to allow the polymer to crystallize. The second cycle was performed from 35 °C to 130 °C at a temperature rate of 1 °C min⁻¹ and flow rate of 1 mL min⁻¹.



Method CEF-160



V.4.2.5. Rheology

Sample preparation The polymer is compressed into a plate of 20 mm diameter and 1 mm at 125 °C, under the force of 5 tons for 30 minutes. Three 0.8 mm disks are cut using a metal punch.

Moduli measurement Rheological measurement were performed with a MARS 60 rheometer from ThermoScientific equipped with 16 mm concentric geometry heated by a Peltier cell. The disk is kept at 100 °C under a nitrogen flow to prevent polymer degradation. The sample is heated at 10 °C min⁻¹ from 130 to 160 °C. The dynamic amplitude sweep test is performed at a fixed frequency of 1 Hz to determine the linear viscoelastic region. The dynamic time sweep test is performed at a fixed frequency of 1 Hz and 0.5 % strain at 130 °C.

VI. REFERENCES

- 1 R. Duchateau, F. F. Karbach and J. R. Severn, *ACS Catal.*, 2015, **5**, 5068–5076.
- 2 S. Ishii, T. Nakano, K. Kawamura, S. Kinoshita, S. Ichikawa and T. Fujita, *Catal. Today*, 2018, **303**, 263–270.
- 3 H. Audouin, R. Bellini, L. Magna, N. Mézailles and H. Olivier-Bourbigou, *Eur. J. Inorg. Chem.*, 2015, **2015**, 5272–5280.
- 4 H. Audouin, PhD thesis, Ecole normale supérieure de Lyon - ENS LYON, 2015.
- 5 D. W. Imhoff, L. S. Simeral, S. A. Sangokoya and J. H. Peel, *Organometallics*, 1998, **17**, 1941–1945.
- 6 A. Sattler, J. A. Labinger and J. E. Bercaw, *Organometallics*, 2013, **32**, 6899–6902.
- 7 Y. Suzuki, S. Kinoshita, A. Shibahara, S. Ishii, K. Kawamura, Y. Inoue and T. Fujita, *Organometallics*, 2010, **29**, 2394–2396.
- 8 United States, US8258361B2, 2012.
- 9 J. A. Suttill, D. S. McGuinness, M. G. Gardiner and S. J. Evans, *Dalton Trans.*, 2013, **42**, 4185–4196.
- 10 G. B. Galland, R. F. de Souza, R. S. Mauler and F. F. Nunes, *Macromolecules*, 1999, **32**, 1620–1625.
- 11 X.-Y. Wang and R. Salovey, *J. Appl. Polym. Sci.*, 1987, **34**, 593–599.
- 12 P. Lehmus, O. Härkki, R. Leino, H. J. G. Luttikhedde, J. H. Näsman and J. V. Seppälä, *Macromol. Chem. Phys.*, 1998, **199**, 1965–1972.
- 13 E. Adisson, M. Ribeiro, A. Deffieux and M. Fontanille, *Polymer*, 1992, **33**, 4337–4342.
- 14 E. Cossoul, L. Baverel, E. Martigny, T. Macko, C. Boisson and O. Boyron, *Macromol. Symp.*, 2013, **330**, 42–52.
- 15 M. Zhang, D. T. Lynch and S. E. Wanke, *Polymer*, 2001, **42**, 3067–3075.
- 16 M. Haager, G. Pinter and R. W. Lang, *Macromol. Symp.*, 2004, **217**, 383–390.
- 17 A. A. Alghyamah and J. B. P. Soares, *Macromol. Symp.*, 2012, **312**, 43–50.
- 18 K. Liu, E. L. de Boer, Y. Yao, D. Romano, S. Ronca and S. Rastogi, *Macromolecules*, 2016, **49**, 7497–7509.

Chapter 3. Kinetic studies and activation process investigations

TABLE OF CONTENT

I. INTRODUCTION	138
II. KINETIC STUDIES.....	139
II.1. KINETICS ACCORDING TO REACTION TEMPERATURE	139
II.1.1. KINETIC MODEL APPLIED TO THE SFI SYSTEM.....	139
II.1.2. REACTION RATE EVOLUTION FOR THE TEMPERATURE STUDY.....	142
II.1.3. EARLY STAGE REACTION.....	144
II.2. STUDY OF THE SFI SYSTEM AT SEVERAL REACTION TIMES	146
II.2.1. EQUIPMENT	146
II.2.2. KINETIC STUDIES AT 40, 60 AND 80 °C.....	147
II.2.2.1. Catalytic test conditions	147
II.2.2.2. Reproducibility of catalytic tests	149
II.2.2.3. Evolution of reaction rate at 40, 60 and 80 °C	151
II.2.2.4. Evolution of products formation and features over time	153
II.3. DISCUSSION ON ACTIVE SPECIES FORMATIONS BASED ON KINETIC CONSIDERATIONS	158
III. PARAMETERS INFLUENCING THE ACTIVATION PROCESS.....	160
III.1. GOAL AND STRATEGY.....	160
III.2. INFLUENCE OF ADDITIONAL 1-HEXENE.....	161
III.2.1. ACTIVITY & SELECTIVITY.....	161
III.2.2. POLYMER PROPERTIES.....	164
III.3. INFLUENCE OF HYDROGEN.....	166
III.3.1. ACTIVITY & SELECTIVITY.....	166
III.3.2. PRODUCTS PROPERTIES	167
III.3.2.1. Evolution of molar mass distribution with hydrogen pressure.....	167
III.3.2.2. Impact of hydrogen on 1-hexene incorporation in the polymer.....	168
III.4. INFLUENCE OF TMA AND PREMIX	169
III.4.1. ACTIVITY & SELECTIVITY.....	169
III.4.2. INFLUENCE OF TMA AND MAO PREMIX ON POLYMER FEATURES	173
III.4.2.1. Comparison of molar mass distribution of polymers.....	173
III.4.2.2. Chemical composition of polymer obtained with MAO premix.....	174
IV. CONCLUSION.....	176

V. EXPERIMENTAL SECTION.....	178
V.1. GENERAL CONSIDERATION	178
V.2. CATALYTIC TESTS CONDITIONS FOR KINETICS STUDIES.....	178
V.2.1. STOPPED-FLOW REACTOR	178
V.2.2. SYNTHESIS AND CATALYTIC TEST ON CHEMSPEED UNIT.....	179
V.2.2.1. Complex I synthesis.....	179
V.2.2.2. Tests with ethylene on Chemspeed reactors.....	179
V.3. CATALYTIC TESTS WITH THE 1 LITER SFS REACTOR	180
V.3.1. INTRODUCTION OF 1-HEXENE	180
V.3.2. USE OF HYDROGEN	181
V.3.3. USE OF TMA AS CO-CATALYST	181
V.3.4. PREMIX COMPLEX I/MAO	181
VI. REFERENCES	182

I. INTRODUCTION

The rationalization of active species formation for the SFI system aims at identifying the key step for polymerization catalysts generation. From the temperature study detailed in the previous chapter, it appears that, contrary to trimerization reaction, polymerization activity and selectivity are promoted upon increase of reaction temperature but little is known regarding their evolution throughout the catalytic tests. Thus, no clear link has been identified regarding trimerization and polymerization species formation.

In the purpose of preventing the generation of polymerization active species, deeper investigations on active species formations during the catalytic tests should be undertaken. Kinetic studies are considered to track the evolution of activity over time and to follow product formation. This way, initiation of polymer production can be clearly identified with respect to the stage of reaction (early, mid, last stage), which informs on the relationship between trimerization and polymerization active species formation.

Even once polymer production is associated with a stage of reaction, the mechanism of active species formation remains unknown. In the literature, the activation process is often incriminated in side catalysts formation. In this view, hypotheses can be formulated by alteration of catalytic test conditions and studying the impact of each parameter on the reactivity of the system.

This chapter mainly focusses on the effect of temperature and activation process on the kinetics of the system as well as its selectivity and the polymer properties. First, kinetics of reactions performed in the temperature study (Chapter 2) are analyzed and additional kinetic studies of complex I/MAO at several reaction times were implemented on dedicated set-ups. This study targets the favored trimerization conditions (40 °C, 60 °C) and polymerization conditions (80 °C). In a second section, the activation process was altered by varying reaction conditions: use of TMA as cocatalyst, premixing of precatalyst and MAO and addition of 1-hexene or hydrogen (Figure 1). The response of the system is assessed with respect to kinetics, selectivity and polymer properties.

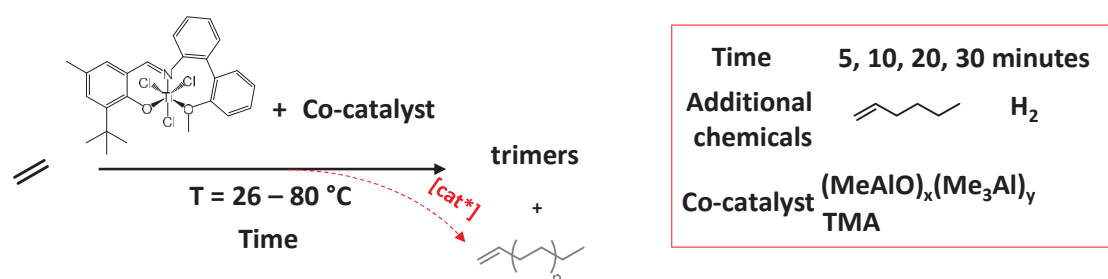


Figure 1. Parameters studied for the investigation of the SFI system kinetics and activation process

II. KINETIC STUDIES

II.1. Kinetics according to reaction temperature

II.1.1. Kinetic model applied to the SFI system

From the evolution of reaction rates, it is possible to determine the order of reaction relatively to ethylene concentration. A first or second order profile informs whether the rate determining step of the overall process involves rather one or two ethylene molecules. In the early literature on the SFI system, Fujita *et al.* reported a second order reaction for the production of 1-hexene (see Chapter 1, IV.3.2.2. Trimerization mechanism).¹ However, DFT calculations performed by the same group indicate that the insertion of ethylene in the pentacycle kinetically limits this reaction owing to a high free energy (122.3 kJ mol⁻¹).²

In this study, a comparison between first and second order is made based on the evolution of reaction rate.³ In the case of a first order dependence, $\ln(R_p)$ is linear with time. On the contrary, $\frac{1}{R_p}$ is linear for second order reactions. This difference results from the definition of reaction rate (Equation 1).

$$R_p = \frac{d[C_2]}{dt} \quad \text{and (i) } R_p = k[C_2] \text{ (1}^{\text{st}} \text{ order reaction)}$$

$$\text{(ii) } R_p = k[C_2]^2 \text{ (2}^{\text{nd}} \text{ order reaction)}$$

Equation 1. General reaction rates equations according to the order of reaction

For all experiments performed at $T < 42^\circ\text{C}$ and $T > 49^\circ\text{C}$, both $\ln(R_p)$ and $\frac{1}{R_p}$ were plotted as a function of time (Figure 2).

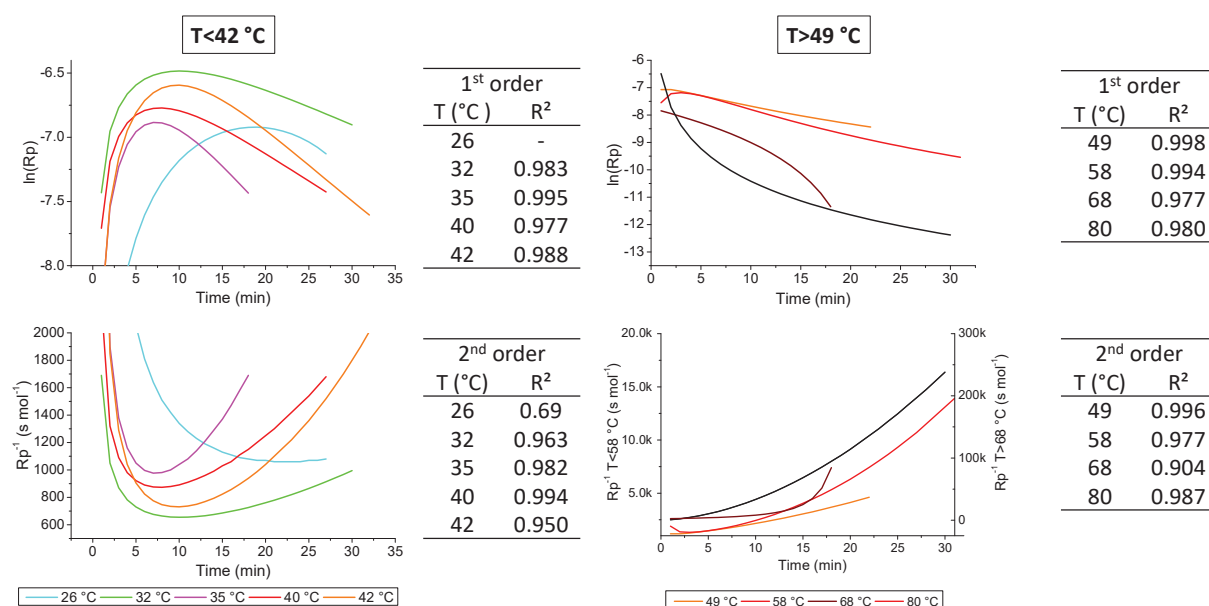


Figure 2. Determination of the order of reaction in “trimerization conditions” ($T < 42^\circ\text{C}$, left) and “polymerization conditions” ($T > 49^\circ\text{C}$, right)

For most of the reactions, reaction rate evolutions are in favor of first order kinetics. At low temperature ($T < 42\text{ }^{\circ}\text{C}$) and after 10 minutes of reaction, $\ln(R_p)$ is closer to a linear trend than $\frac{1}{R_p}$ (Figure 2). At higher temperature ($T > 49\text{ }^{\circ}\text{C}$), the comparison of $\ln(R_p)$ and $\frac{1}{R_p}$ does not enable to draw a straightforward conclusion but the results tend to support a first order kinetics (Figure 2). As a result, the evolution of reaction rate can be fitted with a model describing similar kinetic profiles. Kissin's model was found to be adequate for this system.

Kissin's model was developed to describe the polymerization reaction in the case of a heterogeneous Ziegler-Natta polymerization catalyst.⁴ This model was applied to the SFI system since there are at least two active species in the system, i.e trimerization and polymerization catalysts. Kissin's kinetic model relies on several steps detailed in Scheme 1. Based on the observations and hypotheses made in the literature, a proposition of kinetic steps for the trimerization mechanism attributed in analogy with the model for polymerization mechanism is detailed in Scheme 1.

		<i>Kissin's model for polymerization</i>	<i>Analogy with trimerization reaction</i>
Activation	k_f	$C \rightarrow C^*$	$C' + C_2 \rightarrow C'^*$
Initiation	k_i	$C^* + C_2 \rightarrow C-P$	$C'^* + 2 C_2 \rightarrow C'^*-C_4$
Propagation	k_p	$C^*-P_n + C_2 \rightarrow C^*-P_{n+1}$	$C'^*-C_4 + C_2 \rightarrow C'^*-C_6$
Transfer	k_t	$C^*-P \rightarrow C^* + P$	$C'^*-C_6 \rightarrow C'^* + C_6$
Deactivation	k_d	$C^* \rightarrow D$	$C'^* \rightarrow D$

Scheme 1. Kissin's model adapted to the trimerization system

For the trimerization reaction applied to Kissin's model, the formation step was assumed to be the reduction Ti^{IV} (C') to Ti^{II} (C'^*) corresponding to the insertion of ethylene into the Ti-Me bond before the concomitant β -H transfer and reductive elimination.² The formation of the pentacycle (C'^*-C_4) *via* oxidative coupling would be the initiation step while the propagation is associated with the insertion of the third ethylene molecule in the metallacycle. Eventually, transfer reactions are assimilated to the release of 1-hexene by concerted β -H intramolecular transfer of the heptanacycle (C'^*-C_6) and the deactivation of the trimerization species affords an unidentified and inactive species (D). In the literature, the formation of an inactive Ti^{III} species is assumed to explain the death of trimerization active species.⁵

Based on the reaction scheme, Kissin developed Equation 2 for modeling the evolution of reaction rate over time. In this model, initiation, propagation and deactivation rate steps are sufficient to describe the behavior of the catalytic system. Moreover, ethylene and titanium concentration contributes to the activity rate of the system with a first order.

$$R_p = k_p [Ti][C_2] \frac{k_i}{k_d - k_i} (e^{-k_i t} - e^{-k_d t})$$

Equation 2. Kissin's reaction rate equation for the model described in Scheme 1 in the case of heterogeneous ZN catalysis with k_i and k_d in s^{-1} , k_p in $L^2 mol^{-2} s^{-1}$, $[Ti]$ and $[C_2]$ in $mol L^{-1}$

For the records, the concentration of ethylene was calculated from Kissin's relationship adapted to the chosen conditions, i.e in toluene as solvent, under 10 bar of ethylene at a given temperature (Equation 3).⁶

$$[C_2] = 1.74 \times 10^{-3} P_{C_2} e^{1284/T}$$

Equation 3. Relationship between ethylene concentration ($mol L^{-1}$) in toluene under the ethylene pressure P_{C_2} (bar) at temperature T (K)

Using Equation 2 and Equation 3, the resulting fitted curves (dashed lines) are superimposed to the experimental curves (solid lines) in Figure 3. All data fitting using Kissin's model were in agreement with experimental R_p curves, except at 26 and 80 °C. As a result, this model can be applied in both "trimerization conditions" and "polymerization favored conditions". This conclusion implies that the mechanism of active species formation, especially polymerization species, is the same in each conditions ($T < 50$ °C and $T > 50$ °C).

From this model, initiation, propagation and deactivation steps seem to have the highest impact on the reactivity of the SFI system. However, another model should be applied for experiments performed at 26 and 80 °C. Indeed, their reaction rate profiles are quite different from other profiles, explaining maybe why experimental data would not properly overlap with the curve following Kissin's Equation 2.

II.1.2. Reaction rate evolution for the temperature study

A kinetic study was undertaken on the SFI system complex I/MAO to quantify the evolution of its activity over time depending on reaction temperature. The reaction rate evolution informs on the behavior of the catalytic system in terms of initiation, propagation and deactivation over time. Comparing the reaction rate profiles according to reaction temperature is complementary to the temperature study (Chapter 2) where the activity, the selectivity and polymer properties were studied after 30 minutes of reaction. Therefore, it was necessary to clarify the active species formation schemes (Chapter 2, Scheme 3) by ruling out hypotheses based on kinetic considerations. In this purpose, kinetic studies were performed to track the evolutions of the reaction rate of the system over time and compare them according to reaction temperature. The corresponding reaction rate profiles are distinguished between reactions performed in the “trimerization conditions” ($T < 50\text{ }^{\circ}\text{C}$) and the “polymerization favored conditions” ($T > 50\text{ }^{\circ}\text{C}$) (Figure 3, left and right respectively). These data are fitted with a kinetic model (Figure 3, dashed lines) detailed in Scheme 1.

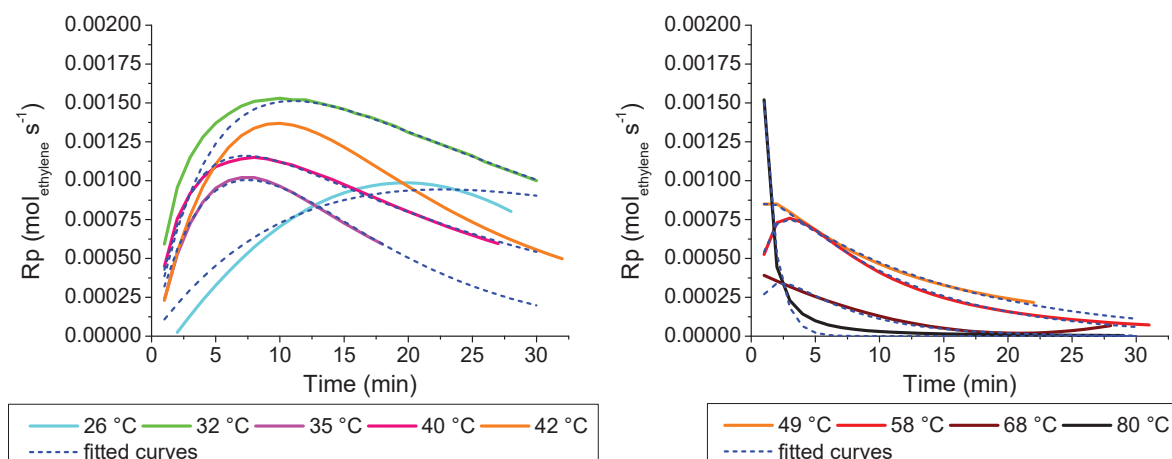


Figure 3. Reaction rate profile of complex I/MAO tested from 26 to 42 °C (left, solid lines) and 49 to 80 °C (right, solid lines) and fitted curves (dashed lines)

For all reaction temperatures, reaction rate profiles exhibit a similar pattern (Figure 3, solid lines). In fact, most of the activities increases rapidly during the first minutes of the test and decreases with a different decay profile according to reaction temperature. One can note a clear difference in reaction rate profiles for reactions performed below and above 50 °C. Moreover, two reaction rate evolutions at 26 °C and 80 °C are distinguished from others profiles for similar conditions.

In the case of “trimerization conditions” ($T < 50\text{ }^{\circ}\text{C}$) (Figure 3, left), the activity rates are similar during the ascending phase and reach a maximum value around $400\text{ mol}_{\text{ethylene}}\text{ mol}_{\text{Ti}}^{-1}\text{ s}^{-1}$ ($844\text{ kg}_{\text{ethylene}}\text{ g}_{\text{Ti}}^{-1}\text{ h}^{-1}$). After 5 to 10 minutes, the system starts to deactivate. For this second phase, the activity of the system decreases with a higher rate as the reaction temperature

increases. Interestingly at 26 °C, it takes 22 minutes for the system to reach the same maximum activity value than at 35 °C.

Regarding reactions performed above 49 °C (Figure 3, right), the highest reaction rates are reached within the first two minutes of reaction. The maximum activity rate are significantly lower at higher reaction temperature, with a decrease from 200 to 100 mol_{ethylene} mol_{Ti}⁻¹ s⁻¹ (420 and 210 kg_{ethylene} g_{Ti}⁻¹ h⁻¹ respectively). At 80 °C, the system deactivates since the early stage of reaction and becomes inactive after 10 minutes.

From the reaction rate profiles in the “trimerization conditions, it was observed that:

- (i) Despite a high concentration in ethylene, activity increases with a lower rate at 26 °C than at higher temperature;
- (ii) Although maximal reaction rates (400 mol_{ethylene} mol_{Ti}⁻¹ s⁻¹) are reached within the same range time (5-10 minutes), these maximum values decrease as reaction temperature increases;
- (iii) For reactions performed between 32 and 42 °C, the main difference lies in the decay profile displaying a faster deactivation with temperature.

From (ii), it seems that the amount of active species is rather stable within the range of temperature 32-42 °C. Differences in speed of deactivation (iii) can be attributed to an effect of the temperature favoring deactivation reaction.

In contrast, the evolution of activity in the “polymerization favored conditions” shows that:

- (i) The deactivation is initiated within the first two minutes of reaction;
- (ii) The maximal activity rate decreases with the reaction temperature;
- (iii) Decay curves display a similar slot, except at 80 °C.

Therefore, one can conclude from (ii) that the number of active species decreases with reaction temperature. (i) and (iii) implies that the difference between each experiment is only linked to their maximal reaction rate, i.e the amount of active species at the initial stage. One can assume that higher temperature limits either the formation of active species and/or favored deactivation of the trimerization catalyst, while maintaining a continuous production of polymer. This polymer activity follows the same trend over time at the expense that the number of polymerization active species seems to decrease. Indeed, reaction rate profiles could be superimposed by translation along the y-axis. It is important to note that the production of a high amount of polymer in the reaction medium may explain or at least favor the deactivation of the system. It can be the case for the experiment performed at 80 °C since the reaction stops after 10 minutes.

To accurately compare the influence of temperature on each kinetic step, a comparison of kinetic constants is required. k_i , k_p and k_d were calculated for each experiment of the temperature study using Excel Solver (Table 1).

Table 1. Kinetic constants according to reaction temperature calculated from Kissin's Equation 2

Entry	T (°C)	[ethylene] (mol L ⁻¹) ^a	k_i (s ⁻¹)	k_p (L mol ⁻¹ s ⁻¹)	k_d (s ⁻¹)
1	26	1.275	7.354x10 ⁻⁴	216.76	7.350x10 ⁻⁴
2	32	1.171	4.872x10 ⁻⁴	1099.21	3.462 x10 ⁻³
3	35	1.124	2.232x10 ⁻³	287.82	2.229x10 ⁻³
4	40	1.052	5.547x10 ⁻³	143.07	6.51x10 ⁻⁴
5	42	1.025	1.675x10 ⁻³	303.09	1.671x10 ⁻³
6	49	0.938	1.206x10 ⁻³	3439.47	4.641x10 ⁻²
7	58	0.842	1.638x10 ⁻³	676.45	1.432x10 ⁻²
8	68	0.751	2.920x10 ⁻³	318.53	1.455x10 ⁻²
9	80	0.661	2.264x10 ⁻¹	464.27	1.750x10 ⁻²

^a calculated with Equation 3

For each experiment, initiation and deactivation constants are in the same order of magnitude. These constants decrease at higher reaction temperature as well as the ratio k_d/k_i , which is about 1 in "trimerization conditions" (Table 1, entries 1-3 and 5) and between 6 and 38 in "polymerization conditions" (Table 1, entries 6-8). Thus, at low temperature, propagation reactions are preferentially favored followed by initiations and eventually deactivations. On the contrary, reaction rate is mainly impacted by propagation and deactivation reactions at T > 49 °C.

Although this study gives a clear picture of the evolution of the SFI system activity over time, it does not allow to draw straightforward conclusions regarding the dependence of trimerization and polymerization active species. Moreover, it is not possible to associate each phenomenon (increase in activity rate and deactivation) with the evolution of trimers and polymer production over time because their formation could not be tracked with this set-up. For example, the fast activation during the early stage of reaction could be associated with trimerization, polymerization or both. Therefore, early-stage reaction studies were undertaken using a reactor designed for short time reactions.

II.1.3. Early stage reaction

The monitoring of trimerization and polymerization production for shorter reactions was implemented on a slurry “stopped-flow” reactor. CO₂ was injected after the desired reaction time to quench the reaction. The reduced volume of the reactor and *a fortiori* loading of catalyst, oriented toward conditions where a sufficient amount of both oligomers and polymer are yielded. Therefore, catalytic tests were carried out at 60 °C given that 1-hexene and polyethylene selectivities are alike. All experiments are performed with 0.6 μmol of complex I and MAO as co-catalyst (Al/Ti = 1 580) in 30 mL of toluene. The evolution of product formation was analyzed at the early stage of reaction after 1, 3 and 5 minutes (Figure 4).

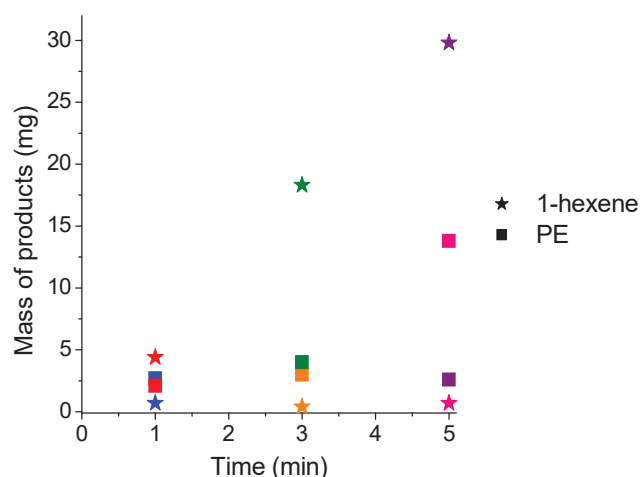


Figure 4. Evolution of products formation over time using a “stopped-flow” reactor
0.61 μmol Ti, 1 580 eq. Al/Ti, 30 mL toluene, 60 °C, 10 bar ethylene
Each color corresponds to one catalytic test

The duplication of experiments for each reaction time shows variations in 1-hexene and polymer yields for the reaction times (Figure 4). For each time of reaction, the main product is either 1-hexene or polyethylene. At 3 and 5 minutes, a significant gap in mass of products is observed. The selectivity of each product is either 10-20 or 80-90 wt % at each reaction time, which stresses a major reproducibility issue.

Despite this lack of reproducibility, kinetics experiments reveal the formation of polyethylene even at the first stage at reaction. Moreover, polymer formation seems to be continuous for the first 5 minutes of reaction. Polymerization species are therefore generated within the first minutes of reaction, implying that they are not solely afforded by the deactivation of the trimerization catalyst.

As the “stopped-flow” reactor set up is clearly not adapted for short time experiments, three identical reactors operated in an automated Chemspeed platform were used as an alternative to perform a reliable kinetic studies.

II.2. Study of the SFI system at several reaction times

II.2.1. Equipment

Chemspeed platform is a fully automated medium-throughput unit dedicated to catalysts synthesis and testing under inert atmosphere (argon). This unit is integrated in a glovebox (Figure 5) to limit contamination during the synthesis of air- and moisture-sensitive homogeneous catalysts and polymerization reactions. This device is unique in Europe and is located in Axel'One Campus, Villeurbanne, France.

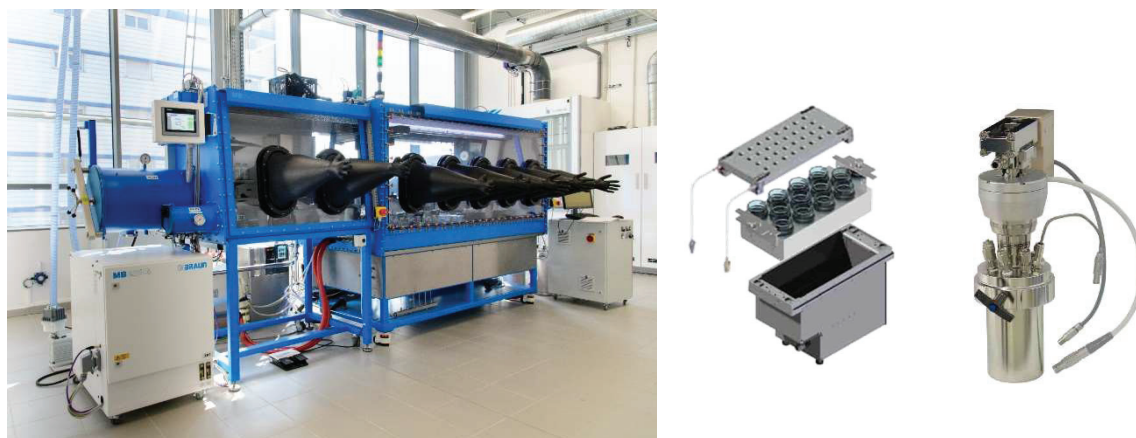


Figure 5. Chemspeed platform (left), ISYNTH© module (middle) and 270 mL-autoclave (right)

The Chemspeed platform brings major advantages compared to the reactors available in the C2P2 laboratory. In the case of standard procedure, catalytic tests are performed in a 1L-reactor, which involves multiple material and steps for catalytic testing (glovebox and Schlenk handling, reactor inertization and loading). Chemspeed unit is automated and all-inclusive, equipped with precatalyst synthesis module (ISYNTH©) and medium-pressure reactors in the same glovebox (Figure 5), offering a considerable gain of time. Indeed, three catalytic tests can be performed simultaneously. Regarding temperature control during catalytic tests, an efficient system combining a heating and cooling circuit enables the management of exothermal reactions. The temperature of the reactor is monitored by the electrical heating while the cooling temperature is fixed at 5 °C. This way, a constant temperature is guaranteed during the catalytic test. Eventually, the automation and the controlled atmosphere provides reproducible working conditions and thus reliable results. In fact, a reproducibility study was performed with a polymerization system before implementing the SFI trimerization system complex I/MAO on this unit.

The reproducibility study of the three reactors was conducted with the polymerization CGC catalyst from Dow Chemical (Chapter 1, Figure 7). This study confirmed the high level of reproducibility after several repetitions of the tests. It should be highlighted that the three reactors are also consistent with one another. Chemspeed autoclaves were also found to be

reliable for short time reactions. Their efficient heating/cooling system was well-adapted to face the temperature control issues involved by other reactors. Consequently, kinetic studies were implemented on this powerful device.

II.2.2. Kinetic studies at 40, 60 and 80 °C

II.2.2.1. Catalytic test conditions

Having proven the achievement of catalytic test reproducibility using Chemspeed autoclaves, both complex I synthesis and catalytic tests were performed simultaneously by the mean of sequences created and adapted for each condition tested. Examples of sequences for the complex synthesis and catalytic tests are given in the experimental section. Analyses of complex I synthesized using this procedure were consistent with the complex synthesized using Schlenck and glovebox technique.

Catalytic tests were performed in 120 mL toluene using 1.8 μmol of precatalyst and 1 500 equivalents of aluminum from a solution of MAO 30 wt % in toluene. Compared to the standard conditions presented in Chapter 2, a higher amount of titanium was purposely employed to afford a sufficient amount of polymer for further analyses. Moreover, such high titanium concentrations are not an issue given a satisfactory temperature control achieved with the efficient heating/cooling system.

Regarding the catalytic test procedure, the succession of several steps are executed differently with the Chemspeed unit compared to the 1 L-reactor. The workflow is presented in Figure 6 and a sequence programmed for catalytic test is exemplified in the experimental section. Contrary to the standard procedure, the precatalyst solution is injected under pressure in the reactor once the ethylene pressure (10 bar) and desired temperature are stabilized (Figure 6). This difference can have an impact on the reactivity of the system since the contacting of precatalyst and cocatalyst occurs in presence of ethylene in this case. The activation process and the kinetics may therefore be altered compared to the case where the reactor is pressurized after the introduction of complex in the solution of MAO in toluene (standard procedure).

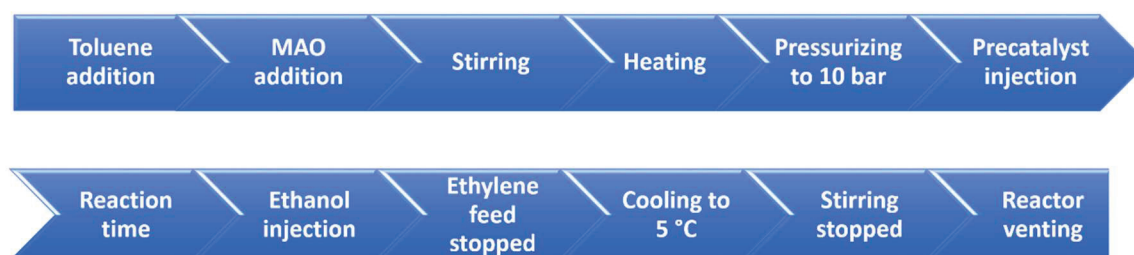


Figure 6. Workflow for catalytic tests with complex I/MAO

Kinetic studies were performed at 3 temperatures and 4 reaction times. The choice of temperature was restricted to 40 °C (“trimerization conditions”), 60 °C (“isoselectivity conditions”) and 80 °C (“polymerization conditions”). For each temperature, tests were carried out for 5, 10, 20 and 30 minutes. To guarantee the accuracy of experiments, temperature is fixed for the same series in the three reactors. It will be demonstrated later on that a satisfying reproducibility was obtained for reactions performed at the same temperature but in a different series.

For the kinetics studies, a series of 11 experiments were performed using the three autoclaves available on the Chemspeed platform. The conditions for each catalytic test are presented in Table 2. It is noteworthy that the titanium loading may differ between series, which slightly alter the Al/Ti ratio. Indeed, the mass of complex slightly varies during preparation of precatalyst solution with the SWILE© module while the volume of MAO 30 wt % in toluene injected is kept constant (0.6 mL).

Table 2. Catalytic tests conditions for the kinetic studies of complex I/MAO

Entry	T (°C)	t (min)	n _{Ti} (μmol)	Al/Ti
1	40	5	1.73	1 550
2	40	10	1.90	1 400
3	40	20	1.90	1 400
4	40	30	1.90	1 400
5	60	5	1.73	1 550
6	60	20	1.95	1 500
7	60	30	1.73	1 550
8	80	5	1.79	1 500
9	80	10	1.84	1 500
10	80	20	1.84	1 500
11	80	30	1.78	1 150

Conditions: complex I, 120 mL toluene, 0.6 mL of MAO 30 wt % in toluene, 10 bar of ethylene

II.2.2.2. Reproducibility of catalytic tests

The kinetics studies enable to have detailed view of the evolution of activity over time. The first concern to focus on is the reproducibility between the tests, which is necessary to confidently compare formation of products and their selectivities. Therefore, the first consideration is to verify the evolution of temperature and ethylene consumption at each instant of the reaction (Figure 7).

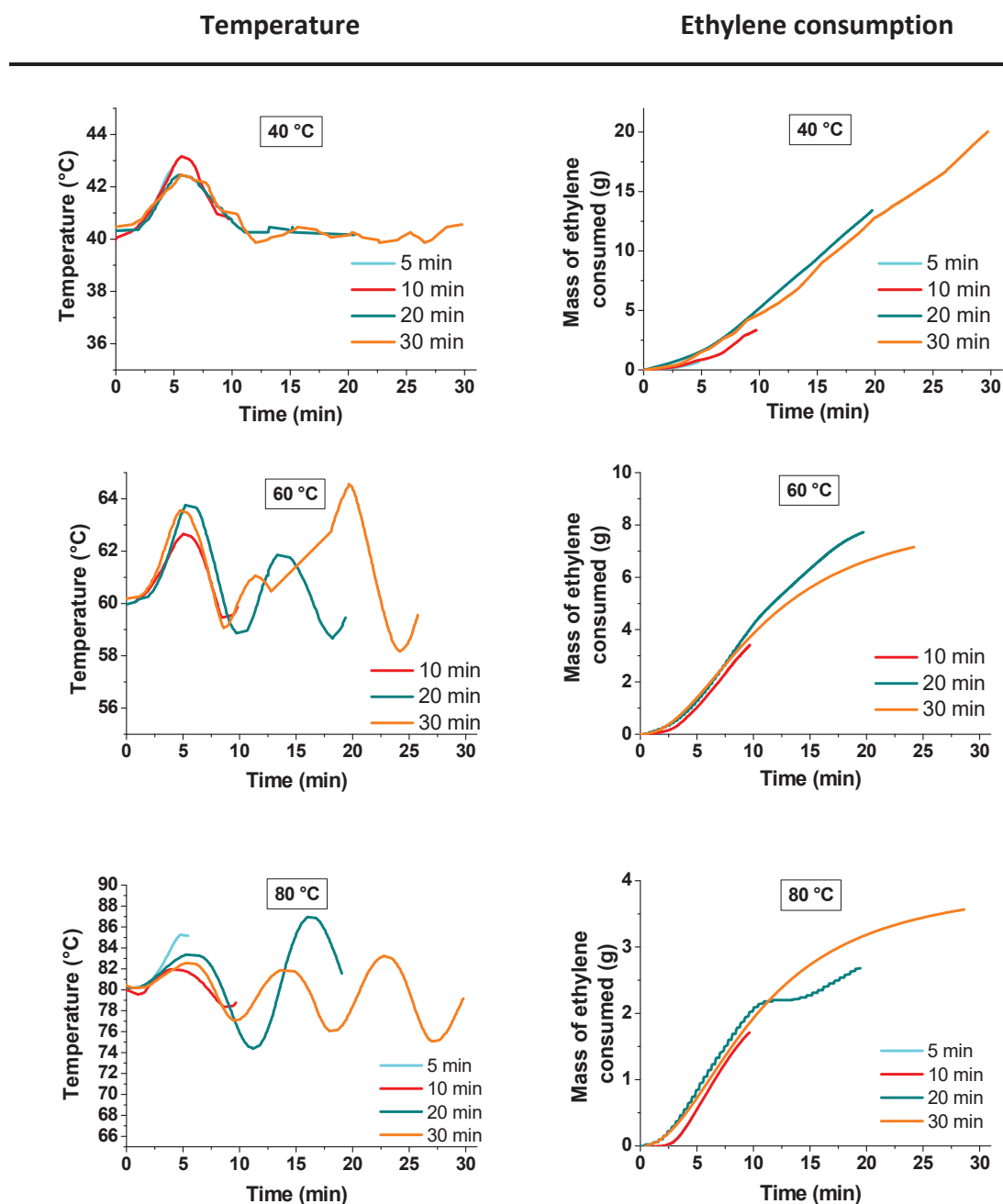


Figure 7. Evolution of temperature (left) and ethylene consumption (right) over time

For most of experiments performed at the same desired temperature, the reproducibility in temperature is achieved. It is quite impressive to see the superimposition of temperature

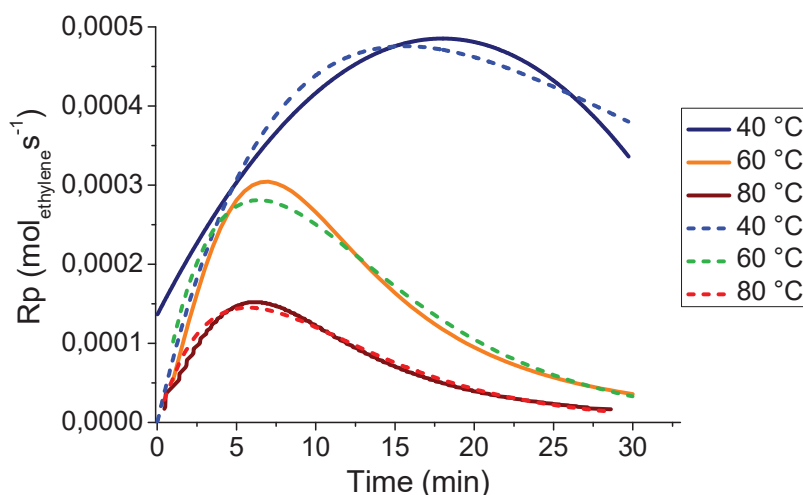
profiles for reactions performed at 40 °C (Table 2, entries 1-4). Moreover, temperature variations are similar for tests carried out at 60 °C and 80 °C, except for experiments lasting 30 and 20 minutes respectively (Table 2, entries 7 and 10). At the early stage of all experiments, temperature increases owing to a fast exotherm observed previously and favored by the high concentration of active species in this case. Still, the efficiency of the cooling system enables to limit the temperature overshoot to 4 °C on average.

For $T > 40$ °C, fluctuations of temperature are observed in the ranges 58-64 °C and 74-88 °C when temperature is set at 60 and 80 °C respectively. One reason for explaining such variations, which are actually reproducible, is the formation of polymer around the thermowell. The swollen solid limits the thermal transfer between the reaction medium and the sensor. Therefore, the control system over compensates the biased slow thermal response from the reaction medium, explaining the larger fluctuations of temperature at 80 °C than 60 °C.

Regarding the reproducibility of ethylene consumption at a given time of reaction, one can observe a similar consumption over time for each temperature. At 40 °C, the mass of ethylene consumed over time is consistent for all tests (Table 2, entries 1-4). At 60 °C and 80 °C, the evolution of monomer consumption for tests performed for 30 and 20 minutes respectively, seems to deviate from other tests. In fact, similarities and differences in ethylene consumption are found to be directly linked to the quality of temperature control. These results show that the conditions selected for the kinetic studies are a satisfactory compromise between the control of temperature, thus reproducibility, and the minimum amount of polymer required for further analysis.

II.2.2.3. Evolution of reaction rate at 40, 60 and 80 °C

From the ethylene consumption extracted from Figure 7, the reaction rates could be compared between 40, 60 and 80 °C. Since a satisfying reproducibility was achieved, only reactions lasting 30 minutes were considered for the comparison. The experimental data are fitted with Kissin's model described by Equation 2 and the resulting kinetic constants were calculated using excel Solver. The superimposition of experimental and fitted curves at 40, 60 and 80 °C is presented in Figure 8.



T (°C)	[ethylene] (mol L ⁻¹)	k _i (s ⁻¹)	k _p (L mol ⁻¹ s ⁻¹)	k _d (s ⁻¹)
40 °C	1.052	5.965x10 ⁻⁴	146.08	1.735x10 ⁻³
60 °C	0.822	2.604x10 ⁻³	57.19	2.603x10 ⁻³
80 °C	0.661	2.902x10 ⁻³	39.98	2.901 x10 ⁻³

Figure 8. Evolution of reaction rates from experimental data (solid line) and fitting with Kissin's model (dashed lines) at 40, 60 and 80 °C (Table 2, entries 4, 7 and 11 respectively).

For experiment performed at 40 °C, 60 °C and 80 °C, the comparison of reaction rate profiles in Figure 8 shows a clear difference in kinetic behavior. Although for all experiments the activity increases and progressively decreases, the maximum reaction rate of 540 kg_{ethylene} g_{Ti}⁻¹ s⁻¹ at 40 °C is 1.5 and 3-fold the activity at 60 °C and 80 °C respectively. Moreover, the system deactivates faster at higher reaction temperature. Indeed, the decay in activity is initiated within the first 10 minutes of reaction at 60 and 80 °C and the system becomes inactive after 30 and 25 minutes respectively. At 40 °C, the system initiates a progressive deactivation after 18 minutes but remains active after 30 minutes. This study reveals a lower activity at higher temperature, which is consistent with the general trend extracted from the temperature study performed on a 1 liter SFS reactor.

Applying the same Kissin's kinetic model for ethylene polymerization, a reliable fitting with experimental data confirmed a first order dependence of the reaction rate with ethylene concentration. This model accurately corroborates with experimental data especially in conditions of enhanced polymer productivity, i.e 60 °C and 80 °C (Figure 8). Applying Kissin's model at 40°C is relevant although the fast initial activation could not be fitted. In fact, one should bear in mind that the data fitting is applied to a system with a dual reactivity: trimerization and polymerization. Although polymerization is predominant at 60 and 80 °C, trimerization is the main reaction at 40 °C. It is conceivable that this kinetic scheme is not a complete model for describing the behavior of this dual system. Indeed, 1-hexene concentration is not taken into account and most probably impact the reaction rate in conditions of high 1-hexene activity. In kinetic studies performed on Hessen's Titanium-based derivatives, trimerization and polymerization were considered separately and the kinetic fitting was applied on trimers and polymer formation, not ethylene consumption.⁷ In this case, deactivation was linked to the polymerization reaction however no clear model taking into account both reactions was proposed.

Similarities in kinetic behavior are observed between the 30-minutes reactions performed in 1 L-reactor (Figure 3) and the Chemspeed autoclaves (Figure 8). Overall reactions, the SFI system displays the same evolution of reaction rate although activity values are lower in the 270 mL reactors than the 1-L one. Consequently, more active species are generated in the latter case. At 60 and 80 °C, deactivations occur earlier and faster in the case of the temperature study (1 liter SFS reactor) than the kinetic studies (Chemspeed reactors). However, straightforward conclusions can hardly be extracted from the comparison of k_i and k_d contributions. Still, initiation and deactivation reactions display a close kinetic constant ($k_i/k_d = 0.99$), slightly higher at 80 °C than 60 °C (Figure 8). At 40 °C, the evolution of reaction rate is not governed by a higher k_d , which is actually equal in both temperature and kinetic studies (Table 1, entry 4 and Figure 8), but rather a lower k_i value. In this case, a sustainable formation of numerous active species maintained for 18 minutes before the decay of reaction rate. Differences in kinetic behavior highlighted so far can surely be associated to a scale effect but also the reaction conditions. Indeed, the activation process differs as ethylene is introduced either before or after that the precatalyst and cocatalyst are contacted. Importantly, the control of temperature, especially during the first minutes of catalytic test can have a significant impact on the evolution of activity over time.

II.2.2.4. Evolution of products formation and features over time

The reproducibility of Chemspeed reactors and the accuracy with the results obtained in the temperature study (chapter 1) allow to confidently analyze the products formation over time. As product selectivities were previously obtained after 30 minutes of reaction, this study gives more details regarding the appearance of products at given reaction times. The evolution of selectivities over time at 40, 60 and 80 °C are shown in Table 3.

Table 3. Product selectivities and yields for different reaction times at 40, 60 and 80 °C

Entry	T (°C)	t (min)	1-hexene		C ₁₀ H ₂₀		Polyethylene	
			m (g)	wt %	m (g)	wt %	m (g)	wt %
1	40	5	4.5	85.7%	0.67	12.8%	0.08	1.5%
2	40	10	5.6	84.8%	0.88	13.4%	0.12	1.8%
3	40	20	11.1	83.4%	2	15.0%	0.21	1.6%
4	40	30	11.6	82.5%	2.2	15.7%	0.26	1.8%
5	60	5	3.2	72.4%	0.26	5.8%	0.970	21.7%
6	60	20	4.2	69.0%	0.11	1.8%	1.780	29.2%
7	60	30	4.3	69.7%	0.43	6.9%	1.450	23.4%
8	80	5	0.4	15.6%	0.01	0.4%	1.990	84.0%
9	80	10	0.4	21.0%	0.01	0.5%	1.530	78.5%
10	80	20	0.6	25.9%	0.02	0.9%	1.550	73.1%
11	80	30	0.4	11.6%	0.013	0.4%	3.047	88.1%

Conditions: Table 2, complex I, 120 mL toluene, 0.6 mL of MAO 30 wt % in toluene, 10 bar of ethylene

For each temperature, selectivities for the main reaction product are rather constant over time. At 40 °C, trimerizations remain the main reactions with an overall selectivity > 98 wt % over time (Table 3, entries 1-4). The increasing selectivity in branched C₁₀H₂₀ oligomers at higher reaction time is explained by a higher 1-hexene concentration in the reaction medium over time. Surprisingly, ethylene trimerization is also the main reaction at 60 °C with a selectivity around 70 wt % for 1-hexene, whatever the time of reaction. As a matter of fact, the system was expected to afford as much 1-hexene as polymer, based on the results of the temperature study (Chapter 2, Table 3). One should also note that selectivity in polyethylene is higher after 20 minutes than 30 minutes (entries 6 and 7). This out-of-trend results can be explained by the deviation in temperature observed previously during the catalytic test performed for 30 minutes (Figure 7). At 80 °C, polyethylene is the main product (> 70 wt %) appearing as soon as 5 minutes of reaction. Interestingly, 1-hexene and polyethylene selectivities are inverted at 60 and 80 °C. Contrary to the cases where trimerizations are the main reactions (entries 1-7), the selectivity of the main product, i.e polyethylene, increases over time from 80 wt % to 88 wt % at 80 °C. The same remark can be made for experiment 10

(Table 3), regarding its lack of consistency with other experiments. Note that experiments 7 and 10 will not be considered for the rest of the kinetic studies given their deviations in terms of temperature, ethylene consumption and product selectivity in comparison with other experiments performed at the corresponding temperature.

Comparing experiments lasting 30 minutes of reaction in the case of the temperature (Chapter 1, Table 3) and kinetic studies (Table 3, entries 4, 7 and 11), selectivities are in the same range with the one obtained with the 1 L-reactor at 40 °C (83.7 wt % for 1-hexene, 13.9 wt % in C₁₀H₂₀ and 2.2 wt % for polyethylene) and 80 °C (19.6 wt % in 1-hexene, 0 wt % in C₁₀H₂₀ and 80.4 wt % for polyethylene). However, a surprisingly high 1-hexene selectivity (70 wt %) is obtained at 60 °C for the kinetic studies whereas the system was expected to be isoselective toward

1-hexene and polyethylene (50/50 wt %). It could be explained by a difference in temperature fluctuation, especially at the beginning of the reaction, which is better controlled using Chemspeed autoclaves than the SFS reactor. It is therefore another illustration of the high temperature sensitivity of the SFI system.

From this study, the evolution of the relative yield for each product over time can be analyzed to identify a relationship or independence between trimerization and polymerization product formation. The relative yield is calculated by dividing the amount of a product by its final yield, i.e mass of product obtained after 30 minutes of reaction (Table 3, entries 4, 6 and 11). This way, one can hypothesize or rule out paths for the formation of trimerization and polymerization active species. The relative yield of each product (1-hexene, C₁₀H₂₀ and polyethylene) was investigated over time in conditions of favored trimerization (40 °C) and polymerization (80 °C) (Figure 9).

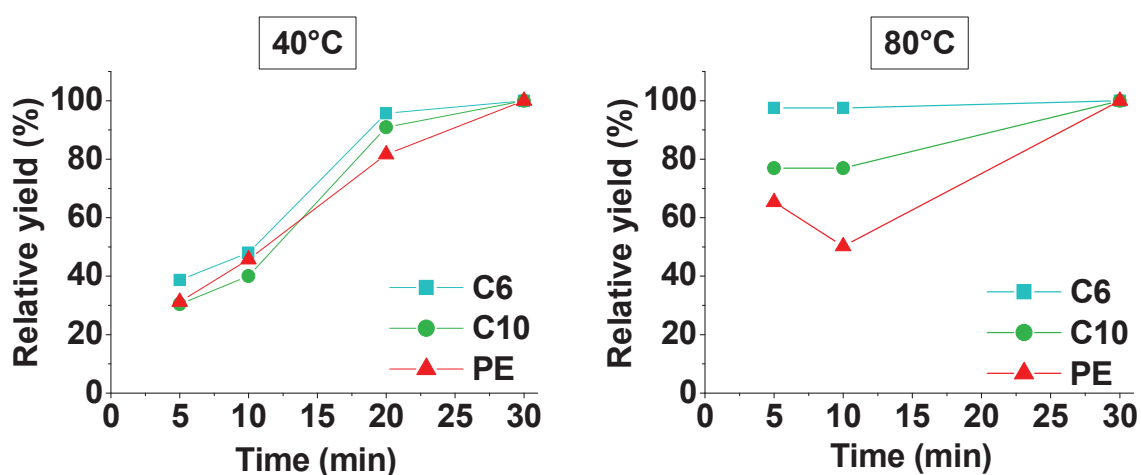


Figure 9. Evolution of relative yield ($m_t/m_{30 \text{ min}}$) over time

From Figure 9, it is clear that the processes of oligomers and polymer production are different at 40 °C and 80 °C. In conditions of favored trimerization, all products are continuously generated and their relative yields follow the same trend. Indeed, for each compound, about 40 wt % of the overall yield is obtained within the first 5 minutes of reaction. Despite a similar evolution of product formation, one should bear in mind that there are significant differences of selectivities between 1-hexene, C₁₀H₂₀ and polyethylene (Table 3). Based on a similar evolution of relative yield, one could hypothesize that the ratio between trimerization and polymerization active species is kept constant over time. As a consequence, these species would be formed from the same source in a parallel process at the early stage of reaction.

In contrast, trimers and polymer production seem to be independent at 80 °C. 1-hexene is only generated within the first 5 minutes of reaction as its amount is stable over time with 0.39-0.4 g for 1-hexene formed. On the contrary, the quantity of polymer evolves from 1.99 g after 5 minutes to 3.05 g after 30 minutes. Note that the increase of C₁₀H₂₀ oligomers corresponds to the evolution from 0.010 to 0.013 g, which is in the range of incertitude. These results reveal that the trimerization system deactivates rapidly while polymerization species produces polymer continuously. Thus, trimerization and polymerization species formation at 5 minutes may also be concomitant in analogy with the hypothesis made at 40 °C. However it is also possible that part of trimerization species are converted into polymerization species after 5 minutes of reaction, explaining the increase of polymer production at 80 °C (Figure 8).

Performing experiments at different reaction times enables to track the evolution of the chemical composition of the polymer formed throughout the process. This way, the ability of the polymerization species to incorporate 1-hexene can be followed. The evolution of 1-hexene content for all polymers collected from experiments 1-11 is presented in Figure 10. 1-hexene content was calculated from Equation 2 (Chapter 2) found for complex I/MAO and applied to the melting temperature measured by DSC. For the sake of clarity, polymers produced with Chemspeed reactors at the temperature T and after t minutes are labeled PE-CR-T_t in the rest of this manuscript.

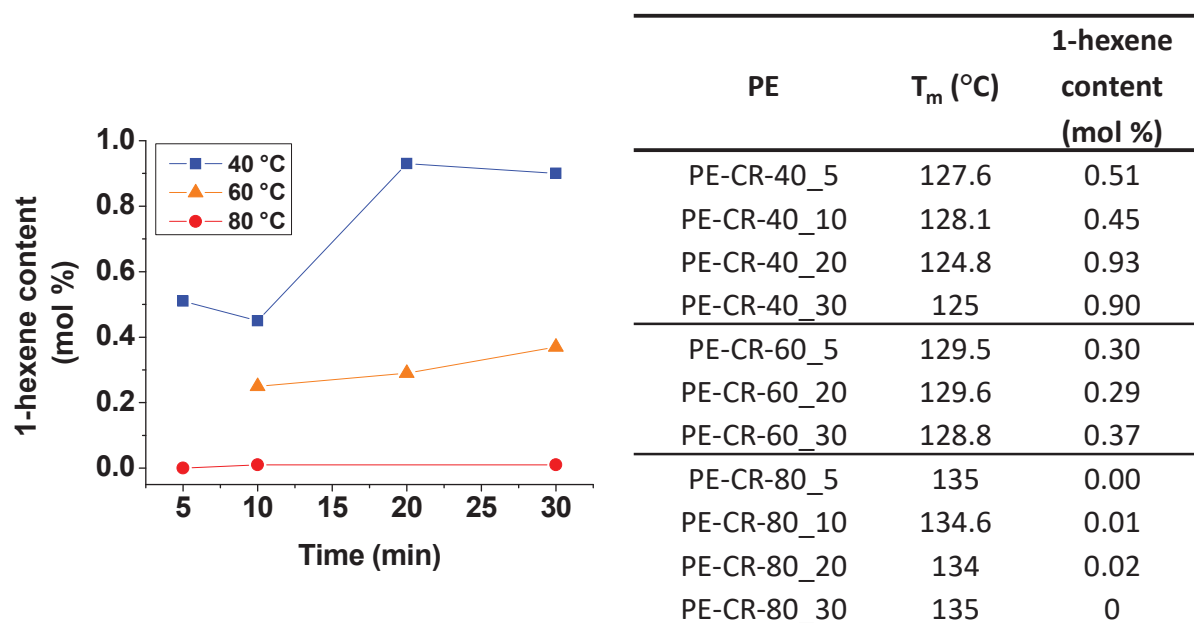


Figure 10. Evolution of the 1-hexene content over time at 40, 60 and 80 °C

The incorporation of 1-hexene in the polymer over time is a reliable indicator of a potential evolution of active species throughout the catalytic test. At 40 °C and 60 °C, 1-hexene content in the polymer increases owing to the 1-hexene enrichment in the reaction medium (Table 3). This continuous increase of 1-hexene content in the polymer confirms that the polymerization species remain active during the catalytic tests. Without great surprise, homopolyethylenes are produced at 80 °C since a small amount of 1-hexene (0.4 g) is available in the reaction medium.

To accurately compare the behavior of the polymerization active species, 1-hexene incorporation has to be put in perspective with the concentration of titanium species and 1-hexene in the reaction medium. The relationship between 1-hexene content in the PE and in the reaction medium follows the same correlation at 40 °C and 60 °C (Figure 11). Little can be concluded for PE-CU-80 given the low 1-hexene concentration in the liquid phase. A similar 1-hexene response characterizes an identical polymerization catalyst. Thus, it seems that the same polymerization species produces PE-CR-40 and PE-CR-60.

Chemical composition of polymer can also be compared with respect to the 1-hexene content in the liquid phase for both temperature and kinetic studies. The evolutions of 1-hexene content in the polymer are shown in Figure 11.

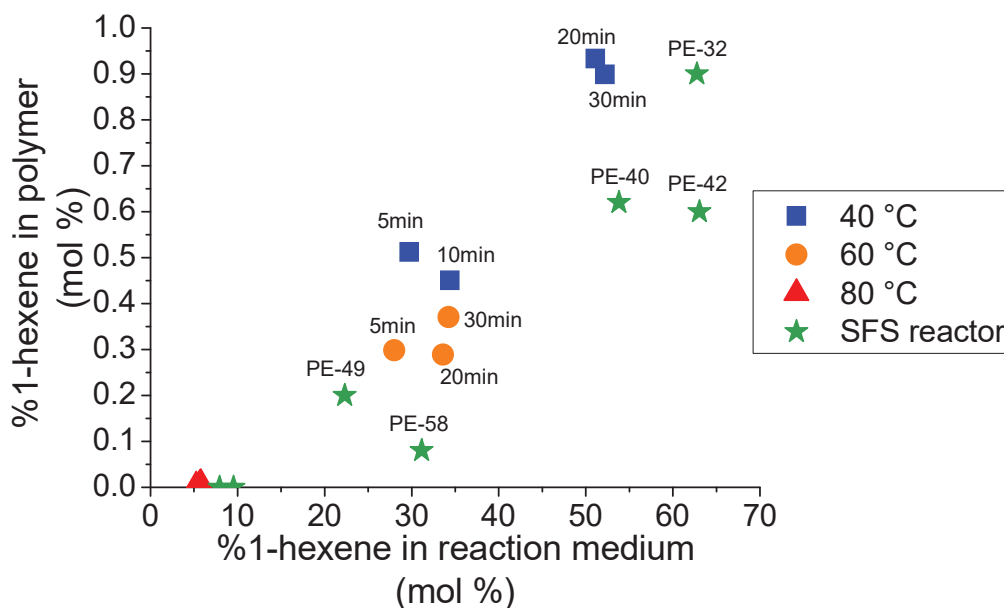


Figure 11. Comparison of the 1-hexene content in the polymer and in the reaction medium relatively to the titanium loading. Results for polymer obtained in the temperature study are included (green stars)

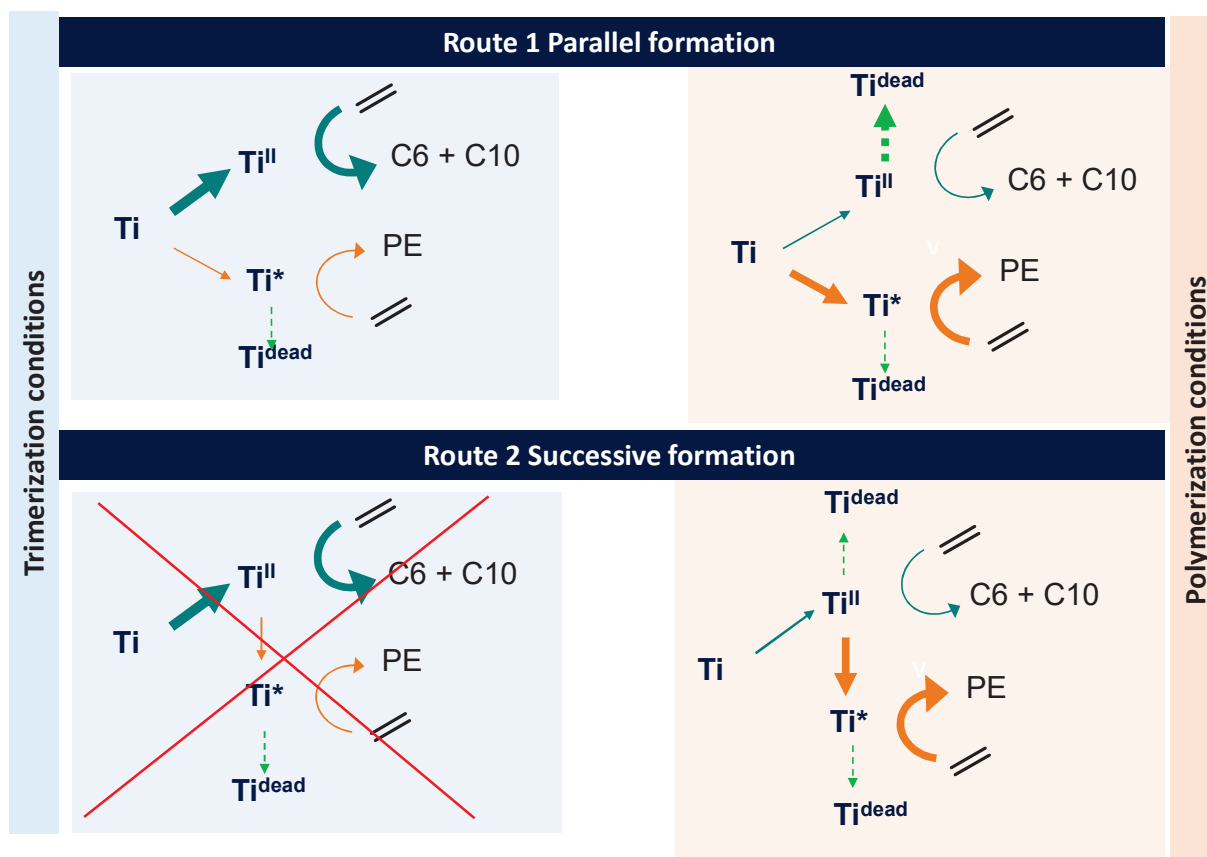
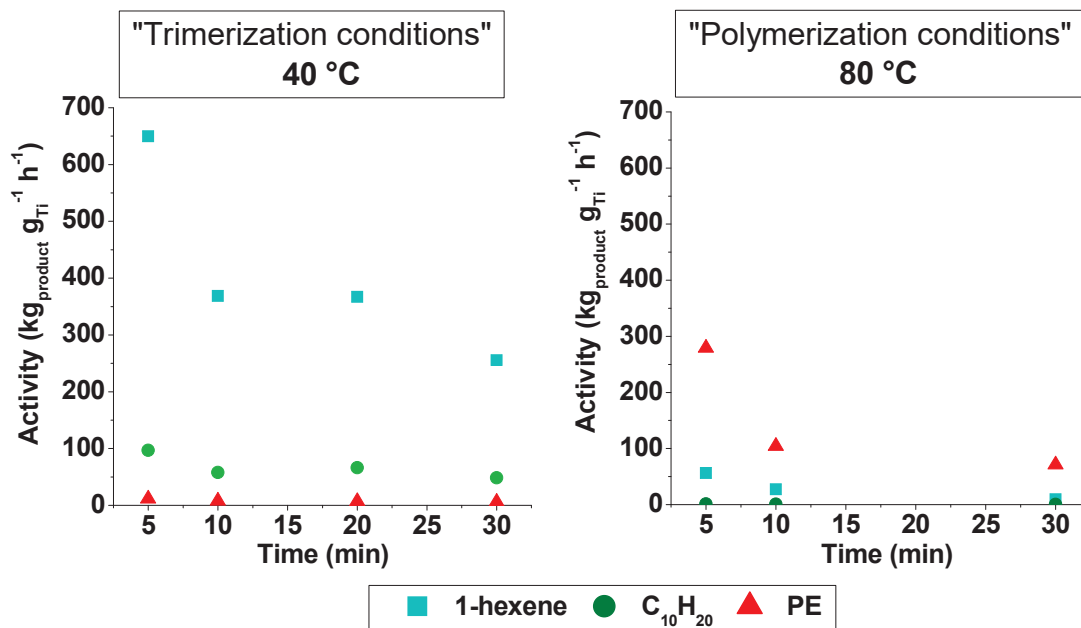
A different 1-hexene response of polymerization species is revealed by two close but different trends describing the 1-hexene content in the polymer and liquid phase in the SFS reactor and Chemspeed autoclaves. In the kinetic studies, polymers obtained after 30 minutes display a higher amount of 1-hexene (entries 4 and 7) than PE-SFS-40 (0.6 mol %) and PE-SFS-58 (0.08 mol %) produced in the 1 L-reactor. However, considering the 1-hexene content in the liquid phase, a lower incorporation is observed between PE-SFS-40 (0.62 mol % of 1-hexene in the polymer) and PE-CR-60 obtained after 30 minutes (Figure 10, entry 7). These differences could be due to a different control of the temperature in the liquid phase in the case of the 1-L and 270-mL reactors. Polymerization species would incorporate more 1-hexene in the case of the SFS reactor probably because fluctuations of temperature promote the copolymerization. This method is relevant for comparing the ability for 1-hexene incorporation between the polymerization species in the SFI system and species suspected to cause this side reaction.

II.3. Discussion on active species formations based on kinetic considerations

The kinetics studies focused on the evolution of reaction rates and products formation revealed a dependence between trimerization and polymerization active species. In the temperature range 40-80 °C, trimers and polymer are jointly generated at the early stage of reaction. Therefore a parallel formation is hypothesized for all reaction temperatures (Scheme 2, Route 1).

At 40 °C, the presence of trimers and polymer at the early stage of reaction combined with their continuous formation implies that two catalysts emerged at the beginning of the reaction from the same precatalyst source. In contrast at 80 °C, trimerization catalyst deactivates within the first 5 minutes of reactions and the polymerization catalyst displays a higher activity compared to lower temperature conditions. Although temperature surely increases the kinetics of polymerization reactions, it seems that more polymerization species are generated at 80 °C than 40 °C. This switch of trimerization active species reactivity implies an alteration of the latter promoted by thermal input. Indeed, the deactivation of trimerization probably causes the enhancement of polymerization at 80 °C. As a result, the combination of both scenari seems to better describe the formation of polymerization active species at higher temperature (Scheme 2, Route 1 and 2).

Since a parallel formation of trimerization and polymerization active species occurs at the early stage of reaction, side reactions during the activation process should first be considered. In this purpose, conditions of active species formations at the initial stage of catalyst tests have been modified. The investigation of selected parameters influencing the activation process is presented in the next section.



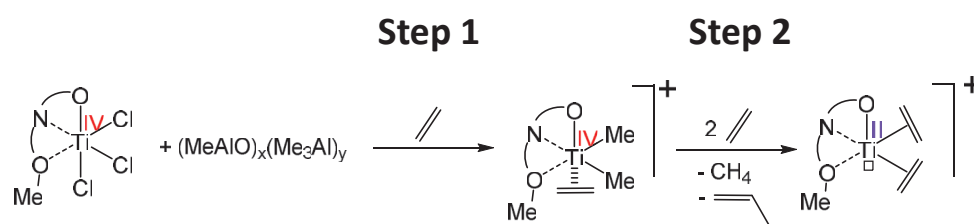
Scheme 2. Formation of polymerization active species: favored routes deduced from the temperature and kinetic studies

III. PARAMETERS INFLUENCING THE ACTIVATION PROCESS

III.1. Goal and strategy

For all reaction temperatures, the presence of polymerization active species was identified as early as 5 minutes of reaction in the kinetic studies and also shorter reaction times using “stopped flow” reactor. Thus, it seems that the polymerization active species is formed at the early stage of reaction, like the trimerization species. Consequently, the activation process would be the key step where the polymerization catalyst is generated.

As explained in the literature review (Chapter 1), the activation process involves several steps that are still not clearly described due to limitation in intermediate identification. The proposed mechanism relies on the formation of a cationic Ti^{IV} complex prior to the generation of a reduced cationic Ti^{III} active species involving ethylene (Scheme 3). Step 1 remains debatable because cationization could occur either *via* MAO-Cl⁻ formation or $AlMe_2^+$ transfer.⁸ Regarding Step 2, DFT calculations support a concerted β -H transfer although no route for polymerization species formation were considered.



Scheme 3. Activation process for the trimerization active species formation

From this scheme, the formation of Ti^{III} species assisted by the co-catalyst can explain the reason for polymer production. To justify this assumption, a drastic decrease of trimerization activity from 10.1 to 0.35 $kg_{1-hexene} g_{Ti}^{-1} h^{-1}$ along with a higher polymer selectivity (1.6 to 85.7 wt %) was observed once TMA is premixed with the precatalyst and then activated with MAO at 28 °C under 28 bar of ethylene.⁹ Thus, one can hypothesize deviations caused by “free-TMA” in MAO solution or MAO itself.^{10–13} In addition to deviation in the activation step, it is important to consider the possibility of a structure modification. As stressed in the literature review, structure alterations of the ligand or the complex lead to polymerization active species, unless subtle changes of the substituents of the phenyl ring are made.

After Step 2, one can hypothesize an alteration of the geometry of the complex, which would prevent the oxidative coupling. A formation of Ti^{III} is also conceivable at this stage resulting from the comproportionation of Ti^{IV} and Ti^{II} species.

To investigate the activation process, the response of the SFI system to several parameters suspected to alter this key step was analyzed. First, the behavior of the system is studied in the case where 1-hexene is introduced prior to the catalytic system activation. This addition

aims at verifying potential limitations or inhibition of active species by coordination of this olefin during the activation process, i.e before introduction of ethylene. Then, it is verified whether hydrogen could block the reactivity of the polymerization active species or at least limit, and especially reduce the molar masses of the HDPEs produced by the SFI system. Eventually, a special attention was paid to the co-catalyst as it is directly involved in the activation process. The use of TMA as alkylating agent was considered to check whether the alkylated complex could trimerize or polymerize ethylene. In the purpose of favoring the formation of trimerization active species, the influence of a prolonged contact between precatalyst and cocatalyst was studied by premixing complex I with MAO.

III.2. Influence of additional 1-hexene

III.2.1. Activity & selectivity

The influence of additional 1-hexene was tested in conditions where trimerization is the main reaction (36-38 °C) or is as favored as polymerization (60 °C). The amount of 1-hexene introduced in the reactor before ethylene supply, was chosen from 0 to 10 000 equivalents relatively to complex I. A mixture of 1-hexene and MAO were introduced in the reactor before injection of the precatalyst solution. The influence of the 1-hexene addition on both activity and selectivity can be analyzed from Table 4.

Table 4. Impact of the addition of 1-hexene on the SFI reactivity at 40 °C and 60 °C

Entry	n_{Ti} (μmol)	T (°C)	t (min)	m_{C_6} introduced (g) equivalent	Activity ($\text{kg}_{\text{ethylene}}$ $\text{g}_{Ti}^{-1} \text{h}^{-1}$)	m_{C_6} (g) ^a wt %	$m_{C_{10}}$ (g) wt %	$m_{C_{14}}$ (g) wt %	m_{PE} (g) wt %
1	3.1	38	30	0	509	33.46	3.59	0.02	1.01
				0		87.8%	9.4%	0.1%	2.7%
2	3.6	37	30	0.3	440	32.89	4.58	0.04	0.70
				889		86.1%	11.8%	0.1%	2%
3	3.8	36	32	1.4	319	26.83	3.28	0.03	0.59
				4 300		87.3%	10.6%	0.1%	2.0%
4	3.4	36	25	2.6	233	13.64	1.83	0.00	0.33
				9 500		86.3%	11.6%	0.0%	2.1%
5	4.6	58	31	0	172	9.61	0.38	0.00	9.55
				0		49.2%	1.9%	0.0%	48.9%
6	2.7	59	29	1.4	164	4.34	0.3	0	5.36
				6 000		43.4%	3.0%	0	53.6%
7	3.6	58	31	2.7	139	4.65	0.32	0	7.33
				9 000		37.8%	2.6%	0%	59.6%

Conditions: complex I, 300 mL toluene, MAO, Al/Ti = 1 000-1 500, 10 bar, 30 min

^a mass of 1-hexene produced by the catalytic system

At low temperature (Table 4, entries 1-4), the activity of the SFI system decreases with the increasing amount of 1-hexene added in the reactor. In fact, 1-hexene productivity dropped from 454 to 200 $\text{kg}_{1\text{-hexene}} \text{g}_{\text{Ti}}^{-1} \text{h}^{-1}$ upon introduction of 2.6 g of 1-hexene. This effect can be explained by the 1-hexene molecules coordination to the metal center, which competes with ethylene coordination. The main impact of 1-hexene addition is seen on the activity while the selectivities are unchanged. Indeed, the amount of C_{10} and C_{14} oligomers remains constant whilst an increase of cotrimerization would have been predicted. The activity of polymerization reaction is also affected by the presence of 1-hexene, highlighted by the decrease from 13 to 5 $\text{kg}_{\text{PE}} \text{g}_{\text{Ti}}^{-1} \text{h}^{-1}$ upon contacting with 2.6 g of 1-hexene (Table 4, entries 1 and 4). From these observations, it is concluded that polymerization catalysts are generated at the same time as the trimerization species, i.e once contacted with ethylene, in these temperature conditions.

At 59 °C, polymer production is close to that of trimers in standard conditions (Table 4, entry 5). Despite a slight decrease of the activity induced by the addition of 1-hexene (entries 5-7), the selectivity of the polymer produced is improved at the expense of 1-hexene. Therefore, the addition of 1-hexene in the reaction medium disfavors more specifically trimerization active species than polymerization catalysts. Indeed, the 1-hexene productivity decreased from 85 to 52 $\text{kg}_{1\text{-hexene}} \text{g}_{\text{Ti}}^{-1} \text{h}^{-1}$ (calculated for entries 5 and 8). Polyethylene activity remains stable between 84 and 83 $\text{kg}_{\text{polyethylene}} \text{g}_{\text{Ti}}^{-1} \text{h}^{-1}$ whereas 2.7 g of 1-hexene was added in the reactor.

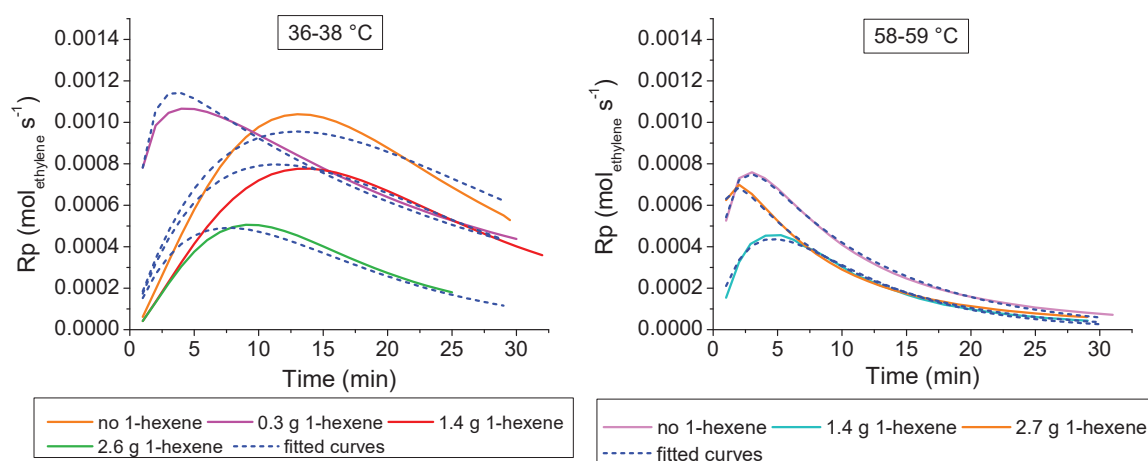
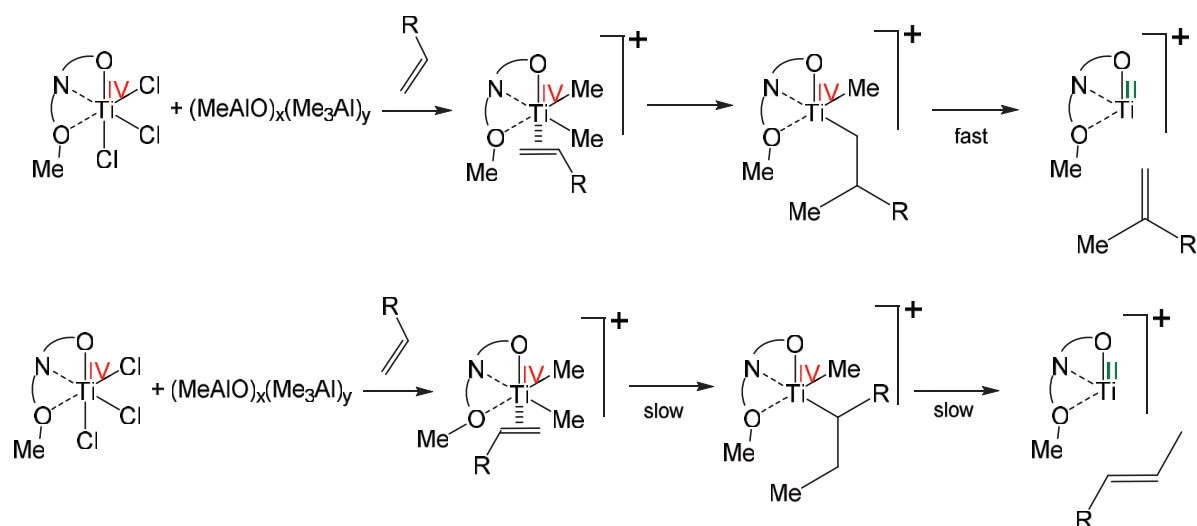


Figure 12. Influence of the presence of 1-hexene during the activation process on the reaction rate of the catalytic system

From the comparison of reaction rate profiles (Figure 12), 1-hexene seems to have a different effect on the kinetic of reaction in both range of temperature. At 36-38 °C, an earlier deactivation and/or a lower activity is observed as the amount of 1-hexene injected increases. 1-hexene seems to hamper the activation process, affording less trimerization active species, and also promotes deactivation reactions. In contrast, the system is less sensitive to the introduction of 1-hexene at 58-59 °C since a very similar evolution of reaction rate is observed in Figure 12 (right).

Consequently, the presence of 1-hexene prior to the contact between the precursor and the co-catalyst hampers the formation of active species. The same phenomenon is observed when the contact between the precursor and MAO occurs in presence of ethylene (Figure 8 versus Figure 3, see procedures of the catalytic tests performed on Chemspeed autoclaves and 1 liter SFS reactor). When 1-hexene is introduced prior to ethylene in the reaction medium, the 1,2 or 2,1-insertion of this olefin in the Ti-Me bond can have an impact on the kinetics of the activation process (Scheme 4).



Scheme 4. Possible limitations of trimerization active species formations (cationic Ti^{II}) caused by 1-hexene

Trimerization active species seems to be more impacted by the presence of LAO than the polymerization active species (Table 4, entries 5-7). Bearing in mind the hypothesis of a dependence between polymerization active species and trimerization catalyst, it seems that another process occurs at higher temperature since polymer production is stable while trimerization reaction is deactivated upon contact with 1-hexene. Bearing in mind that two populations of PE were identified, it is possible that the addition of 1-hexene enhanced the formation and/or activity of the polymerization catalyst that incorporates more 1-hexene than the other one.

III.2.2. Polymer properties

Since 1-hexene can play the role of comonomer in ethylene polymerization, the influence of its addition before catalytic reaction, on the chemical composition of the polymer was quantified. Once again, it was showed that polymerization species poorly copolymerizes 1-hexene in standard conditions. Thus, it was important to check their behavior towards 1-hexene before the formation of this alpha-olefin by the trimerization system. Polymer properties and 1-hexene content are gathered in Table 5.

Table 5. Chemical composition of polymers according to the amount of 1-hexene introduced.

Entry	T (°C)	1-hexene introduced (g) equivalent	T _c (°C)	T _m (°C)	χ (%)	1-hexene content (mol %) ^a
1	38	$\frac{0}{0}$	113	127.4	40	-
2	37	$\frac{0.3}{900}$	114	127.6	39	0.6
3	36	$\frac{1.4}{4\ 300}$	114	128.3	37	0.3
4	36	$\frac{2.6}{9\ 500}$	114	128.5	38,5	0.28
5	58	$\frac{0}{0}$	117	133.5	45.5	0.08
6	59	$\frac{1.4}{6\ 000}$	117	132.2	44.5	-
7	58	$\frac{2.7}{9\ 000}$	116	131.5	43,5	0.11

^a determined by high temperature ¹³C NMR

At low temperature, the increasing of 1-hexene amount introduced in the reactor led to a higher melting temperature and a lower 1-hexene content in the polymer (Table 5, entries 1-4). These results correspond to the case when both 1-hexene and polyethylene activities decreased. Therefore, a lower 1-hexene incorporation can be linked to a lower 1-hexene production. In this case, the decrease of trimerization activity upon addition of 1-hexene can result from issues during the activation step. From the kinetic profiles in Figure 12, one can intuit that less active species are formed upon activation in presence of 1-hexene for both polymerization and trimerization reactions. It is therefore important to check whether polymerization active species are altered or if it remains intact despite the addition of 1-hexene before activation.

The goal is to check whether polymerization active species behaves differently when 1-hexene is added or not. To do so, comonomer content in the polymer must be put in perspective with the amount of 1-hexene in the reaction medium and the loading of titanium. A comparison between standard polymers (PE-SFS-32 to PE-SFS-80) and polymers produced in conditions where 1-hexene is added before the reaction (Table 5, entries 2-4, 6 and 7) is provided in Figure 13.

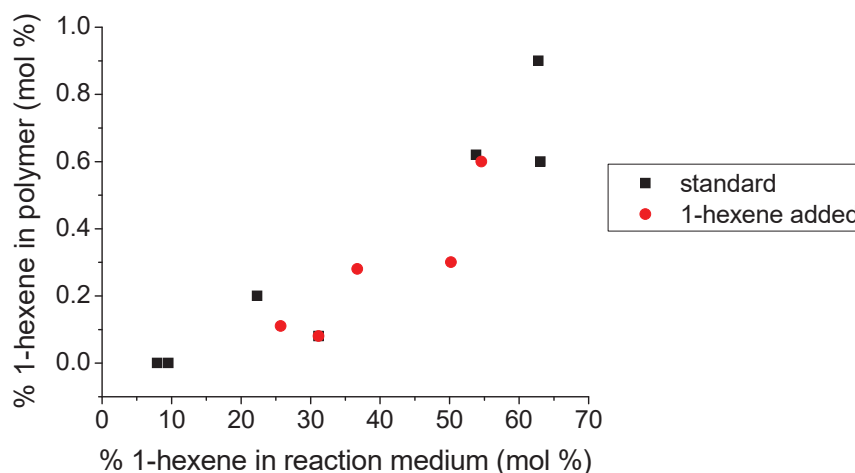


Figure 13. Evolution of 1-hexene content in the polymer and in the reaction medium in the case of 1-hexene addition (red) and standard conditions (black, Chapter 2, Figure 11)

Polymers obtained when 1-hexene is added in the reaction medium (Figure 13, red) or not (black) follow the same trend regarding the comonomer content in the polymer and the reaction medium. Indeed, even when extra 1-hexene is introduced, there is an accurate fit between the curves obtained with all the PE-SFS. As a consequence, the polymerization species behaves identically in both conditions since its ability for 1-hexene incorporation remains unchanged. Thus, polymerization species formed in presence of 1-hexene or not seems to be the same in each case, at 35 and 60 °C.

Eventually, the addition of 1-hexene during the activation of the SFI system limits its reactivity and has a little impact on the production of polymer. This behavior being unsatisfactory with respect to the objective of this project, another parameter that is known to reduce molar masses, consequently process inconveniences, is the addition of hydrogen.

III.3. Influence of hydrogen

III.3.1. Activity & selectivity

The effect of hydrogen on the SFI system was studied with respect to the polymer molar mass distribution and the reactivity of the system. Indeed, hydrogen is commonly used with chromium trimerization systems to lower the molar masses of the side polymer product.¹⁴ Based on this observation, it was speculated that hydrogen could also reduce polyethylene chain length with the titanium-based SFI system. Moreover, hydrogen can have an effect on the reactivity of the trimerization and polymerization active species. It would be greatly beneficial if hydrogen poisons preferentially the polymerization catalyst while maintaining a high 1-hexene activity. Addition of hydrogen prior ethylene pressurization enables to determine whether active species formation is impacted by the presence of hydrogen or not.

Since the SFI system displays the highest 1-hexene activity at low temperature, the effect of hydrogen was tested in conditions of favored trimerization ($T < 50\text{ }^{\circ}\text{C}$) with the hydrogen/ethylene ratio of 1/9 and also 6/4 bar. Hydrogen was introduced prior to ethylene and the overall pressure was kept constant at 10 bar during the tests. The pressure was set to 10 bar, which is the maximum pressure to operate the SFS-reactor. A series of three experiments were conducted in these conditions (Table 6).

Table 6. Activity and selectivity of complex I/MAO in absence and presence of hydrogen

Entry	T ($^{\circ}\text{C}$)	t (min)	P_{H_2} bar	n_{Ti} (μmol)	Al/Ti	Activity ($\text{kg}_{\text{ethylene}} \text{g}_{\text{Ti}}^{-1} \text{h}^{-1}$)	1-hexene (g) (wt %)	$\text{C}_{10}\text{H}_{20}$ (g) (wt %)	PE (g) (wt %)
1	40	27	0	3.42	1 300	362	21.8 81.8	2.9 10.7	1.92 7.2
2	38	2 ^a	1	2.95	1 650	92	0.33 76.7	0.03 7.3	0.07 16
3	40	1.5 ^a	6	3.23	1 400	3	0.005 55	0 0	0.004 45

Conditions: complex I, MAO 30 wt % in toluene (new bottle), 300 mL toluene, $P_{\text{hydrogen}} + P_{\text{ethylene}} = 10\text{ bar}$

^a time corresponding to the exotherm during pressurization of reactor

The activity is severely impacted by the presence of hydrogen introduced before the reaction. Depending on the hydrogen pressure, the system is only active during the first 2 minutes (Table 6, entry 2) or almost inactive under 6 bar of hydrogen (Table 6, entry 3). This strong limitation of the reactivity can be explained by a lower ethylene concentration in the reaction medium of 0.97 and 0.42 mol L⁻¹ (Table 6, entries 2 and 3) compared to the hydrogen-free experiment (1.052 mol L⁻¹, Table 6, entry 1). However, when comparing reactions performed with a similar ethylene concentration (Chapter 2, Table 1, 49 $^{\circ}\text{C}$, $[\text{C}_2] = 0.938\text{ mol L}^{-1}$), the SFI system displays a significantly higher activity of 527 $\text{kg}_{\text{ethylene}} \text{g}_{\text{Ti}}^{-1} \text{h}^{-1}$ at a reaction time of

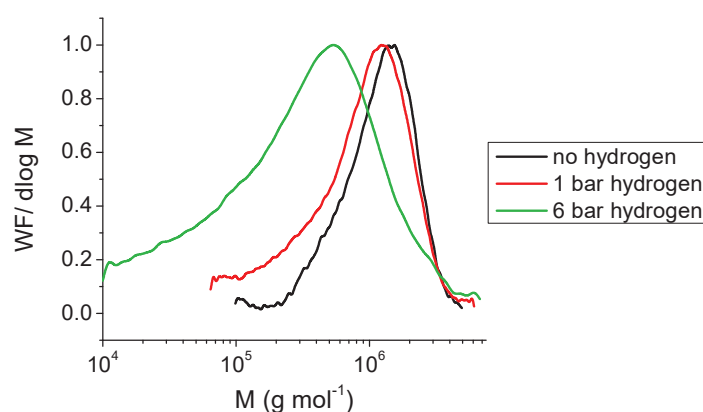
2 minutes of reaction (Figure 3). Although the temperature is different, it shows that hydrogen has an impact on active species by either limiting their formation or reactivity. Owing to a fast deactivation of the SFI system in presence of hydrogen, reaction rate could not be compared. An exothermal phenomenon is identified during the pressurization of the reactor with ethylene. However, it is not possible to extract the evolution of reaction rate for such short reaction times.

In terms of product formation, trimers and polymers are yielded in a very limited amount (< 0.5 g). It is noteworthy that there were no oligomers products other than the one usually identified (1-hexene and branched $C_{10}H_{20}$). Under 1 bar of hydrogen, the selectivity of 1-hexene is reduced from 81.8 to 76.7 wt %. In counterpart, polymer selectivity is more than doubled with an increase from 7.2 wt % to 16 wt %. When ethylene concentration is very low (Table 6, entry 3), the system is almost isoselective for both trimerization and polymerization reactions.

III.3.2. Products properties

III.3.2.1. Evolution of molar mass distribution with hydrogen pressure

Originally the use of hydrogen aimed at reducing the molar masses of the polyethylene formed as side reaction. This way the process operations could be greatly improved as the product separation is faster and more convenient. In this study, it was proven that the SFI system produces high molar masses polyethylene in standard conditions. Thus, the effect of hydrogen on molar masses distribution of polymers was verified by SEC analysis (Figure 14).



Entry	P_{H_2} (bar)	M_w (g mol ⁻¹) ^a	\bar{D} ^a
1	0	1 350 000	1.5
2	1	960 000	2.2
3	6	550 000	5.8

^a determined by SEC in TCB at 150 °C

Figure 14. Molar mass distributions for polymers obtained with the mixture hydrogen/ethylene of 0/10 (black), 1/9 (red) and 6/4 (green)

Hydrogen was found to have the expected effect on molar masses distribution. Indeed, a drastic decrease of the molar masses from 1.5 to 0.96 and even $0.55 \times 10^6 \text{ g mol}^{-1}$ is observed when hydrogen/ethylene ratio increases. In fact, hydrogen is involved in transfer reaction by hydrogenolysis. Thus, shorter polymer chains with saturated chain ends are afforded. Besides, the frequency of transfer reaction increase with the hydrogen concentration, i.e pressure, and the lower ethylene pressure leading to lower molar masses.¹⁵ Nevertheless, observing higher dispersities associated with higher hydrogen pressure is unusual. In the case of the homogeneous system $\text{Cp}_2\text{ZrCl}_2/\text{MAO}$, a narrower MMD was obtained under a hydrogen partial pressure of 0.15 bar ($\mathcal{D} = 2.7$) than without hydrogen ($\mathcal{D} = 3.7$).¹⁶ A more heterogeneous behavior of the polymerization species is probably related to the instability of hydrogen and ethylene concentration during the pressurization of the reactor, during which polymerization occurs.

III.3.2.2. Impact of hydrogen on 1-hexene incorporation in the polymer

Although the trimerization reaction was shortly interrupted and a very limited yield in 1-hexene was afforded, the ability of the polymerization species to incorporate 1-hexene was still checked (Table 7).

Table 7. Influence of hydrogen on polymer properties

Entry	P_{H_2}	T_m (°C)	χ (%)	1-hexene content (mol %) ^a
1	0	128.3	38.5	0.43
2	1	134.5	41	0.01
3	6	133.7	48	0.03

^a calculated from the Equation 2 (Chapter 2)

As expected, melting temperatures of the polymers are in the range of HDPEs displaying a negligible amount of comonomer content ($T_m \sim 134$ °C). One should note the lower melting temperature in the case of isoselective conditions (Table 6 and Table 7, entries 3). The influence of hydrogen on the ability of the polymerization species for 1-hexene insertion depending on the concentration of 1-hexene available in the reaction medium could not be determined in this case. Indeed, the poor 1-hexene content in the polymer and the solvent being close to zero, it is not possible to draw straightforward conclusions on a potential similarity of active species.

Unfortunately, hydrogen has a negative effect on both polymerization and trimerization active species and especially the latter. The addition of hydrogen during trimerization with the SFI system would therefore not be a relevant method for improving the productivity and

selectivity of the targeted product, which is 1-hexene. Therefore, further investigations were focused on the co-catalyst, having a direct role in the activation process.

III.4. Influence of TMA and premix

III.4.1. Activity & selectivity

As explained previously, the activation process seems to play an important role on the selectivity of the system. Based on the observation of Duchateau *et al.*, premix with MAO enhances catalytic performances of the trimerization system while the use of TMA favors polymerization reaction.⁹ Therefore, replacing MAO by TMA was considered to compare the properties of the polymer in both cases. Then, complex I and MAO were premixed in the view of promoting alkylation and methyl abstraction (Scheme 3, Step 1). The comparison of polymers in both cases indicates whether TMA could cause the formation of polymerization species in this system. Thus, in the purpose of clarifying the activation process, the influence of both MAO premix and substitution by TMA were studied with respect to the reactivity of the system and the polymer properties.

The performances of the catalytic system in both conditions were compared in Table 8. TMA was in the reactor before the precatalyst solution, following the standard procedure. Two premix experiments were performed under similar conditions. The difference between these two catalytic tests is the quality of the MAO. The effect of a “normal” MAO (solutions usually used for all other catalytic tests) and an “old” solution of MAO (visual modification of the solution), were compared. The precontacts between MAO and complex I were conducted inside the reactor at 40 °C for 30 minutes before introduction of ethylene.

Table 8. Influence of TMA and MAO premix on catalytic performances of the SFI system

Entry	T (°C)	t (min)	Co-catalyst	n_{Ti} (μmol)	Al/Ti	Activity (kg _{ethylene} g _{Ti} ⁻¹ h ⁻¹)	C ₆ H ₁₂ (g) (wt %)	C ₁₀ H ₂₀ (g) (wt %)	PE (g) (wt %)
1	42	32	MAO	3.8	1 200	540	44.2	5.8	1.7
							85.4	11.1	3.3
2	42	1.5 ^a	TMA	3.2	200	11 ^b	0.03	0	0.01
							80	0	20
3	40	28	MAO ^c	3.6	1 250	390	26.2	3.2	1.84
							83.9	10.2	5.9
4	41	29.5	“Old” MAO ^c	3.0	1 600	195	12.6	1.43	0.03
							89.6	9.7	0.2

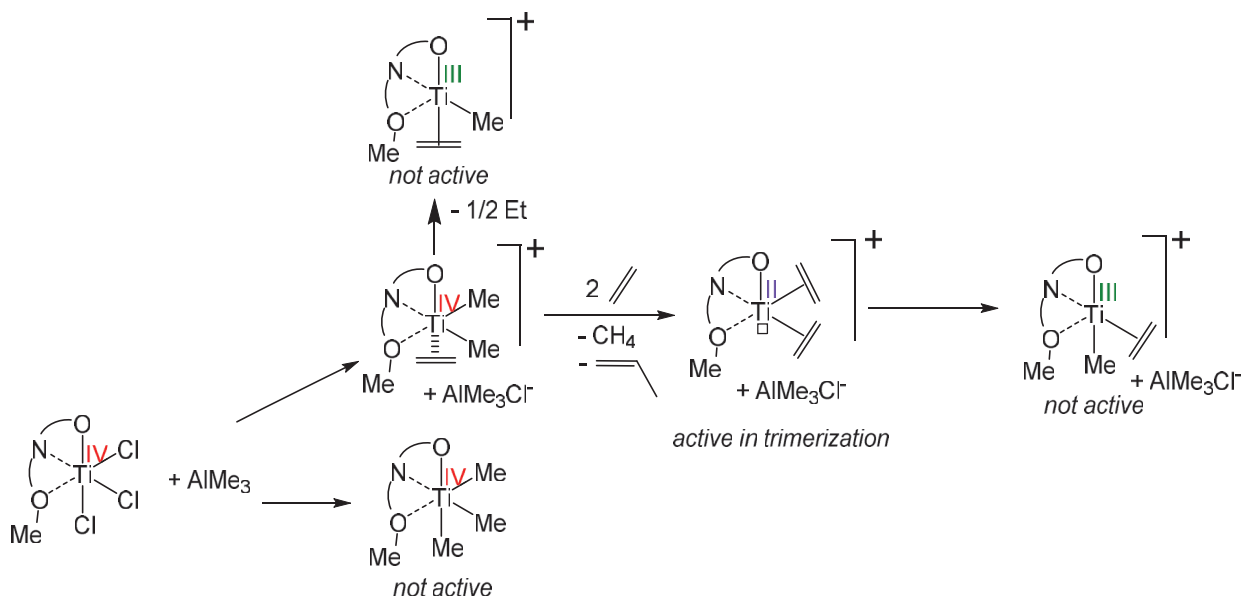
Conditions: complex I, MAO 30 wt % in toluene, 300 mL toluene

^a time corresponding to the temperature increase during pressurization of reactor

^b calculated based on the duration of the exothermicity

^c premix performed at 40-41 °C for 30 minutes

As expected, the use of TMA has a significant impact on the activity of the system. Indeed, a small amount of product was afforded despite the absence of ethylene consumption over time (Table 8, entry 2). It was noted an increase of temperature during the pressurization of the reactor, which was ascribed to the short-time reaction between ethylene and the catalytic system releasing heat. Thus, complex I/TMA is not a viable catalytic system and deactivates during the early stages of reaction. In spite of a strongly limited activity, the system produced both 1-hexene and polyethylene. This observation is in line with the assumption that polymerization and trimerization active species are jointly generated during the activation process. As a consequence, formation of trimerization and polymerization active species is possible but strongly limited and leads to a fast degradation of the latter. One can hypothesize the formation of inactive (FI)TiMe₃ complexes and seldom cationic Ti^{IV} with AlMe₃Cl⁻ as counter-anion. From this cationic species, an inactive cationic Ti^{III} can be formed by homolytic cleavage of Ti-C bond¹⁷ or the cationic Ti^{II} complex, which performs ethylene trimerization² (Scheme 5). In addition, comproportionation between Ti^{II} and Ti^{IV} species would afford inactive Ti^{III} species.



Scheme 5. Proposed activation mechanism and deactivation involving TMA

Precontacting the precatalyst with MAO has an effect on both the activity and the selectivity of the system. In the case of “normal” and “old” MAO premix (Table 8, entry 3 and 4), the system is a 1.4-fold and a 2.7-fold less active after 30 minutes, respectively. This lower activity is associated with a higher selectivity in 1-hexene at the expense of polyethylene in the case of “old” MAO premix. Indeed, a significant decrease in polyethylene selectivity from 3.3 wt % to 0.2 wt % is observed. However, an increase of PE selectivity is observed in the case of “normal” MAO premix, which emphasizes the impact of the quality of MAO the behavior of the catalytic system. As a result, it seems that the premix of complex I and an older MAO could be beneficial for lowering polymer production. In contrast, slight increase of polymer selectivity with a substantially equal activity was reported by Duchateau *et al.* when complex II is premixed and not directly engaged in trimerization with 2 250 equivalents of MAO.

Conditions of premix involved 750 equivalents of MAO before an additional activation with 1 500 equivalents of MAO under 28 bar, at 28 °C, in 75 mL of Isopar for 1 hour.⁹ Audouin also highlighted the increase of polymer selectivity from 1 % to 10 % along with a halved activity after 1h30 premix with 500 equivalents of MAO.¹⁸ Therefore, there are clear evidences that premixing MAO with the pre-catalyst has an effect on active species formation however the reasons explaining the preferential formation of either 1-hexene or polymer remain unclear.

Lower activities observed upon MAO premix and TMA activation maybe due to the formation of inactive species. In fact, a Ti^{III} species is detected by EPR analysis performed by Audouin as well as Bercaw and coworkers.^{5,18} The latter assumed the inactivity of such species towards ethylene. In addition, polymerization being selectivity more disfavored than trimerization reactions, one could conclude upon a parallel active species formation during the pre-activation step (Scheme 3, Step 1).

As a matter of fact, alteration during the second step of this process could be checked by testing the reaction of well-characterized $[(FI)TiMe_2^+]$ complexes with ethylene. Bercaw *et al.* reported the synthesis of such species $[(FI)TiMe_2^+][MeB(C_6F_5)_3^-]$ which also affords a lower polymer yield once contacted with ethylene. Thus, deviations in activation process are also likely to occur during the formation of active species (Scheme 3, Step 2).

As a result, the formation of side products can occur at several stages of the reaction. The profile of reaction rate was compared in the case of standard and premix conditions (Figure 15). All profiles follow a similar trend with a maximal activity rate of $847 \text{ kg}_{\text{ethylene}} \text{ g}_{Ti}^{-1} \text{ h}^{-1}$ (standard) reached after 10 minutes of reaction, 672 and $326 \text{ kg}_{\text{ethylene}} \text{ g}_{Ti}^{-1} \text{ h}^{-1}$ achieved after 6 minutes ("normal" MAO) and 10 minutes ("old" MAO). Therefore, the difference in terms of activity rate between experiments performed with and without premix, are linked to the number of actives species in the reaction medium.

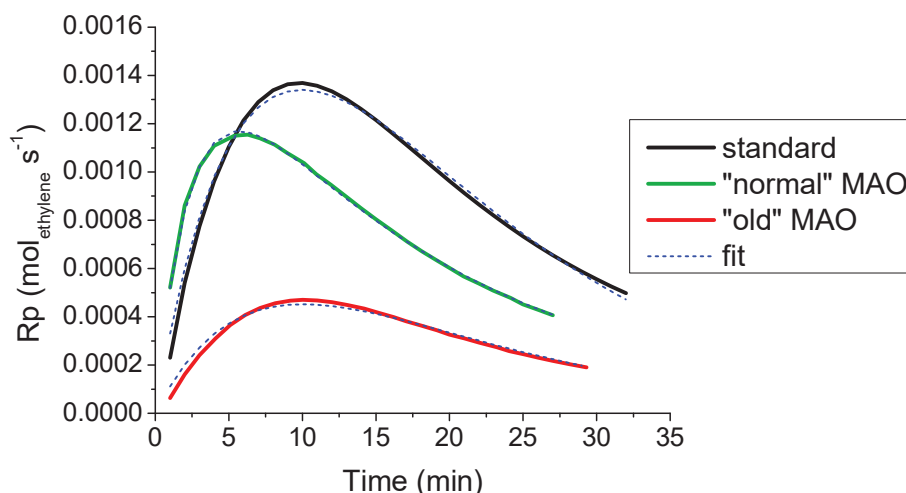


Figure 15. Evolution of reaction rate in the case of complex I/MAO premix with "old" MAO (red), "normal" MAO (green) and without premix (black). Fitted curves using Kissin's model are included (blue dashed lines)

Reaction rate profiles for the premix experiments were successfully fitted using Kissin's kinetic model (Equation 2). Comparing the kinetic constants (Table 9), there is no difference between k_i and k_d for "old" MAO premix. The same observation is made for the test conducted in standard conditions. Moreover, one should note the similar initiation and deactivation constants values between the standard and for "old" MAO premix experiments (Table 9). Therefore, differences in reaction rates relies on the propagation step. Assuming that premix has no effect on the activity of the system, one would expect similar propagation constants with standard conditions.

However, the ratio between k_p for standard and for "old" MAO premix conditions implies that about 40 % of potential active species are effectively formed upon contacting "old" MAO and complex I. Consequently, less active species are generated in this case, which could be explained by an evolution of MAO composition over time, i.e the formation of more MAO oligomers.¹⁹ Regarding the effect of "normal" MAO premix, another behavior of the catalytic system is observed. In fact, initiation and deactivation constants are substantially different from the ones calculated from the standard test (Table 9). From the ratios of $k_{\text{no premix}}/k_{\text{normal MAO}}$ of the initiation and deactivation steps, it is concluded that active species are rapidly formed but deactivate faster upon premix. This surprising trend is associated with a higher selectivity in polyethylene (Table 8, entry 3). Consequently, "normal" MAO premix has a different impact on active species formation and behavior, which could be linked to the amount of "free" TMA available in the "normal" MAO solution. This comparison stresses the complexity of MAO activation, which limits its understanding.

Table 9. Comparison of kinetic constants for experiments performed with and without premix

	No premix	« normal » MAO	$k_{\text{no premix}}/k_{\text{normal MAO}}$	« old » MAO	$k_{\text{no premix}}/k_{\text{old MAO}}$
[Ti] (mol L ⁻¹)	1.17x10 ⁻⁵	1.20x10 ⁻⁵		1.01x10 ⁻⁵	
k_i (s ⁻¹)	1.673x10 ⁻³	6.73x10 ⁻³	0.25	1.660x10 ⁻³	1.01
k_d (s ⁻¹)	1.673x10 ⁻³	9.40x10 ⁻⁴	1.78	1.660x10 ⁻³	1.01
k_p (L mol ⁻¹ s ⁻¹)	303.3	128.5	2.36	117.1	2.59
$k_p \times [\text{Ti}]$ (s ⁻¹)	3.55x10 ⁻³	1.55x10 ⁻³	2.29	1.18x10 ⁻³	3.00

III.4.2. Influence of TMA and MAO premix on polymer features

III.4.2.1. Comparison of molar mass distribution of polymers

Since polymerization active species formation and/or activity are impacted by the use of TMA and premix with MAO (Table 8, entries 3 and 4), the properties of the polymers obtained in both conditions were compared in terms of molar mass distributions (Figure 16).

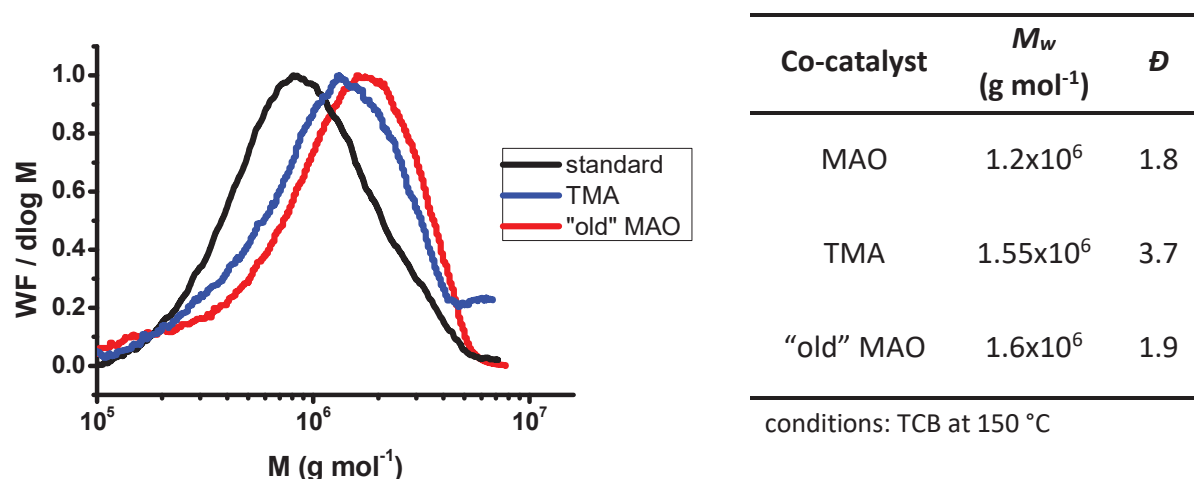


Figure 16. Molar mass distribution of polymers obtained in the standard catalytic test procedure (black), with TMA as cocatalyst (blue) and after premix with "old" MAO (red)

From the MMDs in Figure 16, it is clear that the polymer obtained with TMA displays a higher average molar mass and dispersity than the one produced in standard conditions. Interestingly, an opposite effect was reported for metallocenes system activated by a large excess of TMA compared to MAO ($Al_{TMA}/Zr = 9\,000$ and $Al_{MAO}/Zr = 1\,000$). In such conditions, both the decrease of molar masses from 403 to 94 kg mol⁻¹ and of the activity from 77.4 to 2.8 t_{PE} mol_{Zr}⁻¹ h⁻¹ was observed for Cp₂ZrCl₂/(TMA+MAO).¹⁶

At this stage, it is important to question the reactivity of TMA with the precatalyst. This study proves that the activation with TMA actually generates both polymerization and trimerization active species. One can assume that "free-TMA" contained in MAO has the same effect. From these results, the hypothesis of a partial cationization illustrated in Scheme 5 seems relevant. Besides, alteration of the ligand or even the whole complex structure, ought to be considered.

Owing that less active species are formed upon premixing the precatalyst and "old" MAO, the resulting polymerization species may be equivalent to the one present in standard conditions. Interestingly, the use of TMA and the premix with "old" MAO (Table 8, entry 4) led to polyethylenes with similar molar masses of 1.55×10^6 and 1.6×10^6 g mol⁻¹ (Figure 16), which questions whether similar polymerization active species are formed in both cases or not.

III.4.2.2. Chemical composition of polymer obtained with MAO premix

Regarding 1-hexene incorporation in polymers afforded after premix or not, melting temperature and 1-hexene content are gathered in Table 10.

Table 10. Properties of polymer afforded after premix or not

Entry	Premix	T _m (°C)	1-hexene content (mol %)
1	no	127.5	0.6
2	"normal" MAO	127	0.59 ^a
3	"old" MAO	126	0.74 ^a

^acalculated from Equation 2 (Chapter 2)

A lower melting temperature of the polymer, i.e higher 1-hexene content, was obtained in the case of "old" MAO premix compared to the standard conditions (Table 10, entry 2 and 1). However, 1-hexene composition is very similar for polymer produced in standard conditions and "old" MAO premix. To verify whether the same polymerization active species are formed upon premixing with MAO or not, it is still necessary to compare the 1-hexene content in the polymer with respect to the amount of 1-hexene available in the reaction medium, which is presented in Figure 17.

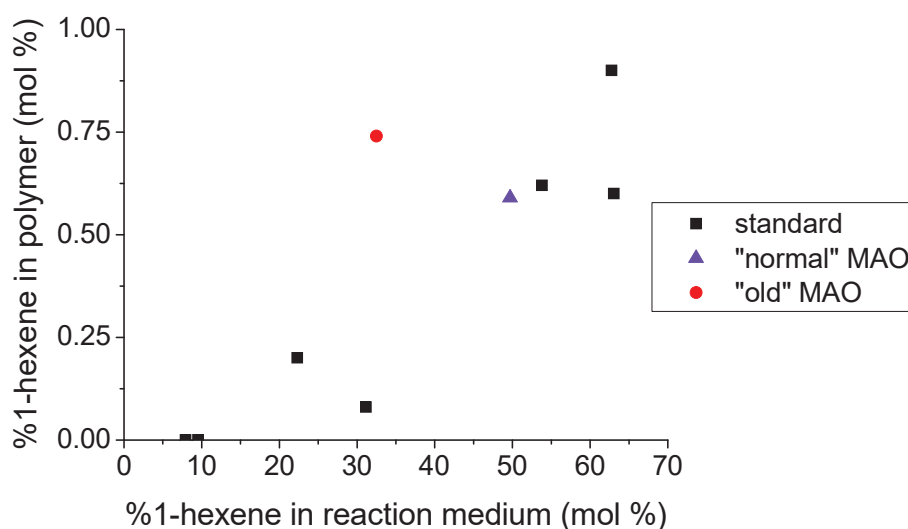


Figure 17. Relationship between 1-hexene content in the polymer and reaction medium for polymers obtained in standard conditions and after premix

The incorporation ability of the polymerization species is different for both premix. In fact, the 1-hexene content in the polymer is higher with “old” MAO than in standard conditions (Figure 17). As the amount of 1-hexene produced is substantially lower after premix than in the standard conditions (Table 8, entries 4 versus 1), one would have expected a 1-hexene content between 0.2 and 0.25 % instead of 0.74 % (Figure 17). One explanation for these antagonist results may lie in a potential delay of polymerization active species formation. On the contrary, polymerization active species afforded with “normal” MAO or in standard conditions exhibit the same response to 1-hexene (Figure 17).

To conclude, an alteration of the activation process by using TMA and premixing MAO with complex I has a different impact on activity, selectivity and polymer properties. Even though polymerization and trimerization active species are present in both cases, the overall activity is highly limited. Thus, these parameters have a negative effect on the formation of active species. Nevertheless, it can be advantageous to premix the precatalyst and MAO to hamper polymerization reactions in some cases (evolution of MAO composition). As a result, there are indisputable proofs that alkylaluminium derivatives involve side reactions, especially the deactivation of the catalytic system.

IV. CONCLUSION

In this chapter, kinetics considerations enabled to draw several conclusions regarding the behavior of the catalytic system over time and temperature. For all experiments performed between 26 and 80 °C, the kinetics of reactions were successfully described by a model developed by Kissin *et al.* In most cases, reaction rates were shown to be first order dependent towards ethylene concentration, implying that trimerization reactions are not limited by the formation of the metallacycle. The SFI system appears to be highly active during the first minutes of reaction before a decay is initiated. Moreover, the elevation of temperature favors an early deactivation of the system and reduces its global activity. It is translated by the increasing kinetic constants of initiation and deactivation with temperature.

Reactions implemented on a “stopped-flow reactor” and the highly reproducible Chemspeed autoclaves were very informative regarding the evolution of product formation over time. In both trimerization (40 °C) and polymerization (80 °C) conditions, polymerization active species are formed in parallel to the trimerization ones at the early stage of reaction, suspecting that the activation process is the key step where side reactions occur. At 80 °C, more polymerization active species would be formed from the alteration of trimerization active species. In the latter case, this species transformation would be explained by an effect of temperature.

The investigation of the activation process reinforced the hypothesis of a concomitant formation of trimerization and polymerization active species. It was shown that if 1-hexene is introduced before activation or generated during the reaction, the polymerization active species remains identical. In addition, 1-hexene addition only impacts the activity of the system maintaining similar selectivities and polymer properties. The presence of olefin (ethylene, 1-hexene) before pre-activation limits the formation of active species. In lieu of 1-hexene, the addition of hydrogen was efficient for reducing molar masses of polymers but also caused a severe deactivation of the system. Both TMA, used as co-catalyst, and the premix of complex I with MAO highly impairs the activity of the system and polymer is afforded in both cases. This observation stresses that “free-TMA” inherently present in MAO may be involved in side active species activation. This study also shed light on potential benefits of premixing the pre-catalyst and “aged” MAO in view of limiting polymer production.

Overall, these studies focused on kinetics and activation process of the SFI system demonstrated that both the activation process and temperature have an effect on the generation of polymerization active species. Since a better picture of the SFI system behavior was extracted from both temperature and kinetic studies, several assumptions can now be made concerning the nature of polymerization active species and the mechanism involved. The most plausible hypotheses on secondary reactions leading to secondary active species are detailed in the next chapter. Each assumption is verified by comparing catalytic performances and polymer features with the complex I/MAO system.

V. EXPERIMENTAL SECTION

V.1. General consideration

Solvent used for the syntheses and catalytic tests performed on the automated Chemspeed platform are collected from the same purification system as reported in Chapter 2. The same grade of ethylene is also employed and purified with activated molecular sieves, alumina and BASF copper oxide catalyst.

V.2. Catalytic tests conditions for kinetics studies

V.2.1. Stopped-flow reactor

Short time reactions were performed on a liquid-phase “stopped-flow” reactor presented in Figure 18.

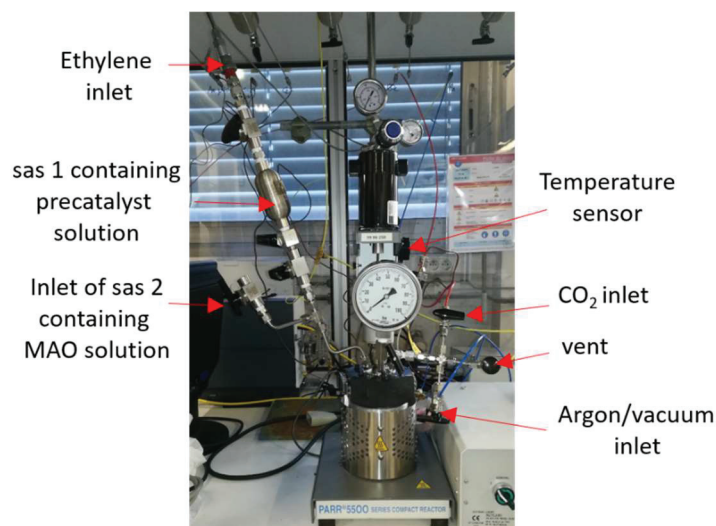


Figure 18. “Stopped-flow” reactor set-up

Conditioning of the 50 mL stopped-flow reactor is performed at 60 °C under vacuum for 45 minutes. Meanwhile, precatalyst and cocatalyst solution were prepared separately in the glovebox. The solution of complex I (0.6 μmol) in 5 mL toluene, prepared from a stock solution, is transferred in sas 1 (10 mL). Similarly, 25 mL of a solution of MAO (0.91 mmol, 1 512 eq. of aluminum) in toluene is transferred in sas 2 (30 mL). sas are quickly connected to the reactor. Ethylene inlet is connected to sas 2 and the MAO solution is injected under 2 bar of ethylene. The reaction medium is stirred at 500 rpm. Ethylene is then quickly connected to sas 1 and the precatalyst solution is introduced in the reactor applying 10 bar of ethylene. Ethylene feed is stopped once the pressure reaches 10 bar and ethylene consumption is qualitatively followed by pressure decrease. Reaction is stopped by injecting 20 bar of CO₂ in the reaction medium. The reactor is cooled with an ice bath to 5 °C, slowly depressurized before collecting the liquid and solid phase. Product isolation and purification is conducted as described in the experimental section of Chapter 2.

V.2.2. Synthesis and catalytic test on Chemspeed unit

The kinetic studies were performed on a fully automated Chemspeed homogeneous catalysis platform located at Axel'One Campus, Villeurbanne, France. This unit is included in a Glovebox to guarantee a controlled atmosphere.

V.2.2.1. Complex I synthesis

Sequence for the synthesis of complex I was developed with the Autosuite software provided by Chemspeed technologies. ISYNTH© module is employed for the synthesis and purification of complex I.

In the Chemspeed unit, the ligand (200 mg, 0.53 mmol) is introduced manually in a 100 mL glass reactor disposed in the ISYNTH© module. The rest of the procedure is performed automatically. 10 mL of toluene is added *via* the 25 mL-syringe connected to the 4-needle head (4-NH). The module is cooled to -20 °C by the mean of a cryostat while stirred at 300 rpm. 0.53 mL of a solution of titanium tetrachloride in toluene (0.53 mmol, 1 mol L⁻¹) is added using 1-mL syringe connected to 4-NH, with a rate of 0.3 mL min⁻¹. At the end of addition, reactor is warmed up to 25 °C at 0.5 °C min⁻¹. 50 mL of heptane is added and stirred for 5 minutes. Stirring is interrupted for 10 minutes and the supernatant is removed through a filter-tip plugged to the 4-NH. Washings are performed 2 more times with 10 mL of heptane. The complex powder is dried for 2 hours at 40 °C *via* an external vacuum pump connected to the ISYNTH© module.

V.2.2.2. Tests with ethylene on Chemspeed reactors

The reproducibility and kinetic studies were performed following the same procedure regarding precatalyst solution preparation and catalytic test with ethylene.

Catalytic tests were performed in three independent 270 mL-reactors. Toluene (120 mL) and MAO 30 wt % in toluene solution (0.6 mL, 1 500 mmol) were introduced in each reactor and stirred at 300 rpm. Once the desired temperature was reached, reactors were pressurized to 10 bar of ethylene. Using SWILE© technology, a stock solution of complex I (3.2 mg, 1.56 mmol) in 10 mL of toluene from which 3 mL were injected *via* a high pressure pump in each reactors. The reaction were run in a semi-batch mode for the desired reaction time. Ethanol was introduced under pressure to quench the reaction. Reactors were cooled to 5 °C before depressurization. Further treatments of the solid and liquid phases were performed as described in Chapter 2.

These catalytic tests being operated automatically, a sequence of elementary steps was programmed to perform experiments in three reactors at the same time and in the same conditions (reproducibility studies) or at different reaction time (kinetic studies).

V.3. Catalytic tests with the 1 liter SFS reactor

The procedure for the catalytic tests performed with 1-hexene, hydrogen, TMA and after premix complex I/MAO are based on the standard procedure detailed in the experimental section of Chapter 2. This procedure is summarized hereafter:

The reactor is heated at 80 °C under vacuum for 20 minutes. It is scavenged with 300 mL of a solution of TEA in heptane (15 mol L⁻¹). The reactor is cooled down to the desired temperature and a commercial solution of MAO 30 wt % (1 mL, 1 200 eq) in 280 mL of toluene is injected. Once temperature is stable, the solution of complex (3 μmol) in 20 mL of toluene is introduced before feeding the reactor with purified ethylene. The catalytic test is carried out at 10 bar and the ethylene consumption is followed by the ethylene pressure decrease in the ballast. After 30 minutes of reaction, the ethylene feed is stopped and 5 mL of methanol is introduced in the reactor *via* an injection sas. The reactor is cooled to 6 °C to preserve the 1-hexene in the liquid phase. The pressure is slowly released before opening the reactor. The liquid phase is treated with sulfuric acid and analyzed by GC with dodecane as internal standard. The solid is washed with acidified methanol then methanol and it is dried *in vacuo* at 90 °C for two hours.

The modifications of this procedure is explained for each case in the following sections.

V.3.1. Introduction of 1-hexene

1-hexene (> 98 %) was purchased from Sigma Aldrich. It was dried over CaH₂ and distilled before use.

For reactions performed in the presence of 1-hexene, this LAO is added to the solution of MAO before injection in the reactor. Once the temperature of the liquid is stable, the precatalyst solution is injected and the reactor is pressurized with ethylene to 10 bar. As a result, 1-hexene is present during the activation process.

V.3.2. Use of hydrogen

Hydrogen (> 99.999 %) was supplied by Air liquid and purified by passing through three columns containing activated molecular sieves, alumina and BASF copper oxide catalyst. After introduction of MAO solution and injection of the precatalyst solution, the reactor is pressurized with hydrogen to either 1 or 6 bar and ethylene is continuously added to guarantee an overall pressure of 10 bar during the catalytic test.

V.3.3. Use of TMA as co-catalyst

A solution of trimethylaluminum 2.0 M in toluene was purchased from Sigma-Aldrich. It was handled and stored under inert atmosphere (glovebox).

The procedure involving TMA as precatalyst is performed following the usual procedure for standard catalytic tests. Instead of MAO, 1 mL (0.8 mmol, 250 eq.) of a diluted solution of TMA in toluene (0.8 mol L⁻¹) is introduced in 300 mL toluene before being introduced in the 1 Liter SFS reactor. The solution of TMA was prepared in the glovebox by diluting 4 mL of the commercial solution TMA in toluene (2.0 mol L⁻¹) in 6 mL of toluene.

V.3.4. Premix complex I/MAO

For MAO premix studies, standard solution of MAO (“normal”) supplied by Albermarle Methylaluminoxane 30 % in toluene (13.6 wt % of aluminum, 5.24 wt % TMA, 26.2 wt % MAO) was purchased from Albermarle. The “old” solution of MAO was sampled from the same batch of MAO about 6 month before the “normal” solution used for all other tests. This “old” MAO had a different physical aspect (more viscous). Both solutions were stored under inert atmosphere at -21 °C except when sampled at room temperature before catalytic tests.

For premixing complex I and MAO, the precatalyst solution is injected in the reactor containing the MAO solution at 40 °C. The reaction medium is then stirred for 30 minutes at 40 °C before ethylene pressurization.

VI. REFERENCES

- 1 Y. Suzuki, S. Kinoshita, A. Shibahara, S. Ishii, K. Kawamura, Y. Inoue and T. Fujita, *Organometallics*, 2010, **29**, 2394–2396.
- 2 S. Ishii, T. Nakano, K. Kawamura, S. Kinoshita, S. Ichikawa and T. Fujita, *Catal. Today*, 2018, **303**, 263–270.
- 3 J. B. P. Soares and T. McKenna, in *Polyolefin Reaction Engineering*, John Wiley & Sons, Ltd, 2012, pp. 131–185.
- 4 Y. V. Kissin, R. I. Mink and T. E. Nowlin, *J. Polym. Sci. Part Polym. Chem.*, 1999, **37**, 4255–4272.
- 5 J. E. Bercaw, A. Sattler, D. C. Aluthge, J. R. Winkler and J. A. Labinger, *ACS Catal.*, 2016, **6**, 19–22.
- 6 Z. Yao, D.-F. Ma, Z. Xiao, W. Yang, Y.-X. Tu and K. Cao, *RSC Adv.*, 2017, **7**, 10175–10182.
- 7 H. Hagen, *Ind. Eng. Chem. Res.*, 2006, **45**, 3544–3551.
- 8 M. Linnolahti and S. Collins, *ChemPhysChem*, 2017, **18**, 3369–3374.
- 9 R. Duchateau, F. F. Karbach and J. R. Severn, *ACS Catal.*, 2015, **5**, 5068–5076.
- 10 E. Y.-X. Chen and T. J. Marks, *Chem. Rev.*, 2000, **100**, 1391–1434.
- 11 V. Busico, R. Cipullo, F. Cutillo, Nic. Friederichs, S. Ronca and B. Wang, *J. Am. Chem. Soc.*, 2003, **125**, 12402–12403.
- 12 F. Ghiotto, C. Pateraki, J. R. Severn, N. Friederichs and M. Bochmann, *Dalton Trans.*, 2013, **42**, 9040–9048.
- 13 V. Busico, C. Ehm, R. Cipullo and P. H. M. Budzelaar, *Dalton Trans.*, 2016, **45**, 6847–6855.
- 14 Phillips petroleum company, WO1999019280A1, 1999.
- 15 Y. V. Kissin, R. I. Mink, T. E. Nowlin and A. J. Brandolini, *Top. Catal.*, 1999, **7**, 69–88.
- 16 L. D'Agnillo, J. B. P. Soares and A. Penlidis, *Macromol. Chem. Phys.*, 1998, **199**, 955–962.
- 17 A. Grassi, A. Zambelli and F. Laschi, *Organometallics*, 1996, **15**, 480–482.
- 18 H. Audouin, PhD thesis, Ecole normale supérieure de Lyon - ENS LYON, 2015.
- 19 H. S. Zijlstra, M. Linnolahti, S. Collins and J. S. McIndoe, *Organometallics*, 2017, **36**, 1803–1809.

Chapter 4.
Hypotheses of
polymerization active
species

TABLE OF CONTENT

I. INTRODUCTION	186
II. HYPOTHESIS OF LIGAND ABSTRACTION	188
II.1. CHARACTERIZATION OF LIGAND TRANSFER TO TMA	188
II.1.1. REACTIVITY OF TMA TOWARD COMPLEX I	188
II.1.2. SYNTHESIS OF AND CHARACTERIZATION OF (FI)ALME ₂	190
II.2. TiCl₄/MAO AS MOLECULAR ZIEGLER-NATTA CATALYST	193
II.2.1. CATALYTIC PERFORMANCE OF TiCl ₄ /MAO IN ETHYLENE POLYMERIZATION AND COPOLYMERIZATION WITH 1-HEXENE	193
II.2.2. COMPARISON OF POLYMER FEATURES OBTAINED WITH COMPLEX I /MAO AND TiCl ₄ /MAO	195
II.2.2.1. Molar mass distribution of polymers	195
II.2.2.2. Chemical composition of polymers	197
II.3. DISCUSSION ON THE HYPOTHESIS OF LIGAND ABSTRACTION	198
III. HYPOTHESIS OF LIGAND ALTERATION	200
III.1. POSSIBLE MODIFICATIONS OF COMPLEX INDUCED BY A TEMPERATURE EFFECT	200
III.2. THERMAL MODIFICATION OF COMPLEX I	201
III.2.1. COMPLEX I DEGRADATION	201
III.2.1.1. Release of MeCl	201
III.2.1.2. Identification of a secondary complex	203
III.2.2. SYNTHESIS OF COMPLEX III	205
III.3. CATALYTIC TEST WITH A MIXTURE OF COMPLEX I AND COMPLEX III	209
III.3.1. ACTIVITY AND SELECTIVITY WITH THE MIXTURE COMPLEX I + COMPLEX III	209
III.3.2. COMPARISON OF POLYMER PROPERTIES	210
III.4. TEST OF COMPLEX III/MAO TOWARD ETHYLENE POLYMERIZATION AND COPOLYMERIZATION WITH 1-HEXENE	212
III.4.1. INFLUENCE OF TEMPERATURE ON ACTIVITY OF COMPLEX III/MAO	212
III.4.2. POLYMERS PROPERTIES OBTAINED WITH COMPLEX III/MAO IN PRESENCE OF 1-HEXENE	214
III.5. RATIONALIZATION OF COMPLEX III FORMATION	215
III.5.1. PROPOSED MECHANISM	215
III.5.2. DFT CALCULATIONS	216
III.5.3. THERMAL ALTERATION DURING CATALYTIC TESTS	218

IV. HYPOTHESIS OF Ti^{III} FORMATION.....	220
IV.1. HYPOTHESIS OF $(FI)Ti^{III}Cl_2$ COMPLEX	220
IV.1.1. SYNTHESIS OF $(FI)Ti^{III}Cl_2(THF)$	220
IV.1.2. ACTIVITY, SELECTIVITY AND POLYMER PROPERTIES.....	223
IV.2. HYPOTHESIS OF A $Bis(FI)TiCl_2$ SPECIES AS POLYMERIZATION ACTIVE SPECIES.....	225
IV.2.1. EVIDENCES OF THE FORMATION OF $(FI)_2TiCl_2$	225
IV.2.2. ACTIVITY, SELECTIVITY AND POLYMER PROPERTIES.....	229
V. CONCLUSION.....	231
VI. EXPERIMENTAL SECTION.....	232
VI.1. DFT CALCULATION METHOD.....	232
VI.2. GENERAL CONSIDERATIONS.....	232
VI.3. COMPLEX SYNTHESIS AND CHARACTERIZATION.....	233
VI.4. HEATING AND DEGRADATION OF COMPLEX I.....	236
VI.5. CATALYTIC TESTS	237
VI.5.1. TESTS IN THE 1 LITER SFS REACTOR	237
VI.5.2. CATALYTIC TESTS WITH CHEMSPEED AUTOCLAVES.....	238
VII. REFERENCES	239

I. INTRODUCTION

This final chapter relates the extension of the “polymer-to-catalyst” approach and focuses on the potential polymerization active species formed in the trimerization system. The idea behind this strategy is to identify the main elements that characterize the polymerization active species in terms of activity and polymer properties. On the basis of the observations made in the previous chapters and in the literature, several hypotheses were formulated regarding the parameters influencing the formation of polymerization active species and the nature of the latter.

Deviations over time

A dependence between trimerization and polymerization active species was demonstrated in the kinetic studies by a rapid formation of both catalysts at the early stage of the reaction. From this observation, the activation process was identified as a key step for the generation of side reactions. Therefore, the co-catalyst plays an important role in the formation of secondary active species. Noteworthy, this step is also associated with a fast exothermicity, which favors potential side reactions.

Effect of activator

Using alkylaluminum-based activators other than MAO, was found to shift the selectivity of the system towards polymerization. To explain this observation, the formation of a “TiR_x” species was proposed by Duchateau *et al.*¹ It was postulated that the FI ligand was abstracted from the titanium center by the “free” TMA contained in MAO. Such homogeneous molecular Ziegler-Natta species would poorly copolymerize LAOs with ethylene.^{2,3} Trialkylaluminum were also reported for the modification from a phenoxy-imine to phenoxy-amido ligand, leading exclusively to polymerization active species.⁴ Therefore, a special attention should be drawn to the effect of TMA on the structure of the complex.

Effect of temperature

Bearing in mind that temperature greatly influences the reactivity of the SFI catalytic system (Chapter 2), it is interesting to check its impact on the structure of the complex. Indeed, the increasing PE production at higher temperature denotes a potential modification of the catalytic system. As highlighted in the literature review (Chapter 1), slight alterations of the (FI)TiCl₃ precatalyst can lead to dramatic changes in activity and selectivity of the system.^{1,5} Consequently, thermally-assisted modification of complex I could generate new polymerization active species. Related examples of polymerization complexes reported in the literature are based on bis(phenoxy-imine) complexes ([O⁻,N]-FI)₂TiCl₂, phenoxy-amido ([O⁻,N⁺,O]-FI)TiCl₂ complexes or even diphenoxy-imine compounds ([O⁻,N,O⁻]-FI)TiCl₂.⁶

It is also important to stress that temperature can promote side reactions between complexes. For instance, Bercaw *et al.* proposed the formation of an inactive Ti^{III} species by comproportionation of the Ti^{IV} and Ti^{II} complexes involved in the metallacycle mechanism. Thus, this hypothesis also deserves to be verified.⁷

For the sake of clarity, the aforementioned assumptions were gathered into three main categories (Figure 1). The previous overview suggests that polymerization active species are the result of side reactions between the trimerization active species and the co-catalyst, e.g. TMA, or other titanium species. In both cases, these side reactions involve a redox process and a structure modification (ligand transfer or alteration). In this work, we focused on three main assumptions for the formation of polymerization active species. First, the investigation of a ligand transfer from titanium to aluminum is reported. Then, the effect of temperature on the structure of complex I was studied combining thermal analyses and catalyst testing. Eventually, the formation of a trivalent titanium complex was verified. For each hypothesis, active species were synthesized, characterized and tested towards ethylene polymerization. The idea again is to compare catalytic performances and polymer properties with the ones of the polymerization active species generated by complex I/MAO.

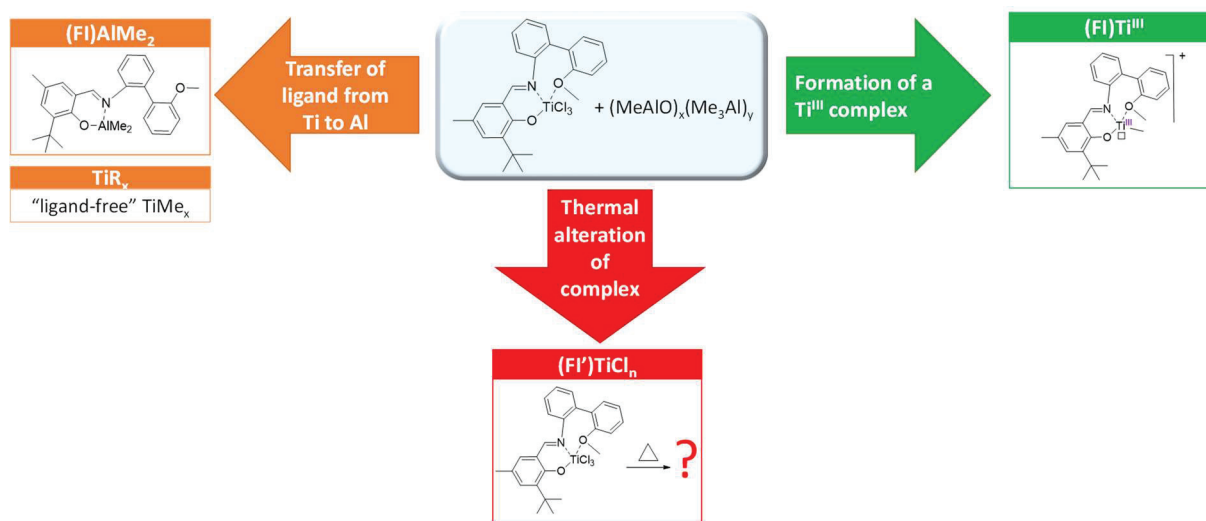


Figure 1. Main hypotheses of polymerization active species considered in this chapter.

II. HYPOTHESIS OF LIGAND ABSTRACTION

II.1. Characterization of ligand transfer to TMA

II.1.1. Reactivity of TMA toward complex I

There are several evidences that TMA is incriminated in the formation of polymerization active species in the SFI system. Although it was proven in Chapter 3 that complex I/TMA affords a limited amount of polymer, the polymerization active species resulting from this combination is not yet identified. The first hypothesis relies on the reducing effect of trialkylaluminum compounds on titanium species.⁸ The resulting Ti^{III} complex could be active in ethylene polymerization. Another possible reaction between TMA and complex I is a ligand abstraction generating a ligand-free “TiMe_x⁺” species and a (FI)AlMe₂ compound. Such TMA-assisted ligand transfer can also be hypothesized for other titanium-based trimerization complexes such as Hessen’s hemi-metallocenes.

To identify a potential reactivity between TMA and complex I, a mixture of these two compounds was analyzed by ¹H NMR (Figure 2). This solution was prepared by reacting 30 equivalents of TMA with a solution of complex I in toluene-*d*₈.

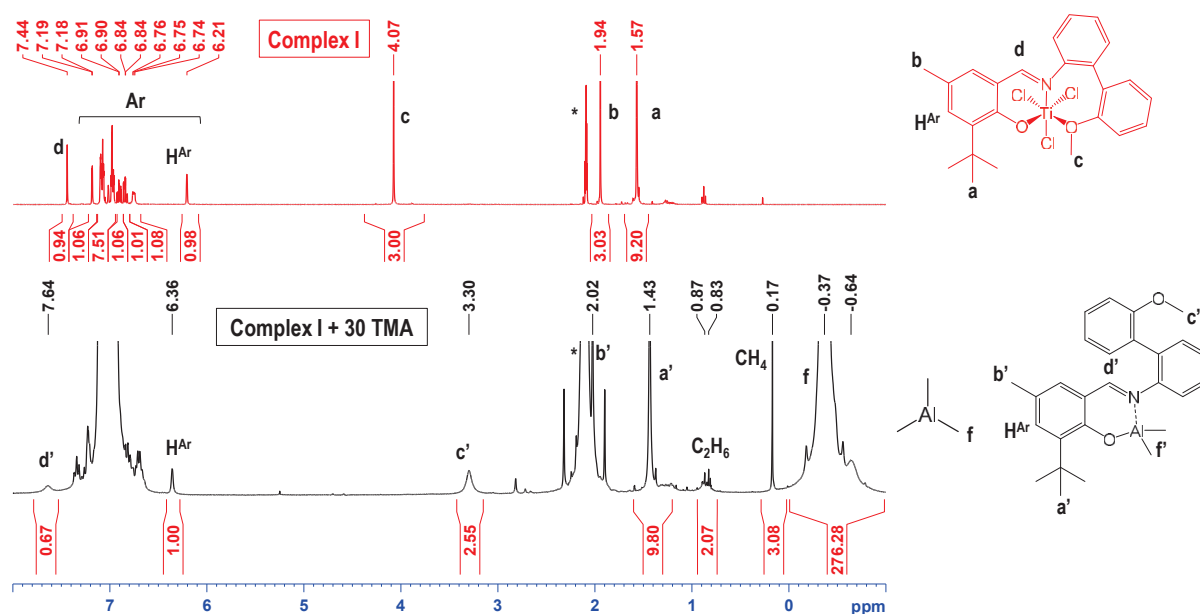


Figure 2. ¹H NMR of complex I (top) and complex I/TMA (Al/Ti = 30) (bottom) in toluene-*d*₈

¹H NMR analysis confirmed the alteration of complex I once contacted with TMA. NMR spectra of complex I+TMA displays signals corresponding to the *tert*-butyl (a', 1.43 ppm) and methyl (b', 2.02 ppm) moieties of the ligand (Figure 2). The broad signal at 3.30 ppm (c') is associated with the methoxy group, which is significantly upfield shifted in presence of TMA compared to complex I (c, 4.07 ppm). In fact, this signal is close to the methoxy group of the ligand (ligand **1**, O-CH₃: 3.36 ppm in toluene-*d*₈, Figure 4). In addition, an imine group (d', 7.64 ppm) is also observed as a deshielded broad signal compared to complex I (d, 7.44 ppm). As a result,

the overall structure of the phenoxy-imine fragment remained intact. In parallel, the signal of the methyl groups of TMA (f, -0.37 ppm) displays a shoulder at -0.64 ppm, which could be assigned to a secondary methylaluminium-based species. The presence of methane (0.18 ppm) and ethane (0.8 ppm) should also be noted.

In the case of the mixture (FI)TiCl₃/TMA, one can expect the formation of (FI)TiMe₃ species along with AlClMe₂. A (FI)AlMe₂ species can also result from the transfer of ligand from the titanium to the aluminum center. Regarding (FI)TiMe₃ complex isolated by Bercaw and coworkers, a single signal at 1.72 ppm is ascribed to the Ti-CH₃ bonds in C₆D₆.⁷ Soshnikov *et al.* reported chemical shifts in the region of 1.78-1.73 ppm and 1.66-1.56 ppm for each Ti-CH₃ moiety of (FI)TiMe₂⁺ species in toluene-*d*₈.⁸ In Figure 2, these regions are free from significant signals, implying the absence of (FI)Ti^{IV}Me₃ or (FI)Ti^{IV}Me₂⁺ complex.

Interestingly, Soshnikov *et al.* reported a similar spectrum pattern as the one presented in Figure 2 (bottom).⁹ In the case of the a bis(imino)pyridine V(III) trichloride complex mixed with AlMe₃/[Ph₃C][B(C₆F₅)₄] (Al/Ti = 15) in presence of ethylene, a cationic bis(imino)pyridine [N,N,N]AlMe₂⁺ was identified along with the formation of ethane (0.86 ppm) and methane (0.17 ppm) (Figure 3). In fact, signals corresponding to the bis(imino)pyridine [N,N,N] ligand are broad and the chemical shifts for TMA and AlMe₂⁺ signals are similar (in the region -0.6 ppm to -0.2 ppm). In comparison, similar signals (f and f') are also observed for the mixture (FI)TiCl₃/TMA (Figure 2, bottom).

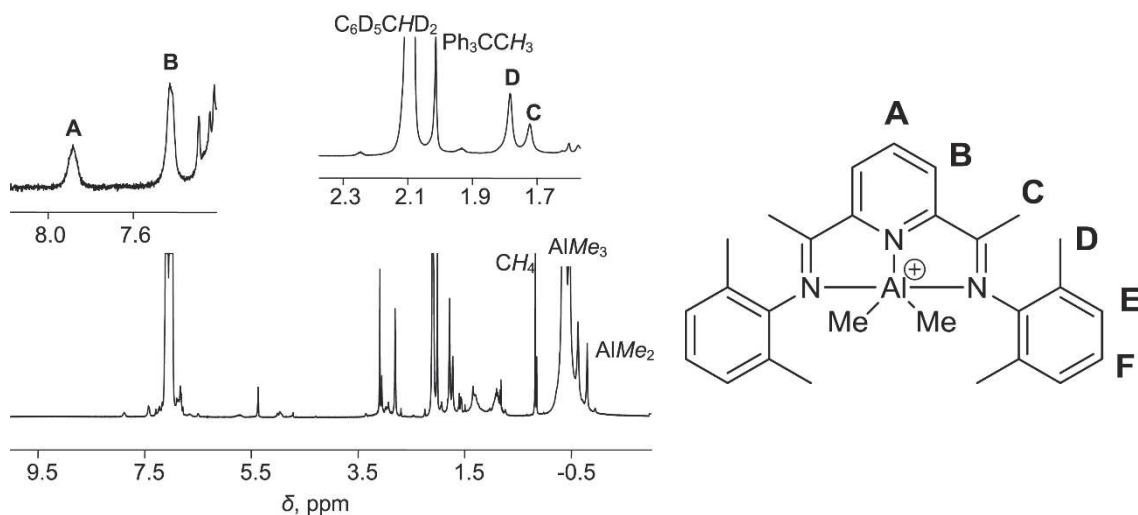
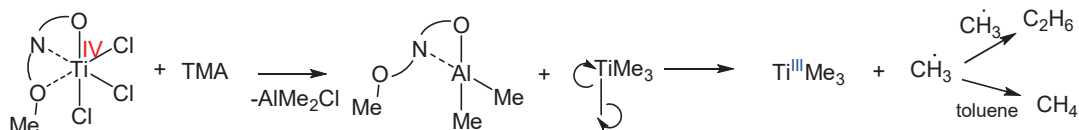


Figure 3. ¹H NMR spectrum of bis(imino)pyridine [[N,N,N]AlMe₂][B(C₆F₅)₄] in toluene-*d*₈
Reprinted with permission from [9] Copyright 2018 Elsevier

To go further, Soshnikov *et al.* also mentioned a correlation between the appearance of the aluminum-based bis(imino)pyridine and the deactivation of the system. The presence of both ethane and methane was explained by the homolytic cleavage of V^{III} -Me affording V^{II} species. Based on this assumption, a similar mechanism can be proposed in the case of (FI)TiCl₃/TMA (Scheme 1). A paramagnetic Ti^{III}Me₃ species should be formed in this case but was not identified in the spectral range of -10 to 14 ppm.

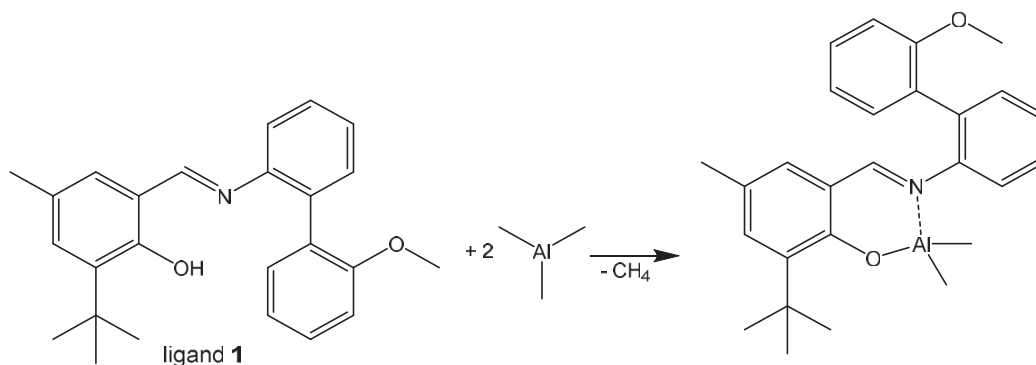


Scheme 1. Proposed mechanism for ethane and methane formation when contacting (FI)TiCl₃ and TMA (Figure 2)

Eventually, (FI)TiCl₃/TMA spectrum analysis showed that TMA is not innocent towards the SFI precatalyst as it would alter the geometry of the complex or even its structure. In fact, one could at least assume the decoordination of the methoxy moiety (c) from the titanium center. Moreover, the hypothesis of ligand transfer is supported by examples reported in literature. At this stage, ¹H NMR comparison is not sufficient to draw straightforward conclusions regarding the ability of TMA for a ligand abstraction. In this context, the synthesis of (FI)AlMe₂ was undertaken.

II.1.2. Synthesis of and characterization of (FI)AlMe₂

To check the possibility of a transfer of ligand, it was decided to synthesize the corresponding aluminum derivative (FI)AlMe₂. Similar compounds are described in the literature.¹⁰ The procedure simply consisted in reacting 2.7 equivalents of TMA (from a diluted solution in toluene) with a solution of phenoxy-imine-ether ligand (ligand **1**) in toluene-*d*₈ at room temperature (Scheme 2). The resulting bright yellow liquid notified a reaction between the ligand and TMA.



Scheme 2. Synthesis of (FI)AlMe₂

Based on the ^1H NMR comparison in Figure 4, the formation of $(\text{FI})\text{AlMe}_2$ was confirmed by:

- (i) the disappearance on the hydroxy group signal of the ligand (e);
- (ii) the presence of methane ($\delta_{\text{CH}_4} = 0.17$ ppm);
- (iii) two close signals f and f'' accounting for Al-CH_3 methyl groups of TMA and $(\text{FI})\text{AlMe}_2$, respectively.

In addition, a similar amount of TMA (f) and $(\text{FI})\text{AlMe}_2$ (f'') were identified presuming an equimolar reaction between TMA and the ligand. One can remark that for the integrations of Al-CH_3 , $I(f) = I(f'')$ instead of 1.5 times $I(f'')$ owing that TMA was partially evaporated during the reaction.

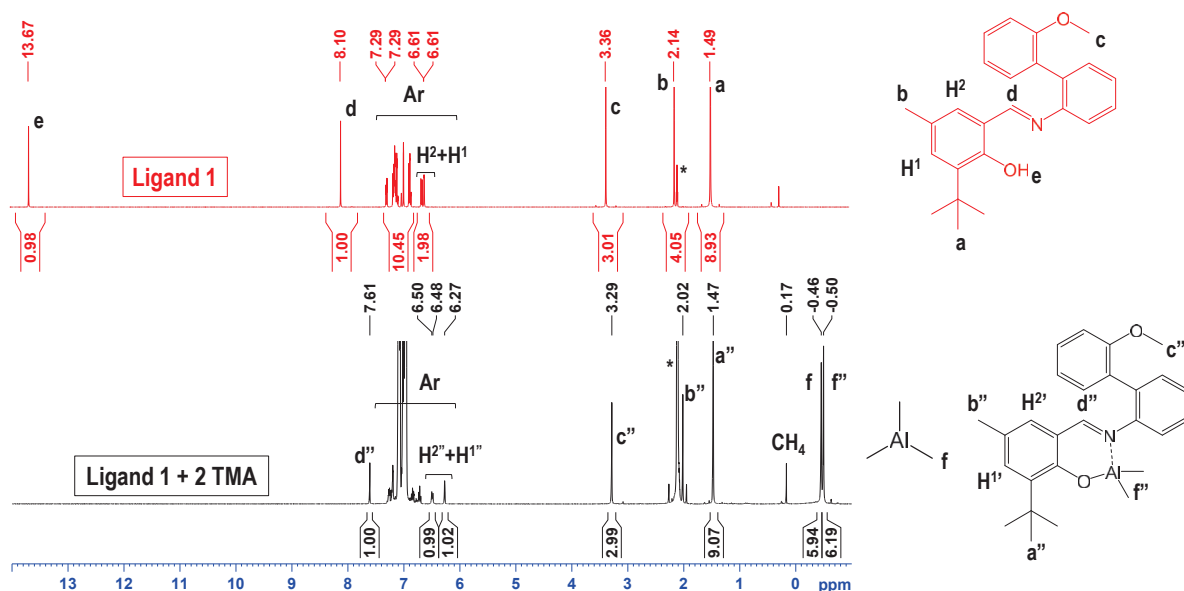


Figure 4. ^1H NMR of the mixture of the phenoxy-imine-ether ligand (ligand **1**, red) and the mixture of ligand **1** with trimethylaluminum ($\text{Al/Ti} = 2$) (black) in toluene- d_8 .

Comparing now the ^1H NMR spectra of $(\text{FI})\text{AlMe}_2$ (Figure 4) and of complex I/TMA mixture (Figure 2, bottom), a good correlation was found between the ligand signals. Indeed, the imine (d'' : 7.61 ppm), methoxy (c'' : 3.29 ppm) and *tert*-butyl (a'' : 1.47 ppm) groups identified for $(\text{FI})\text{AlMe}_2$ display close chemical shifts with the mixture $(\text{FI})\text{TiCl}_3/\text{TMA}$ (a' : 1.43 ppm, b' : 3.30 ppm and d'' : 7.64 ppm). Consequently, the species afforded by the mixture of $(\text{FI})\text{TiCl}_3$ with TMA exhibits a similar structure to $(\text{FI})\text{AlMe}_2$, which supports the hypothesis of a ligand transfer from the titanium center to aluminum.

Although there were few doubts on the incapability of $(\text{FI})\text{AlMe}_2$ for ethylene polymerization in the catalytic conditions studied in this project ($T = 20\text{--}80$ °C, 10 bar of ethylene), the possibility of an Aufbau reaction was verified. Generally speaking, Aufbau reactions are carried out at very high temperatures and pressures (100 °C, 100 bar) with triethylaluminum.¹¹ Under

these conditions, long C₁₀₀ oligomers are obtained. As expected, (FI)AlMe₂ did not polymerize ethylene in our operating conditions.

To conclude, there are evidences that TMA can abstract the phenoxy-imine-ether ligand from complex I but the resulting Al-based species is not active towards ethylene polymerization (at low pressure and temperature). The possibility of a ligand-free titanium polymerization catalyst “TiR_x” should therefore be considered even though its exact structure is undefined.¹ In fact, the formation of a “TiMe_x⁺” species in the case of complex I/MAO system would result from a transfer of the ligand assisted by the “free” TMA contained in MAO.

Considering that this side reaction occurs during the activation process, three steps would occur concomitantly:

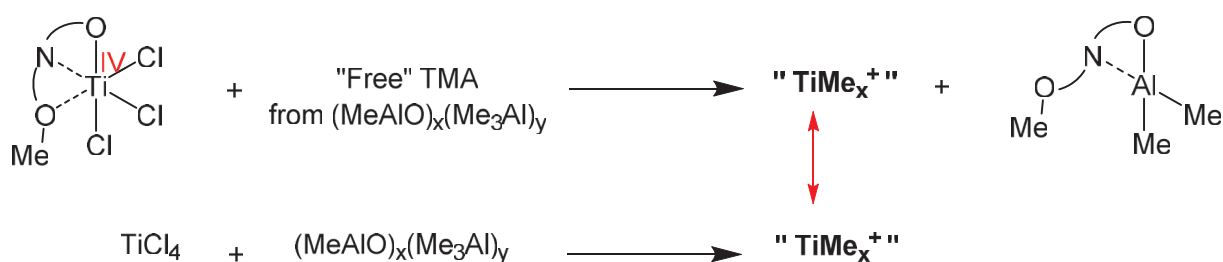
- (i) the alkylation of (FI)TiCl₃ by the MAO into (FI)TiMe₃;
- (ii) the cationization of (FI)TiMe₃ by MAO leading to (FI)TiMe₂⁺;
- (iii) the abstraction of ligand from (FI)TiMe₂⁺ by the “free” TMA affording a “TiMe_x⁺” species.

In the view of verifying whether this “TiMe_x⁺” species is the polymerization active species in the SFI system, its synthesis is necessary although not reported. To circumvent this limitation, a judicious alternative to generate this “ligand-free” titanium species was found and explained in the following section.

II.2. TiCl₄/MAO as molecular Ziegler-Natta catalyst

II.2.1. Catalytic performance of TiCl₄/MAO in ethylene polymerization and copolymerization with 1-hexene

A possible model for “ligand-free” molecular Ziegler-Natta “TiMe_x⁺” mentioned in the literature is the TiCl₄/MAO system. The choice for TiCl₄ was naturally driven by the absence of any organic ligand coordinated to the titanium center. As co-catalyst, MAO was selected to generate the “TiMe_x⁺” species for its double role of alkylating and cationizing agent (Scheme 3). In fact, as highlighted in the literature review, MAO is the prominent co-catalyst for molecular Ziegler-Natta systems based on metallocenes and post-metallocenes but not for TiCl₄. Indeed, few trials were attempted with the system TiCl₄/MAO but quickly abandoned because of irrelevant catalytic performances compared to AlR₃-activated heterogeneous systems.¹² Given the absence of literature regarding the performance of TiCl₄/MAO, it was important to check the reactivity of this unusual system toward ethylene and ethylene/1-hexene.



Scheme 3. Presumed and considered routes for “TiMe_x⁺” species formations.

In order to properly assess the catalytic behavior of this system, TiCl₄/MAO was tested in similar conditions as complex I/MAO in terms of titanium loading and MAO equivalent (Al/Ti = 1/130). The amount of TiCl₄ was fixed at 4 μmol to ensure a sufficient polymer yield. This way, the amount of “TiMe_x⁺” species engaged in the reaction is purposely higher than the theoretical amount of polymerization species in the SFI system. This catalytic system was studied at the key temperatures of 40, 60 and 80 °C towards ethylene polymerization (Table 1, entries 1-3) and ethylene/1-hexene copolymerization (Table 1, entries 4-6). All catalytic tests were conducted in the 1-L SFS reactor following the standard procedure. As a reminder, 1-hexene was introduced in the reactor along with MAO, i.e. before the solution of titanium tetrachloride.

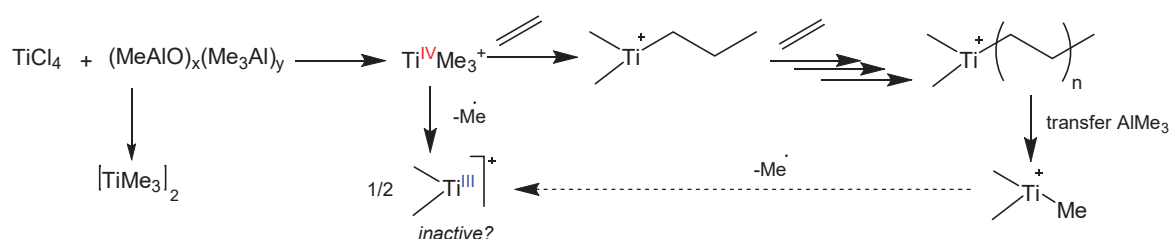
In the case of TiCl₄/MAO for ethylene/1-hexene copolymerization, the amount of MAO introduced was approximated to the yield of 1-hexene obtained with the SFI system (Chapter 2, Table 3), after 5 minutes of reaction. At this stage of reaction, 1-hexene production amounts to 40 % (17.7 g) and 75 % (1 g) of the global yield at 42 °C and 80 °C respectively. Half of the amount of 1-hexene formed at 58 °C (9.6 g) was arbitrarily chosen.

Table 1. Ethylene polymerization and ethylene/1-hexene copolymerization with TiCl_4/MAO at 40, 60 and 80 °C.

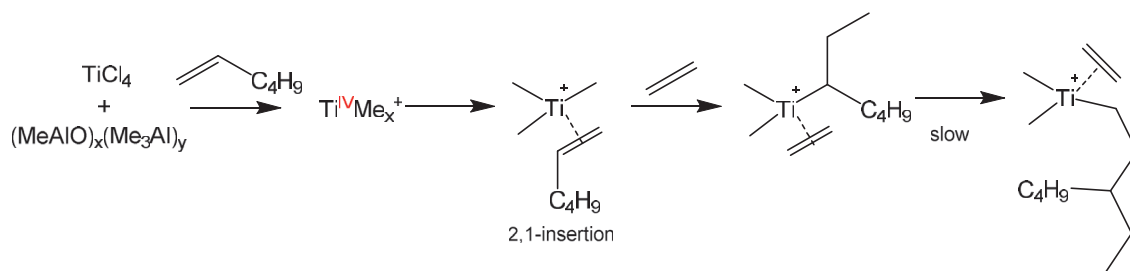
Entry	T (°C)	t (min) ^a	1-hexene introduced (g)	PE yield (g)	Activity ($\text{kg}_{\text{ethylene}} \text{g}_{\text{Ti}}^{-1} \text{h}^{-1}$)
1	42	2	0	1.45	230
2	61	1	0	0.66	210
3	79	1	0	0.78	245
4	42	1.5	10.2	0.36	75
5	62	1.5	5.5	0.31	80
6	80	1.5	1.0	0.14	35

Conditions: 4 $\mu\text{mol TiCl}_4$, MAO 30 wt % in toluene, Al/Ti = 1 130, 300 mL toluene, 10 bar of ethylene
^a time corresponding to the increase of temperature during reactor pressurization

First, testing TiCl_4/MAO from 40 to 80 °C evidenced its limited activity in ethylene polymerization, especially at elevated reaction temperature. The system deactivates during the first minutes of the catalytic test yielding to less than 1.5 g of polymer between 40 °C and 80 °C (Table 1, entries 1-3). It can be concluded that the polymerization active species emerging from TiCl_4/MAO becomes rapidly inactive, probably because of degradations leading to an inactive species as proposed in Scheme 4.

Scheme 4. Proposed degradation of "TiMe_x⁺" in presence of MAO

In the case of ethylene/1-hexene copolymerization, the presence of 1-hexene impacts the activity of the system. At 42 °C, a high 1-hexene composition of 28.3 mol % in the liquid phase leads to a decrease in activity by four (entry 4 versus 1). The same negative effect is observed even with a low 1-hexene content of 5.6 mol % at 80 °C. Consequently, an interaction between 1-hexene probably occurs during the pre-activation step and explains this additional limitation of polymerization. For example, 2,1 insertions of 1-hexene in the Ti-C bond can limit further insertion of ethylene (Scheme 5). A similar effect of LAO introduced before the pre-activation step has also been demonstrated for complex I/MAO in Chapter 3 (III.2. Influence of additional 1-hexene).



Scheme 5. Proposed interaction between 1-hexene and “ TiMe_x^+ ” species limiting the catalyst activity.

Considering now the copolymerizations with complex I/MAO, catalytic tests showed that the temperature has an opposite effect on the polymer production, which may be correlated to the concomitant deactivation of the trimerization system (see Chapter 2). Although a similar polymer yield is afforded at low temperature (1.69 g at 42 °C, Chapter 2, Table 3), it cannot be only ascribed to the “ TiMe_x^+ ” species. Indeed, 4 μmol of TiCl_4 were necessary to yield a similar PE amount as complex I (3.78 μmol) whereas the latter also produces 44 g of 1-hexene. Besides, one could still consider a ligand transfer to explain the formation of polymer in the first 2 minutes of the catalytic test. On that basis, the analyses of polymers produced by TiCl_4/MAO and complex I/MAO were compared in terms of MMD and 1-hexene content.

II.2.2. Comparison of polymer features obtained with complex I /MAO and TiCl_4/MAO

II.2.2.1. Molar mass distribution of polymers

The molar masses of the poly(ethylene-co-1-hexene) obtained at 40 and 60 °C using TiCl_4/MAO were determined by SEC analysis. Even though it was previously shown that such “ TiMe_x^+ ” species would not be the main polymerization catalyst of the SFI system, it is still interesting to determine the average molar masses and the broadness of chain length distribution with this “ligand-free” catalyst.

SEC analyses were performed on the polymer obtained with TiCl_4/MAO and compared with polymers produced by complex I/MAO in the 1-L SFS reactor in similar conditions (PE-SFS-42 and PE-SFS-58). A comparison of molar mass distributions of the polymers is provided in Figure 5.

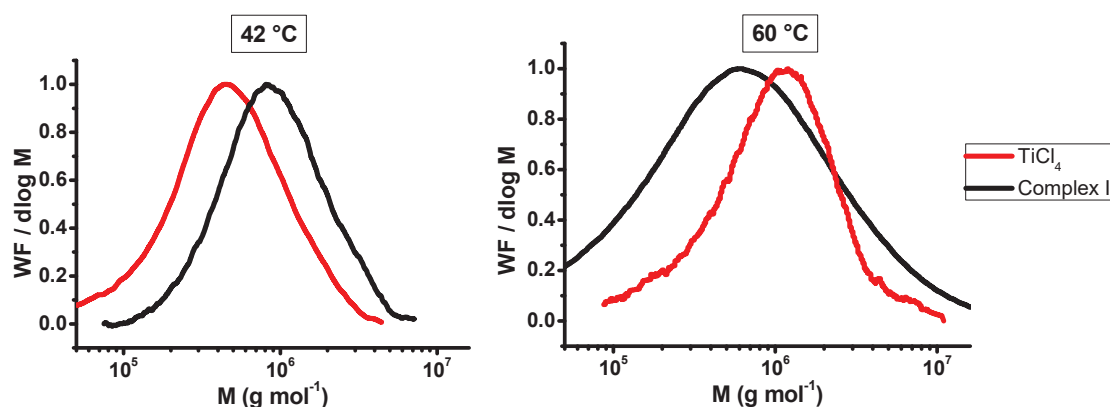


Figure 5. Comparison of molar mass distributions of polymers obtained at 42 and 60 °C by complex I/MAO (black) and TiCl_4 /MAO in presence of 1-hexene (red)

The MMD analyses of polymers produced with TiCl_4 /MAO revealed the formation of high molar mass PE at 42 °C and 60 °C. Indeed, an increase of molar masses from 0.63×10^6 to $1.59 \times 10^6 \text{ g mol}^{-1}$ is observed as the amount of 1-hexene is decreased (Table 1, entries 4 and 6). One explanation lies in the presence of 1-hexene and more precisely the negative impact of 2,1-insertion of this comonomer in the growing polymer chain (Scheme 5). As a result, a higher concentration of 1-hexene in the reaction medium at 42 °C (Table 1, entries 4 versus 1) impacts both the polymerization rate and polymer chain lengths. This phenomenon is actually observed when 1-hexene is added to complex I/MAO (Chapter 3, Table 4).

Interestingly, the two MMDs at 42 °C display a dispersity of 2 but a different average molar mass. In addition, MMD of the polymer afforded by TiCl_4 /MAO at 60 °C is encompassed in the MMD of PE-SFS-58 (Figure 5, right). From these observations, the hypothesis of “ TiMe_x^+ ” species formed at the early stage of reaction cannot be completely rejected. In addition, polymers obtained by TiCl_4 /MAO exhibit a homogeneity in chain length given the low dispersity value ($2 < \mathcal{D} < 2.6$). One possibility is that the “ TiMe_x^+ ” species behaves as a single site. One must remain cautious in hypothesizing the structure of the presumed “ TiMe_x^+ ” active species from pure polymer properties. Indeed, polymerization conditions were unstable with temperature and pressure variations at the early stage of reaction. Despite this limitation, it was worth comparing polymer properties between these two systems in terms of 1-hexene content in the polymer.

II.2.2.2. Chemical composition of polymers

This approach enables to check the ability of the TiCl_4/MAO catalyst to incorporate linear alpha-olefins compared to complex I/MAO. The analysis of polymer properties indicated a poor copolymerization ability of the TiCl_4/MAO system (Table 2).

Table 2. Polymer properties resulting from ethylene/1-hexene copolymerization with TiCl_4/MAO

Entry	T (°C)	t (min) ^a	1-hexene introduced (g)	T _m (°C)	1-hexene content (mol %) ^a
1	42	1.5	10.2	125	0.85
2	62	1.5	5.5	128	0.28
3	80	1.5	1.0	131	0.13

Conditions: 4 μmol TiCl_4 , MAO 30 wt % in toluene, Al/Ti = 1 130, 300 mL toluene, 10 bar of ethylene
^a determined by high temperature ^{13}C NMR in o-DCB-*d*₄/o-DCB (1/9)

Although the reaction time was very limited, polymerization catalyst incorporated 1-hexene to some extent. High melting temperatures (from 125 °C to 131 °C) and low 1-hexene content revealed by high temperature ^{13}C NMR were observed for these polymers. As expected, 1-hexene content decreases along with its initial concentration in the liquid phase. This poor 1-hexene response is a common point with the polymerization active species of the SFI system.

Putting in perspective the content of 1-hexene in the reaction medium and in the polymer, it can be concluded that a “ TiMe_x^+ ” catalyst is a better ethylene/LAO copolymerization species than the polymerization catalyst formed by combination of complex I and MAO. Indeed, for both systems, polymer CCD diverges despite a similar 1-hexene composition in the liquid phase (Figure 6). Still, both catalysts display a poor tendency for LAO copolymerization. Thus, it is conceivable that the polymer produced by a “ TiMe_x^+ ” species could constitute part of the material afforded after 30 minutes in the case of complex I/MAO.

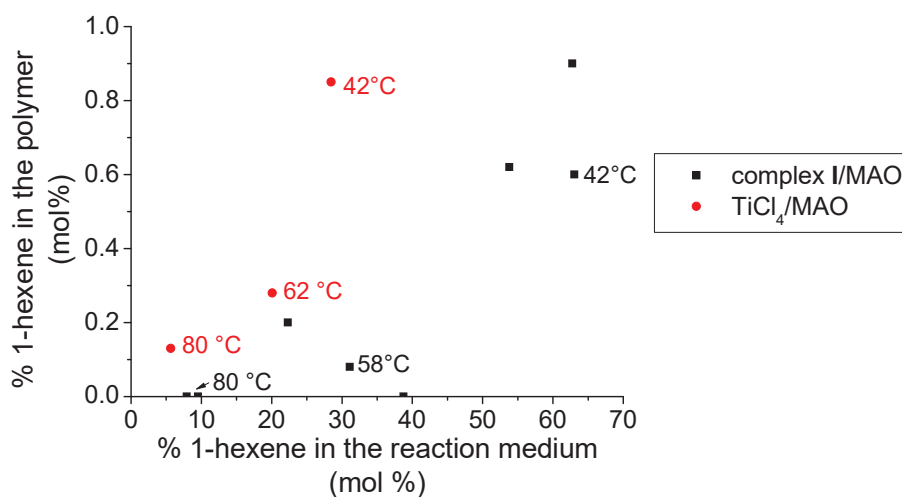


Figure 6. Comparison of 1-hexene copolymerization ability of TiCl₄/MAO and complex I/MAO systems

II.3. Discussion on the hypothesis of ligand abstraction

The hypotheses involving TMA for the formation of a polymerization active species were:

- (i) the formation of a “TiMe_x⁺” complex assumed to behave as a molecular Ziegler-Natta catalyst;
- (ii) a reduction of the imine group highlighted by neosilylated precursors¹³;
- (ii) a reduction to Ti^{III}.

Regarding (i), the present study showed undeniable evidences that TMA can react with complex I. The comparison with (FI)AlMe₂ spectrum tends to support the hypothesis of ligand abstraction by this alkylaluminium compound. Concerning (ii), there is no proof that TMA would not eventually undergo imine reduction during catalytic tests although this reaction was not identified by ¹H NMR. Regarding (iii), no paramagnetic species were identified by ¹H NMR. Therefore, a ligand abstraction is the most probable path describing the reactivity of complex I with TMA.

Considering that the active species resulting from the mixture TiCl₄/MAO is equivalent to the structurally undefined “TiMe_x⁺” catalyst, it was proven that such species cannot afford the entire amount of polymer formed in the case of complex I/MAO. To exemplify this conclusion, an arbitrary proportion of the overall (FI)TiCl₃ is designated as polymerization active species, “TiMe_x⁺” in this case. Since the temperature study detailed in Chapter 2 highlights the increasing production of polymer at higher temperature, the content of “TiMe_x⁺” would increase. For instance, it was conjectured that “TiMe_x⁺” content evolves from 25 mol % (42 °C) to 50 mol % (62 °C) and 75 mol % (80 °C) (Table 3), which are probably overestimated. Based on the yield of polymer obtained at these temperature, the “TiMe_x⁺” species would produce at most 20 wt % of the polymer actually obtained with the SFI system.

Consequently, one can exclude that such “ligand-free” species is at the origin of the whole polymer produced by the SFI system, but maybe a part of it.

Table 3. Proportion of PE theoretically afforded by TiMe_x^+ in complex I/MAO system

	42 °C	62 °C	80 °C
% TiMe_x^+ (mol %)	25%	50%	75%
% PE (wt %)	20.2%	4.0%	9.5%

To conclude, the hypothesis of ligand abstraction proposed by Duchateau *et al.* is not sufficient to explain the side polymerization reaction in the SFI system, especially at low temperature. Other side reactions should lead to polymerization active species that are more active but also poorly 1-hexene responsive. On the basis of the studies detailed in the previous chapters, investigations were oriented toward potential alterations of complex I structure by several parameters, such as reaction temperature.

III. HYPOTHESIS OF LIGAND ALTERATION

III.1. Possible modifications of complex induced by a temperature effect

In this project, it was demonstrated that temperature plays a significant role in polymer production since this undesired reaction is promoted at $T > 50\text{ }^{\circ}\text{C}$. The main asset of increasing temperature in chemical transformation is to favor the kinetics of reactions of the targeted reaction but side reactions may also be promoted. In the case of the SFI system, it is possible that high temperature induces an alteration of the global structure of complex I. Indeed, the miscellaneous phenoxy-imine-based polymerization catalysts reported in the literature provide diverse possibilities of complexes able to polymerize ethylene.⁶ The formation of such phenoxy-imine derivatives could result from a transformation from a mono to a dianionic ligand or a transfer of ligands leading to a complex bearing two bidentate phenoxy-imine ligands (Figure 7). Noteworthy, these modifications can be also assisted by the co-catalyst or result from side reactions between complexes.

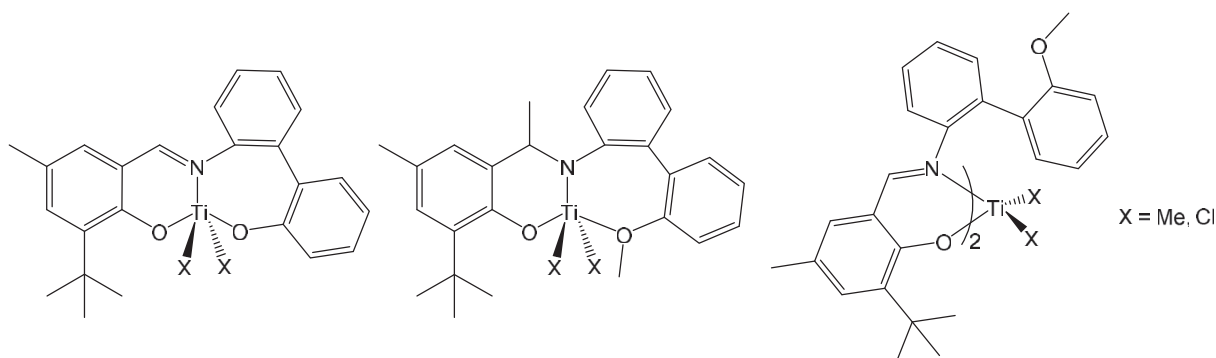


Figure 7. Potential polymerization post-metallocenes derived from the phenoxy-imine complex I

In the purpose of verifying the formation of a new complex, the effect of temperature on complex I was investigated. The strategy was to highlight any thermal modification, identify the resulting complex, test its reactivity towards ethylene and if successful, compare it with complex I/MAO in terms of catalytic performance and polymer properties.

III.2. Thermal modification of complex I

III.2.1. Complex I degradation

III.2.1.1. Release of MeCl

The strategy is to investigate the thermal stability of complex I and to highlight any ligand alteration or reorganization. In this purpose, several thermal techniques were employed and analyses were combined to determine the process leading to a potential new complex.

First, the stability of complex I was studied according to temperature. Its degradation was forced by thermogravimetric analysis (TGA). This technique consists in measuring the mass of a compound upon heating. This way, any mass loss can be quantified and associated to a temperature. Thus, one can formulate hypotheses regarding the nature of moieties released upon heating based on its mass and its temperature of formation. TGA was performed on 5.1 mg of complex I which was heated from 25 °C to 600 °C with a rate of 10 °C min⁻¹ under inert atmosphere. The resulting thermogram is shown in Figure 8.

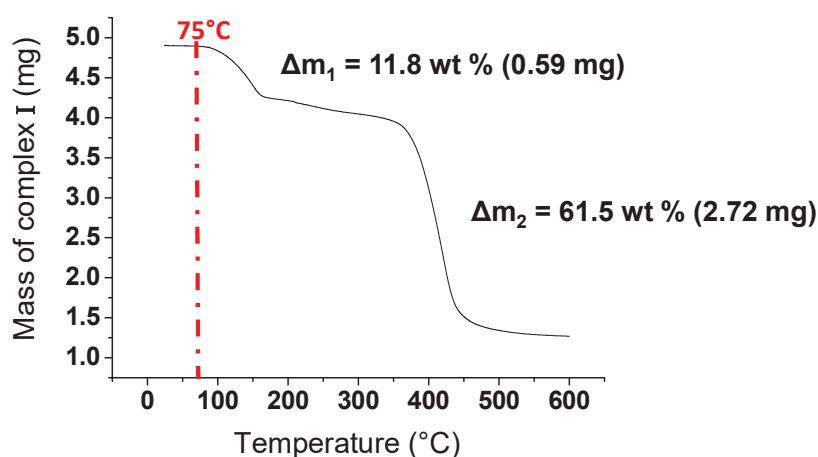


Figure 8. TGA thermogram of complex I heated from 25 °C to 600 °C at 10 °C min⁻¹

TGA analysis of complex I revealed two thermal events corresponding to the degradation of the phenoxy-imine compound (Figure 8). The first minor event is ascribed to the release of a small and volatile molecule from 75 to 150 °C amounting to 11.8 wt % of complex I (Figure 8, Δm_1). A significant degradation is observed from 350 to 450 °C (Figure 8, Δm_2) after which it remains 26.5 wt % (1.35 mg) of residues of complex I at $T > 450$ °C.

Considering possibilities for complex degradation, the first hypothesis involves the release of a ligand moiety. Knowing that the ligand represents 70.8 wt % of the complex, a total degradation can be assumed at $T > 450\text{ }^{\circ}\text{C}$. Considering the first molecule released ($\Delta m_1 = 0.59\text{ mg}$, Figure 8), its molar mass has been assessed to 60 g mol^{-1} , which cannot be ascribed to a fragment of ligand. As a result, this volatile molecule should involve a chlorine and a moiety of the phenoxy-imine-ether molecule.

TEA experiment showed that complex I is subject to structure alteration at high temperature. It is an interesting phenomenon that could take part in the formation a polymerization active species at elevated temperature. To go further and identify the molecules released during complex I degradation, DRIFT-GC/MS analyses were performed under inert atmosphere. This combination of characterization techniques enables to identify the structure of the heated compound by separating the volatile molecules by gas chromatography and identifying them using mass spectroscopy. The heating of 50 mg of complex I was monitored at $2\text{ }^{\circ}\text{C min}^{-1}$ under nitrogen flow and gas phase chromatograms were recorded at $20\text{ }^{\circ}\text{C}$, $50\text{ }^{\circ}\text{C}$ and then every $36\text{ }^{\circ}\text{C}$ (Figure 9).

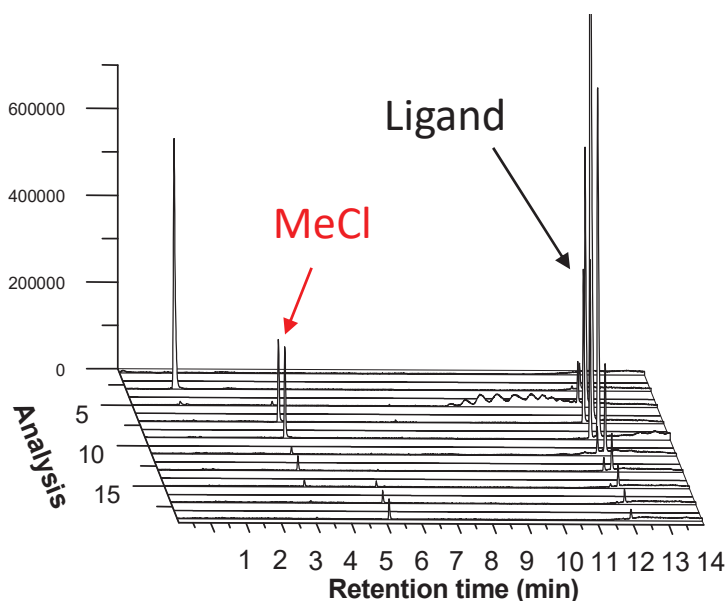


Figure 9. GC signals of volatiles molecules released upon heating of complex I. GC analyses are performed each $36\text{ }^{\circ}\text{C}$ from $20\text{ }^{\circ}\text{C}$.

MS analyses performed for each of the 20 GC records enabled to identify the molar masses of the molecules released during complex I heating. In Figure 9, a peak is detected at 3.1 min and corresponds to a molecule with $m/z = 50$, attributed to chloromethane. This molecule is released from $122\text{ }^{\circ}\text{C}$ to $300\text{ }^{\circ}\text{C}$ (Figure 9, analyses 4-9). The second main signal (13 min) is assigned to a molecule with $m/z = 254$. In this case, a larger moiety is released from 50 to $586\text{ }^{\circ}\text{C}$ but could not be associated with an accurate fragment of the ligand. This experiment enables to clearly identify the structure of the complex rearranged upon heating, which is accompanied by the release of chloromethane. As a result, the first mass loss observed in TGA

(Figure 8) is mainly associated to the release of this volatile molecule, accounting for 9.3 wt % of complex I.

III.2.1.2. Identification of a secondary complex

To go even further with the identification of structure alteration, ^1H NMR analyses of complex I in toluene- d_8 were performed at high temperature (Figure 10). The NMR tube was heated within the NMR spectrometer and signals were recorded at 25, 40, 60, 80, 100 °C and at 25 °C after cooling. The temperature was stabilized for 15 minutes before signal recording.

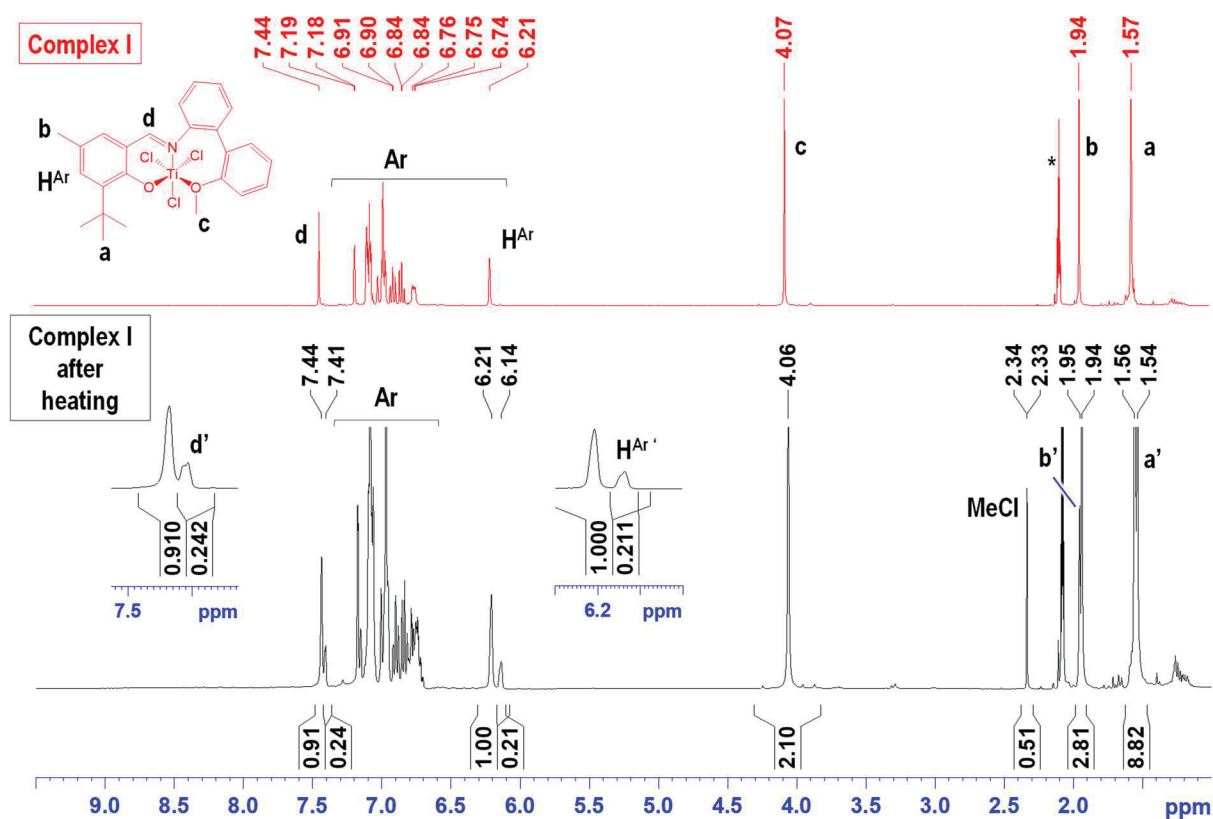


Figure 10. ^1H NMR of complex I in toluene- d_8 at 25 °C (red) and at 25 °C after heating to 100 °C (black)

The comparison of ^1H NMR spectra between the intact (red) and heated (black) complex I confirmed the formation of chloromethane and allowed the identification of the induced complex (Figure 10). ^1H NMR monitored at high temperature indicates that part of complex I remains unchanged. Indeed, characteristic signals of complex I labeled a (1.56 ppm), b (1.94 ppm), H^{Ar} (6.21 ppm) and d (7.44 ppm) are still present. Chloromethane is identified with a single resonance at 2.33 ppm. In addition, a new complex (complex III, Figure 11) is also identified whose signals a' (1.54 ppm), b' (1.95 ppm), $\text{H}^{\text{Ar}'}$ (6.14 ppm) and d' (7.41 ppm) are close to the ones of complex I. Interestingly, no secondary signal is observed in the region of c (4.06 ppm). Consequently, the structure of the complex after heating is essentially equivalent to complex I, at the expense of the methoxy group that is gradually transformed in

chloromethane. In addition, this new compound arose from a slight but irreversible alteration of complex I. A hypothesis of its structure is proposed in Figure 11.

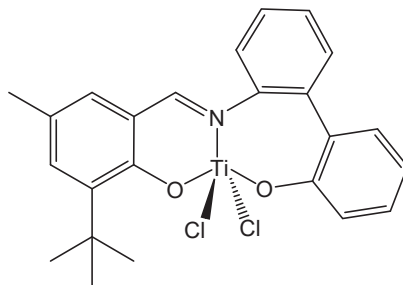


Figure 11. Hypothesis of complex III structure

As mentioned earlier, the formation of complex III was followed by ^1H NMR from 40 to 100 °C. To quantify the evolution of complex III/complex I ratio, the sum of integral $I(\text{H}^{\text{Ar}})+I(\text{H}^{\text{Ar}'})$ was normalized to one. A progressive decrease of $I(\text{c})$, corresponding to the methoxy group of complex I, and concomitant appearance and intensification of the chloromethane signal is a proof that complex III does not display a methoxy group upon increase of temperature (Table 4).

Table 4. Evolution of the ratio complex III/initial complex I upon heating complex I from 40 to 100 °C in toluene- d_8

Entry	T (°C)	Complex III (mol %)	$I(\text{c})^b$	$I(\text{MeCl})^c$
1	40	2	2.93	0
2	60	3	2.90	0
3	80	3	2.82	0.07
4	100	13	2.39	0.46
5	25 ^a	21	2.10	0.50

Conditions: 35 μmol complex I, 0.6 mL toluene- d_8 , 15 min temperature stabilization before acquisition

^a after cooling

^b integration of the signal at 4.07 ppm (methoxy group of complex I)

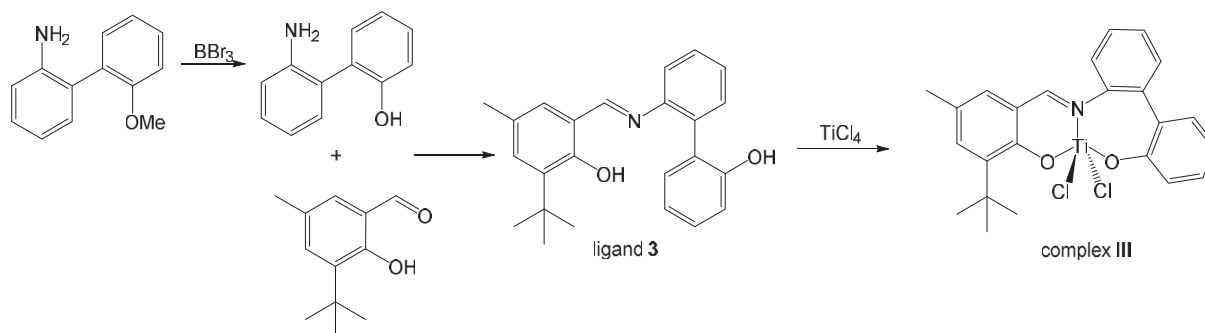
^c integration of the signal appearing at 2.33 ppm

In addition, the gradual formation of complex III started from 40 °C. Indeed, the secondary complex amounts from 2 mol % (40 °C) to 21 mol % (100 °C) of the initial amount of complex I (Table 4). Therefore, heating complex I to 100 °C led to the transformation of a part of this species. To force the formation of complex III, the thermal treatment of complex I was performed at 100 °C for 24 hours under argon. Even in these conditions, the alteration of complex I remains incomplete with 80 mol % of complex III formed.

Based on thermal stability studies of complex I, there are indisputable proofs that the structure of this complex is altered at high temperature but also in toluene. This modification induces a compound displaying a similar structure with complex I, revealed by close ^1H NMR signals. Furthermore, the balance between methoxy disappearance and chloromethane formation reveals the involvement of Ti-Cl and Me-O bounds. As a result, one could propose the transformation from a mono-anionic $([\text{O}^-, \text{N}, \text{O}]\text{-FI})$ to a di-anionic $([\text{O}^-, \text{N}, \text{O}^-]\text{-FI})$ complex presented in Figure 11.

III.2.2. Synthesis of complex III

To further confirm the formation of complex III, this compound was synthesized and characterized by ^1H NMR in toluene- d_8 . Being a derivative of complex I, its synthesis was simply based on a ligand moiety alteration. In fact, hydrolysis of the 2'-methoxy-1,1'-biphenyl-aniline assisted by BBr_3 enabled the formation of the corresponding hydroxy compound (Scheme 6).¹⁴ After the Schiff condensation between this fragment and the salicylaldehyde derivative, the resulting ligand (ligand 3) was reacted with TiCl_4 at -78°C affording the LX_2 -species. Details of the synthesis of each ligand moiety can be found in the experimental section. Such diphenoxo-imine complexes were described in the literature and were synthesized by conventional route, employing two equivalents of *n*-butyllithium as deprotonating agent before reacting the ligand with titanium tetrachloride.¹⁵



Scheme 6. Steps for complex III synthesis

^1H NMR spectrum of complex III in toluene- d_8 revealed that this synthesized LX_2 species displays the same chemical shifts as the secondary complex formed upon heating of complex I (Figure 10). In fact, the imine group (d) is identified at 7.40 ppm while signals for the methyl and *tert*-butyl substituents are observed at 1.95 and 1.54 ppm, respectively (Figure 12). The absence of the methoxy group and the agreement between theoretical and measured integrals of the aforementioned signals enable to conclude that the same complex is formed upon thermal treatment of complex I.

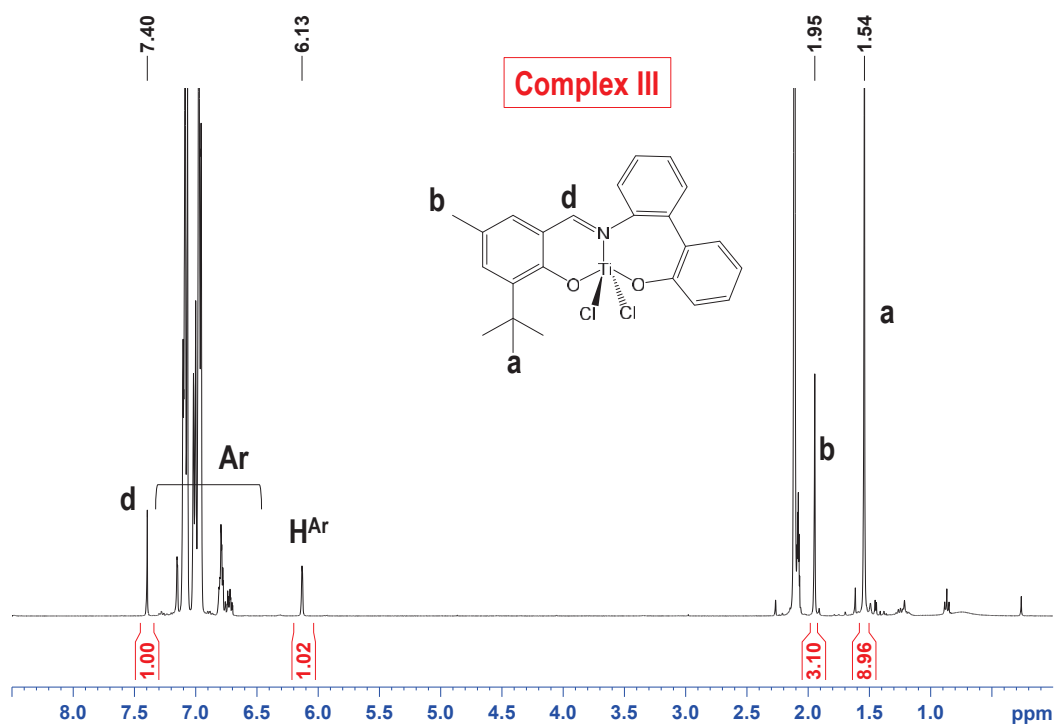


Figure 12. ¹H NMR spectrum of complex III in toluene-*d*₈

To determine the structure of complex III by X-ray diffraction, several recrystallization trials were performed in different conditions. The liquid and vapor diffusion of pentane as antisolvent in a solution of complex in toluene did not permit the growth of monocrystals but rather the precipitation of an orange solid. Eventually, light orange crystals were afforded by slow evaporation of toluene from a concentrated solution of complex III. X-ray diffraction of a monocrystal shed light on the formation of an unexpected complex (Figure 13).

Instead of a complex bearing one [O⁻,N,O⁻] ligand, a bis(diphenoxy-imine) complex was identified in the solid state (Figure 13). Such disubstituted species adopts a distorted octahedral geometry with the coordination of both ligands in a *fac* fashion. The *o*-*tert*-butyl phenoxy groups (O(7) and O(5) in Figure 13) are in *cis* position, which is rather surprising considering the steric hindrance provided by *tert*-butyl groups in *ortho*-positions. This peculiar mode of coordination involves that distances between metal and each heteroatoms are different since Ti-O(7) < Ti-O(5), Ti-N(4) > Ti-N(3) and Ti-O(8) > Ti-O(6).

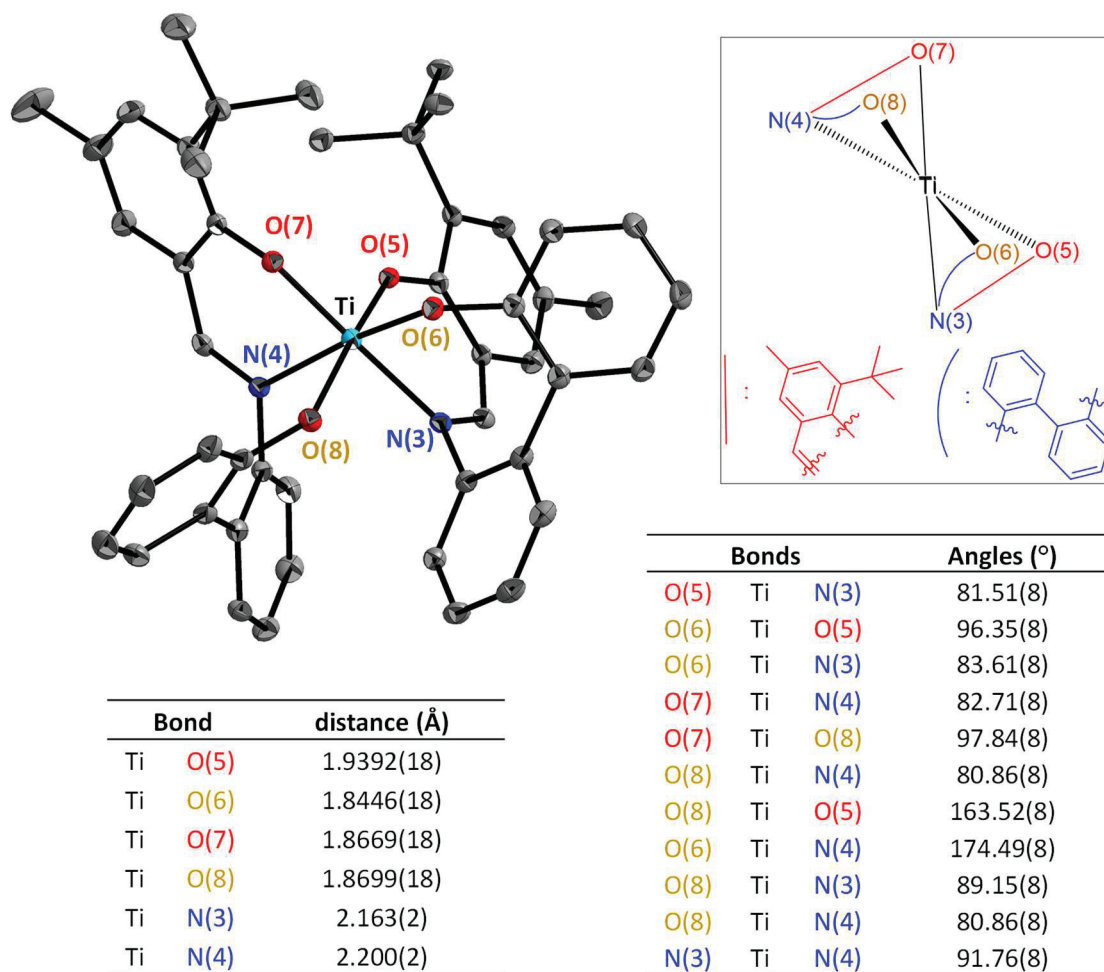


Figure 13. ORTEP diagram of the complex obtained after recrystallization of complex III (complex IV) Protons are omitted for clarity.

The thermal alteration of phenoxy-imine-ether [O⁻,N,O]-FI into diphenoxy-imine [O⁻,N,O⁻]-FI complex demonstrated in this work has also been highlighted in the literature for another system.¹⁶ In this case, the resulting active species was found to actually polymerize ethylene. By analogy, one can expect that the ([O⁻,N,O⁻]-FI)TiCl₂/MAO system also undergoes ethylene polymerization, which would constitute an additional argument as potential polymerization species.

Few bis(diphenoxy-imine) complex structures are reported in the literature.^{17–19} A similar compound displaying a phenyl group linked to the imine moiety was identified by Owiny *et al.* (Figure 14).¹⁷ Average bond lengths are very similar to the ones observed for complex IV (Figure 13, Ti-N = 2.17 Å, Ti-O = 1.87 Å and Ti-O = 1.92 Å).

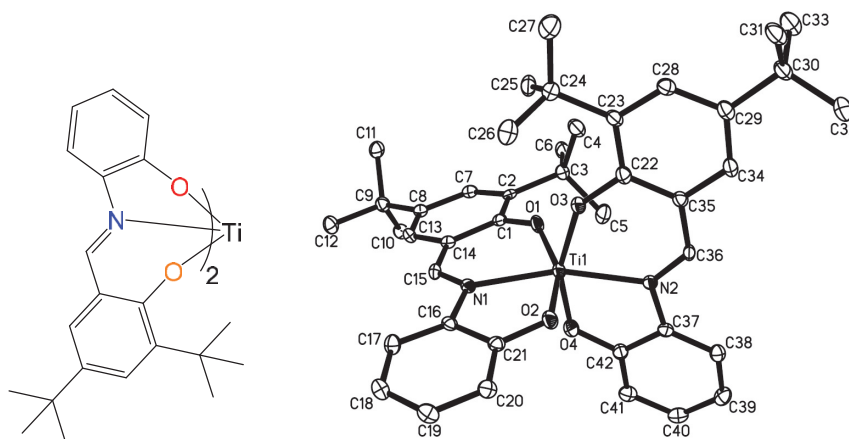
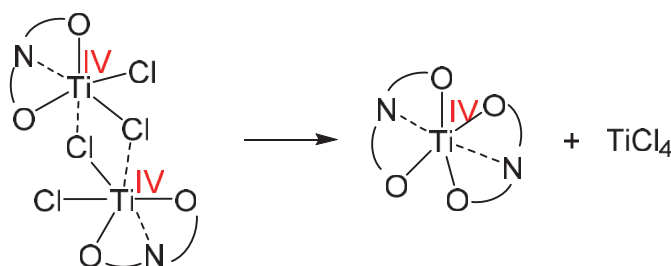


Figure 14. Bis($[\text{O}^-, \text{N}, \text{O}^-]\text{-Fi}$)Ti complex isolated by Owiny *et al.* and ORTEP diagram (50 % thermal ellipsoid probabilities)¹⁷ Reprinted with permission from [17] Copyright 2003 Elsevier

In our case, it is not possible to conclude whether one or two diphenoxy-imine ligands (ligand **1**) are coordinated to the titanium center from the NMR shown in Figure 12. However, one should stress that the formation of $([\text{O}^-, \text{N}, \text{O}^-]\text{-Fi})_2\text{Ti}$ species required two equivalents of ligands in the literature.^{17,19} Thus, one would expect that the synthesized complex displays the structure proposed in Figure 11.

The formation of a bis-phenoxy-imine complex $([\text{O}^-, \text{N}, \text{O}^-]\text{-Fi})_2\text{Ti}$ can arise from a ligand exchange during crystallization. This ligand transfer can involve a chloro-bridged dimer as proposed in Scheme 7. This ligand exchange implies the formation of titanium tetrachloride, which could induce polymerization if generated in presence of co-catalyst and ethylene. However, the resulting “ TiR_x^+ ” species would poorly copolymerize ethylene with 1-hexene as reported in the previous section (TiCl_4/MAO as molecular Ziegler-Natta catalyst).



Scheme 7. Proposed formation of $([\text{O}^-, \text{N}, \text{O}^-]\text{-Fi})_2\text{Ti}$ from $([\text{O}^-, \text{N}, \text{O}^-]\text{-Fi})\text{TiCl}_2$

Even though a doubt remains on the exact structure of the complex $([\text{O}^-, \text{N}, \text{O}^-]\text{-Fi})\text{TiCl}_2$ or $([\text{O}^-, \text{N}, \text{O}^-]\text{-Fi})_2\text{Ti}$, it has been proven that this species displays the same chemical shifts as the one formed by thermal degradation of complex **I** (Figure 12 versus Figure 10). Therefore, testing its reactivity in ethylene polymerization will enable to conclude whether the formation of such active species bearing $([\text{O}^-, \text{N}, \text{O}^-]\text{-Fi})$ ligand causes the polymerization in complex **I**/MAO system.

III.3. Catalytic test with a mixture of complex I and complex III

III.3.1. Activity and selectivity with the mixture complex I + complex III

It is essential to test the synthesized complex (complex III) in the presence of ethylene and MAO to determine its catalytic performances and the properties of the polymer induced. It will further enable to conclude whether complex III could be at the origin of polymer at higher reaction temperature or not. To verify whether the complex III/MAO is active in ethylene polymerization and to compare the polymer properties of both polymer, two strategies were followed. First, the mixture complex I/complex III (obtained by thermal modification of complex I) was tested to determine whether the polymer produced displays the properties of a single-site or multi-sites catalytic system. Then, the synthesized complex III is tested alone in ethylene polymerization and ethylene/1-hexene copolymerization.

First, the *in situ* formation of the LX₂ complex from complex I enabled to check the reactivity of this system toward ethylene. As complex III was obtained after a thermal treatment of complex I, its formation was forced by heating complex I in solid state at 100 °C. Given that only 13 % of complex III are formed after 15 minutes at this temperature in toluene (Table 4, entry 4), the powder was heated for 3 h, 24 h and 48 h to force this transformation. Eventually, heating complex I at 100°C for 24h afforded a mixture complex III/complex I with a rough molar ratio of 80/20.

This mixture was tested under mild conditions at 41 °C in the 1-L SFS reactor. At this temperature, trimerization is the major reaction in the case of the complex I/MAO. Activities and selectivities of complex I and the mixture complex I + III are compared in Table 5.

Table 5. Catalytic performance and selectivity of complex I and the mixture complex I/complex III

Entry	T (°C)	Complex	n _{Ti} (μmol)	Al/Ti	Activity (kg _{ethylene} g _{Ti} ⁻¹ h ⁻¹)	C ₆ H ₁₂ (g) (%)	C ₁₀ H ₂₀ (g) (%)	C ₁₄ H ₂₈ (g) (%)	PE (g) (%)
1	40	I	3.1	1 400	560	30.96 83.7	5.14 13.9	0.07 0.2	0.83 2.2
2	41	I	1.9	1 000	56	6.02	0.62	0	3.87
		III	7.6			57.3	5.9	0	36.8

Conditions: 30 min, 300 mL toluene, 10 bar of ethylene

Concerning the activity of the catalytic system, a ten-fold decrease was observed for the mixture of complexes compared to complex I alone. Subsequently, the mixture of complex I and III afforded a lower 1-hexene selectivity than complex I (Table 5). Such results were expected since 80 mol % of the (FI)TiCl₃ complex was converted into the LX₂-type complex.

Additionally, 1.9 μmol of complex **I** would have produced 19 g of 1-hexene by extrapolating results obtained in entry 1. However, only 6.02 g of this trimer were yielded. The trimerization catalyst seems to be impacted by the presence of another species in the reaction medium.

Concerning polymerization reaction, the mass of polymer produced compared to the amount of complex **I** is $0.27 \text{ g}_{\text{PE}} \mu\text{mol}_{\text{Ti}}^{-1}$ (entry 1). Therefore, the expected mass of polymer produced by 1.9 μmol of complex **I** should be 0.51 g. However, 3.87 g of polyethylene were obtained with the mixture of complexes **I+III** (entry 2). Thus, complex **III** is a polymerization species and is responsible for the production of 3.37 g of polymer. The corresponding activity of complex **III** would thus be $46 \text{ kg}_{\text{ethylene}} \text{ g}_{\text{Ti}}^{-1} \text{ h}^{-1}$, which is similar to the moderate activities reported for $([\text{O}^-, \text{N}, \text{O}^-]\text{-FI})\text{TiCl}_2/\text{MAO}$ systems.¹⁵

III.3.2. Comparison of polymer properties

In the case of a mixture of complex **I** and **III**, the chemical composition of the polymer gives a hint on the ability of the polymerization active species for 1-hexene copolymerization. Since there is substantially less 1-hexene produced in the case of the mixture of complex **I+III** than complex **I** alone (Table 5), the polymer displays a low 1-hexene content (0.12 mol %) revealed by a melting temperature of 132.5 °C. While engaging a mixture of polymerization catalysts, one would expect to obtain polymer with different properties compared to a single active species.

Comparing the amount of branching in the polymer in the case of complex **I/MAO** and complex **I+III/MAO** (Table 6), it is seen that the polymerization active species exhibit the same response to 1-hexene. Indeed, using the mixture complex **I+III**, the polymer obtained contains the same amount of 1-hexene as the one expected in the case of complex **I** only. This observation encourages further exploration of complex **III/MAO** as polymerization system in the SFI system.

Table 6. Comparison of 1-hexene content in polymer and reaction medium in the case of complex **I** and complex **I+III**

Complex	Tm (°C)	1-hexene content (mol %)	
		Reaction medium	Polymer
I	130	22.3	0.2
I	133	31.1	0.08
I +III	132.5	18.7	0.08 ^a

^adetermined from Equation 2, Chapter 2

It is then worth analyzing the broadness and modality of molar mass distribution of the polymer produced in the case of the mixture complex I+III/MAO. In the case where several polymerization active species would be present in the system complex I+III/MAO, one would expect a multimodal distribution or at least its broadening. In fact, the opposite is observed for the MMD of the polymer produced by complex I+III/MAO. Figure 15 shows narrower MMDs for this system than in the case of complex I/MAO. Yet, the resulting polyethylene displays lower molar masses ($6.3 \times 10^5 \text{ g mol}^{-1}$) than PE-SFS-42 ($1.2 \times 10^6 \text{ g mol}^{-1}$). Nonetheless, these similarities in MMD implies that complex III/MAO could be a polymerization species in the SFI system.

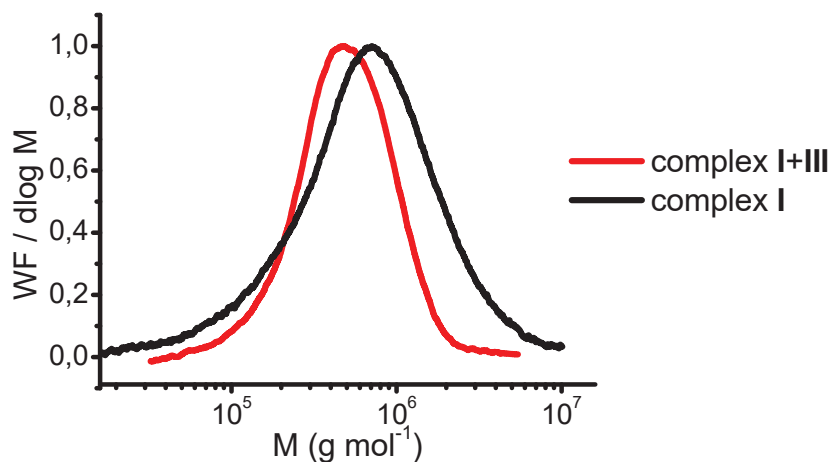


Figure 15. MMD for the polymers obtained by complex I+III/MAO (red) and complex I/MAO at 42 °C (PE-SFS-42, black)

Now that the analysis of reactivity in ethylene polymerization and polymer properties proved that complex III/MAO is a polymerization species, it is important to study the behavior of the isolated complex III in ethylene polymerization and copolymerization with 1-hexene.

III.4. Test of complex III/MAO toward ethylene polymerization and copolymerization with 1-hexene

III.4.1. Influence of temperature on activity of complex III/MAO

As highlighted previously, there are evidences that complex III/MAO is a polymerization system displaying a moderate activity. Therefore, it is important to quantify the reactivity of this system for ethylene polymerization and copolymerization with 1-hexene to be able to make a comparison with the performances of the polymerization active species in complex I/MAO system. Moreover, combining this study with the effect of temperature is indispensable to further conclude whether this LX_2 species could be at the origin of polymer production or not.

In the literature, Chen *et al.* reported a similar modification of ligand in the case of a zirconium complex bearing both cyclopentadienyl and phenoxy-imine ligands when refluxed for 4 hours in THF.¹⁶ The synthesized $[(O^-,N,O^-)FI]CpTiCl$ species activated with MAO (Al/Ti = 2 000) was found to be active towards ethylene polymerization but with a moderate activity of $10 \text{ kg}_{PE} \text{ mol}_{Zr}^{-1} \text{ h}^{-1}$ (30 °C) and $272 \text{ kg}_{PE} \text{ mol}_{Zr}^{-1} \text{ h}^{-1}$ (80 °C). These values are lower than the ones reported with $[(O^-,N,O^-)FI]CpTiCl_2$ in the same conditions ($59 \text{ kg}_{PE} \text{ mol}_{Zr}^{-1} \text{ h}^{-1}$ at 30 °C and $769 \text{ kg}_{PE} \text{ mol}_{Zr}^{-1} \text{ h}^{-1}$ at 80 °C).

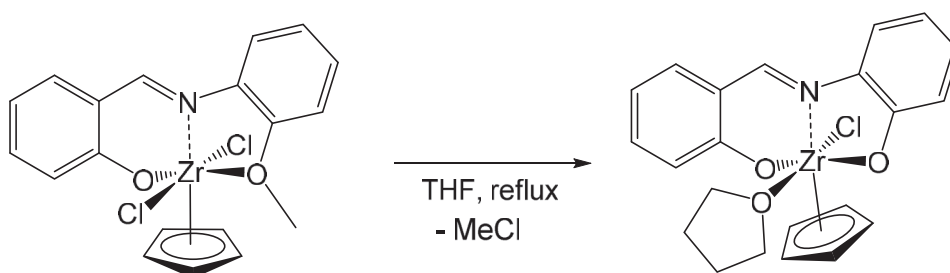


Figure 16. Thermal modification of a $[(O^-,N,O^-)FI]CpTiCl_2$ into $[(O^-,N,O^-)FI]CpTiCl(THF)$ observed by Chen *et al.*¹⁶

Complex III/MAO was tested at 40, 60 and 80 °C in ethylene polymerization and copolymerization with 1-hexene using the three autoclaves of the Chemspeed platform. Catalytic tests were performed under the same conditions as for complex I/MAO. For this study, 1-hexene was introduced once the system is activated, meaning that complex III was already contacted with MAO and ethylene beforehand. The amount of 1-hexene injected was adapted from the 1-hexene concentration after 5 minutes of reaction with the trimerization system (Chapter 3, Table 4, 4 g at 40 °C, 3 g at 60 °C and 0.4 g at 80 °C).

Table 7. Catalytic performances of complex III/ MAO with ethylene and ethylene/1-hexene

Entry	T (°C)	n _{Ti} (μmol)	Al/Ti	1-hexene introduced (g)	Activity (kg _{ethylene} g _{Ti} ⁻¹ h ⁻¹)	PE yield (g)
1	40	1.62	1 520	0	2.9	0.11
2	60	1.62	1 520	0	5.4	0.21
3	80	1.62	1 520	0	9.8	0.38
4	40	1.26	1 000	3.6	0.3	0.01
5	60	1.35	1 500	1.8	3	0.10
6	80	1.35	1 500	0.6	6.7	0.22

Conditions: complex III, MAO 30 wt % in toluene, 120 mL toluene, 30 minutes, 10 bar of ethylene

First of all, no oligomer were identified by GC analysis, which showcases the absence of trimerization active species with this system. In agreement with previous observations, complex III/MAO exhibits a limited activity in ethylene polymerization even at 80 °C (Table 7, entries 1-3). A similar LX₂-complex (Figure 17) also produces a low amount of polymer (0.3 g) in presence of 250 equivalents of MAO, at 25 °C, under 1 bar of ethylene and after 5 minutes of reaction.²⁰

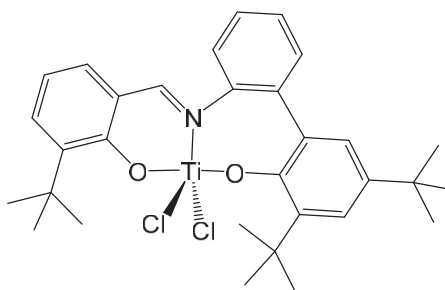


Figure 17. Diphenoxo-imine [O,N,O] complex with a similar structure as complex III²⁰

The moderate activity of complex III/MAO in ethylene polymerization was also observed in the case of copolymerization with 1-hexene. In fact, the system is inactive at 40 °C (Table 7, entry 4) and twice less active than in homopolymerization conditions at 60 and 80 °C (entries 5 versus 2 and 6 versus 3). For these two catalytic tests, the same titanium loading of complex III and complex I affords a similar polymer yield. Therefore, complex III/MAO cannot account for the total amount of polymer produced by the SFI system, especially at high temperature. Still, the generation of this active species cannot be completely excluded. The comparison of 1-hexene content in the polymer provides further information on the behavior of this LX₂-type species.

III.4.2. Polymers properties obtained with complex III/MAO in presence of 1-hexene

Once again, polymer properties were investigated to determine common or divergent points between polymerization species in complex III/MAO and complex I/MAO systems. Analyses of MMD and chemical composition were performed on the polymers produced in presence of 1-hexene (Table 7, entries 4-6). Unsuccessful attempts for polymer dissolution in the view of SEC analyses are a proof of the high molar masses ($> 10^6 \text{ g mol}^{-1}$) of the polyethylenes produced.

On the basis of the 1-hexene available in the reaction medium, differences in terms of 1-hexene incorporation ability are observed between polymerization species derived from complex I and complex III. The catalytic system being poorly active at 40 °C, the 1-hexene content in the polymer is highly impacted by its fast deactivation. Interestingly, both polymerization species afford polymer with a close 1-hexene content of 0.3 mol % even though the amount of 1-hexene in the liquid phase is different (Figure 18). Surprisingly, the polymerization active species was found to incorporate more 1-hexene at higher temperature, even for lower 1-hexene content in the liquid phase (15 mol %). This trend can be explained by a limitation of the polymerization activity due a higher 1-hexene concentration at 40 °C than at 80 °C.

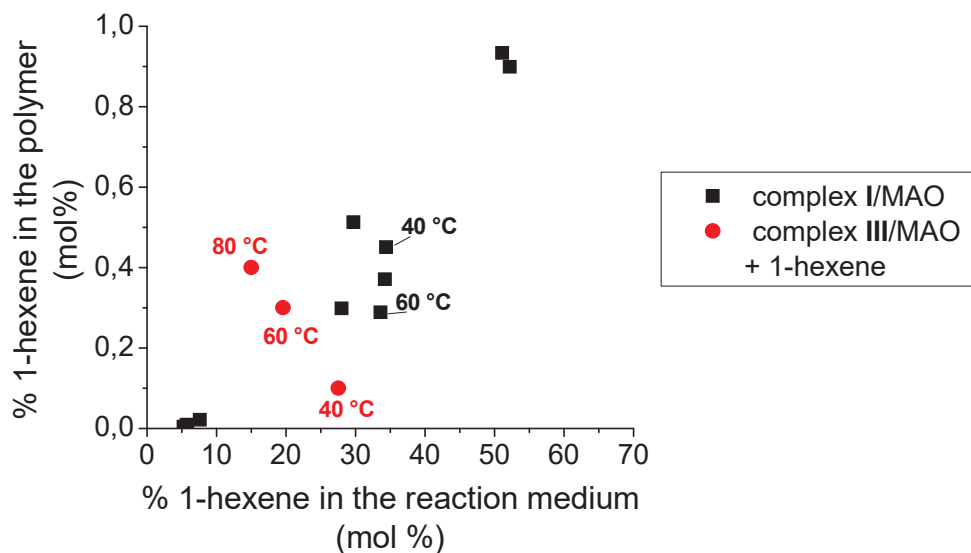


Figure 18. 1-hexene incorporation ability of complex III/MAO depending on the amount of 1-hexene available in the liquid phase (red) and comparison with the SFI system (black)

To sum up, complex III/MAO most probably produces high molar-mass polyethylenes, which is a common feature with the polymers obtained in the case of the SFI system. Besides, this species would be more prone to insert 1-hexene than the unknown polymerization species.

Eventually, polymerization active species $([O^-,N,O^-]-FI)TiMe^+$ can be one of the active species in the case of complex I/MAO. Indeed, it displays a similar reactivity, although more limited, as the polymerization active species in the SFI system. The same observation can be made regarding the higher but still moderate copolymerization of 1-hexene at 80 °C. At this stage, it is important to combine all conclusion drawn in this study to rationalize the hypothesis of thermal alteration of complex I affording a $[O^-,N,O^-]$ -type polymerization species.

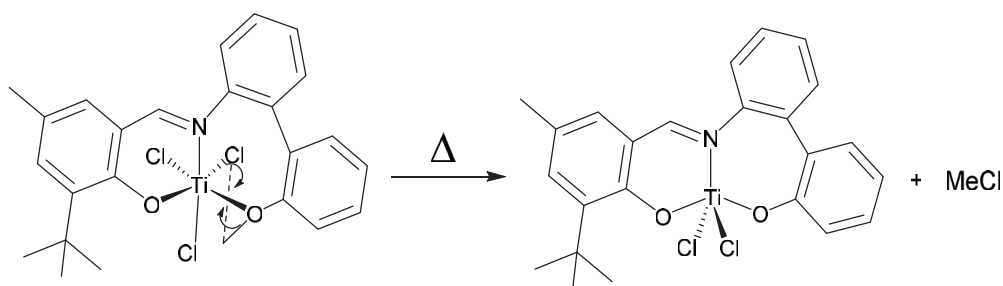
III.5. Rationalization of complex III formation

The formation of a polymerization active species complex III/MAO induced by temperature-alteration of complex I was demonstrated but not yet proven to occur during catalytic tests with complex I/MAO. Several questions arose from this consideration:

- (i) What mechanism is involved in the thermally favored formation of complex III?
- (ii) Could such species be formed during catalytic tests, especially in presence of MAO?
- (iii) Is the amount of polymer produced by such species relevant with respect to the polymer yielded with the SFI system?

III.5.1. Proposed mechanism

To answer (i), one should take into consideration the procedure leading to the formation of the LX_2 species. Indeed, the thermal degradation of complex I sets aside any reaction involving compounds other than the complex. Actually, the simplest explanation for rationalizing the concomitant formation of a second covalent Ti-O bond and release of chloromethane is an intramolecular substitution involving the Ti-Cl and O-Me bonds (Scheme 8). The ability of titanium for such ether cleavage was reported in the case of $TiCl_4$ and diethyl ether or THF.²¹ Therefore, one could consider that such oxophilic species can undergo bond cleavage to covalently coordinate with oxygen atoms. In fact, Chen *et al.* reported the same modification of ligand in the case of a zirconium complex bearing both cyclopentadienyl and phenoxy-imine ligands when refluxed for 4 hours in THF.¹⁶ Authors proposed a thermocyclization between Zr-Cl and O-Me bonds to explain the formation of the diphenolate ligand. It is noteworthy that no XRD structure is provided, their conclusion relies on ¹H NMR spectra comparison between the thermally induced and synthesized $([O^-,N,O^-]-FI)ZrCl_2(THF)$ complexes.



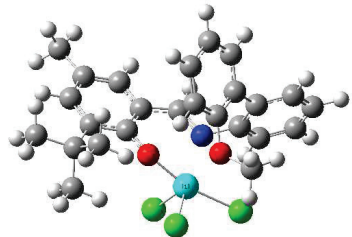
Scheme 8. Proposed intramolecular substitution reaction leading to a diphenoxy-imine LX_2 complex

Taking into account the structure of the complex, it is entirely possible that the longest Ti-Cl bond reacts with the methoxy group. In fact, the oxygen of the phenoxy group destabilizes a Ti-Cl bond by *trans* effect. Heating the complex probably promotes the torsion and rotation of the biphenyl group, and eventually lead to a conformation favoring the reaction between this Ti-Cl bond and the methoxy group. To verify the plausibility of this assumption based on entropic and enthalpic consideration, DFT calculations were performed at IFPEN using the structure of complex I as determined by XRD.

III.5.2. DFT calculations

DFT calculations were conducted at IFP Energies nouvelles. Calculation method is detailed in the experimental section. By means of first principles *ab initio* calculations, energies determined are the ones associated to the possibility of decomposition of phenoxy-imine titanium chloride complex I, which crystalizes as the *fac* isomer. DFT calculations performed on both isomers (*fac* and *mer*), confirmed that the *fac* isomer is more stable, in agreement with the experimental observations. It must be noted that the energy difference between the two isomers is not large, although it remains significant regarding the accuracy expected from DFT calculations (Table 8).

Table 8. Phenoxy-imine complex I conformation

Complex	I
Most stable optimized structure	
$G_{mer}^0 - G_{fac}^0$ (kJ.mol ⁻¹)	+11

From the most stable optimized structure, calculations were performed to locate possible transition states for the formation of chloromethane as proposed in Scheme 8. Figure 19 shows the corresponding energy diagram for complex I, while Table 9 summarizes the energetics of the reaction. Reaction rate constants k have been calculated according to the Eyring equation (Equation 1).

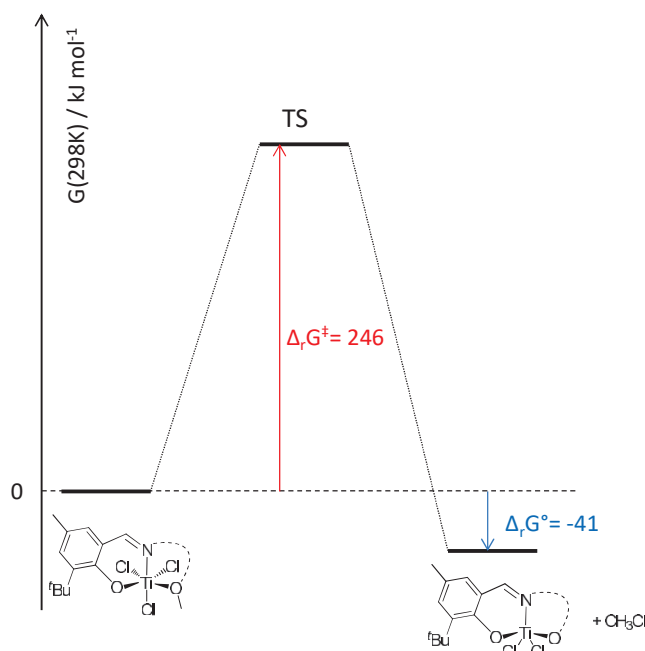


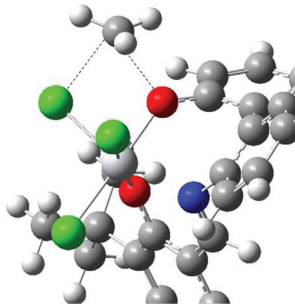
Figure 19. Energy diagram for the transformation of complex I to III (Energy are calculated in kJ mol^{-1})

$$k = \frac{k_B T}{h} \exp\left(\frac{-\Delta_r G^\ddagger(T)}{RT}\right)$$

Equation 1. Eyring equation

The reaction Gibbs free energy profile is negative (about -40 kJ mol^{-1}) essentially due to the gain in entropy related to the formation of an additional molecule of chloromethane. The activation Gibbs free energy at $25 \text{ }^\circ\text{C}$ is in the range $240\text{-}250 \text{ kJ mol}^{-1}$ (essentially enthalpic contribution), which is a significant energy barrier that can hardly be reached. Consequently, the reaction rate constants calculated on that basis are in the order of magnitude of 10^{-31} s^{-1} at $25 \text{ }^\circ\text{C}$, and increase to about 10^{-22} s^{-1} at $100 \text{ }^\circ\text{C}$. In either case, low reaction rates constants reveal that the reaction is extremely limited, kinetically speaking. Thus, according to these calculations, the formation of chloromethane observed seems very unlikely to occur *via* the reaction mechanism proposed in Scheme 8.

Table 9. Gibbs free energy and rate constant at 25 °C and 100 °C

Complex	I
TS Structure	
$\Delta_r G^\circ$ (298 K)	-24
$\Delta_r H^\circ$	+11
$\Delta_r S^\circ$	+177
$\Delta_r G^\ddagger$ (298 K)	246
$\Delta_r H^\ddagger$	248
$\Delta_r S^\ddagger$	+7
k (298 K)	$4.0 \cdot 10^{-31}$
k (373 K)	$2.8 \cdot 10^{-22}$

One has to bear in mind that these calculations were conducted on the isolated (FI)TiCl₃ complex. Even though it gives an idea of the energy demand of such reaction, it does not take into account external factors that can influence this transformation (solvent, cocatalyst).

III.5.3. Thermal alteration during catalytic tests

There are common point between the polymerization active species complex I/MAO and complex III/MAO. First, ([O⁻,N,O⁻]-FI)TiCl₂/MAO is described in the literature as a polymerization species and it was confirmed in our experiments. It was shown that the polymerization activity increases with temperature for both systems. Moreover, this diphenoxy-imine species is poorly active and its ability for 1-hexene incorporation is limited.

In contrast, it is important to stress several differences and issues related to the actual transformation of the complex in the conditions of catalytic tests. First, the transformation involves the presence of a Ti-Cl bond, which should not remain after activation with MAO. Indeed, contacting complex I with MAO leads to the instantaneous methylation as revealed by ¹H NMR characterization of this mixture.²² It is however still possible that such ([O⁻,N,O⁻]-FI) complex is formed *via* another path in presence of activator. In this case, one should discuss the relevance of this hypothesis with respect to the amount of polymer yielded.

By applying the same strategy as for TiCl_4/MAO system, it is possible to deduce the theoretical amount of polymer produced by an estimated fraction of complex **III** in complex **I**. It was shown by ^1H NMR that up to 13 mol % of complex **III** is formed upon heating to $100\text{ }^\circ\text{C}$ in toluene (Table 6). Assuming now that the increase of temperature observed during the first minutes of reactions can promote this side reaction, 75 % polymerization active species would only cover 7 wt % of polymer produced by the SFI system at $80\text{ }^\circ\text{C}$ (Table 10).

Table 10. Proportion of PE theoretically afforded by complex **III**/MAO in complex **I**/MAO system

	40 °C	60 °C	80 °C
% $\text{Ti}_{\text{complex III}}$ (mol %)	5%	50%	75%
% PE (wt %)	0.3%	4.3%	7%

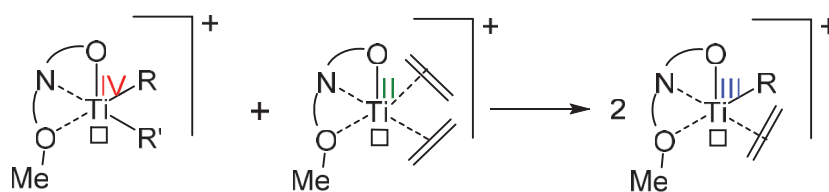
To sum up, the formation of an active species based on $([\text{O}^-, \text{N}, \text{O}^-]\text{-FI})\text{TiCl}_2$ complex is possible but in very limited proportions. Therefore, investigations on the identification of active species should be pursued towards other ligand alterations occurring in presence of cocatalyst and ethylene. In this purpose, the hypothesis of Ti^{III} species emerging from side reactions during the catalytic tests is investigated hereafter. So far, the hypothesis of complex modification was based on the transformation of complex **I** into complex **III**, which is promoted by temperature. However, other complex alterations can involve the variation of titanium oxidation state and the modifications of the complex structure.

IV. HYPOTHESIS OF Ti^{III} FORMATION

IV.1. Hypothesis of (FI)Ti^{III}Cl₂ complex

IV.1.1. Synthesis of (FI)Ti^{III}Cl₂(THF)

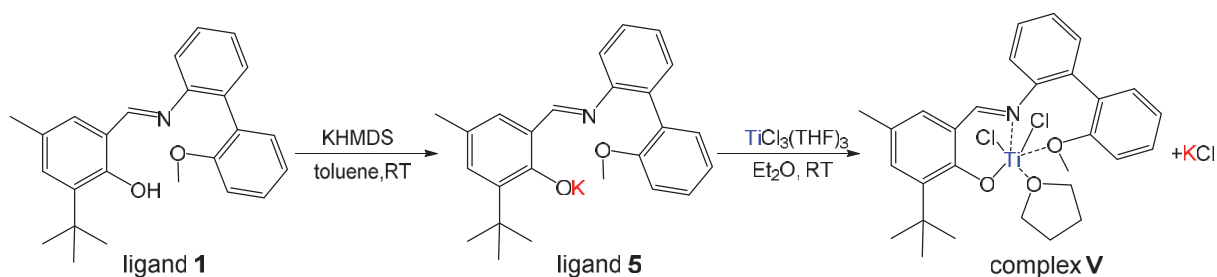
The hypothesis of formation of a Ti^{III} species was highlighted in the literature in the case of the SFI system. In fact, the presence of a Ti^{III} species in the complex I/MAO and (FI)TiMe₃/B(C₆F₅)₃ system has been reported but no Ti^{III} species were identified.^{8,23} One can assume that a phenoxy-imine Ti^{III} derivative could be induced by a one-electron reduction of Ti^{IV} complex during the activation process or by comproportionation of Ti^{II} and Ti^{IV} complexes involved in the metallacycle mechanism. According to Scheme 9, the [(FI)Ti^{III}R]⁺ complex is the most probable species formed during catalytic tests. From this scheme, the reversible mechanism is also possible.



Scheme 9. Comproportionation reaction leading to Ti^{III} species

One can question the ability of such trivalent titanium for polymerization reactions. Even though, Bercaw *et al.* demonstrated that the Ti^{III} formation is correlated to the deactivation of the system, it is possible that such species could polymerize ethylene. The hypothesis of Ti^{III} as polymerization active species is supported by scarce examples reported for polyethylene production.^{24–28} In the case of the SFI system, (FI)Ti^{III}Cl₂ complex was considered as a potential polymerization active species when combined with MAO. The goal of studying this trivalent species was to identify whether this Ti^{III} complex is directly involved in ethylene polymerization or in side reactions leading to secondary polymerization catalysts. The model to study this system was based on ([O⁻,N,O])Ti^{III}Cl₂(THF) (complex **V**) activated by MAO.

This procedure was adapted from the synthesis of a bis(aryloxy) Ti^{III} complexes reported by Allouche *et al.*²⁸ The synthesis of the air- and moisture-sensitive Ti^{III} complex was conducted in a glovebox to avoid any degradation of the trivalent species. Complex **V** was prepared by reacting 1 equivalent of the aryloxy potassium salt (ligand **5**) with TiCl₃(THF)₃ in diethyl ether at room temperature (Scheme 10). The solution turned into a deep green slurry after 10 minutes of reaction. The formation of KCl as a greyish solid showcases the complexation of the ligand leading to (FI)TiCl₂(THF) species. After 12h at room temperature, part of the filtered reaction medium was condensed to perform crystallization. A green solid was afforded after drying the rest of the solution.

Scheme 10. Synthesis of (FI)Ti^{III}Cl₂ (complex **V**)

Given that Ti^{III} complexes are paramagnetic species, the green product was first analyzed by elemental analysis to determine the number of ligand and THF molecules coordinated to the titanium center. It was found that an equivalent amount of THF *versus* phenoxy-imine ligand is present in the product (see the experimental section). Noteworthy, ether coordination in lieu of THF could also occur but would be limited by the steric hindrance provided by the phenoxy-imine ligand.

One should bear in mind that such complexes are prone to disproportionation and potential ligand transfer, as revealed previously in the case of the ([O⁻,N,O⁻]-FI)TiCl₂ complex (Figure 13). To verify this assumption, ¹H NMR analysis in toluene-*d*₈ of a concentrated solution of complex **V** in diethylether was attempted. In agreement with the presence of a paramagnetic species, it was not possible to record the spectrum. Another attempt enabled to record ¹H NMR spectrum of a concentrated solution of complex **V** in diethylether (Figure 20, bottom). Broad signals are observed while a'', b'', Ar'' and d'' can be attributed to diamagnetic species. This compound does not correspond to complex **I**, which imine group is identified at 7.46 ppm (Figure 20, top). In addition, the absence of signals of complex **I** emphasizes that this precursor is generated upon reaction of TiCl₃(THF)₃ and ligand **5** (Scheme 10). As a result, a mixture of diamagnetic and paramagnetic species is probably afforded either during the synthesis of (FI)Ti^{III}Cl₂(THF) or once in solution in C₆D₆. Note that the intensity of the diamagnetic signal is low, which informs on its limited concentration. Noteworthy, similar issues were encountered at IFPEN for characterizing NMR spectra of the reaction medium.

Given the paramagnetism highlighted by ¹H NMR and the result of elemental analysis, it is possible to hypothesize the formation of the (FI)TiCl₂(THF) complex. Crystallization of a solution of complex **V** afforded a disubstituted complex, which will be presented later on. Despite the identification of secondary complexes, it was still worth testing the behavior of the presumed (FI)TiCl₂(THF) complex in ethylene polymerization.

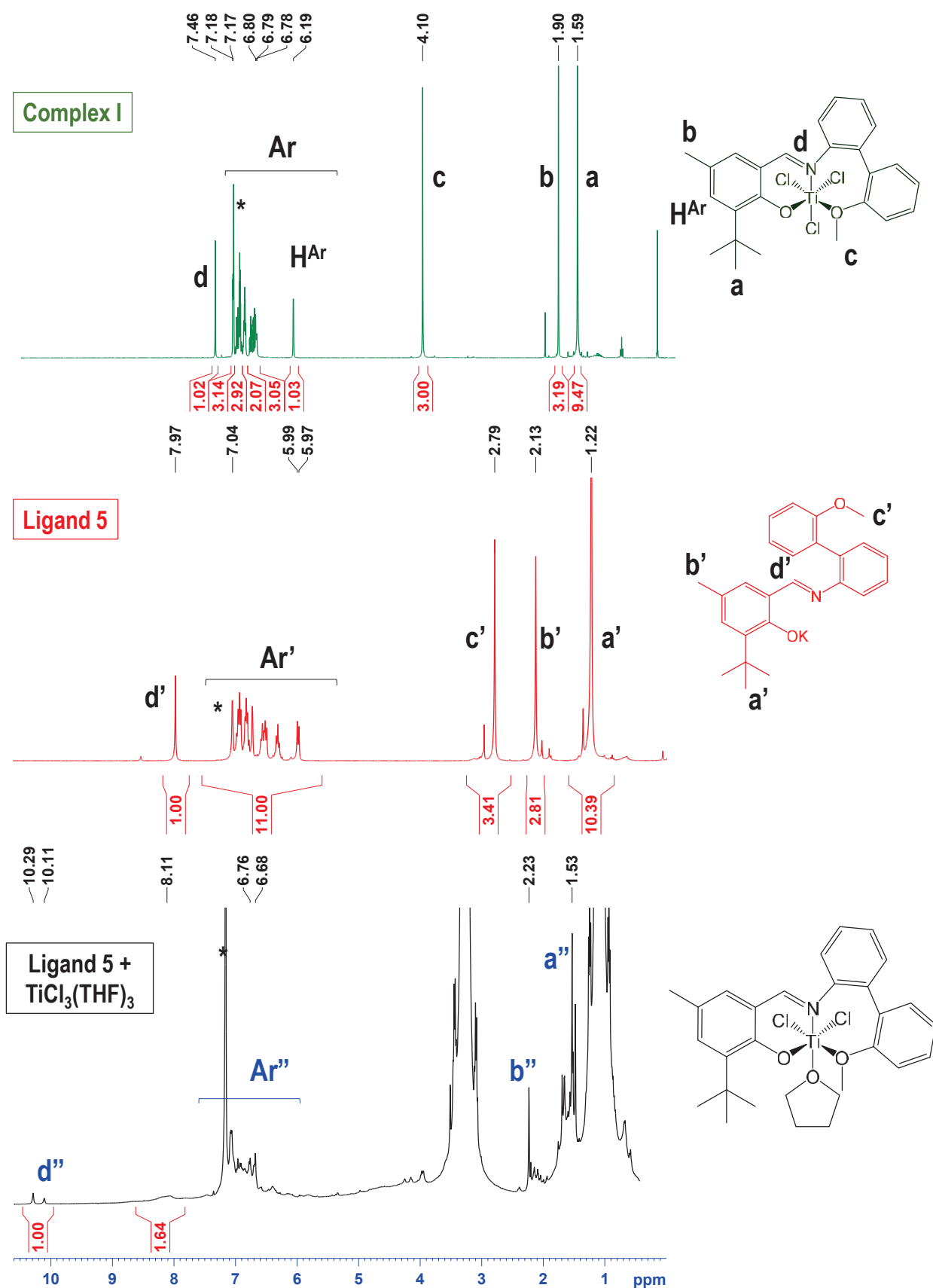


Figure 20. ¹H NMR in C₆D₆ of complex I (green), ligand 5 (red) and ligand 5+TiCl₃(THF)₃ in diethylether (filtrated and concentrated solution) (black)

IV.1.2. Activity, selectivity and polymer properties

After the synthesis of complex **V**, the reactivity of the system (FI)Ti^{III}Cl₂(THF)/MAO was tested towards ethylene in the same conditions as complex **I**/MAO. The analysis of the activity and selectivity has a double stake:

- (i) Verify the production of polymer and conclude on a possible (FI)Ti^{III}Cl₂ complex as a polymerization precursor;
- (ii) Identify a potential formation of 1-hexene resulting from the presence of Ti^{II} species, which implies a disproportionation of Ti^{III} complexes.

The catalytic tests were performed in the 1 liter SFS reactor at 60 °C, under 10 bar of ethylene and for 30 minutes. Catalytic performances and selectivities were also compared with TiCl₃(THF)₃/MAO to check any common features with this FI-ligand-free species (Table 11). Both complex **V** and TiCl₃(THF)₃ were solubilized in 2 mL of THF before introduction in the reactor containing the solution of MAO in toluene.

Table 11. Comparison of catalytic performances between complex **I**/MAO and complex **V**/MAO

Entry	Complex	n _{Ti} (μmol)	Al/Ti	Activity (kg _{ethylene} g _{Ti} ⁻¹ h ⁻¹)	C ₆ H ₁₂ (g) (wt %)	C ₁₀ H ₂₀ (g) (wt %)	PE (g) (wt %)
1	I	4.6	1 000	170	9.62 49.2%	2 0.38%	9.55 48.9%
2	V	3.9	1 150	17	0.34 20.7%	0 0%	1.25 76.5%
3	TiCl ₃ (THF) ₃	8.1	1 200	5 ^a	0.03 15%	0 0%	0.17 85%

Conditions: 60 °C, 30 min, 300 mL toluene, 10 bar of ethylene

^a calculated for 2 minutes reaction

It was found that (FI)Ti^{III}Cl₂/MAO mainly produces polyethylene with a moderate activity of 17 kg_{ethylene} g_{Ti}⁻¹ h⁻¹ (Table 11, entry 2). In comparison, complex **I**/MAO is ten times more active and produces 6.5 times the amount of polyethylene yielded by complex **IV**/MAO (Table 11, entry 1). In contrast, TiCl₃(THF)₃/MAO exhibits the lowest activity in ethylene polymerization since it deactivates within the first minutes of reaction (Table 11, entry 3). It is important to note that for solubility issues, a small amount of THF was introduced in the reaction medium. This compound is known for decreasing the activity of titanium catalysts, which could explain the low activities observed for complex **V** and TiCl₃(THF)₃.

From these results, it is first interesting to note that both Ti^{III} species yields trimerization as a side reaction with a 15-22 wt % of 1-hexene produced (Table 11, entries 2,3). This observation is a hint of the presence of the reduced Ti^{II} species in the reaction medium. Reactions of disproportionation of Ti^{III} species into Ti^{II} and Ti^{IV} complexes has been mentioned in the literature and can be applied in this case.⁷ As a result, it seems that reaction between titanium complexes are hardly avoidable and independent from the structure of the trivalent complex.

Few information can be extracted from the analysis of polymer properties. Indeed, polymer obtained by complex **V**/MAO (Table 11, entry 2) contains an insignificant amount of 1-hexene as revealed by a high melting temperature of 135.9 °C. The reason for this low incorporation of 1-hexene lies in the limited 1-hexene content in the liquid phase (1.6 mol %).

Eventually, complex **V**/MAO cannot be considered as main polymerization active species given its lower productivity compared to complex **I**/MAO. Moreover, the lack of characterization of complex **V** and the potential side reactions leading to several active species are a hurdle for the identification of polymerization active species. As a result, further characterizations are necessary to determine possible complex transformations that could spontaneously occur or be promoted in the presence MAO and ethylene. In this purpose, efforts were focused on the determination of complex **V** structure since no Ti^{III} -based phenoxy-imine complexes are reported in the literature so far. During the attempts of $(FI)TiCl_2(THF)$ recrystallization, an unexpected complex was identified, as presented hereafter.

IV.2. Hypothesis of a Bis(FI)TiCl₂ species as polymerization active species

IV.2.1. Evidences of the formation of (FI)₂TiCl₂

Recrystallization of complex **V** was performed from a concentrated solution of the complex in diethylether (obtained after filtration of the reaction medium and concentration of the filtrate). After a slow diffusion of a layer of pentane in the liquid at -35 °C under inert atmosphere, small black needle-shaped crystals were obtained. X-ray diffraction enabled to identify once again an unexpected complex (Figure 21).

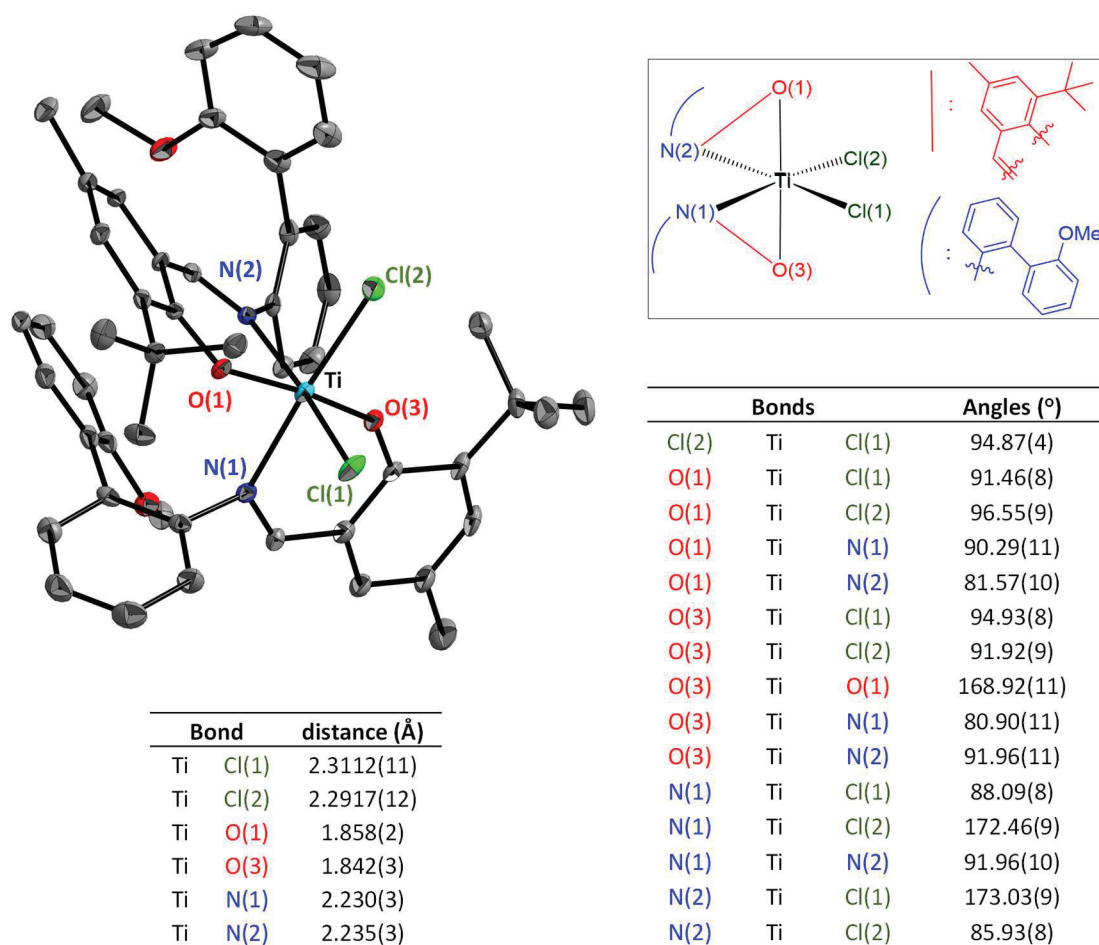


Figure 21. ORTEP plot of the complex obtained after recrystallization of complex **V** (complex **VI**) Protons are omitted for clarity.

Thermal ellipsoids are drawn at the 30 % probability level

A bis(phenoxy-imine) Ti^{IV} complex (complex **VI**) was obtained from crystallization of a solution of complex **V**. It is actually the second example of an unintended disubstituted phenoxy-imine complex isolated from a mono(phenoxy-imine) complex (Figure 13). The crystallized compound displays an octahedral geometry around the titanium center comprising two phenoxy-imine ligands coordinated in a *O-trans*, *N-cis* and *Cl-cis* fashion (Figure 21). As a result, a Ti^{IV} species was formed and can be compared to the extensive library of bis(phenoxy-imine) complexes reported in the literature.⁶

To further analyze this new complex, a comparison with a similar species reported by Ivanchev *et al.* (Figure 22, complex **VII**) is made.²⁹ The only difference between these two phenoxy-imine complexes is the nature and size of the group connected to the nitrogen atom (referred to as R^1 substituent). Average lengths of Ti-heteroatom bonds are in the same range as for a similar bis(phenoxy-imine) complex shown in Figure 22 (Ti-Cl = 2.306 Å; Ti-O = 1.344 Å and Ti-N = 2.212 Å).²⁹ However, several differences compared to other $(\text{FI})_2\text{TiCl}_2$ should be highlighted. Complex **VI** exhibits wider bond angles for N-Ti-N than Cl-Ti-Cl whereas the opposite is usually observed for other complexes bearing less bulky R^1 substituents.²⁹⁻³¹ In fact, for the complex presented in Figure 22, bond angles for N-Ti-N and Cl-Ti-Cl are 86° and 94° , respectively. Moreover, a diastereoisomer is observed in this case of complex **VI** (Figure 21) as for most of the $(\text{FI})_2\text{TiCl}_2$ species reported. One exception among others is the Δ configuration adopted by the complex presented in Figure 22. However, it is noteworthy that a mixture of diastereoisomers are often observed, caused by their inherent ability for functional isomerization.⁶

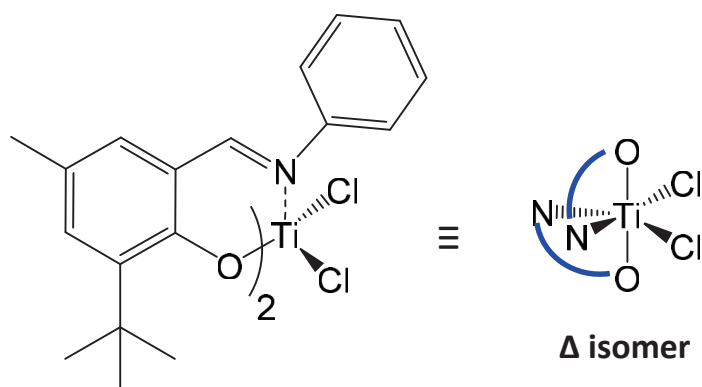
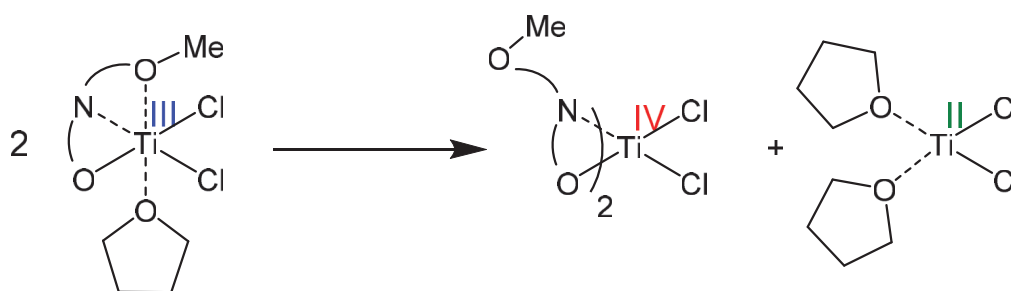


Figure 22. Bis(phenoxy-imine) titanium complex (complex **VII**) used as comparison with complex **VI**

This bis(phenoxy-imine) complex belongs to the family of precursors for olefin polymerization.⁶ It was very surprising to observe a disubstituted species with such hindered R^1 substituents. Indeed, to quote Fujita *et al.*:⁶ “Bulky R^1 (for example, 2,6-disubstituted phenyl) and/or an extra donor (L) are usually required to avoid the formation of bis-ligated $(\text{LFI})_2\text{MCl}_2$ complexes.” This excerpt is reprinted from [6] with permission (Copyright 2011 American Chemical Society).

As a consequence, the possibility of a double coordination of sterically demanding phenoxy-imine ligands has been discarded so far. To the best of our knowledge, complex **VI** is the first example of titanium-based bis(phenoxy-imine) complex bearing a 2-substituted phenyl R^1 group reported in the literature.

The formation of such $\text{Bis}(\text{FI})\text{Ti}^{\text{IV}}$ species from a $\text{mono}(\text{FI})\text{Ti}^{\text{III}}$ complex involves both a ligand transfer and a disproportionation reactions (Scheme 11). From this scheme, it is also important to note the formation of a reduced Ti^{II} species which would be coordinated to two THF molecules. Such $\text{TiCl}_2(\text{THF})_2$ species have been reported in the literature as black aggregates, which is in line with the deep dark colors of the reaction medium.³²



Scheme 11. Proposed mechanism for complex **VI** formation

To rebound on the catalytic tests performed with complex **VI** (Table 11), the mixture of Ti^{IV} and Ti^{III} complexes could probably afford polyethylene and possibly 1-hexene after activation with MAO, excluding complex alterations. Therefore, one can hypothesize that $(\text{FI})_2\text{TiCl}_2(\text{THF})/\text{MAO}$ would polymerize ethylene if it is generated by the SFI system during the activation step and/or throughout the catalytic test.

The bis(phenoxy-imine) complex was synthesized at IFPEN by reacting two equivalents of ligand with TiCl_4 at room temperature. The resulting deep red powder was analyzed by ^1H NMR in toluene- d_8 (Figure 23, black) and shows a mixture of several species. The ^1H NMR spectrum of complex **VI** revealed the presence of several signals, implying a mixture of complexes. Indeed, characteristic signals of complex **I** (a' , b' , c' and d') can be found among numerous signals. Several signals are identified for the imine (7.63 ppm), methoxy (3.5, 3.3 and 3.05 ppm), methyl (1.62-1.72 ppm) and *tert*-butyl (1.25-1.09 ppm) groups.

By comparing ^1H NMR spectra of complex **I** and the corresponding ligand, one can note that the signal for the methoxy group (c , 3.36 ppm) is deshielded once coordinated to the metal center (c' , 4.08 ppm). Regarding the $(\text{FI})_2\text{TiCl}_2$ complex, one would expect that the signal of the methoxy group is present in between c and c' , which is indeed the case (Figure 23, black, c'' area). Moreover, 65 mol % of complex **I** are identified based on the integrations of the methoxy region (c''). Therefore, several bis(phenoxy-imine) complexes should be formed in toluene and the generation of complex **I** seems unavoidable.

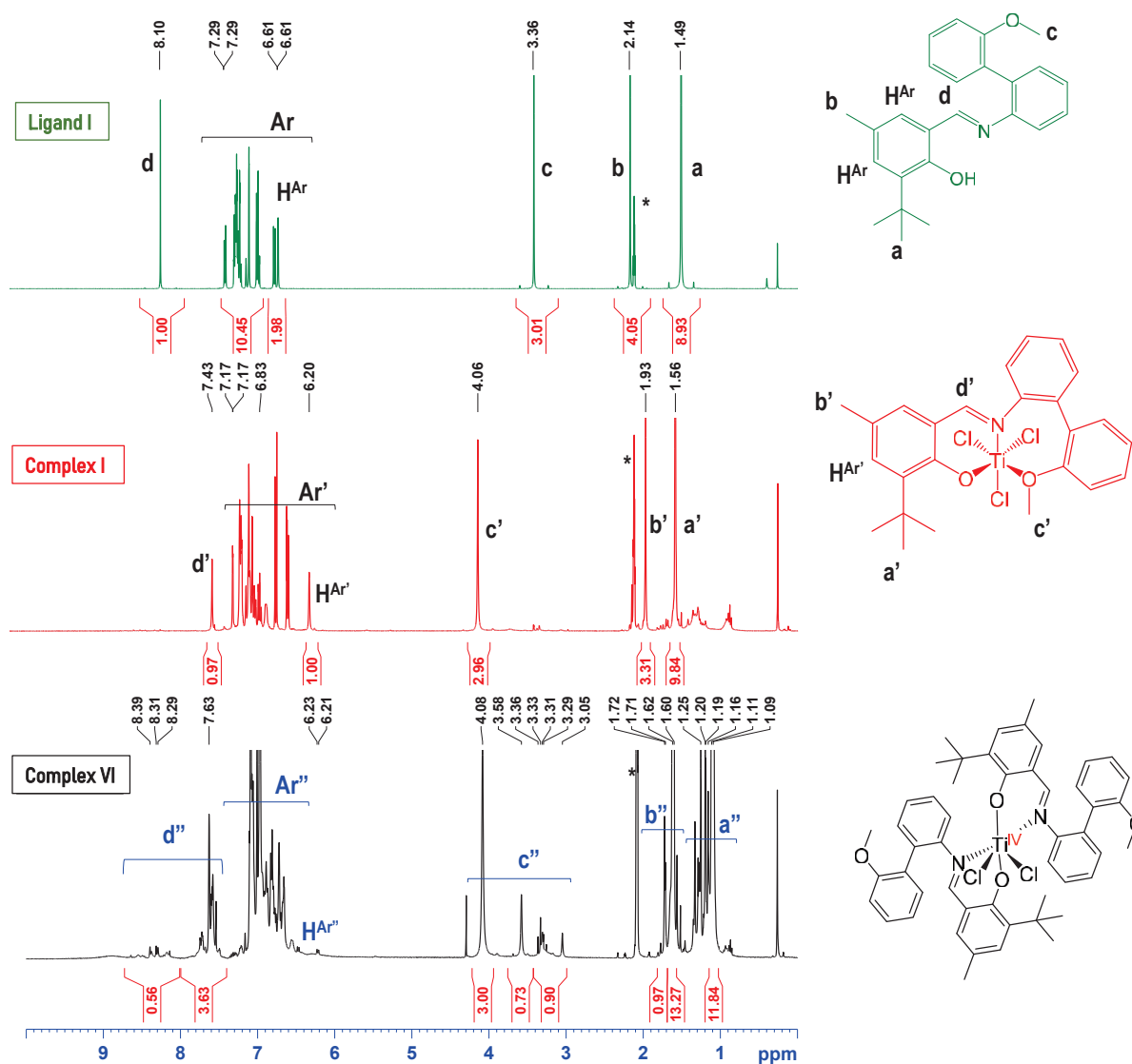


Figure 23. ^1H NMR spectra in toluene- d_8 of complex I (red), the corresponding ligand (green) and the synthesized bis(phenoxy-imine) complex (black)

Although it was not possible to assign each peak to a complex structure, similar spectra pattern were reported in the case of the C_6F_5 -substituted bis(phenoxy)-imine zirconium-based system.³³ In this case, several single and doublet signals for the imine and *tert*-butyl (in *ortho*- position of the phenol) groups at -25°C . It was concluded that a mixture of *N-cis*, *Cl-cis*, *O-trans/-cis* species were present in solution. It is also noteworthy that the type of solvent has an influence on the formation of these isomers in solution.³⁴ Consequently, the difference in terms of chemical shift between the mixture analyzed in toluene- d_8 and in CD_2Cl_2 (see experimental section) highlights this effect.

Although a mixture of several active species with a significant proportion (65 mol %) of complex I was observed by ^1H NMR, it is worth testing the mixture in ethylene oligo/polymerization.

IV.2.2. Activity, selectivity and polymer properties

Since complex **VI** is a new hindered bis(phenoxy-imine) complex, its reactivity towards ethylene has never been reported but it can be predicted based on several criteria. After the analysis of an extensive number of $(FI)_2TiCl_2$ complexes, general trends have been extracted regarding the structure/reactivity/polymer properties relationships established by Fujita *et al.*:⁶

- (i) β -H elimination is disfavored resulting in high molar-mass polyethylene;
- (ii) larger bite angles affect activity and comonomer incorporation.

On the basis of complex **VI** structure (Figure 21), bulky *tert*-butyl substituent should favor ethylene polymerization activity. The small angle for Cl-Ti-Cl, corresponding to the ethylene coordination sites, would limit 1-hexene intake.

To compare the reactivity of the mixture of complex **I** and complex **VI**, catalytic tests were performed on Chemspeed platform in the same conditions as previously described. Tests were carried out at 40 °C and 80 °C, i.e under conditions where trimerization and polymerization are favored, respectively. The resulting activity and selectivities are compared with complex **I**/MAO (Table 12).

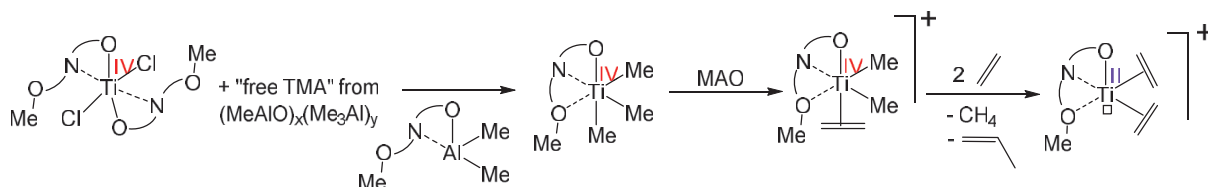
Table 12. Catalytic performances and selectivity of complex **I**/MAO and complexes **I+VI**/MAO at 40 and 80 °C

Entry	Complex	T (°C)	n_{Ti} (μ mol)	Al/Ti	Activity ($kg_{ethylene} g_{Ti}^{-1} h^{-1}$)	C_6H_{12} (g) (wt %)	$C_{10}H_{20}$ (g) (wt %)	PE (g) (wt %)
1	I+VI	40	1.6	1 700	380	11.7 80.5 %	2.6 17.9 %	0.22 1.5 %
2	I+VI	80	1.6	1 700	70	0.33 13%	0.01 0.3%	2.19 86.7%
3	I	40	1.9	1 400	310	11.6 82.5 %	2.2 15.7 %	0.25 1.8 %
4	I	80	1.8	1 150	80	0.4 11.6%	0.01 0.4%	3.05 88.1%

Conditions: MAO 30 wt % in toluene, 120 mL toluene, 30 minutes, 10 bar of ethylene

Catalytic tests with complexes **I+VI** showed that the system is more active at 40 °C than 80 °C (Table 12, entries 1 and 2). In addition, the mixture affords both trimers and polymer with a surprisingly high selectivity in co-trimers $C_{10}H_{20}$ at 40 °C (17.9 wt %). A low production of polymer at 40 °C contrasts with its 10 times higher yield at 80 °C.

Overall, the resulting system is more active than complex **I** alone. Even though complex **I** was found in the mixture complex **I+VI** (Figure 23), it is surprising that the amount of 1-hexene and polyethylene are essentially identical in both cases (Table 12, entries 1 vs 3 and 2 vs 4). In fact, it was expected that secondary species, assumed as $(\text{FI})_2\text{TiCl}_2$ complex, would have produced more polymer in presence of MAO. One hypothesis to rationalize this behavior is a probable ligand transfer in presence of MAO. Indeed, if the complexation of two FI ligands with TiCl_4 is incomplete even with two equivalents of ligand, it is conceivable that a ligand abstraction induced by the TMA contained in MAO occurs (Scheme 12).



Scheme 12. Proposed mechanism for the formation of Ti^{III} active species from the $(\text{FI})_2\text{TiCl}_2$ complex

Polymer properties were analyzed to verify whether polymerization active species can be distinguished or not. A similar copolymerization ability was found between complex **I**/MAO and complex **I+VI**/MAO at both 40 °C and 80 °C (Figure 24). Therefore, the presence of a species complex **VI**/MAO in the SFI system could explain the production of polymer.

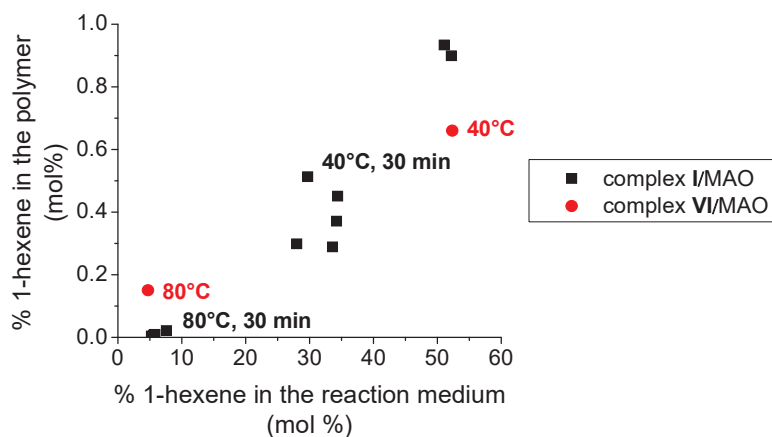
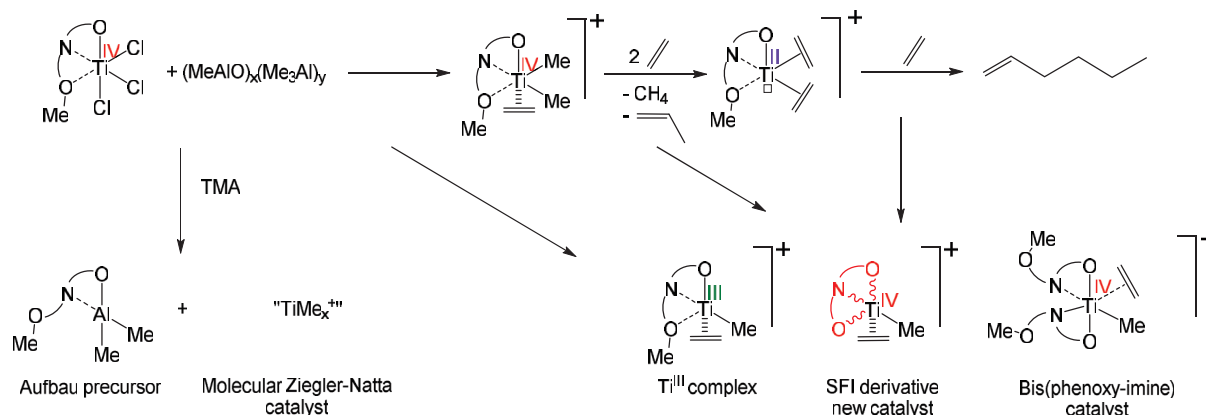


Figure 24. 1-hexene incorporation ability of complex **VI**/MAO depending on the amount of 1-hexene in the liquid phase (red) and comparison with the SFI system (black)

Despite the qualitative aspect of this study, several interesting facts were highlighted. First, there are undeniable evidences that such phenoxy-imine ligands are labile and mobile. Ligand transfers from Ti^{III} or Ti^{IV} species were identified. These new complexes are prevalent for further ligand transfer or isomerization and are assumed as polymerization active species. It is still not possible to conclude whether $(\text{FI})_2\text{TiCl}_2$ is the side active species formed from complex **I** that could produce polymer in the reaction medium. However, it is an interesting and promising hypothesis in which further efforts should be invested.

V. CONCLUSION

In this chapter, three paths were investigated regarding the polymerization active species formed in the trimerization system (FI)TiCl₃/MAO. All the hypotheses considered were integrated in a global reaction scheme (Scheme 13).



Scheme 13. Potential routes for polymerization active species formation during the pre-activation, activation and catalytic test

First, a ligand transfer proposed by Duchateau *et al.* was proven to be likely to occur in presence of TMA. Assuming that such ligand exchange are involved during the activation process of the SFI system is credible. However, it was proven that the resulting "TiMe_x⁺" species would not be the main polymerization species but only a minor catalyst produced at the early stage of the catalytic test.

Considering the hypothesis of ligand alteration, the formation of a secondary active species of [O⁻,N,O⁻]-FI type during the catalytic test is still controverted. The antagonist results of the experimental and theoretical studies revealed that the reaction scheme is not yet ascertained but an intramolecular substitution is unlikely. Although the formation of complex III is strongly supported by the combination of several thermal techniques, this side reaction is not obvious to occur during in catalytic tests. Still, it is conceded that part of the polymer produced by complex I/MAO could be generated by this LX₂ complex.

A reduced Ti^{III} species produced by comproportionation or partial reduction of complex I could not clearly be evidenced as polymerization active species in the SFI system. Indeed, the (FI)₂TiCl₂ derived from Ti^{III} complex alteration, yielded both 1-hexene and polyethylene with a similar activity and selectivities as with complex I/MAO. Such bis(phenoxy-imine) complex, arising from Ti^{III} disproportionation, should be further studied to conclude whether it can be generated from the SFI system.

VI. EXPERIMENTAL SECTION

VI.1. DFT calculation method

Calculations related to the intramolecular transformation of complex I ($[\text{O}^-, \text{N}, \text{O}^-]\text{-FI})\text{TiCl}_3$ into ($[\text{O}^-, \text{N}, \text{O}^-]\text{-FI})\text{TiCl}_2$ were conducted at IFPEN. *ab initio* calculations were performed using Gaussian09 and the results visualized using Gaussview. Calculations were performed at the DFT level of theory using the functional ωB97XD . The electronic density was modeled using a TZVP basis set for C,H,N,O and Cl atoms and def2-TZVP for Ti. Transition state structures were obtained by performing an energy scan according to the adequate atoms displacements, then running a Bery algorithm on the most relevant structure obtained, and finally performing a frequency calculations to check the presence of single imaginary vibration mode characteristic of a transition state.

VI.2. General considerations

All air and moisture sensitive reactions were carried out under an inert argon atmosphere using Schlenk line, glovebox, Young NMR tube and vacuum techniques. All experiments involving titanium(III) species were performed in a glovebox ($\text{O}_2 < 1$ ppm and $\text{H}_2\text{O} < 0.1$ ppm). Toluene, heptane and pentane were supplied by Biosolve and dried with a MBRAUN solvent purification system equipped with activated alumina and copper catalyst columns. THF and diethylether were pre-dried over CaH and distilled over benzophenone/sodium.

Chemicals and solvents used for the organic and complex syntheses are gathered in the following table:

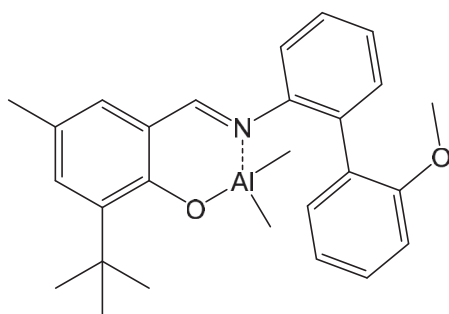
Chemical	Supplier
glacial acetic acid, 99.5 %	Acros organics
boron tribromide solution, 1M in dichloromethane	Sigma Aldrich
potassium bis(trimethylsilyl)amide solution 1M in THF	Sigma Aldrich
trichlorotris(tetrahydrofuran)titanium(III), min. 97 %	Strem
trimethylaluminium solution, 2M in toluene	Sigma Aldrich
Solvent	Supplier
diethylether, anhydrous, > 99 %	Sigma Aldrich
methanol anhydrous 99.8 %	Sigma Aldrich
Tetrahydrofuran 99.8 %	Acros organics

VI.3. Complex synthesis and characterization

Reaction between complex I and TMA

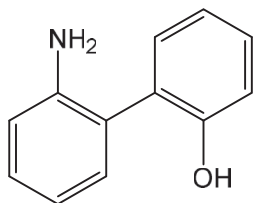
In a NMR Young tube and under inert atmosphere, 11 mg (0.021 mmol) of complex I was dissolved in 0.4 mL of toluene-*d*₈. To the red solution was added 0.06 mL of a solution of TMA 2.0M in toluene (0.4 mmol, 30 eq.). The solution turned dark blue/brown after stirring.

¹H NMR (toluene-*d*₈, 400 MHz): δ (ppm) 7.64 (s, 0.7H, N=CH), 7.7-6.6 (m, ArH), 6.36 (s, 1H, H^{Ar}), 3.3 (s, 2.55H, O-CH₃), 2.02 (s, Ar-CH₃), 1.43 (s, 9.8H, Ar-C(CH₃)₃), -0.37 (broad s, 280H, Al-CH₃)

Synthesis of (FI)AlMe₂

In a NMR Young tube and under inert atmosphere, 20.4 mg (0.055 mmol) of ligand **1** was dissolved in 0.6 mL of toluene-*d*₈, affording a yellow solution. 0.15 mL of a solution of TMA 2.0M in toluene (0.15 mmol, 2.7 eq.) was added in the NMR tube. The resulting solution was bright yellow.

¹H NMR (toluene-*d*₈, 400 MHz): δ (ppm) 7.61 (s, 1 H, N=CH), 7.3-6.6 (m, ArH), 6.5 (d, 1H, Ar-H^{2'}), 6.27 (s, 1H, Ar-H^{1'}), 3.29 (s, 3H, O-CH₃), 2.02 (s, 3H, Ar-CH₃), 1.47 (s, 9.1H, Ar-C(CH₃)₃), 0.17 (s, CH₄), -0.46 (s, 5.9H, Al-CH₃), -0.5 (s, 6.2H, Al-CH₃)

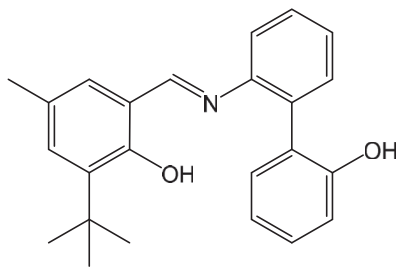
Synthesis of 2'-hydroxy-[1,1'-biphenyl]-2-amine

In a 100 mL Schlenk, a solution of boron tribromide 1.0 N in dichloromethane (10 mL, 10 mol) was added to a solution of 2'-methoxy-[1,1'-biphenyl]-2-amine (0.496 g, 2.5 mmol) in 10 mL of dichloromethane at -78°C. After the addition, the reaction medium was stirred for 3 hours at room temperature before being transferred in 20 mL of ice. The aqueous phase was neutralized with a 1.0 N solution of NaOH and washed with 2x20 mL of dichloromethane. Organic phase is washed with 2x20 mL of brine and water before being dried over MgSO₄. The light brown compound was sublimed at 100 °C under 10⁻² mbar affording a white powder.

Yield: 201 mg, 1.09 mmol, 44 %.

¹H NMR (CDCl₃, 400 MHz): δ 7.35-7.30 (m, 2H, ArH), 7.25-7.23 (m, 2H, ArH), 7.07-7.01 (m, 2H, ArH), 6.98 (td, *J* = 1.16 Hz, *J* = 7.66 Hz, 1H, ArH), 6.88 (dd, *J* = 1.16 Hz, *J* = 7.66 Hz, 1H, ArH), 4.45-3 (br s, 1.5H, OH/NH₂)

¹³C NMR (CDCl₃, 100 MHz): δ 153.5 (C), 142.6 (C), 131.5 (CH), 131.2 (CH), 129.3 (CH), 128.7 (CH), 126.1 (C), 121.5 (C), 120.8 (CH), 120.4 (CH), 117.8 (CH), 117.2 (CH)

Synthesis of the diphenoxy-imine ligand (ligand 3)

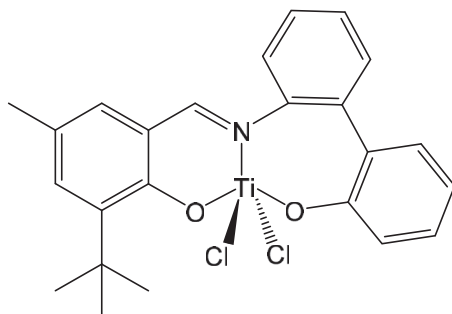
In a 100 mL Schlenk, 2'-methoxy-[1,1'-biphenyl]-2-amine (0.5 g, 2.51 mmol) and 3-tert-butyl-5-methylsalicylaldehyde (0.483 g, 2.51 mmol) were mixed in 20 mL of methanol before adding a drop of acetic acid. The reaction medium was stirred overnight at room temperature with molecular sieve. Some yellow solid precipitated while concentrating the reaction medium. The slurry was condensed and filtered. After 3 washings with 5 mL of pentane, the yellow powder was dried under vacuum.

Yield: 0.7 g, 1.88 mmol, 75 %. MS (EI⁺): (m/z) [M⁺] = 382.2.

¹H NMR (CD₂Cl₂, 400 MHz): δ (ppm) 8.54 (s, 1H, N=CH), 7.52-7.48 (m, 1H, ArH), 7.44-7.37 (m, 2H, ArH), 7.32-7.24 (m, 2H, ArH), 7.20 (dd, *J* = 2 Hz, *J* = 7.8 Hz, 1H, ArH), 7.16 (d, 1H, ArH), 7.00-6.94 (m, 3H, ArH), 2.27 (s, 3H, Ar-CH₃), 1.35 (s, 9H, Ar-C(CH₃)₃)

¹H NMR (toluene-*d*₈, 400 MHz): δ (ppm) 8.03 (s, 1H, N=CH), 7.18-6.72 (m, 1H, ArH), 6.61 (s, 1H, H^{Ar}), 2.15 (s, 3H, Ar-CH₃), 1.5 (s, 9H, Ar-C(CH₃)₃)

¹³C NMR (CD₂Cl₂, 100 MHz): 163.4 (CH), 158.51 (C), 153.10 (C), 148.00 (C), 137.61 (C), 132.32 (C), 132.18 (CH), 131.83 (CH), 131.45 (CH), 130.91 (CH), 129.98 (CH), 129.72 (CH), 127.55 (C), 127.52 (C), 126.49 (CH), 120.96 (CH), 119.24 (C), 119.14 (C), 116.00 (CH), 35.04 (C), 29.43 (3 CH₃), 20.70 (CH₃)

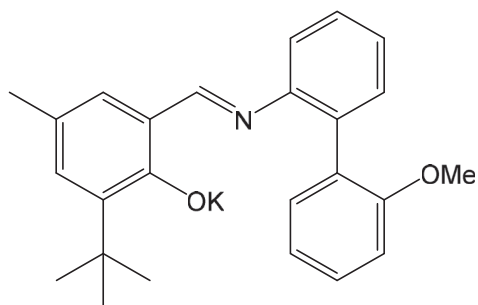
Synthesis of ([O⁻,N,O⁻]-FI)Ti^{IV}Cl₂ (complex III)

In a 100 mL Schlenk, 23 mg (0.064 mmol) of ligand **3** was dissolved in 15 mL of dry toluene. To the yellow solution cooled at -78 °C, 0.06 mL of TiCl₄ 1.0M in toluene (0.065 mmol, 1 eq.) was added dropwise. The red solution was stirred for 15 minutes at low temperature and warmed up to room temperature overnight. 10 mL of pentane was added to precipitate the complex as a red solid.

After removing the supernatant, the bright red precipitate was washed 2 times with 6 mL of pentane and dried under reduced pressure at 40 °C for 1 hour. An orange/red powder was obtained.

Yield: 21 mg, 0.04 mmol, 70 %.

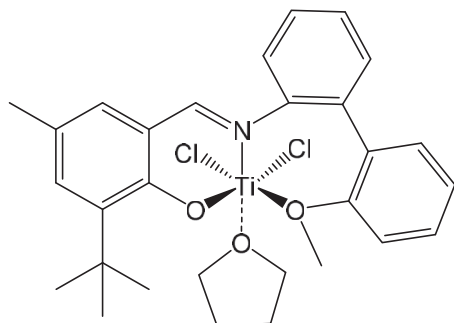
¹H NMR of powder (toluene-*d*₈, 400 MHz): δ (ppm) 7.40 (s, 1H, N=CH), 7.15-6.65 (m, 4H, ArH), 6.13 (s, 1H, H^{Ar}), 1.95 (s, 3H, Ar-CH₃), 1.54 (s, 9H, Ar-C(CH₃)₃)

Synthesis of phenoxy-imine potassium salt (ligand 5)

In the glovebox, 90.6 mg (0.242 mmol) of ligand **1** was dissolved in 5 mL of toluene. To the yellow solution, 0.24 mL (0.24 mmol, 1 eq.) of KHMDS 1 M in THF was added dropwise at room temperature. The bright yellow solution was stirred overnight. The reaction medium was condensed and a yellow precipitate was formed after addition of 5 mL of pentane. The supernatant was filtered off and the solid was washed with 2x5 mL of pentane. A bright yellow powder was obtained after drying under reduced pressure at room temperature for 1 hour.

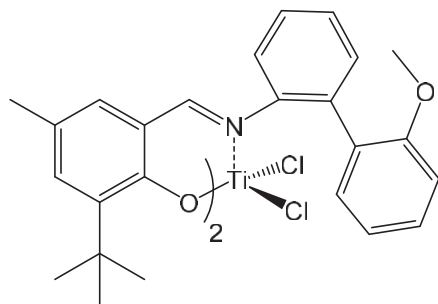
Yield: 45.6 mg, 0.111 mmol, 45.7 %

^1H NMR (C_6D_6 , 400 MHz): δ (ppm) 7.97 (s, 1H, N=CH), 7.04-5.98 (m, 11H, ArH), 2.79 (s, 3H, O-CH₃), 2.12 (s, 3H, Ar-CH₃), 1.54 (s, 10H, Ar-C(CH₃))

Synthesis of $[(\text{O}^-\text{,N,O})\text{-FI})\text{Ti}^{\text{III}}\text{Cl}_2(\text{THF})$ (complex V)

In the glovebox, 40.7 mg (0.099 mmol) of ligand **1** was dissolved in 10 mL of diethylether. To the yellow solution, 36.6 mg (0.099 mmol, 1 eq.) of $\text{TiCl}_3(\text{THF})_3$ (light blue powder) was added at once at room temperature. The bright yellow solution turned dark green/brown after 1 hour. The solution was stirred overnight. The reaction medium was condensed and filtered from the white and green precipitate. The deep green solution was condensed to about 6 mL. 3 mL were placed in the fridge for crystallization at $-30\text{ }^\circ\text{C}$ by diffusion of 1 mL of pentane. The other half was dried under vacuum affording a green powder (16 mg, 0.03 mmol).

Elemental analysis $(\text{FI})\text{TiCl}_2(\text{THF})$ $\text{C}_{29}\text{H}_{34}\text{Cl}_2\text{NO}_3\text{Ti}$: Calc. (wt %) C: 61.83; H: 6.07; N: 2.59. Found: C: 61.49; H: 6.07; N: 2.45.

Synthesis of $[(O^-,N)\text{-FI}]_2\text{Ti}^{\text{IV}}\text{Cl}_2$ (complex VI)

This complex was synthesized at IFPEN. To a solution of titanium tetrachloride (0.1 mL, 0.1 mmol, 1.0 eq.) in dichloromethane (1.4 mL), a solution of ligand **1** (100.0 mg, 0.2 mmol, 2.0 eq.) in dichloromethane (1.0 mL) was slowly added at room temperature. The mixture was stirred during two hours before removing the solvent under vacuum. The residue was washed with

pentane and dried under reduced pressure, affording the desire product as a red solid.

Yield: 76.2 mg, 0.08 mmol, 67 %

^1H NMR (toluene- d_8 , 400 MHz): δ (ppm) 8.39-8.29 (s, 0.5H, N=CH), 7.63 (s, 3.6H, N=CH), 7.18-6.21 (m, ArH), 4.08 (s, 3H, O-CH₃ complex I), 3.58 (s, 0.7H, O-CH₃), 3.31-3.05 (m, 1H, O-CH₃), 6.13 (s, 1H, ArH), 1.94 (s, 3H, Ar-CH₃), 1.54 (s, 9H, Ar-C(CH₃))

^1H NMR (CD₂Cl₂, 300 MHz): δ (ppm) 7.86-7.71 (m, 4H, N=CH and Ar-H), 7.57-7.44 (m, 12H, ArH), 7.11-7.09 (t, J = 6.3 Hz 4H, Ar-H), 7.08-6.96 (d, J = 6Hz, 4H, Ar-H), 3.79 (s, 6H, O-CH₃), 1.53-1.47 (m, 1H, O-CH₃), 1.35-1.30 (s, 1H, ArH), 1.94 (s, 3H, Ar-CH₃), 1.54 (s, 9H, Ar-C(CH₃))

VI.4. Heating and degradation of complex I**Forced thermal modification of complex I**

In a 10 mL Schlenck, 20.8 mg of complex I (red powder) was heated under argon at 100 °C for 24 hours. 0.5 mL of toluene- d_8 was introduced in the Schlenck and the red solution was transferred in a Young tube for ^1H NMR analysis. The yield of complex III produced by complex I modification is 80 mol %, based on the ratio between integration of H^{Ar} signals (6.2 ppm).

High temperature DRIFT with online GC/MS

50 mg of complex I powder was placed in the DRIFT cell in the glovebox and sealed under inert atmosphere. Powder is heated at 2 °C min⁻¹ from 20 °C to 600 °C. A constant argon flow of 1 mL min⁻¹ was applied as carrier gas. Volatiles molecules were analyzed by GC-MS (Agilent technologies 7890A). The column was kept at 35 °C for 7 min before the heating to 250 °C at 20 °C min⁻¹.

The sublimation of a yellow solid during complex I heating led to a deposit on the inner walls of the cell.

Thermogravimetric Analysis (TGA)

Mass loss analysis was performed on a TGA 2 LF module provided by Mettler Toledo. 4.9 mg of complex I powder was placed in a 40 μ L aluminum crucible and sealed in the glovebox. The crucible was automatically pierced under nitrogen (10 mL min⁻¹). The complex was heated for 10 minutes at 25 °C followed by a heating to 600 °C at 10 °C min⁻¹.

VI.5. Catalytic tests

VI.5.1. Tests in the 1 liter SFS reactor

General procedure

The 1 liter SFS reactor is heated at 80 °C under vacuum for 20 minutes. It is scavenged with 300 mL of a solution of TEA in heptane (15 mol L⁻¹) for 20 minutes. The solution is evacuated and the reactor is put under vacuum for 10 additional minutes. The reactor is cooled down to the desired temperature and a commercial solution of MAO 30 wt % (1 mL, 1 200 eq) in 280 mL of toluene is injected. Once the temperature is stable, the solution of complex (3 μ mol) in 20 mL of toluene is introduced before feeding the reactor with purified ethylene. The catalytic test is carried out at 10 bar and the ethylene consumption is followed by the pressure decrease of the ballast. After 30 minutes of reaction, the ethylene feed is stopped and 5 mL of methanol is introduced in the reactor *via* an injection sas. The reactor is cooled to 6 °C to preserve the 1-hexene in the liquid phase. The pressure is slowly released before opening the reactor. The liquid phase is treated with sulfuric acid and analyzed by GC with dodecane as internal standard. The solid is washed with acidified methanol then methanol and it is dried *in vacuo* at 90 °C for two hours.

TiCl₄/MAO

A bulk solution of TiCl₄ (4 mmol L⁻¹) was prepared and 1 mL (4 μ mol of Ti) of this solution was introduced in 9 mL toluene before being transferred in the reactor. For ethylene/1-hexene copolymerizations, 1-hexene was introduced in the reactor together with MAO solution in toluene. The solution of TiCl₄ was injected before pressurizing with ethylene.

The amount of 1-hexene introduced was 7.6 g (90 mmol) at 42 °C, 3.5 g (41 mmol) at 62 °C and 0.8 g (9.5 mmol) at 80 °C.

Complex I/TMA

A stock solution of TMA in toluene (0.8 mol L⁻¹) was prepared in the glovebox. 1 mL (250 eq. TMA) of this solution was introduced in the reactor and temperature was set at 40 °C. The solution of complex I (1.68 mg, 3.19 μ mol) in 10 mL of toluene was prepared in the glovebox before introduction in the reactor containing 1 mL of TMA (250 eq.) in 290 mL of toluene at 60 °C.

Complex IV/MAO

A solution of (FI)Ti^{III}Cl₂(THF) (2.20 mg, 3.91 μmol) in 2 mL of THF and 8 mL of toluene was prepared in the glovebox before introduction in the reactor containing 1 mL of MAO (1 150 eq.) in 290 mL of toluene at 60 °C.

TiCl₃(THF)₃/MAO

A solution of TiCl₃(THF)₃ (3.0 mg, 8.1 μmol) in 2 mL of THF and 8 mL of toluene was prepared in the glovebox before introduction in the reactor containing 2 mL of MAO (1 120 eq.) in 290 mL of toluene at 60 °C.

VI.5.2. Catalytic tests with Chemspeed autoclaves

General procedure

Catalytic tests were performed in three independent 270 mL-reactors. Toluene (120 mL) and MAO 30 wt % in toluene solution (0.45 mL, 1 500 eq.) were introduced in each reactor and stirred at 300 RPM. Once the desired temperature was reached, reactors were pressurized to 10 bar of ethylene. Using SWILE© technology, a batch solution of complex in a defined volume of toluene was prepared and 3 mL of this solution was injected *via* a high pressure pump in each reactors. The reactions were run in a semi-batch mode for the desired reaction time. Ethanol was introduced under pressure to quench the reaction. Reactors were cooled to 5 °C before depressurization. Further treatments of the solid and liquid phases were performed as described in the previous section.

Complex III/MAO

A stock solution of 2.7 mg (5.7 μmol) of complex III in 10.5 mL of toluene was prepared using SWILE© technology. In each reactor, 1.62 μmol of titanium were introduced under ethylene pressure in the solution of MAO (0.55 mL, 1 520 eq.). Reactions were run at 40, 60 and 80 °C for 30 minutes.

A stock solution of 1.5 mg (3.2 μmol) of complex III in 7 mL of toluene was prepared using SWILE© technology. Two reactors were run for 30 minutes with 1.35 μmol of titanium, 0.45 mL (1 490 eq.) of MAO and 1.8 g (42.8 mmol, 60 °C) and 0.6 g (7.1 mmol, 80 °C) of 1-hexene. At 40 °C, 1.26 μmol of complex III were reacted with 0.29 mL (1 031 eq.) of MAO and 3.6 g (24 mmol) of 1-hexene.

Complex V+I/MAO

A stock solution of 2.4 mg of complex V (1.58 μmol containing 1.02 μmol of complex I) in 7 mL of toluene was prepared using SWILE© technology. In each reactor, 1.58 μmol of titanium were introduced under ethylene pressure in the solution of MAO (0.55 mL, 1 700 eq.). Reactions were run at 40 °C and 80 °C for 30 minutes.

VII. REFERENCES

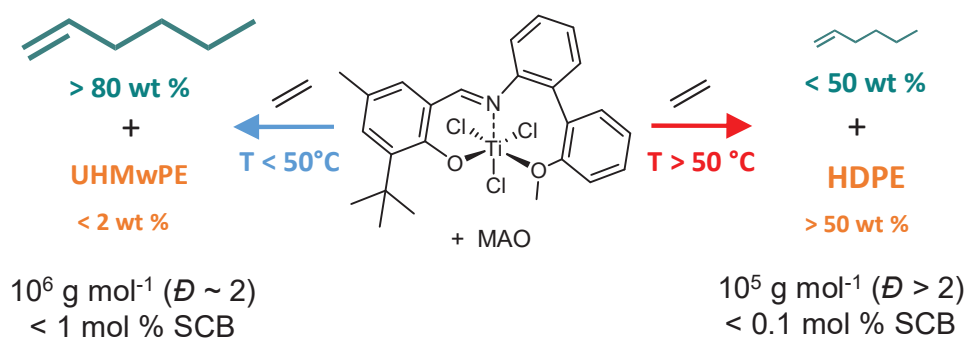
- 1 R. Duchateau, F. F. Karbach and J. R. Severn, *ACS Catal.*, 2015, **5**, 5068–5076.
- 2 J. C. W. Chien and T. Nozaki, *J. Polym. Sci. Part Polym. Chem.*, 1993, **31**, 227–237.
- 3 Y. Imanishi and N. Naga, *Prog. Polym. Sci.*, 2001, **26**, 1147–1198.
- 4 H. Makio, A. V. Prasad, H. Terao, J. Saito and T. Fujita, *Dalton Trans.*, 2013, **42**, 9112–9119.
- 5 H. Audouin, R. Bellini, L. Magna, N. Mézailles and H. Olivier-Bourbigou, *Eur. J. Inorg. Chem.*, 2015, **2015**, 5272–5280.
- 6 H. Makio, H. Terao, A. Iwashita and T. Fujita, *Chem. Rev.*, 2011, **111**, 2363–2449.
- 7 A. Sattler, J. A. Labinger and J. E. Bercaw, *Organometallics*, 2013, **32**, 6899–6902.
- 8 I. E. Soshnikov, N. V. Semikolenova, J. Ma, K.-Q. Zhao, V. A. Zakharov, K. P. Bryliakov, C. Redshaw and E. P. Talsi, *Organometallics*, 2014, **33**, 1431–1439.
- 9 I. E. Soshnikov, N. V. Semikolenova, K. P. Bryliakov, V. A. Zakharov and E. P. Talsi, *J. Organomet. Chem.*, 2018, **867**, 4–13.
- 10 Z. Flisak, G. P. Spaleniak and M. Bremmek, *Organometallics*, 2013, **32**, 3870–3876.
- 11 H. Wesslau, *Justus Liebigs Ann. Chem.*, 1960, **629**, 198–206.
- 12 G. Natta, P. Pino, G. Mazzanti, U. Giannini, E. Mantica and M. Peraldo, *J. Polym. Sci.*, 1957, **26**, 120–123.
- 13 A. Sattler, D. G. VanderVelde, J. A. Labinger and J. E. Bercaw, *J. Am. Chem. Soc.*, 2014, **136**, 10790–10800.
- 14 I. Mori, *Bull. Chem. Soc. Jpn.*, 1975, **48**, 911–913.
- 15 Mitsui Chemical, JP2011016789A, 2011.
- 16 Q. Chen, J. Huang and J. Yu, *Inorg. Chem. Commun.*, 2005, **8**, 444–448.
- 17 D. Owiny, S. Parkin and F. T. Ladipo, *J. Organomet. Chem.*, 2003, **678**, 134–141.
- 18 L. Chen, N. Zhao, Q. Wang, G. Hou, H. Song and G. Zi, *Inorganica Chim. Acta*, 2013, **402**, 140–155.
- 19 T. Xu, J. Liu, G.-P. Wu and X.-B. Lu, *Inorg. Chem.*, 2011, **50**, 10884–10892.
- 20 Mitsui Chemical, JP2011016789, 2011.
- 21 N. V. Shugurova, E. I. Davydova, T. N. Sevast'yanova, A. D. Misharev, M. Bodensteiner and M. Scheer, *Russ. J. Gen. Chem.*, 2016, **86**, 9–17.
- 22 H. Audouin, PhD thesis, Ecole normale supérieure de Lyon - ENS LYON, 2015.
- 23 J. E. Bercaw, A. Sattler, D. C. Aluthge, J. R. Winkler and J. A. Labinger, *ACS Catal.*, 2016, **6**, 19–22.
- 24 G. Natta, P. Pino, G. Mazzanti and U. Giannini, *J. Am. Chem. Soc.*, 1957, **79**, 2975–2976.
- 25 J. L. Barr, A. Kumar, D. Lionetti, C. A. Cruz and J. D. Blakemore, *Organometallics*, 2019, **38**, 2150–2155.
- 26 T. Saito, H. Nishiyama, H. Tanahashi, K. Kawakita, H. Tsurugi and K. Mashima, *J. Am. Chem. Soc.*, 2014, **136**, 5161–5170.
- 27 S. Kanazawa, T. Ohira, S. Goda, N. Hayakawa, T. Tanikawa, D. Hashizume, Y. Ishida, H. Kawaguchi and T. Matsuo, *Inorg. Chem.*, 2016, **55**, 6643–6652.
- 28 F. Allouche, D. Klose, C. P. Gordon, A. Ashuiev, M. Wörle, V. Kalendra, V. Mougél, C. Copéret and G. Jeschke, *Angew. Chem. Int. Ed.*, 2018, **57**, 1–6
- 29 S. S. Ivanchev, V. A. Trunov, V. B. Rybakov, D. V. Al'bov and D. G. Rogozin, *Dokl. Phys. Chem.*, 2005, **404**, 165–168.
- 30 R. Furuyama, J. Saito, S. Ishii, M. Mitani, S. Matsui, Y. Tohi, H. Makio, N. Matsukawa, H. Tanaka and T. Fujita, *J. Mol. Catal. Chem.*, 2003, **200**, 31–42.
- 31 M. Mitani, J. Saito, S. Ishii, Y. Nakayama, H. Makio, N. Matsukawa, S. Matsui, J. Mohri, R. Furuyama, H. Terao, H. Bando, H. Tanaka and T. Fujita, *Chem. Rec.*, 2004, **4**, 137–158.
- 32 J. J. Eisch, A. A. Adeosun and J. M. Birmingham, *Eur. J. Inorg. Chem.*, 2007, **2007**, 39–43.

- 33 Y. Tohi, H. Makio, S. Matsui, M. Onda and T. Fujita, *Macromolecules*, 2003, **36**, 523–525.
34 H. Makio and T. Fujita, *Macromol. Symp.*, 2004, **213**, 221–234.

General conclusion

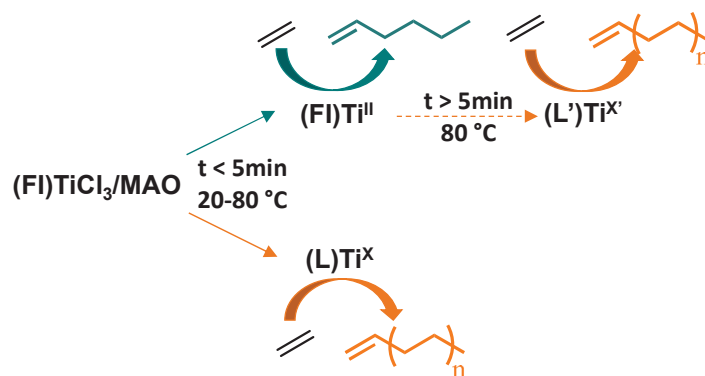
The goal of this PhD project was to determine the nature of the active species responsible for the polymerization in the case of Fujita's ethylene trimerization SFI system ($[\text{O}^-, \text{N}, \text{O}]\text{-FI})\text{TiCl}_3/\text{MAO}$. Studies based a "polymer-to-catalyst" strategy contributed to identify crucial parameters for the activity and selectivity of the system. Several relevant routes explaining the formation of secondary active species also emerged from these investigations.

First, considerable insights have been gained on the influence of temperature on the behavior of the SFI system in tri/polymerization. This study emphasized and quantified a shift of the activity and selectivity of the catalytic system from an efficient trimerization ($25\text{ }^\circ\text{C} < T < 50\text{ }^\circ\text{C}$) to a moderate polymerization ($50\text{ }^\circ\text{C} < T < 80\text{ }^\circ\text{C}$) (Scheme 1). For the first time, the properties of polyethylenes produced with such systems were systematically analyzed and reported. Indeed, the combination of several conventional techniques (DSC, high-temperature NMR, SEC) and advanced analyses (CEF, SIST, rheology) pointed out the formation of high to ultra-high molar mass polyethylenes. This polymer-to-catalyst investigation demonstrated a poor ability of the active species for ethylene/1-hexene copolymerization and transfer reactions. Moreover, a switch from single-site to multi-site catalysis at higher temperature is strongly suspected by the broadening of molar mass distribution.



Scheme 1. Selectivity of the SFI system and polymer features according to temperature

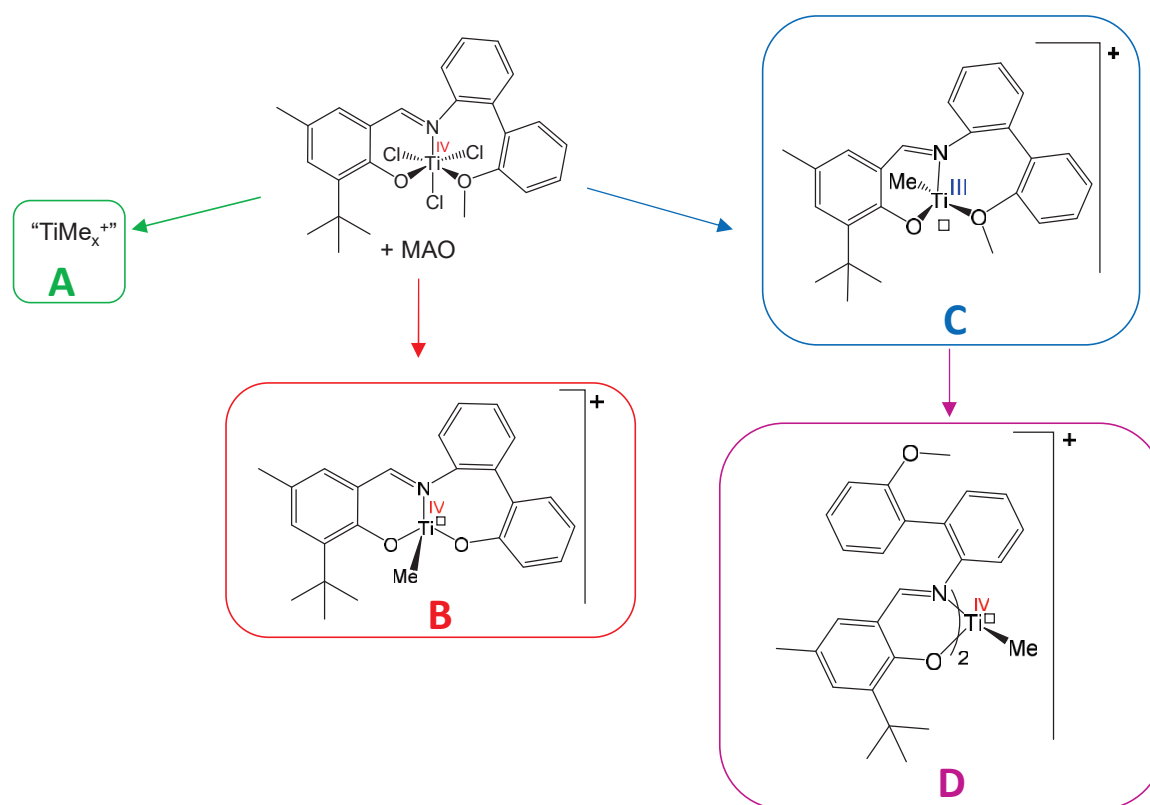
Then, the identification of the activation process as a key step for the formation of polymer species was achieved by kinetic studies implemented on an automated Chemspeed platform. In fact, polymerization and oligomerization active species are produced through a parallel process (Scheme 2). It was found that trimerization and polymerization products are continuously formed during the catalytic tests at $40\text{ }^\circ\text{C}$. In contrast, trimerization species are probably converted into polymerization catalysts at $80\text{ }^\circ\text{C}$, which explains the broadening of MMDs. This dual behavior reinforces the assumption of temperature-promoted side reactions.



Scheme 2. Routes for trimerization and polymerization species formation according to reaction time and temperature

By altering the conditions of the activation process, the concomitant formation of trimerization and polymerization active species was confirmed. A characteristic deactivation of both species in presence of 1-hexene and hydrogen hints that they originate from the same pre-activated species. It was also shown that a prolonged contact between $(FI)TiCl_3$ and MAO of a different composition might have a positive effect on 1-hexene selectivity in some cases. Conversely, the combination of the complex with TMA afforded a limited amount of polymer. Such activator effects shed light on the necessity to investigate alternative activation processes.

Based on previous conclusions and hypotheses from the literature, the main parameters identified for the formation of polymerization active species encompass the oxidation state of titanium, the type and number of ligands coordinated to the latter. Three main catalytic systems were considered as serious candidates for the production of polymer in the $(FI)TiCl_3/MAO$ system (Scheme 3). First, precursors were synthesized and characterized by NMR and XRD when possible. Then, their relevance as secondary active species was ascertained by comparisons with the SFI system in terms of activity and properties of resulting polymers.



Scheme 3. Active species derived from complex I and suspected to induce polymerization

The assumption of a ligand abstraction from (FI)TiCl₃ by TMA was mentioned in the literature by Duchateau *et al.* and evidenced in this work (Scheme 3. A). The resulting "TiMe_x⁺" species was adequately modeled by the TiCl₄/MAO system. Although the presence of a "ligand-free" catalyst is possible, the fast deactivation of "TiMe_x⁺" species reveals that it cannot be the main reason behind the continuous polymer production observed in the case of the SFI system.

A thermal modification of the trimerization precursor ([O⁻,N,O⁻]-FI)TiCl₃ into a polymerization precatalyst ([O⁻,N,O⁻]-FI)TiCl₂ was pointed out (Scheme 3. B). The combination of several thermal techniques (high temperature NMR, TGA, GC-MS of volatile molecules) confirmed the formation of a LX₂-type species. From these analyses, it was proposed that this transformation proceeds through a metathesis reaction between Ti-Cl and O-CH₃ bonds. However, this transformation is not yet elucidated since DFT calculations do not support an intramolecular process. The resulting diphenoxy-imine derivative was active in ethylene polymerization, as predicted from similar ([O⁻,N,O⁻]-FI)TiCl₂ complexes reported in the literature. In agreement with the polymerization species in the SFI system, this new complex exhibits a poor ability for 1-hexene insertion once activated with MAO. However, its catalytic performances do not exceed those of the SFI system, which rules out ([O⁻,N,O⁻]-FI)TiCl₂/MAO as main polymerization active species. Still, this catalyst could be formed and produce polymer especially during exothermic events at short reaction time.

Eventually, the investigation of a phenoxy-imine-ether complex of Ti^{III} gave rise to new possibilities that have not been considered in the literature. Indeed, this $[(O^-,N,O)-FI]Ti^{III}Cl_2(THF)$ complex (Scheme 3. C) led to the serendipitous formation of a bis(phenoxy-imine) derivative $[(O^-,N)-FI]_2TiCl_2$ *via* a disproportionation mechanism (Scheme 3. D). A disubstituted complex was also obtained in the case of the diphenoxy-imine complex $[(O^-,N,O^-)-FI]_2Ti$. Hence, this study demonstrated that such phenoxy-imine species are subject to structural rearrangement on two independent occasions. As a result, the formation of $[[O^-,N)-FI]_2TiMe]^+$ as polymerization active species, is a serious avenue worth exploring in preventing this ligand transfer between titanium centers.

Overall, our investigations enabled to rule out several hypotheses to concerning the main polymerization active species formed by the SFI. This work opened new prospective regarding the mechanism of their formation. We evidenced the possible modification and mobility of ligands in the case of the phenoxy-imine-ether complex, which can be extended to other selective phenoxy-imine-ether-based titanium systems. The paths for SFI complex rearrangements is worth being further investigated in the view of improving the robustness of the trimerization complex, and eventually its selectivity for 1-hexene production.

From a general point of view on the investigations of polymerization active species formation and intermediate, several conclusions and prospective can be proposed to improve the general understanding of the catalytic systems. This work and the reported literature highlighted the versatility of titanium complexes in the SFI system in terms of oxidation state and structure (ligand alterations and transfers). Based on the complexity of this system, the identification of a precise polymerization active species can hardly be achieved. To circumvent this limitation, improvements should be focused on avoiding contact between titanium centers and controlling the activation process. For instance, Duchateau's and Bercaw's research teams showed that supporting the SFI system on a carrier did not provide a drastic limitation of polymerization. To go further in active species separation, one could consider other methods to limit ligand transfer and associated dis/comproportions (e.g ligand grafting). Other improvements rely on the optimization of the activation process. To limit side reactions involved by TMA contained in MAO, the use of "trapping agents" (e.g BHT) can be beneficial. Other activation systems employing non-aluminum-based alkylating agents (e.g Grignard derivatives) and cationizing agents (e.g weakly coordinating anions) would enable a better control over this activation step.

Eventually, a special attention should be drawn to the polymer-to-catalyst strategy developed in this project. This original approach enabled to gain insight in the nature of the polymerization active species. Besides, one should stress that this strategy can be easily implemented on any catalytic system that provides polymer as main or side reaction.

Keywords: homogeneous catalysis, titanium, trimerization, polymerization, ethylene, 1-hexene, polyethylene

1-hexene is one of the most important olefin used as comonomer for the production of value-added polyethylenes (HDPE, LLDPE). In the field of selective ethylene trimerization employing titanium-based catalysts, specific single tridentate phenoxy-imine complexes (SFI) display the highest activity and 1-hexene selectivity upon activation with methylaluminoxane (MAO). However, ethylene polymerization is an unavoidable side reaction affecting both 1-hexene selectivity and process operations. Although being a major drawback, the causes of polymerization remain a grey area since few studies were dedicated to its deciphering. To handle this challenge, an original “polymer-to-catalyst” strategy was implemented. An extensive temperature study (26-80 °C) revealed that the highest 1-hexene activity is reached between 30 °C and 40 °C while polymer production is prominent above 50 °C. Polyethylenes obtained were analyzed by SEC, NMR DSC, and advanced segregation techniques (CEF, SIST, rheology). Molar masses above 10^5 g mol⁻¹ were identified along with a 1-hexene content below 1 mol %. An increase of dispersity ($D > 2$) with temperature was ascribed to an evolution from single to multi-site polymerization catalysis. Kinetic studies proved that polymer is continuously produced even at short reaction time, for any reaction temperature. Other parameters (addition of 1-hexene, hydrogen and use of trimethylaluminum) were found to impair the trimerization selectivity and/or activity of the system. Nevertheless, it was possible to lower the selectivity in polyethylene by premixing the complex with MAO. After analyzing the possible routes for the polymerization catalyst formation, the hypotheses of temperature and MAO-induced complex alterations were considered. Regarding the latter, a molecular ligand-free Ziegler-Natta catalyst, modeled using TiCl₄/MAO, and the synthesized (FI)Ti^{III}Cl₂ activated by MAO could not explain polymer production in the SFI system. Formation of a polymerization species upon thermal alteration of the SFI complex was evidenced. This [O-,N,O]-type species displays common features regarding catalytic response to 1-hexene compared to the polymerization catalyst in the SFI system although it could not reach the same catalytic performances. The formation of a bis(phenoxy-imine) complex (FI)₂TiCl₂ was evidenced in this thesis and is a promising avenue worth exploring. Eventually, although the exact species has not yet been identified, this work enabled to guide the focus of further investigations on activation process and complex rearrangement by ligand mobility.

Mots clés : Catalyse homogène, titane, trimérisation, polymérisation, éthylène, hexène-1, polyéthylène

L'hexène-1 est une des oléfines les plus importantes puisqu'elle est principalement utilisée comme comonomère pour la production de polyethylenes (HDPE, LLDPE), matériaux aux diverses applications à l'échelle mondiale. Dans le domaine de la trimérisation sélective de l'éthylène par voie catalytique, quelques complexes de titane portant un ligand phenoxy-imine tridentate (SFI) et activé par le méthylaluminoxane (MAO) sont les plus actifs et sélectifs parmi les systèmes au titane. Néanmoins, la polymérisation de l'éthylène est une réaction secondaire inhérente à ces systèmes. Même si cette production de polymère impacte à la fois la sélectivité et le procédé de trimérisation, peu d'études sont focalisées sur la rationalisation de cette réaction indésirable. Pour répondre à cette problématique, ce projet s'est appuyé sur une stratégie originale qui consiste à analyser le polymère pour récolter des informations sur le catalyseur. Dans un premier temps, le comportement du système catalytique (activité, sélectivité) a été étudié sur une large gamme de température (26-80 °C). Il a été prouvé que ce système est le plus actif et sélectif en hexène-1 à basse température (30-40 °C) mais produit d'autant plus de polymère que la température est haute ($T > 50$ °C). En combinant des techniques d'analyses classiques (SEC, RMN, DSC) et plus avancées (CEF, SIST, rhéologie), il a été observé que tous les polyéthylènes obtenus entre 26 et 80 °C sont de haute masse molaire (10^{5-6} g mol⁻¹) et contiennent un faible taux de branchement (< 1 mol %). Ces éléments démontrent que l'espèce active en polymérisation a une faible capacité d'incorporation de l'hexène-1 et engendre peu de réactions de transfert. De plus, l'élargissement des distributions de masse molaire à haute température ($D > 2$) témoignent de l'évolution d'un système de polymérisation de mono-site vers multi-site. Par la suite, des études cinétiques ont révélé que quelle que soit la température, la production de polyéthylène est continue pendant la réaction et ce dès les premiers instants de la réaction. Pour étudier le comportement du système SFI, les conditions des tests catalytiques ont été modifiées (ajout d'hexène-1, d'hydrogène, prémélange avec le MAO ou emploi du TMA comme co-catalyseur). Dans tous les cas, l'activité et/ou la sélectivité en hexène-1 en sont impactés. En étudiant les potentielles voies menant à la formation d'espèces polymérisantes, les principaux paramètres impliqués dans ces réactions sont la température et le MAO. Concernant les réactions induites par le co-catalyseur, une espèce active de type Ziegler-Natta ne portant plus de ligand, car potentiellement abstrait par le TMA, a été modélisée par le système TiCl₄/MAO. De plus, l'hypothèse d'une réduction partielle au Ti^{III} a été vérifiée en testant le système (FI)Ti^{III}Cl₂/MAO. Ces deux hypothèses s'avèrent peu probables puisque les performances catalytiques de ces systèmes ne permettent pas d'expliquer la quantité de polymère obtenues avec (FI)Ti^{IV}Cl₃/MAO. Par la suite, la formation d'une espèce de polymérisation par modification thermique du complexe (FI)TiCl₃ a été mise en évidence. Cette espèce portant un ligand tridentate de type [O-,N,O] présente une réponse à l'hexène-1 similaire au système SFI mais ses faibles performances catalytiques montrent qu'il ne s'agit pas de l'espèce de polymérisation principale dans le système SFI. Finalement, même si le catalyseur de polymérisation n'a pas été clairement identifié dans cette étude, ce projet a permis d'orienter de futures recherches en ciblant les paramètres clés à étudier pour expliquer la formation de cette espèce secondaire.